ASSESSING THE IMPACTS OF CLIMATE CHANGE ON BEST MANAGEMENT PRACTICE IMPLEMENTATION STRATEGIES

By

Sean Alexander Woznicki

A THESIS

Submitted to
Michigan State University
in partial fulfillment of the requirements
for the degree of

MASTER OF SCIENCE

Biosystems Engineering

2011

ABSTRACT

ASSESSING THE IMPACTS OF CLIMATE CHANGE ON
BEST MANAGEMENT PRACTICE IMPLEMENTATION STRATEGIES

By

Sean Alexander Woznicki

The effects of climate change on future water availability and water quality are not well understood, making the development of watershed management plans difficult for decision-makers. Agricultural best management practices (BMPs) are commonly implemented to mitigate non-point source (NPS) pollution, but future effectiveness is unknown due to climate change. To address these problems, the following research objectives were developed: (1) quantify the impacts of climate change on water quantity and water quality, (2) assess BMP effectiveness in current and future climate scenarios, and (3) determine the reliability of BMPs in future climates by performing a sensitivity analysis. The Soil and Water Assessment Tool (SWAT), a physically-based watershed model, was coupled with climate change data from the National Center for Atmospheric Research (NCAR) Community Climate System Model (CCSM-3) for the Tuttle Creek Lake watershed of Kansas and Nebraska. Eight agricultural BMPs were represented within the SWAT model framework: conservation tillage, contour farming, filter strips, grazing management, native grass, no-tillage, porous gully plugs, and terraces. Results indicate that water quantity and pollutant yields will likely increase in future climates. Native grass, terraces, and contour farming were determined to have the highest mean annual reduction efficiencies for all pollutants in current and future scenarios, while porous gully plugs were least efficient. Native grass, filter strips and grazing management were the least reliable under all climate scenarios due to high sensitivity.

ACKNOWLEDGEMENTS

I would like to thank all the people that supported me through the completion of this degree. First, I would like to thank Dr. Pouyan Nejadhashemi for this opportunity and his guidance, support, and advice. Without his encouragement and motivation, I would not have been able to write this thesis. I would also like to thank my committee, Dr. James Steffe and Dr. Julie Winkler for their advice and support in completing this degree. Thank you to Dr. Fred Bakker for your emphasis for always having an open office.

I would also like to thank my mom and dad, Michelle and Tom, and my brother, Scott, for their love and support. To my friends, thanks for the distractions and everything else you do. Special thanks to Tom for your coding help. To Stacy, thank you for your support, encouragement, and love.

Finally, I would like to thank my labmates Brad, Matt, Mike, Giri, Yaseen, Edwin, and Sabah for all the laughs and good times over the past year.

TABLE OF CONTENTS

LIST OF TABLES

LIST OF FIGURES

LIST OF ABBREVIATIONS

AnnAGNPS – Annualized Agricultural Non-Point Source Model

ARS – Agricultural Research Service

BASINS – Better Assessment Science Integrating point and Nonpoint Sources

Canmx – Maximum Canopy Storage (mm)

CCSM3 – Community Climate System Model

CH_N1 – Manning's "n" value for the tributary channel

Ch_N2 – Manning's "n" value for the main channel

CH_K2 – Channel effective hydraulic conductivity (mm/hr)

CN2 – initial SCS runoff curve number for moisture condition II

CO_2 – Carbon Dioxide (ppm)

DEM – Digital Elevation Model

EFTMIX – tillage mixing efficiency

Epco – Plant uptake compensation factor

Esco – Soil evaporation compensation factor

ET – evapotranspiration (mm)

FILTERW – width of edge-of-field filter strip (m)

GCM – Global Climate Model

GIS – Geographic Information Systems

GtC – Gigatonnes carbon

Gw_Delay – Groundwater delay time (days)

HadCM2 – Hadley Centre Coupled Model, version 2

HRU – Hydrologic Response Unit

HSPF – Hydrologic Simulation Program-FORTRAN

HUC – Hydrologic Unit Code

HVSTI – Harvest index for optimal growing conditions

IPCC – Intergovernmental Panel on Climate Change

L-THIA – Long-Term Hydrological Impact Analysis

MRLC – Multi-Resolution Land Characteristics Consortium

MUSLE – Modified Universal Soil Loss Equation

NCAR – National Center for Atmospheric Research

NCDC – National Climatic Data Center

NLCD – National Land Cover Database

NPS – Non-Point Source

NRCS – Natural Resources Conservation Service

NSE – Nash-Sutcliffe Efficiency

PLOAD – GIS Pollutant Load

PRISM – Parameter-elevation Regressions on Independent Slopes Model

R^2 – Coefficient of determination

Rchrg_Dp – Deep aquifer percolation fraction

RCM – Regional Climate Model

RMSE – Root mean square error

RUSLE – Revised Universal Soil Loss Equation

S – Relative sensitivity index

SCS – Soil Conservation Service

SDSM – Statistical Downscaling Model

Sol_Alb – moist soil albedo

SOL_AWC – available water capacity of the soil layer (mm H_2O/mm soil)

Sol_K – saturated hydraulic conductivity (mm/hr)

Spcon – Linear re-entrainment parameter for channel sediment routing

Spexp – Exponential re-entrainment parameter for channel sediment routing

SRES – Special Report on Emissions Scenarios

STATSGO – State Soil Geographic Database

SURLAG – Surface runoff lag coefficient

SWAT – Soil and Water Assessment Tool

TCLW – Tuttle Creek Lake Watershed

Timp – Snow pack temperature lag factor

TKN – Total Kjeldahl Nitrogen

TN – Total nitrogen

TP – Total phosphorus

USDA – United States Department of Agriculture

USEPA – United States Environmental Protection Agency

USGS – United States Geological Survey

USLE – Universal Soil Loss Equation

USLE_C – Universal Soil Loss Equation cover factor

USLE_P – Universal Soil Loss Equation support practice factor

WetSpa – Water and Energy Transfer between Soil, Plants and Atmosphere

1 INTRODUCTION

The earth's climate is changing. Due to increased atmospheric greenhouse gases (GHGs) from intensive fossil fuel use, the earth has experienced a warming effect (IPCC, 2007). According the to the Intergovernmental Panel on Climate Change (IPCC), global average surface temperatures have increased by 0.13°C per decade since 1950 (IPCC, 2007). Furthermore, the IPCC (2007) hypothesizes that global average surface temperatures could increase from 1.8°C to 4°C by the end of the 21st depending on the extent of future GHG emissions. The potential impacts of these changes on the well-being of society and the environment are far reaching. Although the extent of the impacts of climate change on humanity and the natural world are not completely known, many predictions have been made as to its effects. The scale of climate change and its influence on society is great: human health, ecosystem health and biodiversity, food production, economic growth, tourism, and water resources are among the potential issues impacted by climate change in the United States and worldwide (Kovats et al. 2005; Ebi et al. 2006; Arnell 2004).

Climate change impacts on human health are generally negative, while low income countries are most vulnerable because of their relative inability to adapt and implement public health programs (Patz et al., 2002; Haines et al., 2006). As temperatures rise, heat waves are expected to increase mortality related to exposure during extreme events (Patz et al., 2005). Infectious disease transmission is related to climatic factors, including temperature, precipitation and humidity (Haines et al., 2006). Changing climate may induce changes in incidence of disease transmission as well as geographic distribution of disease vectors (Haines et al., 2006). Ecosystem dynamics

have been affected by recent changes in climate. Biodiversity is expected to be negatively impacted through reduced habitat suitability and reproduction performance (Hulme 2005). Many organisms in various geographic regions have been affected and common changes are related to timing of spring activities: earlier breeding of birds, spawning of amphibians, and flowering of plants (Walther et al., 2002). Species interaction has been negatively affected, including predator-prey and plant-insect relationships (Parmesan et al., 2006). Climate change has also impacted species distribution, populations, and may lead to increased probability of extinction by the mid-21st century (Thomas et al., 2004).

Food production is expected to be greatly affected by climate change and variability. Agriculture is highly sensitive to climatic variations, including temperature, precipitation, and carbon dioxide (Howden et al., 2007). Changes in rainfall may lead to drought or flooding, while temperature changes alter the growing season; these two extreme weather scenarios may result in decreased crop yields, affecting the global food security through increasing food prices (Easterling and Apps 2005; Gregory et al. 2005; Slingo et al. 2005). Food production is affected by climate change through alterations of crop yields and land suitability (Schmidhuber and Tubiello, 2007). Warming may benefit crop and pasture yields in temperate regions and decrease yields in tropical and arid regions (Tubiello et al., 2007).

Economic growth and tourism are also affected by future climate changes. It is predicted that for most climate change scenarios and most countries, negative climate change impacts are likely to reduce the rate of economic growth (Fankhauser and Tol 2005). Changing lengths and quality of the tourism season has implications for demand and seasonality, which may negatively affect profitability of some destinations (Scott et

al. 2004). Tourism is very sensitive to climatic variations, and popular destinations may become too hot, while other destinations with predominantly cool climates may warm and become more desirable globally (Berritella et al., 2004).

Fresh water is the most important resource in the world to humans, flora, and fauna. As global climate change and its effects become a pressing issue, it is important to understand the consequences it will have on water quality and quantity issues. Human life and well-being depends on having clean water to use for drinking, food production, industrial uses, transportation, and recreation, while ecosystems rely on clean water to provide life and habitat. The IPCC (2008) predicts that higher water temperatures and changes in extremes, such as flood and droughts, are projected to affect water quality and intensify forms of water pollutants, including sediments and nutrients (Bates et al. 2008). For example, in the United States, the western Great Plains are expected to experience decreased streamflows while this area is heavily dependent on regional water supplies for sustaining agriculture (Rosenberg et al. 2003). Already rising temperatures in the western United States have lead to earlier melting of snow and changing of the timing and amount of runoff, which is critical to water resources in the region (Karl et al., 2009). Surface water and groundwater quality are expected to be affected by a changing climate (Karl et al. 2009).

Based on the implications changing climate may have on water quantity and quality, the goal of this project is to determine the impacts of climate change on water quantity and quality in the Tuttle Creek Lake watershed of Kansas and Nebraska. Additionally, the project will investigate the effectiveness of agricultural conservation practices in current and future climate projections through analysis of their pollution

reduction capabilities and sensitivity to change in temperature, precipitation, and atmospheric CO_2 concentration.

There are four specific problems (knowledge gaps) that must be addressed when planning for future climate change and its impact on water quality and quantity

1) *Uncertainty of water quantity and availability*. It is known that climate change will affect water quantity and availability on the watershed scale in varying ways for different basins. Availability of water for consumption and other economic uses is variable and not well understood in detail on a case-by-case basis for individual watersheds under future climate scenarios, and research is in its infancy (Jackson et al. 2001; Hurd et al. 2004; Marshall and Randhir 2008)

2) *Changing magnitudes of NPS pollution*. Degradation of water quality is an important issue because of predicted changes in hydrologic regimes. Storm events are the driving force of nonpoint source (NPS) pollution, and increases or decreases in precipitation (annual average and variability) will affect the quantity of pollutants entering lakes and rivers. Meanwhile, the type of NPS pollution that is affected by climate change will vary from watershed to watershed (Meyer et al. 1999; Murdoch et al. 2000; Senhorst and Zwolsman 2005; Ficklin et al. 2009). Climate change impacts on water quality are poorly understood, and research must be enhanced in this area Kundzewicz et al., 2007).

3) *Uncertainty of BMP effectiveness*. Current best management practices (BMPs) may not be applicable for future climate scenarios. As climate changes, magnitude of NPS pollutants may be more extreme within a watershed and current BMPs may not be appropriate to treat these conditions (Wilby et al. 2006). The IPCC (2008) has concluded

with very high confidence that current water management practices may not be able to cope with the impacts of climate change on water supply and water quality (Bates et al. 2008).

4) *Lack of a decision making tool*. There is a need for a decision-making tool to understand climate change and its impact on agricultural watersheds (National Research Council 2009). Assessments of NPS pollution within a watershed are important for implementing effective management strategies (Parajuli et al. 2008; Behera and Panda 2006; Gitau et al. 2006).

Therefore, the specific objectives of this project located in the Tuttle Creek Lake watershed are as follows:

1) Determine the impacts of climate change on water quantity and water quality
2) Assess the effectiveness of BMPs in current and future climate scenarios
3) Perform a sensitivity analysis of BMP implementation in current and future climate scenarios

2 LITERATURE REVIEW

2.1 OVERVIEW

This literature review describes climate change, its affects on water resources, mitigation methods, and the integration of climate models and hydrological models for climate change impact assessment studies. The first section describes climate change over various geographic scales, development of future global emissions scenarios by the IPCC, and methods of integration of climate change data into hydrological models. The next section outlines various hydrological models and their applications. Next, the effects of climate change on water quantity and water quality are discussed, respectively. Finally, methods for mitigating the effects of climate change on water resources are detailed.

2.2 CLIMATE CHANGE

Humans alter global climate not by the generation of heat in energy usage, but by interfering with natural energy flow through changing atmospheric composition (Karl et al., 2003). Atmospheric composition is altered by humans through the emission of greenhouse gases such as carbon dioxide (CO_2) and methane (CH_4) due to the burning of greenhouse gases (GHGs), known as anthropogenic forcing of the climate system. Global concentration of carbon dioxide has increased 31% since the industrial revolution, and half of this increase has been since 1965 (Karl and Trenberth, 2003). Anthropogenic greenhouse gases affect the natural flow of energy by trapping outgoing radiation produced by the earth leaving the atmosphere, which creates a warming effect that is

observed as an increase in global temperatures (Karl and Trenberth, 2003, National Academies 2008). Solomon et al. (2009) has concluded that anthropogenic climate change taking place due to increases in CO_2 concentration is irreversible for at least one thousand years after emissions stop.

Climate responds to local, regional, and global factors, and climate variability generally increases as scale decreases (e.g. the United States climate varies more than the average global climate does) (Karl et al., 2009). Therefore, it is important to examine the effects of increasing atmospheric concentrations of greenhouse gases on climate at three scales before examining watershed scale climate change: globally, nationally (USA), and regionally (the Great Plains).

Additionally, Nackicenovic et al. (2000) developed future greenhouse gas emissions scenarios based on how the global economy, environment, and population may change to understand how the climate change in the future. These scenarios provide alternative futures about the direction that society and the climate may move and are used as the driving force behind global climate models (GCMs) that attempt to simulate future climate.

The following sections discuss climate change on the global scale, in the United States, and in the Great Plains (which contains the project study area). In addition, future greenhouse gas emissions scenarios and approaches for performing climate change impact assessments are presented. This section lays the framework for integration of climate change projection data into hydrologic models to determine the impacts of climate change on water resources.

2.2.1 Global Climate Change

Globally, the IPCC predicts that continuing GHG emissions at or above current rates will further warm the Earth and induce many changes in the global climate system of the 21st century that are very likely to be larger than those experienced in the previous century (Meehl et al., 2007). Heat waves are expected to be more intense and extend over larger time periods, while cold spells are projected to decrease in a warmer global climate (Meehl et al., 2007). On a daily cycle, daily minimum temperatures are expected to increase faster than daily maximum temperatures (Meehl et al., 2007).

Model outputs regarding global precipitation project that tropical areas around the equator will become wetter, midlatitude areas will generally observe decreases in precipitation, and conversely, high latitudes will become wetter (Meehl et al., 2007). Currently, atmospheric CO_2 concentration is about 385 ppm as of 2008, measured at the National Oceanic and Atmospheric Administration (NOAA) Mauna Loa Observatory in Hawaii, USA (Tans, 2010). As CO_2 concentrations in the atmosphere rise to 450-650 ppm over the next 100 years, dry season- rainfall is expected to decrease significantly (20%) for a global mean warming of 2°C in many regions of the world, including northern Africa, southern Europe, and western Australia (Solomon et al., 2009). Dry-season rainfall is also expected to decrease to a lesser extent (10%) for the same global mean warming in southwestern North America, eastern South America, and southern Africa (Solomon et al., 2009).

2.2.2 Climate Change in the United States of America

Changes in temperature and precipitation in the United States have already been observed in the past half-century, likely due to increased greenhouse gas emissions. In the past 50 years, average air temperatures in the U.S. have increased by more than 1°C, which has amplified drought severity and extent; annual average precipitation has increased by about 5% in that same time period, and about 20% more precipitation has fallen in extreme storm events (Karl et al., 2009).

All of North America is very likely to warm in the 21st century and it is expected to exceed the global mean warming (Christensen et al., 2007). At the same time, climate responses to increased greenhouse gases are expected to vary greatly by region within the United States. Warming is likely to be largest in the winter for the northern United States, while summer temperatures are likely to experience the greatest increase in the southwest. Depending on GHG emissions throughout the 21st century, average U.S. temperature could increase by 2-6°C (Karl et al., 2009). Increases in summer maximum temperatures may be as high as 7°C for the southeastern United States (Mearns et al., 2003).

In regards to precipitation, projections indicate that the northern United States will likely receive more precipitation by the end of the 21st century, while the southwest United States will be come drier, although higher confidence exists for winter and spring than for summer and fall (Karl et al., 2009). Increases in northern precipitation is due to projections foreseeing warm, moist air from the southeast traveling further north than it has in the past, while cold and dry air from the north may not extend as far south as it has

previously (Gutowski et al., 2007; Karl et al., 2009). In the southeastern United States, climate models have projected significant decreases of 20-30% in summer precipitation (Mearns et al., 2003).

2.2.3 Climate Change in the Great Plains

Climate change in the Great Plains (consisting of North Dakota, South Dakota, Nebraska, Kansas, Oklahoma, Wyoming, Montana, and parts of Colorado, Texas, and New Mexico) as defined by the United State Global Research Program (USGCRP) is expected to vary widely due to strong seasonal and regional variations in climate (Karl et al. 2009). Currently, climate in the Great Plains is characterized by uniform topography and steep gradients in temperature and precipitation: mean temperatures increase from north to south, while annual precipitation increases from south to north and from east to west. The Great Plains have experienced increases in average temperature of about 0.8°C since the 1960-1979 baseline period (Karl et al. 2009).

By 2100, temperature increases are expected to be more severe, ranging from 1.4°C to 7.2°C, depending on future GHG emissions (Karl et al. 2009). Winter temperatures are expected to have smaller increases than summer temperatures throughout the region (Christensen et al., 2007). Precipitation increases are expected mostly in the winter and spring of the northern half of the Great Plains, while precipitation decreases are expected for the already arid southern half of the Great Plains (Karl et al. 2009). In addition to these changes, variability and extremes of temperature and precipitation are expected to increase. Heat waves, droughts, and heavy rainfall are projected to be the major factors in future climate change of the 21st century that will

adversely affect water resources, agricultural production, and natural resources (Karl et al., 2009).

2.2.4 Emissions Scenarios

Evolution of GHG emissions in the future is uncertain due to the complexities and somewhat ill-understood nature of their driving forces. Influences on atmospheric GHG concentrations include population growth, socio-economic development, land use change and agricultural productivity, and advancement of technology (Nakićenović et al. 2000). In 2001, the IPCC published the Special Report on Emissions Scenarios (SRES) developed for the Third Assessment Report by Nakićenović et al. (2000) to provide alternative futures of how society and climate may unfold, as well as for use as the driving force behind GCMs to develop scenarios for climate change. Climate change scenarios created from GCMs are then used for studies that assess the impacts of climate change and look for ways to adapt and mitigate climate change.

Scenarios are snapshots of alternative futures; they cannot be considered predictions, but are simply ways in which the future may unfold regarding the global economy, social system, and climate. Due to the complexity of the causes of GHG emissions, accurate prediction of emissions is impossible (Nakićenović et al., 2000). Therefore, a set of scenarios is used to understand future developments of GHG emissions.

SRES scenarios have two main components: a narrative storyline and various quantitative scenarios for each storyline. There are four storylines: A1, A2, B1, and B2, which all detail different directions in which society, the economy, technology, the environment, and policy will progress (Arnell, 2004).

2.2.4.1 A1 Storyline

The A1 storyline and family of scenarios consists of rapid economic development and prosperity (Nakićenović et al. 2000; Arnell, 2004; Abbaspour et al., 2009). At the same time, population growth is relatively low and technology efficiency increases (Joos et al., 2001). Economic relationships change, as distinctions between poor and rich countries are minimized. Demographically, A1 suggests smaller families due to a lower mortality rate and lower fertility rate. Population will peak at nine billion people around the mid-21st century and decline to seven billion by the end of the century. Technology change is variable for each scenario within the A1 storyline to depict how energy source uncertainty is represented in the future (Arnell, 2004). The global population regards environmental issues to be important: environmental quality shifts from a conservation focus to management of natural resources and ecosystems services. There are three scenarios within this family: A1F1 (fossil fuel intensive energy use), A1B (balance between all energy sources), and A1T (extensive use of non-fossil fuel and renewable energy technologies). The A1F1 scenario has the highest GHG emissions of any storyline/scenario. For the period of 1990-2100, cumulative carbon dioxide emissions for the A1F1, A1B, and A1T is projected to be 2189 gigatonnes carbon (GtC), 1499 GtC, and 1038 GtC, respectively (Nakićenović et al. 2000).

2.2.4.2 A2 Storyline

The A2 storyline and its family of scenarios describe a more divided world than the A1 storyline (Nakićenović et al. 2000). Underlying themes include self-reliance and local and regional focus regarding economic and environmental issues (Maurer, 2007;

Githui et al., 2009). Economic development is divided regionally due to lack of trade growth and cooperation between nations (Maurer, 2007; Abbaspour et al., 2009). Subsequently, per capita economic growth is slow and social and cultural interactions are less prevalent on an international scale, which leads to segmented technological advancement when combined with slow economic development. Family life is highly valued, leading to higher fertility rates and the highest projected population of any SRES storyline (Arnell, 2004). In A2, global population reaches 15 billion people by 2100 (more than double that of the A1 storyline). Capacity for food production must increase in the A2 storyline, therefore agricultural production is a substantial focus. High yield agriculture reduces soil erosion and water resource pollution that was initially very high. Environmental concerns vary by country, and are more prevalent on local and regional scales. Energy development is based on the needs and resources of each country: low-income, resource-rich countries develop more resource-intensive economy and food production technology, while high-income, resource-poor countries focus on advancement of alternative technology (nuclear or renewable). For the period of 1990-2100, cumulative carbon dioxide emissions for the A2 scenario are projected to be 1862 GtC (Nakićenović et al. 2000).

2.2.4.3 B1 Storyline

The B1 storyline depicts an ecologically friendly, socially conscious, and convergent world (Nakićenović et al. 2000). In the B1 storyline, the world achieves an environmentally sustainable economy by the middle of the 21st century (Arnell, 2004). Individual life is based on renewable-resource dependency based on clean technology.

Economic growth is rapid, but is based on information and services rather than material resources (Joos et al., 2001; Maurer, 2007). Internationally, global solutions are used to achieve economic, social, and environmental sustainability. Population growth is similar to the A1, scenario where global population is at its maximum (nine billion) by 2050 and decreases to seven billion by 2100. Low mortality and low fertility is a characteristic of B1 due to social and environmental concerns. Industry, governments, the public, and the media are more environmentally conscious in regards to economic development (Abbaspour et al., 2009). This leads to high environmental quality: pollution prevention and material reuse and recycling occurs on every scale, from local to global (Nakićenović et al. 2000). Land use change is managed to prevent further ecological damage. Lower food requirements allow for low-impact agriculture, while less meat is consumed due to increased forested land. Cities are compact and allow for increased public transport; wilderness areas are increased as management becomes more important and less agricultural land is necessary. Alternative energy is dominant as oil and gas resources decline globally and environmental concerns increase (Maurer, 2007; Abbaspour et al., 2009). Conventional and unconventional gas becomes the cleanest fossil in use during the transition between intensive fossil fuel use and renewable energy prevalence. For the period of 1990-2100, cumulative carbon dioxide emissions for the B1 scenario are projected to be 983 GtC (Nakićenović et al. 2000).

2.2.4.4 B2 Storyline

The B2 storyline depicts a divergent world that emphasizes economic, social, and environmental sustainability on a local and regional scale (Nakićenović et al. 2000; Githui et al., 2009). Decision-making structures are implemented locally rather than

internationally (Joos et al., 2001). Economic development is considered intermediate in this storyline. Per capita income increases globally and income disparity decreases between nations due to community scale focus. Population growth is moderate, reaching ten billion people by the end of the 21st century as fertility and mortality slightly decrease (Joos et al., 2001; Arnell, 2004). Technological growth is less rapid than in the A1 and B1 storylines, although it is greater than in the A2 storyline (Joos et al., 2001). Due to a more divergent world, technological research and development is regionally based and disparate internationally. Environmental issues are a priority globally, but national governments are not as successful as local governments in implementing solutions. Land use management is important at the local level, reducing urban sprawl while increasing public transportation and decreasing car usage (Nakićenović et al. 2000). Locally grown produce is significant, decreasing meat consumption in countries with large populations (Nakićenović et al. 2000). Energy type is a function of the natural resources of each country. Fossil-fuel technology is abandoned in favor of renewable energy in countries that need to use resources more efficiently. By 2100 most countries are still using fossil-fuel based technology although transition to other sources of energy begins, reducing GHG emissions. For the period of 1990-2100, cumulative carbon dioxide emissions for the B2 scenario are projected to be 1164 GtC (Nakićenović et al. 2000).

2.2.5 Climate Impact Assessment Approaches

To study the impacts of climate change and water resources, construction of climate change scenarios is necessary. As defined by Githui et al. (2009), there are four general techniques available to accomplish this: (1) climate models, (2) temporal and

spatial analogues, (3) incremental scenarios, and (4) extrapolation of historical trends and empirical relationships between regional climate and projected global changes. Each approach has both advantages and disadvantages, which are explored, along with examples of implementation in climate impact assessments, in the following sections.

2.2.5.1 GCM Approach

The climate model based approach uses Global Climate Models (GCMs), to simulate the response of the global climate system based on changes in atmospheric composition (Githui et al., 2009). GCMs, which are the primary tools for predicting future climate, are mathematical, computer-based models of the physics, chemistry, and biology of the atmosphere, land surface, oceans, and cryosphere and their interactions with each other and the sun (Karl and Trenberth, 2003). The difficulty in using GCM output is that the coarse resolution of GCMs is often not adequate for the fine spatial scale of impact assessments, including hydrology (Stone et al., 2003). Therefore, GCM data is often downscaled. Downscaling refers to using fine spatial scale numerical atmospheric models (dynamical downscaling) or statistical relationships (statistical downscaling) to produce detailed regional or local atmospheric data (Castro et al., 2005). Another method of dealing with GCM inadequacies is the delta change method.

Dynamical downscaling nests a higher resolution regional climate model (RCM) within a coarser resolution GCM (Giorgi and Mearns, 1999; Wilby et al., 2002). RCMs use a GCM to define atmospheric boundary conditions around a finite domain, within which physical dynamics of the atmosphere are modeled at a fine spatial resolution (Wilby et al., 2002). Advantages of RCMs is that they can model small scale atmospheric features and can explore significance of external forcings such atmospheric-chemistry

changes, while disadvantages include high computational demands (restraints on domain size, number of experiments, and duration of simulations), and sensitivity to selected boundary conditions (such as soil moisture) that initiate experiments (Wilby et al., 2002).

Statistical downscaling of GCMs fall into three major categories: regression methods, stochastic weather generators, and weather typing schemes (Dibike and Coulibaly, 2005). Regression-based downscaling techniques use empirical relationships between local-scale climate variables (predictands) and large-scale climate variables (predictors) to develop regression functions (Dibike and Coulibaly, 2005; Wilby et al., 2002). Advantages of regression is that it is easy to apply, but it suffers from only being able to explain a fraction of observed climate variability (especially when using precipitation as the predictand) (Dibike and Coulibaly, 2005; Wilby et al., 2002). Stochastic weather generators are statistical models of observed sequences of weather variables, otherwise known as complex random number generators that produce output that resembles daily weather at a specific location (Dibike and Coulibaly, 2005). Advantages of stochastic weather generators include its ability to reproduced observed climate statistics and the fact that it has been widely used, while disadvantages are related to the arbitrary methods used to define model parameters for future climate conditions (Wilby et al., 2002). Weather typing groups local meteorological variables in relation to classes of atmospheric circulation, where future regional climate scenarios are constructed from samples of the observed variable distributions or by generating synthetic sequences of weather patterns using Monte Carlo simulation (Wilby et al., 2002). Advantages of this method are it logically connects climate at the large scale and weather at the local scale, while disadvantages include inadequacy in simulation extreme

events and that weather patterns generated rarely agree with the parent GCM (Wilby et al., 2002).

The delta change method computes differences between current and future GCM simulations, which are applied to observed time series weather data (Hay et al., 2000). This commonly used method adds an expected temperature increase to the observed temperature record to obtain a future time series, while precipitation is changed using a fraction (Lenderink et al., 2007). The delta change method does not include future changes in variability because it adjusts observed time series data, and therefore, the number of wet days remains unchanged (Graham, et al., 2007).

The GCM approach and downscaling methods to developing climate change scenarios have been used frequently in watershed scale water quantity and quality studies, which are presented in the following.

Eckhardt and Ulbrich (2003) used the GCM approach to determine the impacts of climate change on water quantity in a mountainous German watershed. Using A2 and B1 SRES scenarios from five GCMs, mean winter and summer temperature and precipitation changes on a grid were calculated for 2070-2099. Using a sinusoidal function, annual cycles of monthly average temperature and precipitation changes were calculated to adjust observed daily time series data.

Stone et al. (2003) compared two climate change scenarios at different scales using a GCM and RCM to asses water yield in the Missouri River basin. The Commonwealth Scientific and Industrial Research Organization (CSIRO) GCM was used,, which has a spatial scale of 400 km by 500 km. The National Center for Atmospheric Research (NCAR) RegCM2 model was used for the RCM, which was

driven by CSIRO initial and boundary conditions, where the output grid spacing was 50 km. Precipitation was found to be more spatially variable for the RCM than for the GCM model output. Both simulations were run under a doubling of atmospheric CO_2 concentration. Maximum and minimum temperature change scenarios were created by adding the differences between the current climate and future climate projects to observed records. Daily precipitation was adjusted by the ratio of the future climate projections to the observed records. The authors concluded that using high resolution RCM climate change scenarios produced significantly different results regarding water yield than those found using coarse scale GCMs.

Gosain et al. (2006) used RCM data to determine the impact of climate change on water resources of 12 watersheds in India. Daily weather data (temperature and precipitation) for 1981-2000 and 2041-2060 was generated using the HadRM2 RCM from the Hadley Centre and input into a watershed model.

Jha et al. (2006) used the GCM approach and the incremental approach to perform a climate change sensitivity analysis on the Upper Mississippi River Basin streamflows. In addition to the incremental approach (detailed in the *Incremental Approach* below), future monthly temperature and precipitation data was obtained from six GCM projections under the A2 scenario for 2061-2090: CSIRO-RegCM2, Canadian Climate Model (CCC), Center for Climate Study Research (CCSR), Geophysical Fluid Dynamics Laboratory (GFDL), CSIRO-Mk2, and Hadley Centre for Climate Prediction and Research (HadCM3). Data for each GCM was used as input in the selected watershed model.

The study by Nurmohamed et al. (2007) used both GCM output and hypothetical climate change scenarios to determine changes in the water balance of a large watershed in Suriname. Average outputs of five GCMs were used to simulate monthly change in temperature and precipitation: Had300 (UK Hadley Centre), ECH498 (German Climate Research Centre), GFDL90 (US Geophysical Fluid Dynamics Laboratory), CSI296 (Commonwealth Scientific and Ind. Research Organization, Australia), and CCSR96 (Japanese Centre for Climate Systems Research). Two time periods of GCM output were used: 2035-2064 (centered on 2050) and 2065-2094 (centered on 2080). Daily changes from the averaged model results were added to observed data from 1975-1983. Incremental scenarios used in this study are presented in the *Incremental Approach* section below.

Marshall and Randhir (2008) used GCM data to evaluate the impacts of temperature increases on water quantity and quality of the Connecticut River Watershed in New England. Two GCMs (MRI2 and CCSR/NIES2) run under SRES A2 were downscaled to modify historical temperature observations. The MRI2 model results were selected because it predicts the lowest increase in average temperature (+1.4ºC), while the NIES2 model results were selected because it predicts the greatest increase (+5.8ºC). Warming predictions were added to daily minimum and maximum temperatures in a linear fashion to the 40 year baseline period. Precipitation changes were not included in the climate change scenarios.

Abbaspour et al. (2009) used the Soil and Water Assessment Tool (SWAT) and the Canadian Global Coupled Model (CGCM 3.1) GCM to determine the impact of climate change on water resources in Iran for two time periods: 2010-2040 and 2070-

2100. Three SRES scenarios were used from the GCM: A1B, A2, and B1. Climate change scenarios were downscaled for each weather station in the study area. Precipitation was downscaled using a monthly ratio between the GCM data and the observed data, while temperature downscaling involved the use of a nonlinear regression model.

Franczyk and Chang (2009) conducted a study to determine the impacts of climate change and urbanization on stormwater runoff in the Portland, OR metropolitan area. Climate change scenarios were constructed based on GCM data from the ECHAM5 model using the A1B emissions scenario for 2040-2059. The GCM results were downscaled to a 15 km resolution grid using a statistical downscaling method. Statistical downscaling, rather than dynamical downscaling, was used because it is computationally inexpensive and is applicable for small watersheds, although it does not consider the effect of topography on climate. Incremental scenarios were also implemented for comparison with the downscaled GCM (detailed in the *Incremental Approach* section below).

Githui et al. (2009) used GCM climate change scenarios to determine the impact of climate change on a Kenyan watershed streamflow. Two thirty year periods were studied: 2010-2039 (centered on 2020) and 2040-2069 (centered on 2050). Climate change data was obtained from five GCMs: CCSR, CSIRO, ECHAM4, GFDL, and HADCM3, which used the A2 and B2 scenarios. The models were not downscaled due to lack of adequate data. GCM data was incorporated into the watershed model by adjusting the baseline daily temperature and precipitation through change factors.

Nyenje and Batelaan (2009) used a statistical downscaling method to downscale daily GCM climate projections from the UK HadCM3 climate model to study the impacts of climate change on the hydrology of a Uganda watershed. A statistical downscaling model (SDSM) was used because downscaled data are more reliable for hydrological analysis at the watershed scale than GCM data, which may be too coarse (Karl et al., 1990; Nyenje and Batelaan, 2009). Data was downscaled based on a relationship between large scale predictor variables (e.g. humidity) and locally observed predictants (temperature and precipitation) averaged over each weather station. Two scenarios (A2 and B2) climate projections from HadCM3 were used encompassing the current climate, the 2020s, 2050s, and 2080s.

Göncü and Albek (2010) used a hypothetical watershed (controlling land use and soil type) with weather stations located in Turkey to determine the impacts of temperature and precipitation changes on streamflow and reservoir volume. The climate change scenario was created by applying trends on daily time series weather station data (temperature, precipitation, relative humidity, and cloudiness). Trends were based on gridded GCM climate change projections from the Canadian Climate Centre model for the SRES A2 emissions scenario in western Turkey. Temperature trends were added to each day of the historical observations to create a linear increase in temperature (1.6ºC by 2050). Precipitation trends were applied as surpluses or deficits to monthly totals, which led to an increase in precipitation of about one inch annually by 2050.

Gul and Rosbjerg (2010) used GCM data to evaluate the effects of climate change on regional water quantity in Denmark. Climate change scenarios were based on data from the European continent-scale PRUDENCE project (PRUDENCE, 2005; Gul and

Rosbjerg 2010). Observed temperature and precipitation was changed on a seasonal basis (3 month intervals) using results from the GCM data.

Rosenberg et al. (2010) coupled a watershed model with two downscaled GCM precipitation datasets to determine the impacts of climate change on Washington state stormwater infrastructure in urban areas. The global climate models used were ECHAM5 and CCSM-3, dynamically downscaled using the Weather Research and Forecast (WRF) RCM developed by NCAR. Data output from the RCM was bias corrected and statistically downscaled for each weather station. The authors concluded that the RCM simulations indicated increases in extreme rainfall magnitudes by 2050, but this varied by model and region.

The GCM approach has been widely used in many climate impacts assessment studies regarding water resources. In the studies presented both regional and global scale models were used that were developed by various organizations. Additionally, each SRES emissions scenario was featured in at least one study presented here, demonstrating that the choice of scenarios is largely due to preference of the author.

2.2.5.2 Temporal and Spatial Analogue Approach

Construction of climate scenarios using temporal and spatial analogues involves the use of past climates that may be similar to future climate in a region (Githui et al., 2009). The climate change in this technique has been previously observed; therefore it is consistent and physically based. One drawback to this approach is that the climate change may not be due to changes in greenhouse gas emissions and atmospheric concentrations, but naturally occurring (Githui et al., 2009).

Parker et al. (2008) used a watershed model and the temporal analogue technique to determine the affect of climate change scenarios on fertilizer application rates, filter strips, livestock stream access, and tillage reduction in an Ontario watershed. Construction of climate change scenarios were based on using historical data for one year that could be analogous to future climate change. Using this technique, an average year, warm wet year, warm dry year, cold wet year, and cold dry year were selected from the historical data.

2.2.5.3 Incremental Approach

Incremental scenarios used for climate change studies are based on alteration of observed time series climate data by arbitrary amounts (Githui et al., 2009). The advantage to using this method is that scenarios are consistent and readily applicable between different studies and regions, leading to easy comparisons. Incremental scenarios can be beneficial to climate change impact studies because they give a better indication of the ways in which gradual temperature changes affect the hydrology of a watershed (Nurmohamed et al. 2007). One consequence of using incremental scenarios is that the scenarios may not represent a physically plausible and realistic change (Githui et al., 2009). Changes in temperature and precipitation variability will not be captured by incremental scenarios. In addition, incremental changes selected are often based on results from GCM results for various SRES scenarios. This method has been used consistently in climate change impacts studies regarding water quantity and quality

Liu et al. (2000) coupled a watershed model and a water balance model with IPCC HadCM2 GCM climate projections translated to incremental weather data adjustments to study the impacts of climate change and land use change on water quality

in the Ohio River basin (specifically the Cincinnati watershed and Columbus watershed). Climate projections were translated to incremental scenarios applied to daily temperature and precipitation. The wet scenario used changes of +4°C and +20% precipitation of the current average climatic condition, while the dry scenario applied of +4°C and -20% precipitation of the current average climatic condition.

Jha et al. (2006) used incremental scenarios to perform a climate change sensitivity analysis on the Upper Mississippi River Basin streamflow. The climate change sensitivity analysis used nine distinct scenarios: 50% CO_2 increase, 100% CO_2 increase, temperature increases of +2°C, +4°C, and +6°C, and precipitation changes of ±10% and ±20%. Temperature and precipitation scenarios altered daily data of the 30-year baseline period. In addition, six GCM projections were used for comparison with the incremental scenarios (detailed in the *GCM Approach* section above).

Chaplot (2007) incrementally varied precipitation, temperature, and atmospheric CO_2 concentrations to determine changes in water yield, nitrate, and sediments in two distinct agricultural watersheds: an arid Texas watershed, and a relatively wet Iowa watershed. An atmospheric CO_2 concentration of 970 ppm by the end of the 21st century was used, which represents the A1F1 scenario from the 2001 IPCC Report. Under the A1F1 scenario, winter temperatures were increased by 3.5°C, while summer temperatures were increased by 0.5°C by 2100. The B1 scenario was also used, where winter temperature was increased by 0.5°C by 2100. Daily rainfall was also changed by ±10%, ±20%, and ±40%. The precipitation and temperature changes were scaled on yearly basis,

which led to a small incremental adjusted each year until the maximum change was reached in 2100.

Nurmohamed et al. (2007) used incremental climate change scenarios in addition to GCM output to determine changes in the water balance of a Suriname watershed. The incremental scenarios were combinations of +2ºC and +4ºC and/or precipitation changes of ±10%, ±30%, and ±50%.

Ficklin et al. (2009) and Ficklin et al. (2010) conducted a climate change sensitivity analysis for an agricultural watershed in California. The authors used a stochastic weather generator (LARS-WG) to develop 50 years synthetic climate change time series data based on the A1F1 and B1 scenarios. Precipitation was arbitrarily changed by ±10% and ±20%, while temperature was increased by 1.1°C (B1) or 6.4°C (A1F1). The temperature ranges represent bounds on the most conservative and aggressive projections for 2100. Three atmospheric CO_2 concentrations were coupled with the temperature/precipitation scenarios: 300 ppm (present-day), 550 ppm (corresponds to B1 scenario by 2100), and 970 ppm (corresponds to A1F1 scenario by 2100).

In their study to determine the impacts of climate change and urbanization on stormwater runoff in Portland, OR, Franczyk and Change (2009) used incremental scenarios for comparison with a GCM approach (detailed in the *GCM Approach* section below).Four combinations of +2°C mean monthly temperature, +4°C mean monthly temperature, +10% mean monthly precipitation, and +20% mean monthly precipitation were used.

2.2.5.4 Extrapolation Approach

Extrapolation of historical trends involves comparing model based projection to observed climate trends and extending them to the future (Githui et al., 2009). The disadvantage of this method is the assumption that the historical change trends are based on greenhouse gas emissions and atmospheric concentrations rather than natural variability (Githui et al., 2009). Finding empirical relationships between regional climate and projected global changes technique assumes that past relationships between the two are also applicable for the future climate (Githui et al., 2009).

2.3 WATERSHED MODELS

To determine the possible effects of climate change on water resources, watershed models are required because of the prediction element involved. Many models are available for performing watershed scale hydrology and water quality studies. Although watershed model classification is subjective, there are three general categories: empirical, conceptual, and physically based spatially distributed models (Nurmohamed et al., 2007). Empirical and conceptual models do not take into account spatial distribution of watershed data such as soil type, land use, topography, precipitation, and air temperature. Subsequently, empirical and conceptual models require less parameters and data for operation. Conversely, physically based spatially distributed models are data intensive, complex, and highly parameterized. The following watershed models are generally physically based and spatially distributed, although some are highly complex, while some are designed to be used as a simple screening tools and little expertise is required.

2.3.1 Annualized Agricultural Non-Point Source Model (AnnAGNPS)

AnnAGNPS is daily time step continuous-simulation watershed model used to estimate NPS pollution generation in agricultural watersheds developed by the United States Department of Agriculture – Agricultural Research Service (USDA – ARS) and the USDA Natural Resources Conservation Service (USDA – NRCS) (Bosch et al., 1998). The model divides a watershed into homogenous cells of land use, soil type, and land management (Bosch et al., 1998). For each cell, surface runoff, sediments, nutrients, and pesticides leaving the cell and transported throughout the watershed are simulated

(Bosch et al., 1998). The effect of conservation practices on pollution generation can also be simulated within AnnAGNPS.

2.3.1.1 AnnAGNPS Model Components

Model components included in AnnAGNPS are hydrology, and transport of sediment, nutrients, and pesticides due to snowmelt, precipitation, and irrigation (Borah and Bera, 2003). A daily soil water balance is maintained to determine runoff when precipitation events occur (Yuan et al., 2001). Surface runoff is calculated using the Soil Conservation Service curve number (CN) method. Channel runoff uses Manning's equation assuming a trapezoidal channel shape. Lateral subsurface flow is calculated using Darcy's equation and tile drain flow is calculated using Hooghoudt's equation and parallel drain approximation (Borah and Bera, 2003). Sediment load delivered to the edge of the field is calculated using the Revised Universal Soil Loss Equation (RUSLE) (Das et al., 2007). The modified Einstein equation is used for channel sediment transport and the Bagnold stream power equation determines transport capacity of a reach.

2.3.1.2 AnnAGNPS Applications

AnnAGNPS has been used in a climate impacts assessment studies such as Parker et al. (2008).

2.3.2 Hydrologic Simulation Program-FORTRAN (HSPF)

HSPF is a distributed, lumped-parameter watershed model that is used to simulate the effects of land use change, point source pollution, NPS pollution, reservoir operations, and more (Bicknell et al., 1997) developed by the Environmental Protection

Agency (EPA) National Exposure Research Laboratory. The model integrates land and soil contaminant runoff processes with in-stream processes to predict runoff, flow rate, and water quality constituent loads at any point in the stream. Hydrology and water quality are predicted on time steps ranging from one minute to one day using continuous precipitation and records for study periods of up to hundreds of years.

2.3.2.1 HSPF Model Components

Model components include runoff and water quality constituents on pervious and impervious land areas, in-stream channel and reservoir processes (Borah and Bera, 2003). Subsurface flow is simulated using empirical relationships and overland flow is simulated using the Chezy-Manning equation. Erosion is modeled using rainfall splash detachment and based on transport capacity. In-stream sediment transport is different for sand and silt/clay: sand is modeled using the Colby (1954) or Toffaleti (1968) method, while silt/clay is modeled based on critical shear stress and settling velocity. Physical, chemical, and biological processes within the model are simulated using theoretical and empirical equations, which increases model complexity and the required number of parameters.

2.3.2.2 HSPF Applications

Climate impact assessments have been performed using HSPF in multiple studies such as Göncü and Albek (2010) and Rosenberg et al. (2010).

2.3.3 Long Term Hydrologic Impact Analysis (L-THIA)

The L-THIA model developed by the College of Engineering at Purdue University is a tool used to determine the long-term effects of land use change on water resources (quantity and quality). L-THIA is a user-friendly tool for rapid assessment of hydrologic impacts of land use change (Bhaduri et al., 2001). Readily available data is used and provided by the model, including long-term climate records, soil maps, and land use maps. Model outputs are pollutant loads and runoff on an annual basis.

2.3.3.1 L-THIA Model Components

Components of the L-THIA model include estimation of runoff, recharge, and NPS pollution generation such as sediment and nutrients from fields. The curve number method is used to calculate annual surface runoff and accounts for variations in antecedent moisture condition in the soil (Bhaduri et al., 2000). Snowfall contributions to precipitation to adjust the curve number are not considered. NPS pollution is estimated using a build-up and wash-off calculation, which includes the dry weather processes that lead to pollutant accumulation and the wash-off that occurs during a storm event (Bhaduri et al., 2000). Build-up calculations are based on days between storm events and pollutant accumulation rates, while the wash off function is a nonlinear empirical formula.

2.3.3.2 L-THIA Applications

To the best knowledge of the author, there are no published climate change impact assessments performed using L-THIA. However, this model is reported here

because this model was designed to study the impacts of both landuse and climate changes.

2.3.4 GIS Pollutant Load Application (PLOAD)

The PLOAD model version 3.0, developed by CH2M HILL, is a geographic information systems (GIS) based tool to calculate user-specified NPS pollutant loadings from a watershed on an annual average basis (PLOAD, 2001). PLOAD was designed to be used as a generic screening tool for a variety of applications and is highly customizable (Nejadhashemi and Mankin, 2007). Two NPS pollution calculation methods are available in PLOAD: the export coefficient method (applicable for small and large watersheds) or EPA's Simple Method (applicable for watersheds less than one square mile in size). Required data includes watershed boundary, land use maps, annual precipitation data, optional BMPs.

2.3.4.1 PLOAD Model Components

PLOAD model components include runoff and pollutant load calculations for any constituent. Runoff is calculated using the SCS curve number method. Event mean concentrations (EMCs) for each land use type are required to calculate pollutant loads using the EPA Simple Method, which is based on precipitation, the ratio of storms producing runoff, and a runoff coefficient based on land use type.

2.3.4.2 PLOAD Applications

Liu et al. (2000) has performed a climate change impact assessment using PLOAD.

2.3.5 Soil and Water Assessment Tool (SWAT)

SWAT (ArcSWAT 2005) is a physically based, spatially distributed, watershed-scale water quality model that operates on a continuous daily or sub-daily time step. The SWAT model was developed by the USDA – ARS (Arnold et al. 1998). This model is used to predict the impact of management practices on water, sediment, nutrient, and chemical yields in watersheds with varying soils and land use over long periods of time (Arnold et al. 1998). SWAT allows a watershed to be delineated into subwatersheds based on topography, and then divided into HRUs (area of homogenous land use, soil type, management practices, and slope). Analysis at the HRU level allows critical sources of pollution and major causes of pollution to be identified based on characteristics of the location.

2.3.5.1 SWAT Model Components

SWAT model components include hydrology, weather, soil temperature, crop growth, nutrients, pesticides, agricultural management practices such as fertilization, tillage, pesticides, and grazing, and channel and reservoir routing (Borah and Bera, 2003). Surface runoff in SWAT is simulated using the SCS CN method based on antecedent soil moisture, land use, and soil type (Neitsch et al., 2005). Lateral subsurface flow is modeled using a kinematic storage model and groundwater flow is estimated using empirical equations. Stream routing is based on the variable storage coefficient method and flow is modeled using Manning's equation. Erosion and sediment yield are calculated for each HRU using the Modified Universal Soil Loss Equation (MUSLE),

while Bagnold's stream power for bed degradation and sediment transport is used. Complete nitrogen and phosphorus cycles are also simulated within SWAT.

2.3.5.2 SWAT Applications

Various studies have used SWAT to study the impacts of climate change on water resources. As of 2007, there have been at least 30 published climate change impacts assessments completed using SWAT (Gassman et al., 2007).Such studies have been performed by Eckhardt and Ulbrich (2003), Stone et al., (2003), Jha et al. (2006), Chaplot (2007), Marshall and Randhir (2008), Abbaspour et al. (2009), Ficklin et al. (2009), Franczyk and Chang (2009), Githui et al. (2009), and Ficklin et al. (2010).

Best management practices (BMPs) have also been modeled on the watershed scale using SWAT in the following studies: Behera and Panda (2006), Bracmort et al. (2006), Santhi et al. (2006), Arabi et al. (2007), Jha et al. (2007), Parajuli et al. (2008), Tuppad and Srinivasan (2008), and Tuppad et al. (2010).

2.3.6 Water and Energy Transfer between Soil, Plants and Atmosphere (WetSpa)

WetSpa is a physically based, semi-distributed rainfall-runoff model developed by the Vrije Universiteit, Belgium (Liu and De Smedt, 2004). The model runs on a daily time step and is applicable on the watershed scale for predicting water and energy transfer of the soil, plants, and atmosphere. A basin in WetSpa is comprised of five components: atmosphere, canopy, root zone, transmission zone, and saturation zone. The basin is divided into grid cells and further divided into bare soil and vegetation. A water and energy balance is calculated for each grid cell.

2.3.6.1 WetSpa Model Components

Model components included in WetSpa are generally hydrology based, as surface and groundwater flow are simulated, but the model lacks simulation of water quality constituents. Specific hydrological processes simulated in WetSpa include surface runoff, evapotranspiration, percolation, interflow, groundwater flow, and a water balance for each model layer (Bahremand et al., 2007). Rainfall excess is calculated using the modified rational method, calculating a potential runoff coefficient that is a function of land cover, soil type, slope, rainfall magnitude, and antecedent soil moisture (Bahremand et al., 2007). Overland and channel flow routing is simulated using the diffusive wave equation. Snowmelt simulation is simulated with an energy balance linked to air temperature.

2.3.6.2 WetSpa Applications

The WetSpa model has been used for climate impacts assessments such as Nurmohamed et al. (2007) and Nyenje and Batelaan (2009).

2.4 IMPACTS OF CLIMATE CHANGE ON WATER QUANTITY

Climate change may have a large impact on the water resources of a watershed based on how elements of hydrological cycle are affected. The following sections present the impacts of climate change on water quantity in various watersheds, based on the SRES emissions scenario or incremental method used in each study. Examining watershed specific studies on the impacts of climate change on water quantity allows for determination of relationships regarding the major components of climate change (temperature, precipitation, and atmospheric CO_2 concentration) on streamflow and surface runoff.

2.4.1 A1 Storyline Impacts

Abbaspour et al. (2009) used GCM data for the A1B emissions scenario in 2013-2039 and 2073-2099. Precipitation increases (up to 35%) were generally projected to occur in the northern regions of Iran, while the southern regions may experience decreases in precipitation of up 40% in 2013-2039. This correlates to a decrease of up to 100% in blue water (the sum of river discharge and deep groundwater recharge) for areas with precipitation decreases and up to 200% increases in blue water in areas with increasing precipitation. In 2073-2099 the increases in blue water are greater (+300%) in wet regions but the decreases (90%) are not as severe in dry regions than in the early 21st century simulations, but are still significant. In historically "wet" regions, the number of days with precipitation exceeding 10 mm increases, indicating that these regions will

have larger and more frequent floods in the future, especially in winter and fall (Abbaspour et al., 2009).

Using GCM data for the A1B emissions scenario, Franczyk and Chang (2009) predicted that runoff in a Portland, OR metropolitan watershed will likely see the greatest changes in winter. January was predicted to increase in mean monthly runoff by 12.5% in the 2040s. February was predicted to show the greatest decrease in mean monthly runoff in the same time period. These changes are likely due to the GCM predictions: the greatest mean monthly precipitation increase was January, while February had the greatest mean monthly precipitation decrease (Franczyk and Chang, 2009). Summer runoff experienced negligible changes from the current climate.

2.4.2 A2 Storyline Impacts

Eckhardt and Ulbrich (2003) predicted that streamflow increases by more than 10% due to increased winter precipitation in the form of rain for a mountainous German watershed. Groundwater recharge in spring is predicted to decrease due to lack of snowmelt caused by temperature increases (because of less winter precipitation falling as snow) (Eckhardt and Ulbrich, 2003). Groundwater recharge and streamflow are reduced by more than 50% in the summer due to increased potential evapotranspiration and decreased precipitation (Eckhardt and Ulbrich).

Jha et al. (2006) used six GCM models under the A2 storyline for the Upper Mississippi River basin. Results predicted a wide range of change in annual average streamflows, from a 6% decrease to a 51% increase. The GCM scenarios also generally predicted increases in spring streamflows, likely due to increased precipitation and snowmelt (Jha et al., 2006). Each GCM used demonstrated different patterns for future

streamflow trends, resulting in a conflicting picture of how future climate change will impact the watershed (Jha et al., 2006).

Abbaspour et al. (2009) used GCM data to project the change in Iranian water resources for 2073-2099. Precipitation increases over most of the country in this scenario (many regions experience a 50-100% increase from the observed period of 1980-2002), which in turn results in increases in blue water. Regions of Iran that experienced significant precipitation increases will have increases in blue water by up to and greater than 300%. This demonstrates that precipitation is generally the most important driving factor in Iran for alteration of water resources due to climate change.

Githui et al. (2009) determined that surface runoff and baseflow in the A2 scenario is likely to increase in 2020 and 2050 for a Kenyan watershed. Between the five GCMs used for climate change scenarios, annual average surface runoff was projected to increase between 38% (HADCM3) and 56% (ECHAM4) by 2020 and between 65% (HADCM3) and 115% (ECHAM4) by 2050. Changes in annual average baseflow were of lesser magnitude than surface runoff: the maximum increase by 2020 was 28% using the ECHAM4 model, while the minimum was 8% using CCSR. In 2050, the CCSR model input projected a decrease by 8% in average annual baseflow, while ECHAM4 projected a 50% increase. Streamflow response to temperature changes was determined to be insignificant in the A2 storyline. Conversely, average annual streamflow was positively correlated with increases in temperature (Githui et al., 2009).

Marshall and Randhir (2008) predicted that annual surface runoff will decrease by 22% (high-warming GCM) and 12% (low-warming GCM) over the 40-year study period in the Connecticut River watershed. On a monthly basis, surface runoff was higher than

the baseline scenario in winter months, likely due to a lower proportion of precipitation falling as snow (Marshall and Randhir, 2008). Decreases in surface runoff were predicted in spring months for both GCMs because of less water held in storage as snow and ice (less snowmelt in spring) (Marshall and Randhir, 2008). Summer and fall also were predicted to have less runoff due to increased evapotranspiration: for example, July was predicted to have decreases of 71% and 67% for the high warming and low warming scenarios, respectively (Marshall and Randhir, 2008). As a result of changes in surface runoff, water yield at the watershed outlet increased in November through February and decreased in the rest of the year.

2.4.3 B1 Storyline Impacts

Eckhardt and Ulbrich (2003) observed conflicting effects of temperature and CO_2 on groundwater recharge and streamflow, resulting in minimal changes (3% and 4% decrease, respectively) for a mountainous German watershed. Temperature increases raised potential evapotranspiration, but increasing CO_2 reduces stomatal conductance of vegetation, which decreases evapotranspiration (Eckhardt and Ulbrich, 2003).

Abbaspour et al. (2009) used the B1 scenario for GCM simulations regarding the impact of climate change on blue water in Iran. Precipitation changes were generally similar to those found in the A1B scenario of this study for both time periods. In 2013-2039 and 2073-2099, the majority of the country observes increases in precipitation by up 40%, although most regions average less than 20% increases. Precipitation decreases in the southeast region were generally less than 10% for both time periods. In terms of change in blue water, the changes are less severe than in the A1B scenario. Both time

periods experience decreases in blue water of up to 90% for most of the southeast and east of the country, while the western part of Iran generally experiences increases in blue water by up to 50%, although some northern areas see increases of greater than 100%. Once again, this study demonstrates the importance of precipitation changes in dictating streamflow and deep aquifer recharge.

2.4.4 B2 Storyline Impacts

Githui et al. (2009) projected that changes in baseflow and surface runoff due to altered climates in Kenya may not be as significant for the B2 emissions scenario as they are projected to be for the A2 emissions scenario. Average annual surface runoff is projected to increase by 6% (CCSR) to 20% (ECHAM4) by 2020, while in 2050 it is projected to change by 11% (HADCM3), depending on the GCM used. Average annual baseflow changes are not as severe, although the CCSR model predicted a -15% change in 2020 and a -28% change in 2050, while maximum changes were projected using ECHAM4 (8% in 2020 and 15% in 2050).

2.4.5 Incremental Scenario Impacts

Liu et al. (2000) used wet and dry scenarios to determine climate change impacts on surface runoff of the Cincinnati and Columbus watersheds of Ohio. The wet-climate scenario increased surface runoff the most, primarily on high-density residential, commercial, and agricultural land use types for both watersheds.

Jha et al. (2006) determined that water yield increased by up to 50% in response to a doubling of atmospheric CO_2 concentration in the Upper Mississippi River basin,

with the period of July to November experiencing the greatest increases. The cause of increased water yield was determined to be decreased transpiration due to increased CO_2, which resulted in higher soil moisture content (Jha et al., 2006). In incrementally increased temperature scenarios, decreases in snowpack levels and increases in snowmelt increased winter streamflow, while decreases in streamflow were predicted otherwise (Jha et al., 2006).

Nurmohamed et al. (2007) used incremental scenarios to determine the sensitivity of the Suriname watershed to climate change. Temperature increases accompanying no precipitation change led to decrease in total annual river discharge, surface runoff, and baseflow. Increasing precipitation by 50% leads to an increase of mean annual river discharge by 75% when accompanied by a 2ºC temperature increase, and a mean annual river discharge of 57% when accompanied by a 4ºC temperature increase, which is likely due to the increase in evapotranspiration (Nurmohamed et al., 2007).

Chaplot (2007) projected that an increase in CO_2 concentration from 330 ppm to 970 ppm would increase streamflow in the Walnut Creek, Iowa watershed by 7%, while no significant streamflow changes are likely to occur in the Bosque River watershed of Texas. Higher CO_2 concentrations increasing streamflow may be explained by a decrease in stomatal conductance of vegetation, which decreases evapotranspiration (Chaplot, 2007). Conversely, lack of streamflow and runoff changes with increasing CO_2 in the Texas watershed may be due to increased plant productivity associated with CO_2 increases (greater water requirements) equalizing the decrease in evapotranspiration. Runoff was positively correlated to precipitation in both watersheds (increasing

precipitation leads to runoff increases and decreasing precipitation leads to runoff reduction), while the magnitude of precipitation increase was also important. In Iowa, a 20% precipitation increase leads to a 22% increase in runoff, while runoff increases by up to 164% in the 40% precipitation increase scenario (Chaplot, 2007). Overall, streamflow and surface runoff were more sensitive to precipitation changes than temperature or CO_2 changes (Chaplot, 2007).

In developed incremental precipitation and temperature increase scenarios, Franczyk and Chang (2009) projected variable increases and decreases in annual, seasonal, and monthly runoff for the Portland, OR metropolitan watershed. All incremental scenarios predicted a summer monthly decrease in runoff although precipitation was increased (Franczyk and Chang, 2009). Winter surface runoff generally increased for all incremental scenarios, likely due to decreased snowfall and increased precipitation falling as rain (Francyzk and Chang, 2009).

Ficklin et al. (2010) used incremental scenarios to determine the impacts of climate change on water yield in the highly agricultural San Joaquin watershed, California. Water yield increased with increasing precipitation, although increasing temperature affected the extent of water yield increase (Ficklin et al., 2010). For example, a 20% increase in precipitation coupled with a 1.1°C temperature increase led to a 20% water yield increase, while the same precipitation increase coupled with a 6.4°C temperature increase resulted in an 11.3% increase in water yield. Atmospheric CO_2 increases caused water yield to increase: in the 970 ppm CO_2 scenario water yield increased by 23.8% from the base scenario, CO_2 coupled with a 6.4°C temperature

increase resulted in a 24.4% water yield increase, and the coupled precipitation and CO_2 increase resulted in a 51.8% water yield increase.

2.4.6 Miscellaneous Scenario Impacts

Miscellaneous scenario impacts are generally studies that used GCM/RCM output to perform a climate impact assessment on water resources, but did not specify the emissions scenario or scenarios used.

Stone et al. (2003) projected increased spring and annual water yield in the Missouri River basin based on doubling atmospheric CO_2 GCM and RCM climate change scenarios. The higher resolution RCM data input into the hydrological model predicted more significant increases in water yield, likely due to the higher magnitude of precipitation increases projected by the RCM (Stone et al., 2003). Stone et al. (2003) concluded that using high-resolution climate change scenarios significantly affects estimations of water quantity compared to using GCM data.

Gosain et al. (2006) used RCM data to quantify the impact of climate change on the hydrological processes of major watersheds in India. Resulting changes in water quantity were variable depending on the geographic location of the watershed within the country. In some cases, precipitation increases resulted in slight decreases in surface runoff, likely due to significant increases in evapotranspiration. It was projected that severity and frequency of droughts and floods in India may increase due to increases in GHG concentrations (Gosain et al., 2006).

Nurmohamed et al. (2007) used the average of five GCMs to determine the effects of climate change on the hydrology of a Suriname watershed. Mean annual temperature

increases had a significant impact on river discharge (Nurmohamed et al., 2007). In 2050, mean annual precipitation and mean annual evapotranspiration increased by 12% and 8%, respectively, which led to a mean annual discharge reduction of 24%, surface runoff reduction of 15% and reduction of 40%. By 2080, a small decrease in precipitation (0.6%) and an increase in mean annual evapotranspiration of 17% translate to a mean annual river discharge reduction of 35%, while surface runoff and baseflow decrease by 19% and 56%, respectively.

Gul and Rosbjerg (2010) used GCM data to determine the impacts of climate change on a Danish watershed. It was concluded changes in temperature and precipitation in Denmark per degree of global warming would increase mean annual streamflow at two gauging stations (Gul and Rosbjerg, 2010). Although mean annual streamflow would increase, seasonal streamflow changes tell a different story: average winter streamflow increases by 8%, spring streamflow increases by 7-8%, summer streamflow decreases by 15-16%, and fall streamflow decreases by 3-5%.

2.5 IMPACTS OF CLIMATE CHANGE ON WATER QUALITY

The impacts of climate change on water quality may vary substantially based on the ways in which the hydrological cycle is altered. Examining watershed specific studies on the impacts of climate change on water quality allows for conclusions to be reached regarding the interaction of climate change and water quality indicators such as sediment, nitrogen, and phosphorus. Due to limited studies regarding the impacts of climate change on water quality, results are lumped together for all emissions scenarios and incremental scenarios.

Liu et al. (2000) developed wet and dry climate change scenarios to determine the impacts of climate change on total nitrogen concentrations in the Cincinnati and Columbus watersheds. Changes in total nitrogen concentration were highly dependent on land use: commercial land was projected to have the greatest changes, while forested land was projected to high insignificant changes. The wet scenarios increased total nitrogen concentration by a maximum 50 mg (on commercial land) in Columbus and 4 mg (on commercial land) in Cincinnati. Minimum total nitrogen increases on forested land were 0.08 mg in Cincinnati and 2 mg in Columbus. Conversely, the dry scenario decreased total nitrogen by 4 mg in Cincinnati and 50 mg in Columbus on commercial land; forested land was projected to have decreases in total nitrogen of 0.04 mg in Cincinnati and 1 mg in Columbus.

Chaplot (2007) concluded that precipitation changes significantly affected sediment loads, while CO_2 increases most significantly affected nitrate loadings for the Walnut Creek watershed in Iowa. The correlation between increased precipitation and

increased sedimentation is well understood: runoff and impact forces of water with the soil are driving forces for sedimentation (Chaplot, 2007). Nitrate loads were most sensitive to increases in CO_2 concentrations: elevated CO_2 resulted in increases in nitrate loadings. The relationship between CO_2 and nitrate loadings is hypothesized to be due to increased vegetation assimilation and soil fixation, resulting in more nitrogen in the system (Chaplot, 2007).

Marshall and Randhir (2008) determined that sediment and nutrient pollution would significantly change in the Connecticut River watershed using two GCMs for the A2 emissions scenario. Sediment runoff in spring decreased with decreasing surface runoff, while increases in sediment runoff were predicted for September and October (Marshall and Randhir, 2008). Average annual yields of organic phosphorus at the watershed outlet decreased by 19% for the low-warming GCM, while it decreased by 46% for the high-warming GCM). Average annual yield of organic nitrogen decreased by 7% and 19% for the low-warming GCM and the high-warming GCM, respectively at the watershed outlet. Nitrogen and phosphorus loads were generally correlated with surface runoff (Marshall and Randhir, 2008).

Ficklin et al. (2010) used incremental scenarios to determine the impacts of climate change on agricultural runoff yields including sediment, nitrate, total phosphorus, and pesticide (diazinon and chlorpyrifos) in the highly agricultural San Joaquin watershed, California. Increasing precipitation and holding temperature and CO_2 constant generally led to an increase in all agricultural runoff components, with nitrate yield increasing the most by 40.2%, and chlorpyrifos decreasing the most by 31.9%. Increasing

temperature decreased all agricultural runoff components, and the larger temperature increase led to a greater projected reduction. Nitrate and total phosphorus yield decreased the most in increased temperature scenarios, while the pesticides only had slight decreases. Pollutant yield was generally correlated to precipitation increase when both precipitation and temperature changes were simulated. Phosphorus yields were highly correlated to sediment yield, and therefore precipitation and surface runoff (Ficklin et al., 2010). Atmospheric CO_2 affected agricultural runoff yields in varying ways: increases to 970 ppm caused decreases in sediment and diazinon and increases in nitrate, total phosphorus, and chlorpyrifos. Increases in total phosphorus and nitrate are expected with increasing CO_2 because these nutrients inputs to the system are greater due to plant assimilation and soil fixation (Ficklin et al., 2010).

2.6 MITIGATING THE EFFECTS OF CLIMATE CHANGE ON WATER RESOURCES

There is a need to study the implications of various mitigation strategies to minimize the impacts of climate change on watershed processes (Marshall and Randhir, 2008).

2.6.1 Wastewater Treatment

Wastewater treatment technologies remove contaminants from industrial, commercial, and residential wastewater. Rather than water pollution prevention at the source, a wastewater treatment plant collects polluted water, reduces the pollution in the water, and then discharges to surface water bodies or is reused. Water conservation is promoted by prevented untreated discharges to surface water, groundwater, and soils, which reduces pollutants and requires a smaller volume of water to be treated (Bates et al., 2008). Reuse of treated wastewater is most desirable for agricultural irrigation, aquaculture, and industrial applications.

2.6.2 Afforestation or Reforestation

Afforestation is the process of planting trees on land that has not previously been forested; reforestation is the process of reversing deforestation by planting trees on land that once was forested. Forested lands are generally expected to use more water through transpiration, evaporation, and canopy interception than cropland, grassland, or urban lands (Bates et al., 2008). Beneficial hydrologic effects of afforestation or reforestation include reduction of surface runoff and increasing stream baseflow due to greater water infiltration (Bates et al., 2008). Decreasing surface runoff is expected to decrease erosion

and nutrient transport to streams, and nutrient input into the land will be considerably less than on agricultural land due to lack of nitrogen and phosphorus application. Conversely, afforestation on some lands may have adverse effects on water resources, especially when planting fast growing conifers. High water demand is a characteristic of most conifers, and streamflow can be expected to decrease with instillation of these tree species and can cause water shortage in drought periods (Bates et al., 2008).

2.6.3 Agricultural Conservation Practices

Agricultural conservation practices, also known as BMPs, are implemented in order to reduce surface runoff, erosion, and nutrient transport from agricultural fields. BMPs are either structural or non-structural in nature. Structural BMPs, such as porous gully plugs, terraces, filter strips, native grass, and streambank stabilization, involve instillation of a structure or vegetation on or near an agricultural field to combat runoff and erosion problems. Non-structural BMPs are focused on altering tilling strategies on agricultural land to reduce surface runoff and erosion. Some common non-structural BMPs are contour farming, reduced-tillage farming, no-tillage farming, and grazing management.

2.6.3.1 Contour Farming

Contour farming alters the direction of runoff from downslope to around the hill slope through the use of ridges formed by tillage, planting, and other farming operations (NRCS-NHCP, CODE 330, 2007). Installation of this conservation practice is meant to decrease erosion by reducing erosive power of surface runoff, and therefore diminish sediment and other attached contaminant transport (Arabi et al., 2007). Water infiltration

is also increased through installation of contour farming because surface runoff is impounded in small depressions.

2.6.3.2 Filter Strips

Filter strips are an area of herbaceous vegetation designed to remove contaminants from surface runoff (NRCS-NHCP, CODE 393, 2010). Establishment of filter strips generally lies between cropland, grazing land, or disturbed land and an environmentally sensitive area (such as a stream). The purpose of a filter strip is to reduce suspended solids (and other suspended contaminants) and dissolved contaminants in surface runoff.

2.6.3.3 Grazing Management

Grazing management is defined as managing the harvest of vegetation with grazing animals to maintain vegetative cover and minimize soil erosion (NRCS-NHCP, CODE 528, 2010). Overgrazing exposes bare soil, increases soil compaction, and infiltration, which increases surface runoff and sediment and nutrient transport to surface waters (Tuppad and Srinivisan 2008). The method to control grazing involves adjustment of the intensity, frequency, and duration of animal grazing on rangelands to maintain adequate vegetative cover. Benefits of grazing management to surface water quality include reduced surface runoff and reduced soil erosion due to increased vegetative cover.

2.6.3.4 Native Grass

Native grass replacement of agricultural row crops involves establishment and maintenance of permanent vegetative cover (NRCS-NHCP, CODE 327, 2010). Native tall grasses such as Indian switchgrass or big bluestem are generally used (Nejadhashemi, 2007). Surface runoff, sediment transport, and nutrient transport are expected to be reduced because vegetative soil cover is increased, water infiltration is increased, and tillage and fertilizer are not needed because the need for tillage and fertilizer are eliminated.

2.6.3.5 No-Tillage Farming

No-tillage farming limits the amount of soil disturbing farm activities to those necessary to plant crops and place nutrients (NRCS-NHCP, CODE 329, 2010). By limiting the amount of disturbed soil while increasing vegetative cover, less sediment will be picked up and transported to streams by surface runoff. Additional benefits of no-tillage farming include reduction of wind erosion, improved soil organic matter content, reduction of CO_2 soil emissions, and increased moisture available to crops (NRCS-NHCP, CODE 329, 2010).

2.6.3.6 Porous Gully Plugs

Porous gully plugs are designed to reduce the velocity of surface runoff in concentrated gullies using rocks or logs. These structures limit the erosive power of surface runoff to prevent further erosion and facilitate settling of sediment (Tuppad et al., 2010). Debano and Schmidt (1990) note that when sufficient sediment supply is

available, small structures such as porous gully plugs can retain only a small portion of sediment. This is acceptable because the reduction in surface runoff energy due to porous gully plug implementation prevents further resuspension of sediment.

2.6.3.7 Reduced-Tillage Farming

Reduced-tillage operations result in less soil disturbances than conventional tillage, although some soil disturbing activities do take place prior to planting (e.g. chiseling, disking, mulch tillage) (Tuppad and Srinivisan, 2008). Reduction of the number of tillage operations will limit soil disturbances and increase vegetative cover to reduce sheet (broad sheets of flowing water containing sediment) and rill (small concentrated flow paths of water containing sediment) erosion. Additional benefits include decreased wind erosion, improved soil condition, and increased plant available moisture.

2.6.3.8 Streambank Stabilization

Streambank stabilization utilizes vegetation or other structures such as rocks, to protect banks from erosion and scouring and further loss of land (NRCS-NHCP, CODE 580, 2010; Tuppad et al., 2010). The end result of a stabilized streambank will be decreased sediment deposition downstream due to prevention of bank erosion while maintaining the flow capacity of the stream.

2.6.3.9 Terraces

Terraces are an earth embankment, or combination ridge and channel, constructed across the field slope designed to reduce soil erosion from agricultural fields (NRCS-

NHCP, CODE 600, 2010). Sediment reduction in runoff is achieved through decreasing length of the hill slope to decrease peak runoff rate, increased settling of sediments in surface runoff, and interception and retention of water (Arabi et al., 2007; Tuppad et al., 2010).

3 INTRODUCTION TO METHODOLOGY AND RESULTS

This thesis is in the form of two research papers that have been submitted to scientific journals. The first paper, entitled "Assessing Best Management Practice Implementation Strategies under Climate Change Scenarios", aims to determine the impacts of climate change on water quantity and water quality in the Tuttle Creek Lake watershed. In addition, the effectiveness of BMPs in current and future climate scenarios are assessed. Climate model output from three SRES emissions scenarios (A1B, A2, and B1) were compared to historical model (20C3M) output from the NCAR CCSM-3 climate model and input into the SWAT watershed model. The SWAT model was calibrated and validated for daily streamflow, sediment load, total Kjeldahl nitrogen load, and total phosphorus load using observed water quality and climate data. Twenty years of daily temperature and precipitation data from the climate model output were prepared by using the delta change method of adjusting observed historical climate data. In addition, the CO_2 level was adjusted accordingly. Eight agricultural BMPs (conservation tillage, contour farming, filter strips, grazing management, native grass, no-tillage, porous gully plugs, and terraces) were physically represented within the SWAT model framework to quantify the effects of climate change on reduction efficiency for each climate scenario at the field and watershed scales.

The objective of the second paper, entitled "Best Management Practice Sensitivity Analysis under Climate Change Scenarios" is to quantify the sensitivity of BMP implementation in current and future climate scenarios. Model setup, calibration, climate change scenario input, and BMP representation are performed in the same manner as the first paper. The BMP sensitivity analysis for sediment, total nitrogen, and total

phosphorus under each climate scenario was performed by randomly altering the parameter defining BMP implementation within an acceptable parameter range determined from previously published studies. A relative sensitivity index was calculated to quantify the sensitivity of each BMP under each climate scenario on an annual and monthly basis.

4 ASSESSING BEST MANAGEMENT PRACTICE IMPLEMENTATION STRATEGIES UNDER CLIMATE CHANGE SCENARIOS

Sean A. Woznicki, A. Pouyan Nejadhashemi, Craig M. Smith

4.1 ABSTRACT

As climate changes, the uncertainty of water availability, changing magnitudes of nonpoint source pollution, and uncertainty of BMP effectiveness are issues that watershed managers and stakeholders must consider and plan for. The objective of this study was to determine how best management effectiveness will be affected by climate change using the Soil and Water Assessment Tool. Using downscaled monthly precipitation and temperature data output from the Community Climate System Model (CCSM-3) provided by the NCAR GIS Initiative Climate Change Scenarios, daily precipitation and temperature data was produced based on observed weather station data for the Tuttle Creek Lake watershed in Kansas and Nebraska. The A1B, A2, and B1 SRES emissions scenarios were compared to historical CCSM-3 model output. Eight agricultural BMPs were physically represented within SWAT and compared across climate scenarios: contour farming, filter strips, grazing management, native grass, porous gully plugs, conservation tillage, no-tillage, and terraces. Water yield (up to 44%), surface runoff (up to 43%), baseflow (up to 58%) sediment load (up to 54%), nitrogen load (up to 37%), and phosphorus load (up to 30%) increased in all three future climate scenarios. Terraces, contour farming, and native grass were determined to be the most effective in pollution load reduction and percent efficiency at the field and watershed scale in future scenarios, but also observed increases in variability of pollution reduction.

Porous gully plugs and filter strips showed no significant changes in pollution load or percent reduction and had reduction efficiencies close to 0%. Grazing management, no-tillage, and conservation tillage percent and load reduction in future scenarios varied at the field and watershed scale. This study demonstrates that BMP performance in terms of sediment, nitrogen, and phosphorus reduction significantly changes in future climate scenarios at the field scale, while performance generally does not change significantly at the watershed scale.

4.2 INTRODUCTION

The potential effects of climate change on the well-being of society are far-reaching. Although the extent of the impact of climate change on humanity and the environment are not completely known, many predictions have been made regarding its effects. Water resources, human health, biodiversity, food production, and economic growth are among the potential areas impacted by climate change in the United States and worldwide (Arnell, 2004; Ebi et al., 2006; Kovats et al., 2005). For example, the western Great Plains of the United States are expected to experience decreased stream flows in the future; this area is heavily dependent on regional water supplies for sustaining agriculture (Rosenberg et al., 2003). Biodiversity is expected to be negatively impacted through reduced habitat suitability and reproduction performance (Hulme, 2005). Food production is expected to be greatly affected by climate change and variability due to direct effects on crop production. Precipitation changes may lead to drought or flooding, while temperature changes alter the growing season; these possibilities may lead to decreased crop yields, affecting global food security (Easterling and Apps, 2005; Gregory et al., 2005; Slingo et al., 2005). Economic growth and tourism

are also affected by climate change. Fankhauser and Tol (2005) predicted that for most climate change scenarios and the majority of countries, negative climate change impacts are likely to reduce the rate of economic growth.

Fresh water is an essential resource to humans, flora, and fauna. Human life depends on clean water for drinking, growing crops, and recreation; ecosystems rely on clean water to provide life and habitat. In today's world more and more people believe that global climate change and its effects are becoming a reality. The Intergovernmental Panel on Climate Change (IPCC) has predicted that higher water temperatures and changes in extremes, such as flood and droughts, are projected to affect water quality and to intensify nonpoint source (NPS) pollution (Bates et al., 2008). Therefore, it is important to understand the consequences of global climate change on water quality and quantity.

In planning for future climate scenarios and their impact on water resources, the following problems must be addressed:

- *Uncertainty of water quantity and availability*. Climate change will affect water quantity and availability on the watershed scale in varying ways for different basins. Water availability is variable and not well understood in detail on a case-by-case basis for individual watersheds under future climate scenarios (Hurd et al., 2004; Jackson et al., 2001; Marshall and Randhir, 2008).
- *Changing magnitudes of nonpoint source (NPS) pollution*. Degradation of water quality is an important issue because of predicted changes in hydrologic regimes. Storm events are the driving force of NPS pollution, and increases or decreases in precipitation (annual average and variability) will affect the quantity of pollutants

entering lakes and rivers, as well as how the pollution is transported. Some studies have suggested that surface water and groundwater quality will be affected by a changing climate (Karl et al., 2009). However, the type and magnitude of NPS pollution that is affected by climate change will vary by watershed (Ficklin et al., 2009; Meyer et al., 1999; Murdoch et al., 2000; Senhorst and Zwolsman, 2005).

- *Uncertainty of BMP Effectiveness*. Current best management practices (BMPs) may not be applicable for future climate scenarios. As climate changes, the magnitude of NPS pollutants may be more extreme within a watershed and current BMPs may not be appropriate to treat these conditions (Wilby et al., 2006). The IPCC has concluded with very high confidence that current water management practices may not be able to cope with the impacts of climate change on water supply and water quality (Bates et al., 2008).

The objective of this study is to examine how best management practice efficiency will be affected by climate change in the Tuttle Creek Lake watershed of Kansas and Nebraska at field and watershed scales. The Soil and Water Assessment Tool (SWAT) was used to determine the effects of three IPCC Special Report on Emissions Scenarios (SRES) outputs (A2, B1, and A1B) from the CCSM-3 model on eight agricultural BMPs (no-tillage farming, conservation tillage farming, native grass, filter strips, contour farming, terraces, porous gully plugs, and grazing management).

4.3 MATERIALS AND METHODS

4.3.1 Study Area

The Tuttle Creek Lake watershed (TCLW), part of the HUC-6 Big Blue watershed (Figure 4-1) was selected for this study. Two major rivers (the Little Blue River and Big Blue River) enter the TCLW from the north. In order to incorporate these inputs into the model, the entire Big Blue watershed (HUC 102702) was also modeled (Figure 4-1). The Big Blue watershed consists of seven subwatersheds: the Upper Big Blue (HUC 10270201), Middle Big Blue (HUC 10270202), West Fork Big Blue (HUC 10270203), Turkey (HUC 10270204), the Lower Big Blue (HUC 10270205), Upper Little Blue (HUC 10270206), and the Lower Little Blue (HUC 10270207) watersheds. For this project, the Big Blue was split into three sections: the upper left, upper right, and the TCLW.

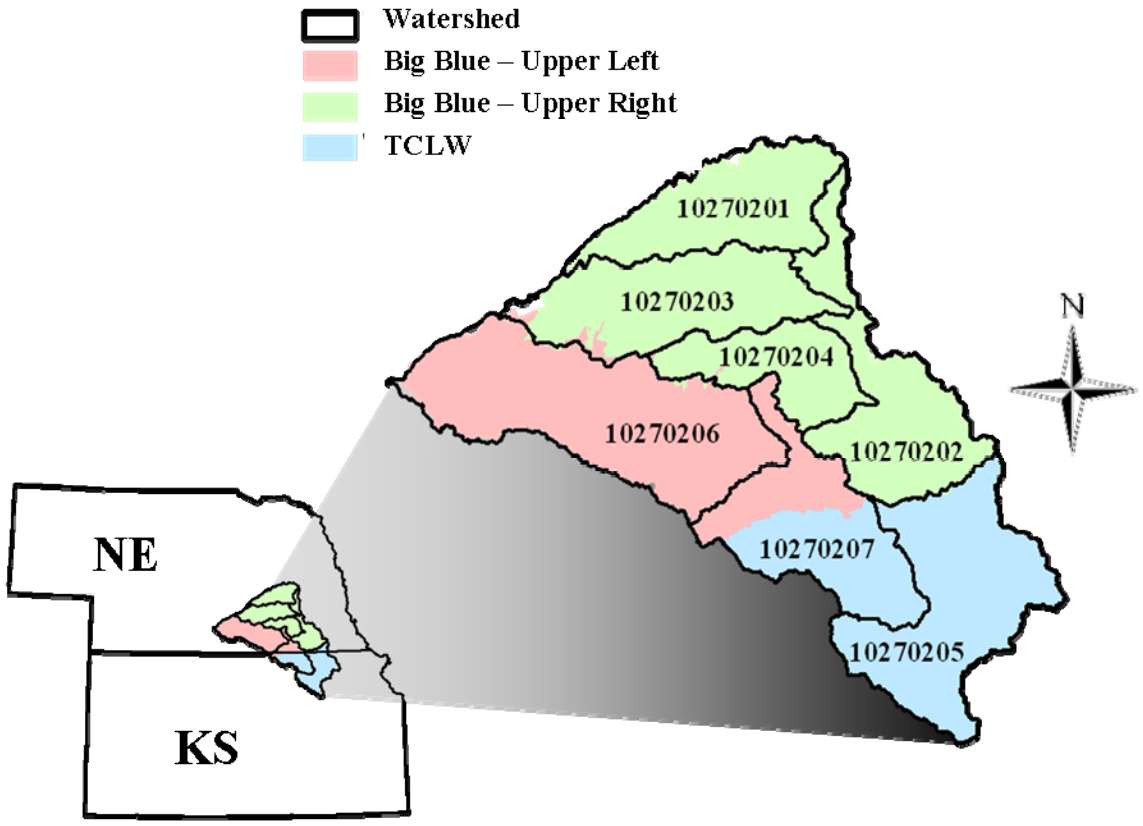

Figure 4-1. Study Area. For interpretation of the references to color in this and all other figures, the reader is referenced to the electronic version of this thesis.

The upper left watershed land use is predominantly agriculture: 66% agricultural row crops and 25% range land, while only 5% of land is urban. Minimum elevation is 381 m and maximum elevation is 668 m above mean sea level (average watershed elevation is 530 m).

The upper right watershed land use is also mostly agricultural. Agricultural row crops make up 79% of the land area, while range grasses are 12% of total land area. Urban land makes up 5% of the watershed. Minimum elevation is 363 m and maximum elevation is 601 m above mean sea level (average watershed elevation is 480 m).

Located in northeastern Kansas and southeastern Nebraska, TCLW contains the Lower Little Blue watershed and the Lower Big Blue watershed. Total watershed area is 6,158 km^2 with an elevation range from 305 m to 513 m. The watershed is highly agricultural with 40% of total area comprised of row crops and 42% consisting of range land. Climate data was obtained from National Climatic Data Center (NCDC) weather stations (Figure 4-2). Average annual precipitation from 1978-2008 in the watershed was 839 mm.

4.3.2 Swat Model

SWAT is a watershed hydrology and water quality model developed by the United States Department of Agricultural Research – Agricultural Research Service (USDA-ARS) (Arnold et al., 1998). SWAT is designed to predict the impact of management practices on water, sediment, and agricultural chemical yields in complex watersheds with varying soils, land use, and land management practices over long time periods (Gassman et al., 2007) The model is physically based, spatially distributed, and operates on a daily time step. In SWAT, a watershed is divided into subwatersheds, which are further divided into hydrologic response units (HRUs). An HRU is an area consisting of homogeneous land use, soil, slope, and management practices. Overland flow, sediment, and NPS pollution are generated at the HRU level, aggregated at subbasin level, and routed through channels to the watershed outlet.

There are two options for calculating runoff volume in SWAT: the SCS curve number procedure or the Green and Ampt infiltration method (Neitsch et al. 2005). The SCS curve number procedure is an empirical equation that calculates accumulated runoff with rainfall depth, initial abstraction (surface storage, infiltration, interception), and

retention (spatial parameter based on soil, land use, management, and slope). The Green and Ampt infiltration predicts infiltration assuming excess water at the surface at all time. This method requires sub-daily precipitation data; therefore the SCS curve number procedure was used in this study.

In SWAT, soil erosion caused by rainfall and surface runoff is computed using the Modified Universal Soil Loss Equation (MUSLE) (Neitsch et al. 2005). MUSLE predicts sediment yield as a function of surface runoff volume, peak runoff rate, area, soil erodibility, land cover, land support practices, topography, and percent coarse fragments in top soil layer.

Transport of nutrients from land areas into the stream network is modeled in various ways depending on the form of the nutrient (Neitsch et al. 2005). Nitrate may be transported with surface runoff, lateral flow, or percolation, and is a function of the nitrate concentration in mobile water. Organic nitrogen attached to soil particles is associated with sediment loading from the HRU. Diffusion is the primary mechanism of phosphorus movement in the soil, which is in response to a concentration gradient. Organic and mineral phosphorus attached to soil particles is a function of sediment loading from the HRU.

Channel sediment routing in SWAT is based on the maximum amount of sediment that can be transported from a reach segment, which is a function of peak channel velocity (Neitsch et al. 2005). Sediment deposition and degradation are the dominant processes in sediment routing, depending on whether sediment concentration is less than (degradation) or greater than (deposition) the maximum amount of sediment that can be transported from a reach segment. Nutrient routing in SWAT is modeled using the

nitrogen cycle and the phosphorus cycle (Neitsch et al. 2005). Organic nitrogen and organic phosphorus may be removed from the stream by settling.

4.3.3 Physiographic Characteristics

The SWAT model requires various datasets for model setup, including topography, land use, and soils data. Topography was obtained from the Better Assessment Science Integrating point and Nonpoint Sources (BASINS) software version 4.0 in the form of a digital elevation model (DEM) with a 90 m resolution (BASINS, 2007).

The National Land Cover Database 2001 (NLCD 2001) map was downloaded from the Multi-Resolution Land Characteristics Consortium (MRLC). NLCD 2001 has a resolution of 30 m and contains 21 different land use classes (Homer et al., 2007). Generic agricultural row crop land within the Tuttle Creek Lake watershed was split into six different land uses based on agricultural statistics (USDA-NASS, 2007) and common crop rotations in the watershed. Agricultural land use allocation was as follows: corn-soybean (25%), continuous soybean (5%), continuous corn (15%), soybean-wheat (25%), continuous soybean (10%), and grain sorghum-soybean-wheat (20%).

Soil data was obtained from the U.S. Department of Agriculture (USDA) State Soil Geographic (STATSGO) dataset. STATSGO data is a 1:250,000 scale map that is linked to tabular data containing estimated physical and chemical soil properties (Muttiah and Wurbs, 2002).

4.3.4 Observed Climate Data

Twenty years of observed daily climate data was attained from the National Climatic Data Center (NCDC) cooperative weather network. Data from eight precipitation stations and six temperature stations were obtained within and around the TCLW. For upper left input watershed, 11 precipitation stations and seven temperature stations were used, while the upper right input watershed used 14 precipitation and 11 temperature stations. Precipitation and temperature stations are presented in Figure 4-2.

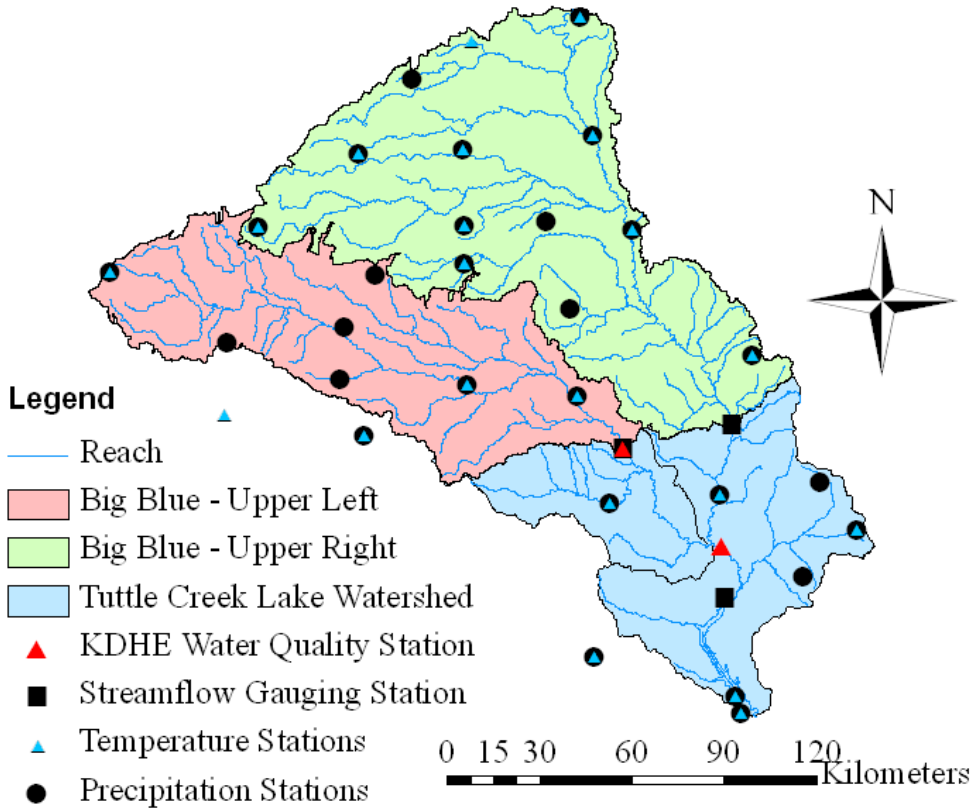

Figure 4-2. Precipitation stations, temperature stations, and model calibration locations

4.3.5 Climate Change Data

Data for the climate change scenarios was provided by the Community Climate System Model (CCSM-3) project (http://www.ccsm.ucar.edu), supported by the Directorate for Geosciences of the National Science Foundation and the Office of Biological and Environmental Research of the U.S. Department of Energy. The National Center for Atmospheric Research (NCAR) GIS Initiative provided CCSM-3 data in a GIS format through GIS Climate Change Scenarios portal (http://www.gisclimatechange.org). Downscaled projections of monthly mean temperature and total precipitation were also provided through this initiative at a spatial resolution of approximately 4.5 km for the contiguous United States (Hoar and Nychka, 2008). Monthly temperature and precipitation projection outputs from the National Center for Atmospheric Research GIS Initiative CCSM-3 are too coarse for use on the watershed scale. Due to the scale of the project, the statistical downscaled monthly temperature and precipitation were used. The statistical downscaling method was developed and performed by Hoar and Nychka (2008). First, a linear model was developed for every location in the domain. The Parameter-elevation Regressions on Independent Slopes Model (PRISM) climate mapping system was used to get a prediction at every CCSM data location. The initially developed linear models for each location were applied to the initial model estimates to obtain the final downscaled estimate.

Three SRES emissions scenarios were used in this study as defined by Nakicenovic et al. (2000): A2, A1B, and B1. Scenarios are not specific predictions or forecasts of future climate, but are plausible alternative futures. The A2 scenario is described by slow development of alternative fuel technologies and prominent fossil fuel

usage. A2 has the highest atmospheric CO_2 concentration (by 2100) of the three scenarios used in this study. The A1B scenario is characterized by rapid economic growth leading to high energy demand. This scenario is "balanced", which means that alternative energy is prominent and no energy technology, fossil fuel or otherwise, controls the market. The B1 scenario illustrates a world relying on resource conservation and ecologically sound solutions. Fossil fuel use decreases to slow the increase of CO_2 emissions. A fourth non-SRES scenario was also used, entitled 20C3M which is a historical experiment characterized by greenhouse gases increasing as observed through the 20^{th} century.

4.3.6 Sensitivity Analysis

Sensitivity analysis is a process that determines the rate of change in model output with respect to changes in model input parameters (Moriasi et al., 2007). A sensitivity analysis was performed to determine which SWAT model parameters impact output variability of streamflow, sediment, nitrogen, and phosphorus the most. The results of the sensitivity analysis conclude which model parameters should be used in calibration. SWAT uses the Latin Hypercube One-factor-At-a Time (LH-OAT) method of sensitivity analysis (van Griensven et al., 2006). In this study, a sensitivity analysis was performed at three separate locations: USGS gauging station #06884025, USGS gauging station #06882000, and the Tuttle Creek Lake US Army Corps of Engineers gauging station at the inlet of Tuttle Creek Lake (Figure 4-2).

4.3.7 Model Calibration and Validation

Calibration is the procedure of adjusting model input parameters to allow model simulation output to emulate observed watershed behavior. The parameters used in calibration were based on the results of the sensitivity analysis. The most sensitive parameters were deemed acceptable for use in calibration. In the auto-calibration procedure, SWAT uses a Shuffled Complex Evolution search algorithm to determine best-fit parameters for the model compared to observed samples (Muleta and Nicklow, 2005). Validation is performed after the calibration time step to ensure model accuracy.

Auto-calibration was used to calibrate the two upstream watersheds and the TCLW using observed data from NCDC weather stations. The same locations that were used for the sensitivity analysis were used in manual and later for the auto-calibration. Calibration was performed on a daily basis for streamflow, sediment, total Kjeldahl nitrogen (TKN) although SWAT does not calculate the ammonia (NH_3) component, and total phosphorus (TP).Time steps for the upper left (USGS #06884025) and Tuttle Creek Lake watershed (US Army Corps Gauging Station) were both from 1998-2000 for calibration and 2001-2000 for validation. The time step for the upper right (USGS #06882000) was 1986-1989 for calibration and 1990-1993. All calibrations used a one year model warm-up. Calibration locations are shown in Figure 4-2. Different time steps were used for different constituents due to data availability, especially concerning sediment and nutrient observations.

Model evaluation is required to determine how well the calibrated model predicts observed watershed behavior. Three statistical methods were used to evaluate model prediction: the Nash-Sutcliffe Efficiency (NSE), coefficient of determination (R^2), and

the root mean square error (RMSE). NSE indicates how well a plot of observed versus simulated data fits a 1:1 line (Moriasi et al., 2007) and is calculated as shown in Equation 1.

$$NSE = 1 - \left[\frac{\sum_{i=1}^{n} \left(Y_i^{obs} - Y_i^{pred} \right)^2}{\sum_{i=1}^{n} \left(Y_i^{obs} - Y^{obs,mean} \right)^2} \right] \quad (1)$$

Where Y_i^{obs} is the observed value for the constituent, Y_i^{pred} is the predicted value of the constituent, and $Y^{obs,\ mean}$ is the mean of the observed data for the constituent. NSE can range from negative infinity to 1, where 1 is the optimal value (perfect fit).

The coefficient of determination describes the proportion of variance in measured data explained by the model (Moriasi et al., 2007). R^2 is calculated as shown in Equation 2.

$$R^2 = \left[\frac{\sum_{i=1}^{n} \left(Y_i^{obs} - Y^{obs,mean} \right) \left(Y_i^{pred} - Y^{pred,mean} \right)}{\sqrt{\sum_{i=1}^{n} \left(Y_i^{obs} - Y^{obs,mean} \right)^2} \sqrt{\sum_{i=1}^{n} \left(Y_i^{pred} - Y^{pred,mean} \right)^2}} \right]^2 \quad (2)$$

Where $Y^{pred,\ mean}$ is the mean of the predicted values for the constituent. R^2 ranges from 0 to 1, where higher values indicate that the model is predicting the y variable with significant confidence.

RMSE indicates the error of a prediction in the squared units of the constituent of interest (Moriasi et al., 2007). The method for calculating RMSE is show in Equation 3.

$$RMSE = \sqrt{\frac{\sum_{i=1}^{n}\left(Y_i^{obs} - Y_i^{pred}\right)^2}{n}} \quad (3)$$

Where *n* is the total sample size. An RMSE equal to zero indicates a perfect fit of predicted data with observed data.

4.3.8 Climate Change Scenarios

Climate change scenarios were developed through the use of downscaled monthly average total precipitation and monthly mean temperature data. The future time period selected was 2041-2060 for each of the SRES emissions scenario model runs to gain an understanding of mid-century climate change. The historical model (20C3M) baseline time period selected was 1980-1999 for comparison with observed data from precipitation and temperature stations during the same time period.

For each precipitation and temperature station, the data for the corresponding 4.5 km by 4.5 km cell was extracted for every month of each year within the period of interest. Unique average values for each station in the future time period and the historical time period were calculated for each month using the delta change method for precipitation and temperature. The delta change method adjusts historical observed daily temperature and precipitation data on a monthly basis (Snover et al., 2003). Assumptions regarding the delta change method are as follows: GCMs are more accurate in simulating relative changes between climate scenarios than the absolute values of a future scenario, there are no changes in climate variability, constant spatial patterns of climate, the number of wet days will remain constant, and minimum and maximum values of climate variables are scaled (Fowler et al., 2007). The daily observed dataset was adjusted using

the 20C3M scenario means for each weather station. Then, the change between the 20C3M scenario and each future scenario were determined for monthly temperature and precipitation. These differences were applied to the adjusted daily dataset for input into SWAT. Assumptions of the delta change method include

Precipitation deltas are based on a percentage change between future time period monthly average and the historical model average (increase or decrease in average monthly precipitation) because precipitation is zero bounded (negative precipitation is not possible). The precipitation delta change method is shown in equation 4.

$$P_{daily,20C3M} = P_{daily,obs}\left(\frac{P_{monthly,20C3M}}{P_{monthly,obs}}\right) \quad (4)$$

Where $P_{daily,\ 20C3M}$ is adjusted daily precipitation, $P_{daily,\ obs}$ is observed daily precipitation, $P_{monthly,\ 20C3M}$ is monthly average for 20C3M (1980-1999) precipitation, and $P_{monthly,\ obs}$ is monthly average (1980-1999) precipitation for the observed data from 1980-1999.

Temperature deltas (additive) are calculated based on the difference between the future time period monthly average and the historical model average. The temperature delta change method is presented in equation 5.

$$T_{daily,20C3M} = T_{daily,obs} + \left(T_{monthly,20C3M} - T_{monthly,obs}\right) \quad (5)$$

Where $T_{daily,\ 20C3M}$ is adjusted mean daily temperature, $T_{daily,\ obs}$ is observed mean daily temperature, $T_{monthly,\ 20C3M}$ is monthly average temperature for 20C3M (1980-1999), and $T_{monthly,\ obs}$ is monthly average temperature for observed data (1980-

1999). Monthly mean temperature deltas were applied to both minimum and maximum observed daily temperature.

To develop daily precipitation and temperature data, observed weather station data was used from 1980-1999. Deltas were calculated between the observed weather data and the 20C3M scenario to obtain daily data statistically similar to the 20C3M monthly averages. The delta ranges between observed data and 20C3M for each weather station are listed in Table 4-1. The 20C3M model over predicts precipitation by up to 116% (January) for one weather station, while under predicts precipitation by up to -72.4% (August) for a weather station. For mean monthly change in temperature, 20C3M under predicts temperature by up to -0.6 °C (November) and over predicts temperature by up to 6.2 °C (August).

Table 4-1. Temperature and precipitation delta ranges and CO_2 concentrations from 20C3M to observed

Month	ΔP (%)	ΔT_{mean} (°C)	CO_2 (ppm)
January	37.2 to 116.0	0.2 to 1.7	330
February	24.4 to 52.1	0.1 to 1.8	330
March	-30.1 to -17.1	0.2 to 1.5	330
April	-27.4 to -12.9	1.2 to 2.6	330
May	-32.0 to -17.0	1.1 to 2.2	330
June	-13.5 to 26.7	-0.1 to 1.1	330
July	-32.2 to 6.1	2.0 to 3.3	330
August	-72.4 to -65.9	4.8 to 6.2	330
September	-66.9 to -56.3	2.9 to 4.1	330
October	-39.8 to -25.1	0.6 to 1.8	330
November	-17.4 to 3.4	-0.6 to 0.3	330
December	-1.0 to 13.5	0.3 to 1.4	330

Using the deltas calculated between 20C3M and each emissions scenario model output, daily precipitation and temperature data were calculated for each model scenario (A1B, A2, B1). Monthly mean temperature deltas were applied to both minimum and

maximum daily observed temperature. Delta ranges for each precipitation station between 20C3M and A2, A1B, and B1 are listed in Tables 4-2, 4-3, and 4-4, respectively. The A2 scenario had the greatest increase in precipitation (66.2% in August), while the A1 and A2 scenarios had temperature increases of up to 3.6 °C (September).

Table 4-2. Temperature and precipitation delta ranges and CO_2 concentrations from 20C3M to A2 for weather stations

Month	ΔP (%)	ΔT_{mean} (°C)	CO_2 (ppm)
January	-7.3 to -2.5	2.3 to 2.4	525
February	4.7 to 6.3	1.8 to 1.9	525
March	4.0 to 8.3	2.1	525
April	20.6 to 24.2	1.9 to 2.0	525
May	16.5 to 19.8	2.1 to 2.3	525
June	9.0 to 12.3	2.5 to 2.7	525
July	12.1 to 16.2	2.3 to 2.4	525
August	43.8 to 66.2	2.6 to 2.8	525
September	7.5 to 10.3	3.4 to 3.6	525
October	-18.8 to -8.8	3.1	525
November	-9.1 to -8.4	3.1 to 3.2	525
December	6.2 to 11.0	2.1 to 2.2	525

Table 4-3. Temperature and precipitation delta ranges and CO_2 concentrations from 20C3M to A1B for weather stations

Month	ΔP (%)	ΔT_{mean} (°C)	CO_2 (ppm)
January	1.2 to 4.2	2.0 to 2.2	525
February	14.9 to 17.7	2.2	525
March	4.1 to 7.1	2.1	525
April	15.7 to 17.8	2.1 to 2.2	525
May	14.0 to 17.3	2.4 to 2.6	525
June	15.4 to 19.0	2.5 to 2.8	525
July	16.3 to 19.2	2.3 to 2.4	525
August	23.8 to 43.1	2.8 to 3.1	525
September	19.5 to 20.4	3.4 to 3.6	525
October	-1.3 to 0.6	3.2 to 3.3	525
November	7.5 to 8.8	2.6 to 2.7	525
December	10.4 to 15.6	2.2 to 2.4	525

Table 4-4. Temperature and precipitation delta ranges and CO_2 concentrations from 20C3M to B1 for weather stations

Month	ΔP (%)	ΔT_{mean} (°C)	CO_2 (ppm)
January	-3.2 to -0.3	1.4	475
February	3.1 to 6.0	1.8	475
March	1.3 to 2.5	1.8 to 1.9	475
April	3.6 to 6.9	1.8 to 1.9	475
May	16.5 to 19.2	1.5 to 1.6	475
June	8.1 to 10.1	1.9 to 2.0	475
July	2.0 to 4.3	1.9 to 2.0	475
August	30.0 to 41.9	1.9 to 2.1	475
September	4.3 to 5.4	2.3 to 2.5	475
October	6.0 to 9.1	2.1	475
November	-2.2 to -1.3	2.0	475
December	15.4 to 17.4	1.3 to 1.4	475

Atmospheric carbon dioxide (CO_2) concentration was considered to be constant for each climate change scenario, based on IPCC predictions for each emissions scenario. The default SWAT value of 330 parts per million (ppm) CO_2 was used for the historical model and the 20C3M scenario. Under the A2 and A1B scenario, 525 ppm CO_2 was used. For the B1 scenario 475 ppm CO_2 was used. SWAT cannot simulate increasing or decreasing atmospheric CO_2 concentrations. Therefore, these baseline values were considered acceptable for each scenario run.

4.3.9 Representation of Best Management Practices in SWAT

Eight agricultural BMPs and a baseline scenario were implemented within SWAT for each climate scenario, for a total of 32 unique scenarios. The BMPs selected for representation were: no-tillage farming, conservation tillage farming, contour farming,

terraces, filter strips, porous gully plugs, grazing management, and replacement of row crops with native grass. The base scenario used applied conventional tillage to all agricultural land, depending on the crop type.

4.3.9.1 Base Scenario (Conventional Tillage)

The base scenario consists of conventional tillage operations throughout the agricultural land of the watershed, with no BMPs applied. Six conventional tillage operations were developed for the six designated agricultural land uses. Within SWAT, one operations schedule was applied to a land use type based on the crops included in the schedule. An example of one of six conventional tillage operations schedules (based on land use) is presented in Table 4-5. In scenarios with BMPs that aren't operations based, the conventional tillage was applied in addition to the BMP. For example, the grazing management, porous gully plug, terrace, and contour farming scenarios also use conventional tillage on agricultural land.

Table 4-5. Example of a corn-soybean conventional tillage operations schedule

Year	Crop	Operation	Application Rate	Date
1	CORN	Tillage		March 27
1	CORN	Knife anhydrous ammonia	96 kg/ha	April 5
1	CORN	Tillage		April 15
1	CORN	Pesticide application	1.7 kg/ha	April 15
1	CORN	Planting		April 16
1	CORN	Nitrogen fertilizer application	16 kg/ha	April 16
1	CORN	Phosphorus fertilizer application	53 kg/ha	April 16
1	CORN	Herbicide application	0.3 kg/ha	May 20
1	CORN	Harvest and kill		October 1
1	CORN	Tillage		November 5
2	SOYB	Tillage		March 27
2	SOYB	Tillage		April 15
2	SOYB	Tillage		May 14
2	SOYB	Planting		May 16
2	SOYB	Phosphorus fertilizer application	33 kg/ha	May 16
2	SOYB	Pesticide application	0.9 kg/ha	June 14
2	SOYB	Harvest and kill		October 1
2	SOYB	Tillage		November 5

4.3.9.2 No-Tillage Farming

No-tillage farming consists of implementing field operations that limit soil-disturbing activities to only those necessary to place nutrients, condition residue, and plant crops. The goal of no-tillage farming is to reduce erosion caused by disturbing the soil.

No-tillage operations were developed for the six crop rotations designated to the agricultural land. One operations schedule was applied to a land use type based on the crops included in the schedule. An example of one of six no-tillage operations schedules (based on land use) is presented in Table 4-6.

Table 4-6. Example of a corn-soybean no-tillage operations schedule

Year	Crop	Operation	Application Rate	Date
1	CORN	Knife anhydrous ammonia	96 kg/ha	April 5
1	CORN	Pesticide application	1.7 kg/ha	April 15
1	CORN	Planting		April 16
1	CORN	Nitrogen fertilizer application	16 kg/ha	April 16
1	CORN	Phosphorus fertilizer application	53 kg/ha	April 16
1	CORN	Pesticide application	0.3 kg/ha	May 20
1	CORN	Harvest and kill		October 1
2	SOYB	Pesticide application	0.9 kg/ha	April 30
2	SOYB	Planting		May 5
2	SOYB	Phosphorus fertilizer application	33 kg/ha	May 5
2	SOYB	Pesticide application	0.9 kg/ha	June 1
2	SOYB	Harvest and kill		October 1
2	SOYB	Herbicide application	0.9 kg/ha	October 10

4.3.9.3 Conservation Tillage Farming

Conservation tillage operations result in less soil disturbance than conventional tillage, although they usually include some tillage practices (Tuppad and Srinivasan, 2008). Implementing conservation tillage will reduce sheet and rill erosion while increasing soil moisture. An example of one of six conservation tillage operations schedules (based on land use) is presented in Table 4-7.

Table 4-7. Example of a corn-soybean conservation tillage operations schedule

Year	Crop	Operation	Application Rate	Date
1	CORN	Knife anhydrous ammonia	96 kg/ha	April 5
1	CORN	Tillage		April 15
1	CORN	Pesticide application	1.7 kg/ha	April 15
1	CORN	Planting		April 16
1	CORN	Nitrogen fertilizer application	16 kg/ha	April 16
1	CORN	Phosphorus fertilizer application	53 kg/ha	April 16
1	CORN	Pesticide application	0.3 kg/ha	May 20
1	CORN	Harvest and kill		October 1
2	SOYB	Tillage		April 15
2	SOYB	Tillage		May 14
2	SOYB	Planting		May 16
2	SOYB	Phosphorus fertilizer application	33 kg/ha	May 16
2	SOYB	Pesticide application	0.9 kg/ha	June 14
2	SOYB	Harvest and kill		October 1
2	SOYB	Tillage		November 5

4.3.9.4 Contour Farming

Contour farming makes use of ridges formed by tillage, planting, and other farming operations to change the direction of runoff from directly downslope to around the hill slope (USDA-NRCS, 2005). This practice is applied to reduce erosion and transport of sediment and contaminants attached to sediment by decreasing energy of surface runoff. Infiltration is also increased through impoundment of water in small depressions and retaining more water on the field (Arabi et al., 2008).

To implement this practice in SWAT, the curve number (CN2) for agricultural land and the USLE practice factor (USLE_P) were adjusted using the technique developed by Arabi et al. (2008) and Tuppad and Srinivasan (2008). USLE_P was reduced from its initial value of 1.0 to 0.5 or 0.6 depending on the land slope. Curve number was reduced by 3 for all agricultural row crops.

4.3.9.5 Terraces

A terrace is an earth embankment, or a combination ridge and channel, constructed across a field slope (USDA-NRCS, 2005). Terraces decrease hill-slope length and prevent gully formation to reduce erosion (Tuppad and Srinivasan, 2008). Surface runoff volume is also decreased by impoundment of water in small depressions, while settling of sediments is increased by reducing flow energy (Arabi et al., 2008).

Terraces are incorporated in SWAT through adjustment of CN2 and USLE_P on agricultural row crop land. Curve number was reduced by 5 for agricultural land, while USLE_P was set to 0.12 or 0.10 based on the land slope (Arabi et al., 2008).

4.3.9.6 Filter Strips

Filter strips are areas of herbaceous vegetation placed between cropland, grazing land, or disturbed land and environmentally sensitive areas (USDA-NRCS, 2005). The purpose of filter strips is to reduce sediment, particulate organics, sediment absorbed contaminants, and dissolved contaminant loadings in runoff (Nejadhashemi and Mankin, 2007). Filter strips may also serve as a riparian buffer along streams.

In SWAT, filter strips were physically represented through alteration of the land use map. A 10 m buffer was created around all streams (identified using the National Hydrography Dataset) bordering agricultural row crop land. The agricultural land was converted to native grass to represent a filter strip between agricultural land and the stream. Maintenance was simulated by harvesting biomass from the filter strip once per year.

SWAT has a filter strip component to add an edge-of-field filter strip of desired width to an HRU (FILTERW). This was not used because the equation used is empirical and not physically based. The method developed here is physically based and the filter strips are placed on an actual location in proximity to the stream.

4.3.9.7 Porous Gully Plugs

Porous gully plugs are rocks or logs used to reduce overland flow velocity in ephemeral gullies (Tuppad and Srinivasan, 2008). The goal is to decrease surface runoff energy to aid in sediment settling. This BMP is represented in SWAT through adjustment of the Manning's roughness coefficient (CH_N1), also known as Manning's "n" value, for tributary channels on subbasins considered erodible. The initial value of CH_N1 is 0.014 in SWAT; in the applied BMP condition it was increased to 0.05 on land with a subbasin slope of greater than 5 percent (Tuppad and Srinivasan, 2008).

4.3.9.8 Grazing Management

Grazing management is used to prevent overgrazing of range grasses through preventing excessive above ground biomass removal by animals. Overgrazing exposes bare soil and increases soil compaction. This leads to decreased infiltration and increased soil erosion and surface runoff, thereby increasing sediment and nutrient yields from range land (Tuppad and Srinivasan).

Grazing management may be incorporated into SWAT through reduction of the harvest index (HVSTI) of range grass (Tuppad and Srinivasan, 2008). The HVSTI is defined as the percentage of biomass removed in a harvest operation (in this case animal grazing). Initially, HVSTI is set to 90% for range grass, while in the BMP

implementation scenario, HVSTI was set to 70%. Decreasing HVSTI increases biomass left on the field, reducing soil exposure.

4.3.9.9 Native Grass

Native grass replacement consists of replacing land containing agricultural row crops with native tall grasses such as Indian switchgrass or big bluestem (Nejadhashemi and Mankin, 2007). Replacing row crops with native grasses is expected to reduce sediment and nutrient transport to streams because it eliminates the need for tillage and fertilizer while increasing vegetative cover on the soil.

To implement native grass within SWAT, all agricultural row crop land was converted to range grass, which represents a mixture of native tall grasses. Row crop management operations are not applicable in the native grass scenario, because row crops are replaced with native grass.

4.4 RESULTS AND DISCUSSION

The results and discussion section details the TCLW sensitivity and calibration results, impacts of climate change on long term water quantity, impacts of climate change on long term water quality, effectiveness of BMPs in the current climate, effectiveness of BMPs in future climate scenarios, and assessing the impacts of climate change on BMP effectiveness.

4.4.1 Sensitivity Analysis

Sensitivity analysis was performed on all three sections of the Big Blue watershed (TCLW, upper left, upper right) for flow sediment, TKN, and TP. The ten most sensitive

parameters for flow and sediment for each watershed and are presented in Table 4-8, while Table 4-9 lists results for TKN and TP. CN2, Esco, Alpha_bf, and Sol_awc were all highly sensitive flow in each watershed. For sediment, Spcon, Spexp, Ch_N2, and surlag were the most sensitive. In the case of TKN, CN2, Surlag, and Ch_K2 were the most sensitive. Surlag, Alpha_Bf, and Ch_K2 were the most sensitive for TP.

Table 4-8. Sensitivity analysis results for flow and sediment

	Streamflow			Sediment		
Rank	TCLW	Upper Left	Upper Right	TCLW	Upper Left	Upper Right
1	CN2	CN2	CN2	Spcon	Spcon	Spcon
2	Esco	Esco	Esco	Ch_N2	Ch_N2	Ch_N2
3	Alpha_Bf	Sol_Awc	Alpha_Bf	Spexp	Surlag	Spexp
4	Ch_K2	Alpha_Bf	Sol_Awc	Ch_K2	Spexp	Surlag
5	Sol_Awc	Blai	Blai	Surlag	CN2	CN2
6	Blai	Sol_Z	Sol_Z	CN2	Ch_K2	Ch_K2
7	Canmx	Surlag	Ch_K2	Alpha_Bf	Blai	Blai
8	Sol_Z	Ch_K2	Timp	Usle_P	Esco	Esco
9	Ch_N2	Canmx	Canmx	Esco	Usle_P	Alpha_Bf
10	Epco	Rchrg_Dp	Surlag	Blai	Usle_C	Usle_P

Table 4-9. Sensitivity analysis results for TKN and TP

	TKN			TP		
Rank	TCLW	Upper Left	Upper Right	TCLW	Upper Left	Upper Right
1	CN2	Surlag	Surlag	Surlag	Surlag	Alpha_Bf
2	Ch_K2	CN2	CN2	CN2	Alpha_Bf	Surlag
3	Surlag	Blai	Usle_P	Esco	CN2	CN2
4	Ch_N2	Usle_P	Blai	Ch_K2	Ch_K2	Ch_K2
5	Sol_Awc	Alpha_Bf	Esco	Alpha_Bf	Timp	Esco
6	Usle_P	Timp	Alpha_Bf	Timp	Canmx	Ch_N2
7	Esco	Canmx	Biomix	Ch_N2	Esco	Blai
8	Blai	Esco	Timp	Sol_Awc	Blai	Biomix
9	Canmx	Sol_Awc	Sol_Z	Sol_Z	Sol_Alb	Sol_Z
10	Alpha_Bf	Biomix	Sol_Awc	Rchrg_Dp	Rchrg_Dp	Sol_K

4.4.2 Model Calibration

The model was calibrated for flow, sediment, TKN, and TP. The calibrated model performed well in reproducing streamflow, sediment load, and TP load. Final calibration parameter values are presented in Table 4-10. Calibration results of TKN load were less satisfactory, especially in the validation period. Poor performance in reproducing TKN load is likely due to lack of observation data, unknown manure applications on agricultural lands, and lack of NH_3 output provided by SWAT. Ten observations of TKN were available over the 20 year study period, while specific manure applications on agricultural fields and septic system usage in the watershed were not modeled. In daily calibration, this volume of observed data is inadequate for satisfactory calibration results. Although the TKN calibration results were unsatisfactory, relative comparisons between model scenarios can still be made. Calibration and validation results for streamflow, sediment load, TKN load, and TP load are presented in Table 4-11 and figures 8-1, 8-2, 8-3, and 8-4 in the appendix.

Table 4-10. TCLW calibrated model parameters

Parameter	Method	Calibrated Value
Alpha_Bf	Replace default with	0.9886
Biomix	Multiply default by	1.4385
Ch_K2	Replace default with	111.1000
Cn2	Multiply default by	1.0323
Esco	Replace default with	0.4976
Sol_Awc	Multiply default by	1.1881
Spcon	Replace default with	0.0015
Spexp	Replace default with	1.8594
Surlag	Replace default with	0.9454

Overall, the results show that the calibrated model is under predicting sediment, TKN, and TP loads for high flow conditions. Under low flow conditions, the model is over predicting for TP, while performing well for flow, sediment, and TKN.

Table 4-11. TCLW calibration results

		Calibration	Validation	Combined
Flow	NSE	0.65	0.58	0.63
	R^2	0.68	0.59	0.63
	RMSE	68.4	67.9	68.2
Sediment	NSE	0.57	0.55	0.56
	R^2	0.86	0.99	0.91
	RMSE	9531	10027	9782
TKN	NSE	0.16	-2.53	0.26
	R^2	0.98	0.14	0.77
	RMSE	221443	31894	151143
TP	NSE	0.87	0.67	0.76
	R^2	0.94	0.85	0.87
	RMSE	5400	9759	7887

4.4.3 Impact of Climate Change on Water Quantity

The impact of different climate scenarios on water quantity (long-term average) under conventional tillage operations (base scenario) is presented in Table 4-12. The study showed that surface runoff, baseflow, and water yield all increased with increasing precipitation for each climate change scenario. Long term average yearly precipitation increases from the current climate scenario were 97.7 mm (3.8 in) for the A1B scenario, 74.2 mm (2.9 in) for the A2 scenario, and 56.7 mm (2.2 in) for the B1 scenario.

The A1B scenario has the greatest impact on water quantity because of has the largest increase in precipitation, while the B1 scenario had the smallest impact on water quantity because it has the smallest increase in precipitation. For example, surface runoff, baseflow, and water yield increased by 43%, 58%, and 44%, respectively, for the A1B

scenario. In the A2 scenario, surface runoff increased by 30%, baseflow increased by 45%, and water yield increased by 31% from the current climate. Finally, the B1 scenario demonstrated that surface runoff increased by 18%, baseflow increased by 26%, and water yield increased by 19% from the current climate, which corresponds with the lowest precipitation increase of the three future climate scenarios.

Table 4-12. Impacts of climate change on water quantity in the TCLW

Scenario	Precipitation (mm)	ET (mm)	Surface Runoff (mm)	Baseflow (mm)	Water Yield (mm)
20C3M	667.2	622.0	56.8	2.6	59.0
A1B	764.9	692.3	81.2	4.2	85.0
A2	741.3	677.2	73.7	3.8	77.1
B1	723.9	667.0	67.2	3.3	70.1

4.4.4 Impact of Climate Change on Water Quality

The impact of different climate scenarios on water quality (sediment, total nitrogen, and total phosphorus) at the watershed outlet (long-term average) under conventional tillage operations is presented in Figure 4-3. This allows for analysis of how climate change affects pollution generation at the watershed scale. In all three future climate scenarios sediment load, nitrogen load, and phosphorus load at the watershed outlet increased from the current climate levels. This may be due to precipitation increases in each scenario. Increase in precipitation generates more runoff and water yield from the field, which leads to an increase in NPS transport to the reach.

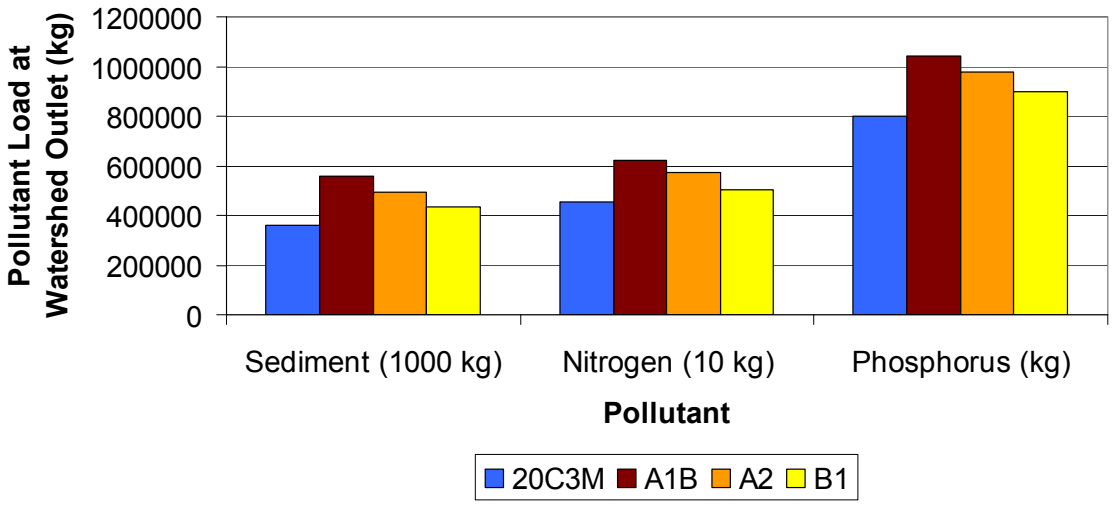

Figure 4-3. Impact of climate change on sediment, nitrogen, and phosphorus load at the watershed outlet (20-year average)

The A1B scenario observed the greatest increases in sediment, nitrogen, and phosphorus loads at the watershed outlet, while the B1 scenario experienced the smallest increases. These results correlate with the increases in precipitation, and consequently runoff, in each scenario. The A1B scenario had the greatest increase in precipitation from the climate and the greatest increase in pollutant loads at the watershed outlet. The B1 scenario had the smallest precipitation increase from the current climate and showed the smallest increase in pollutant loads. In terms of percent increase in pollution generation, the A1B scenario had a 54% increase in sediment load, a 37% increase in nitrogen load, and a 30% increase in phosphorus load from the current climate. In the A2 scenario, sediment, nitrogen, and phosphorus loads increased by 36%, 27%, and 22%, respectively. Finally, for the B1 scenario, smaller increases of 20%, 11%, and 12% in sediment load, nitrogen load, and phosphorus load were observed, respectively.

4.4.5 Effectiveness of BMPs in the Current Climate

BMP efficiency was analyzed in the current climate. Nutrient reduction efficiencies from conventional tillage to BMP are presented in Figure 4-4 (TN) and Figure 4-5 (TP), while sediment reduction is shown in Figure 4-6. Native grass, terraces, and contour farming show the best performance out of the BMPs at the field scale, while porous gully plugs, no-tillage, conservation tillage, and filter strips show limited reduction. Native grass has median percent reductions of 52%, 56%, and 70% for sediment, nitrogen, and phosphorus, respectively. Terraces have a median sediment reduction of 51%, total nitrogen reduction of 54%, and phosphorus reduction of 63%. Contour farming is also performs well, with median reduction efficiencies of 36%, 34%, and 41% for sediment, total nitrogen, and total phosphorus, respectively. Grazing management was the fourth most efficient BMP, with 14% median sediment reduction, 8% median total nitrogen reduction, and 6% median total phosphorus reduction. Filter strips had median reduction of 1% for all three pollutants, while porous gully plugs had almost no reduction. Conservation tillage had median reduction efficiencies of less than 5% for all three pollutants, while no-tillage had an 8% mean sediment reduction efficiency, a -1% median total nitrogen reduction efficiency, and -7% median total phosphorus reduction efficiency.

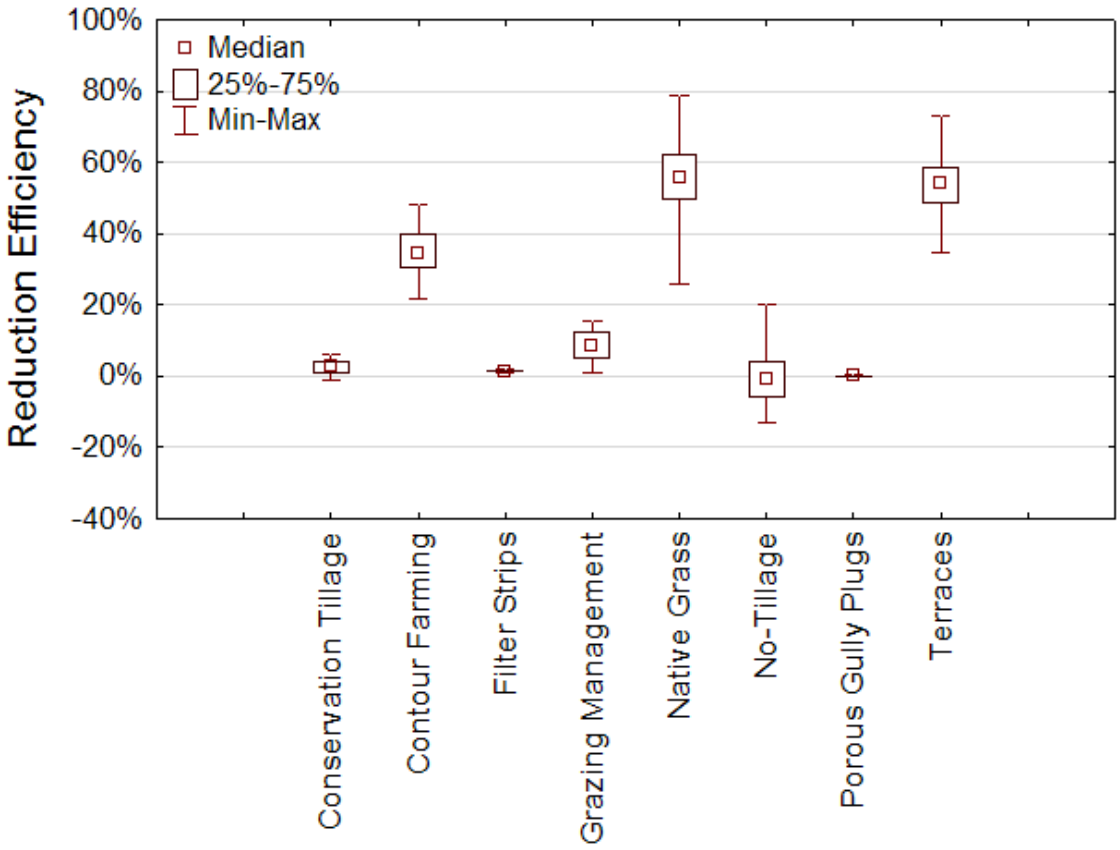

Figure 4-4. BMP TN efficiency at the field scale for the 20C3M scenario

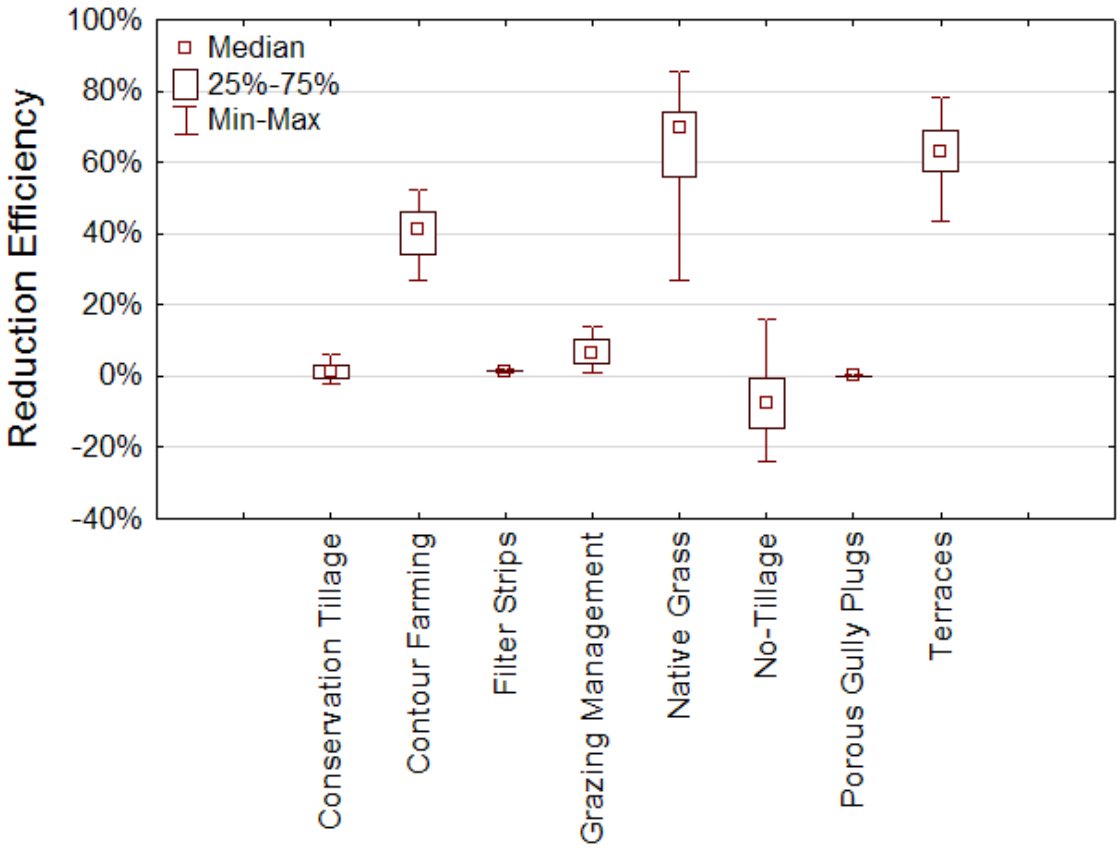

Figure 4-5. BMP TP efficiency at the field scale for the 20C3M scenario

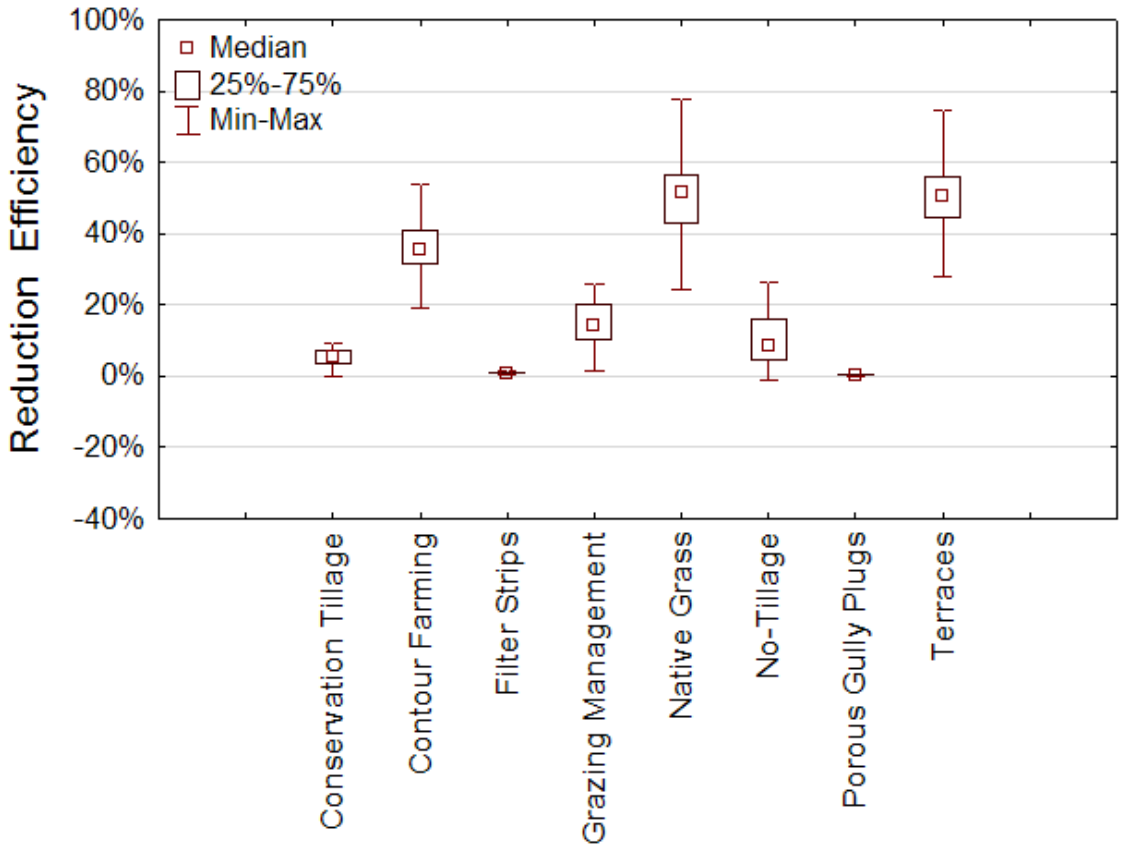

Figure 4-6. BMP sediment reduction efficiency at the field scale for the 20C3M scenario

Contour farming, terraces, and native grass likely had the best performance because of the intensive nature and large scale of the BMPs. Porous gully plugs had limited reduction because of their small scale (suitable only in areas with gully erosion and large slope). Due to the way in which porous gully plugs were defined here, they were implemented in few situations. Filter strips also showed limited reduction because they were only implemented in agricultural fields bordering reaches, which was less than 0.7% of the watershed area. If implemented in more areas (for example, bordering all agricultural fields), it is expected that load reduction would increase. Although erosion decreases in the no-tillage scenario, nitrogen loading from the field to the reach increased because of increased infiltration and transport of nitrate in groundwater.

Variability in pollutant reduction for the BMP scenarios is also an important consideration. BMPs with low variability are more reliable because their efficiency is more predictable in the long-term. Filter strips, grazing management, porous gully plugs, and conservation tillage BMPs have the lowest variability in percent reduction. Native grass, terraces, contour farming, and no-tillage have the greatest variability in percent reduction. The BMPs with highest variability are also the large scale, intensive practices. Due to their large scale, their reduction efficiency at the field scale is related to precipitation.

For example, in the native grass scenario, as yearly precipitation increases, reduction efficiency of each pollutant decreases. Decreased pollutant reduction efficiency in years with relatively higher precipitation is likely due to increased runoff and overland flow rate, where the native grass is unable to trap as much sediment and particulate nutrients. Similar results were seen in a study by Abu-Zreig et al. (2004) where sediment trapping efficiency of native grass generally increased with decreasing overland flow rate.

BMPs with low variability in percent reduction are generally less efficient and smaller scale. In these scenarios, the minimum and maximum predicted reduction was similar to the median reduction. This was the case for filter strips, porous gully plugs, and conservation tillage. This is likely due to the small scale nature of the BMPs, and lack of reduction efficiency at the field scale.

4.4.6 Effectiveness of BMPs in Future Climate Scenarios

Each BMP was compared to the conventional tillage operation (base scenario) in terms of sediment, nitrogen, and phosphorus load reduction and percent reduction

efficiency from the field and at the watershed outlet for each climate scenario. Sediment reduction efficiency from the field for all climate scenarios are presented in Figure 4-6 (20C3M), Figure 4-7 (A1B), Figure 4-8 (A2), and Figure 4-9 (B1). Similar trends were observed for TN and TP. In general, median efficiency is similar for each scenario, while variability increases for some BMPs in the climate change scenarios. For example in the 20C3M scenario for native grass, the maximum and minimum sediment reduction efficiencies were 78% and 25%, respectively, while in the A2 scenario the maximum was 77% and the minimum was 9% over the 20 year study period. Increased variability may be attributed to increases in extreme precipitation events and average yearly precipitation. For example, in 2054 above average precipitation is magnified by precipitation increases in future climate scenarios. In these extreme events native grass only partially slows down surface runoff and is not as effective as in low flow conditions in reducing sediment and phosphorus. This is due to runoff passing above the height of the native grass.

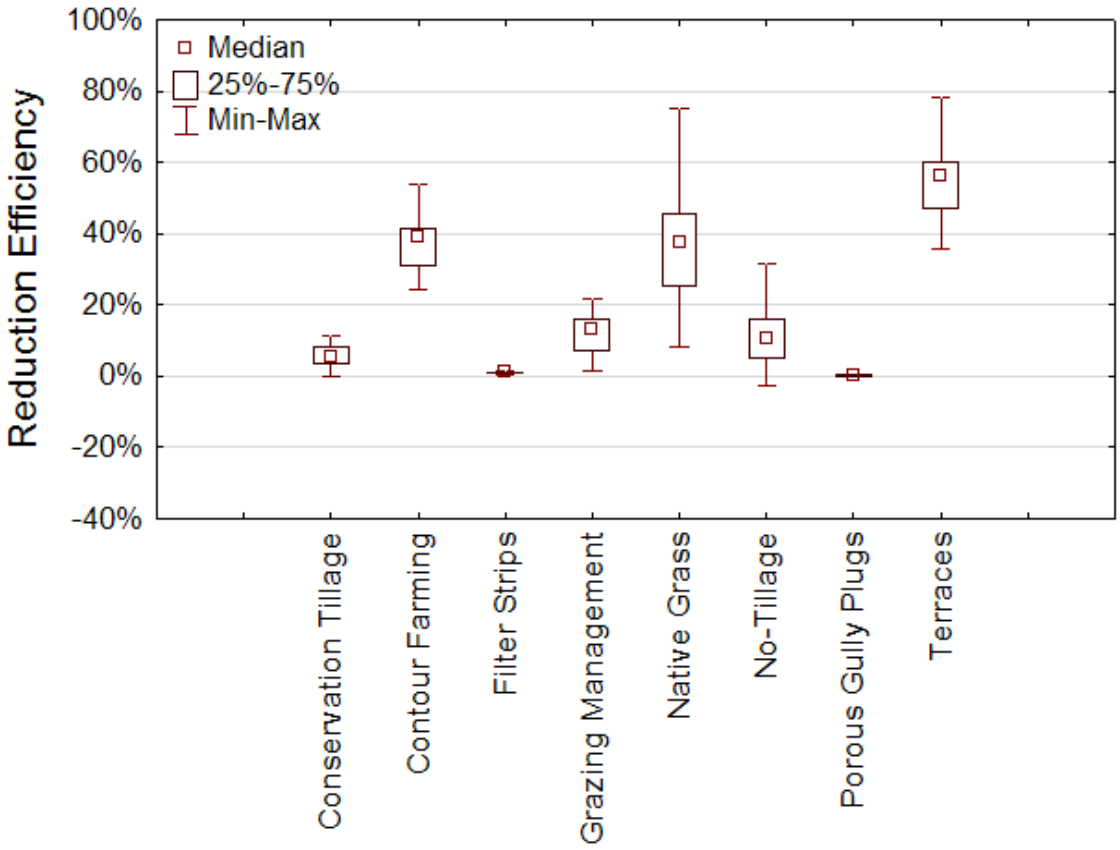

Figure 4-7. BMP sediment reduction efficiency at the field scale for the A1B scenario

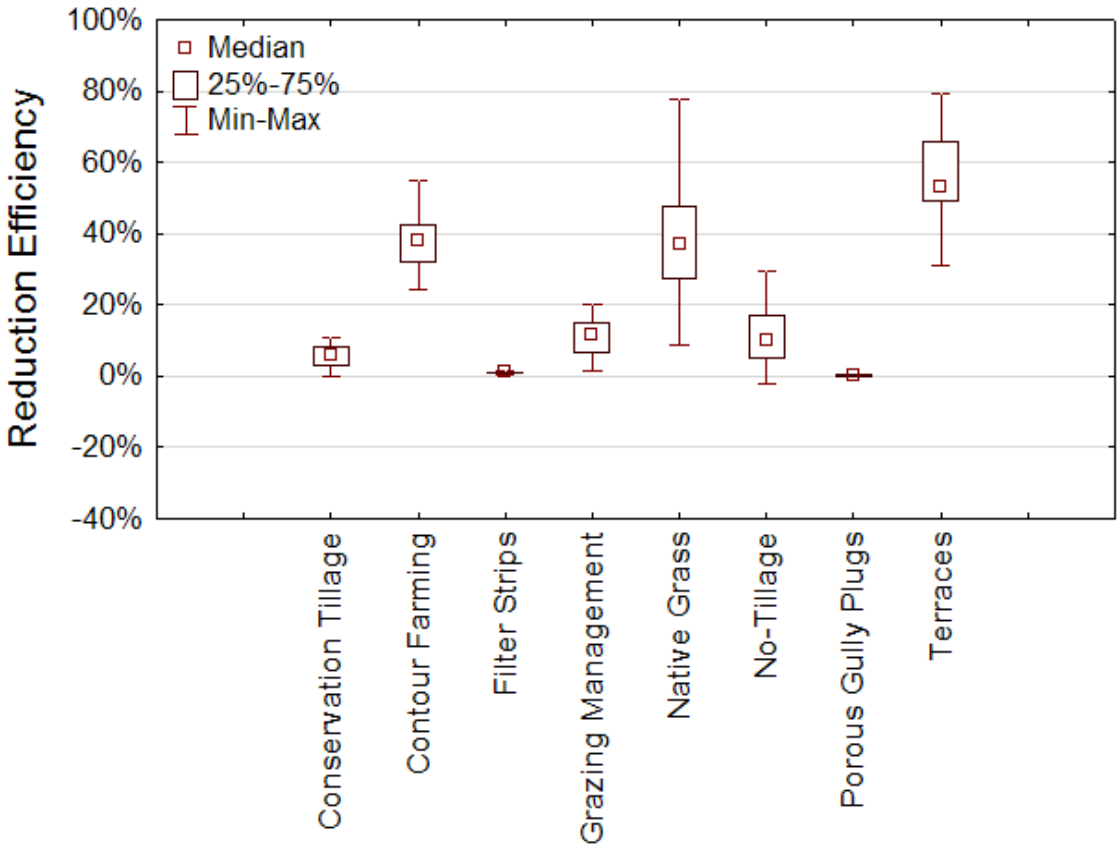

Figure 4-8. BMP sediment reduction efficiency at the field scale for the A2 scenario

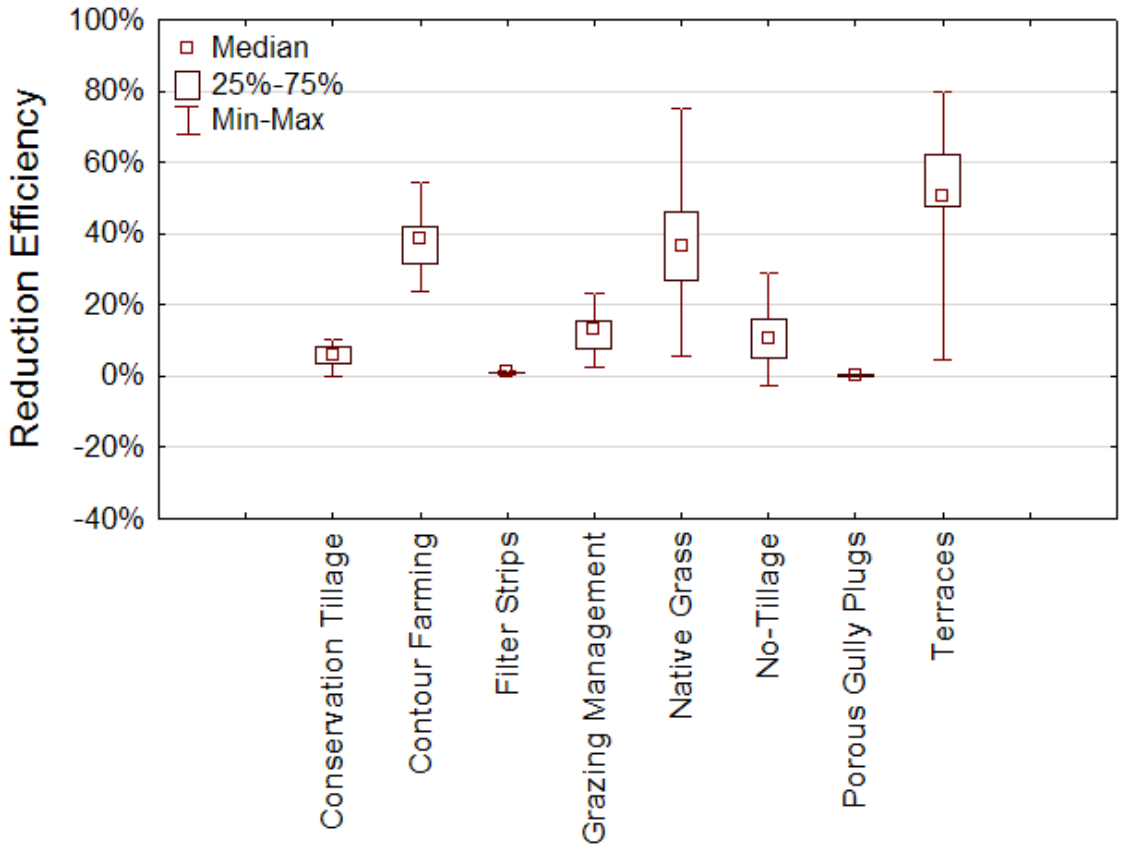

Figure 4-9. BMP sediment reduction efficiency at the field scale for the B1 scenario

Porous gully plugs, conservation tillage, and filter strips were the least efficient in reduction for all scenarios and pollutants, but were also experienced a minimal change in effectiveness in the future. Contour farming, native grass, and terraces all performed well at reducing pollutants from the field, although their variability was often increased in the A1B, A2, and B1 scenarios. Therefore, it can be concluded that these three BMPs are the most effective at NPS pollutant reduction, but their high variability in current and future climate makes them less dependable. Varying efficiencies between BMPs are likely due to the manner in which the BMPs were physically represented in SWAT due to their characteristics. Porous gully plugs, filter strips, and conservation tillage are less intensive

BMPs, while terraces, contour farming, and native grass are meant for large scale reduction in pollution transport and erosion.

Sediment, nitrogen, and phosphorus load reduction at the field and watershed scale were compared for all BMPs under all climate scenarios. Sediment, nitrogen, and phosphorus load reduction for contour farming at the field (HRU) and watershed (outlet) scale is displayed in Figure 4-10, 4-11, and 4-12, respectively.

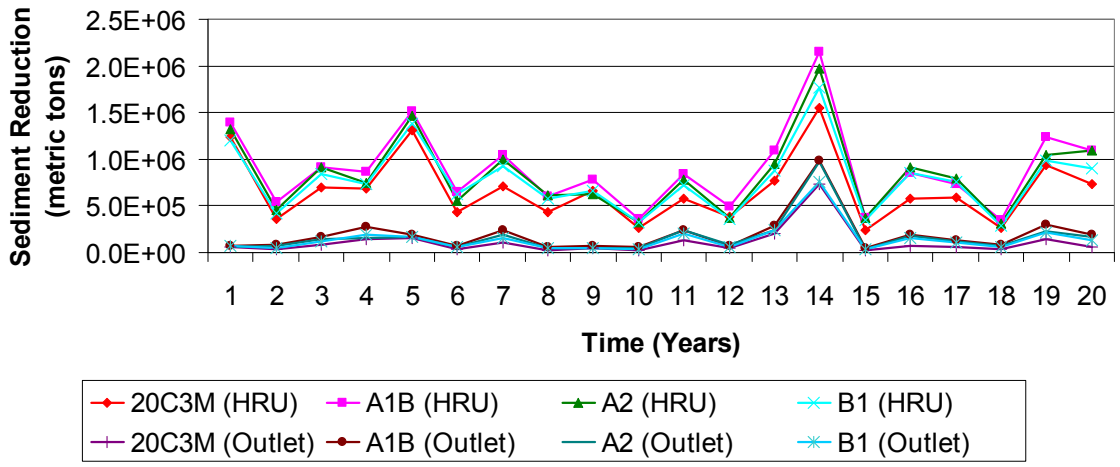

Figure 4-10. Contour farming sediment reduction at the field (HRU) and watershed (outlet) scale

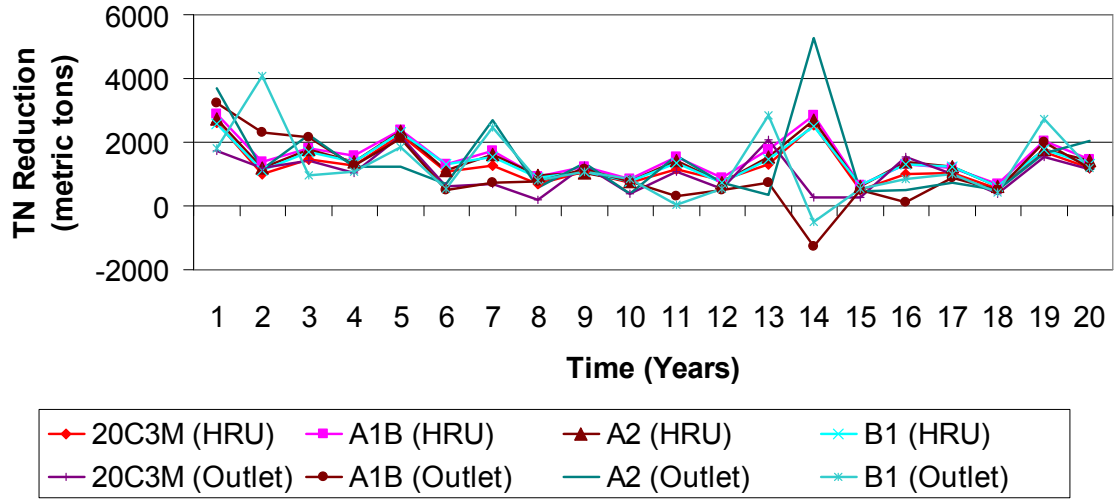

Figure 4-11. Contour farming TN reduction at the field (HRU) and watershed (outlet) scale

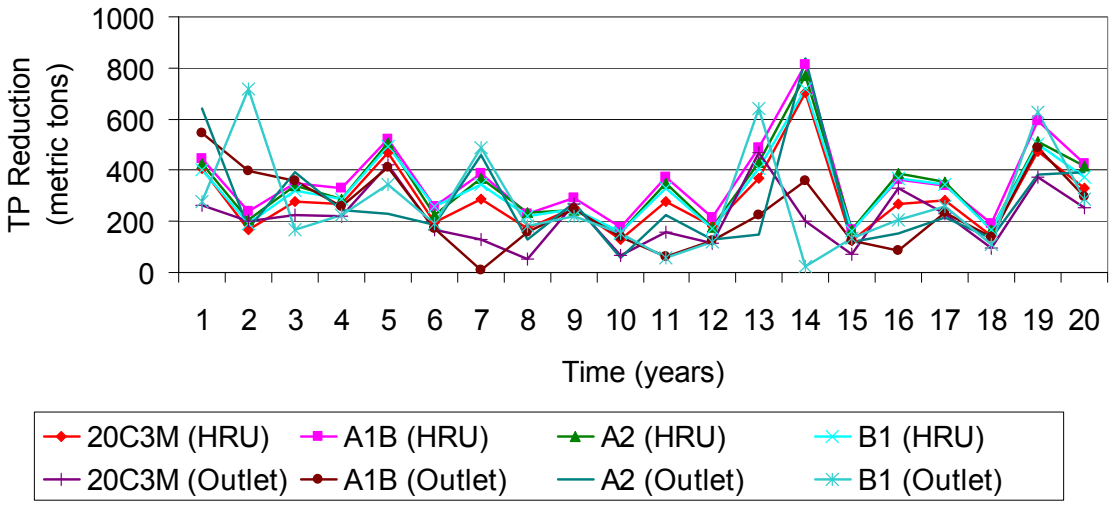

Figure 4-12. Contour farming TP reduction at the field (HRU) and watershed (outlet) scale

Figure 4-10 shows that while very effective at the field scale for sediment reduction, contour farming is about ten times less effective for sediment reduction at the watershed scale, due to channel processes such as deposition, although the field and watershed scale reduction follow a similar reduction trend (when load reduction at the field increases, load reduction at the watershed outlet increases). Contour farming also increases sediment load reduction for all three future climate scenarios at both the field and watershed scale.

Figure 4-11 and Figure 4-12 demonstrate that the difference between field and watershed reduction in nutrients is negligible in most years for contour farming. Field and watershed load reduction follow a similar trend, with the exception being in years of higher precipitation (such as year 14: 1993/2054). In these situations watershed reduction decreases while field reduction is increasing, which may be attributed to increased nitrogen and phosphorus in surface runoff.

4.4.7 Assessing the Impacts of Climate Change on BMP Effectiveness

Two methods can be used to evaluate the effectiveness of BMPs: percent reduction and load reduction. The percent reduction method measures the difference in load reduction divided by the original load reduction, while the load reduction is a measure of the difference in mass pollutant reduction from the base scenario to the BMP scenario. In order to determine if BMP performance changes between current climate and future climate scenarios in terms of percent reduction and load reduction at the field and watershed scale, t-tests were performed. A p-value of 0.05 to determine significance was used. Results of the t-tests are presented in Tables 4-13 and 4-14 for the A1B scenario, while the results for the A2 and B1 scenarios are presented in Tables 8-1, 8-2, 8-3, and 8-4. An up arrow represents a significant increase in percent or load reduction with the application of a BMP between the current and future climate scenarios, while a down arrow represents a significant decrease in percent or load reduction with the application of a BMP between current and future climate scenarios. The p-value is also presented in the tables.

Table 4-13. Significant difference (p-value) in BMP performance at the field scale between 20C3M and A1B.

	Sediment		Total Nitrogen		Total Phosphorus	
BMP	%	Load	%	Load	%	Load
Contour Farming	↑ 0.01	↑ <0.01	0.79	↑ <0.01	0.78	↑ <0.01
Filter Strips	↑ <0.01	↑ <0.01	0.06	↑ <0.01	↑ 0.01	↑ 0.00
Grazing Management	↓ <0.01	0.71	↓ 0.01	0.36	↓ <0.01	0.32
Native Grass	↓ <0.01	0.31	↓ <0.01	0.39	↓ <0.01	↑ 0.03
No-Tillage	0.21	↑ <0.01	↑ <0.01	↑ <0.01	↑ 0.02	↑ 0.17
Porous Gully Plugs	0.08	↑ 0.01	0.20	↑ 0.01	0.07	↑ 0.00
Conservation Tillage	0.17	↑ <0.01	↑ <0.01	↑ <0.01	0.08	↑ <0.01
Terraces	↑ <0.01	↑ <0.01	0.04	↑ <0.01	0.01	↑ <0.01

Table 4-14. Significant difference (p-value) in BMP performance at the watershed scale between 20C3M and A1B.

	Sediment		Total Nitrogen		Total Phosphorus	
BMP	%	Load	%	Load	%	Load
Contour Farming	↑ <0.01	↑ <0.01	0.30	0.98	0.36	0.39
Filter Strips	0.09	↑ <0.01	0.07	0.15	0.15	0.30
Grazing Management	0.94	0.96	↓ 0.02	0.27	↓ <0.01	0.72
Native Grass	↑ <0.01	↑ <0.06	0.19	0.44	0.28	0.79
No-Tillage	0.10	0.06	0.42	0.33	0.23	0.19
Porous Gully Plugs	0.34	0.27	0.11	0.09	0.12	0.15
Conservation Tillage	0.34	0.15	0.06	0.25	0.20	0.30
Terraces	↑ <0.01	↑ <0.01	0.05	0.50	0.08	0.59

The most notable results of the t-tests show that individual BMP performance has more occurrences of significant difference in load and percent reduction between current

and future climate at the field scale than the watershed scale. This is consistent between all three future climate scenarios, which is likely due to in-stream channel processes (such as channel deposition and bank erosion) causing less reduction at the watershed scale although there are reductions at the field.

For example, there are statistically significant changes between scenarios in performance of conservation tillage farming in sediment, total nitrogen, and total phosphorus load reduction at the field scale, while there are no statistically significant changes in performance at the watershed scale. This difference is prevalent even though the conservation tillage practice shows a consistent reduction trend at the field and watershed levels. In addition, the sediment load reduction on the watershed scale is much less than the load reduction at the field scale. A graphical comparison of conservation tillage sediment reduction at the field scale between 20C3M and A1B is presented in Figure 4-13. A similar graph for sediment reduction at the watershed scale is presented in Figure 4-14.

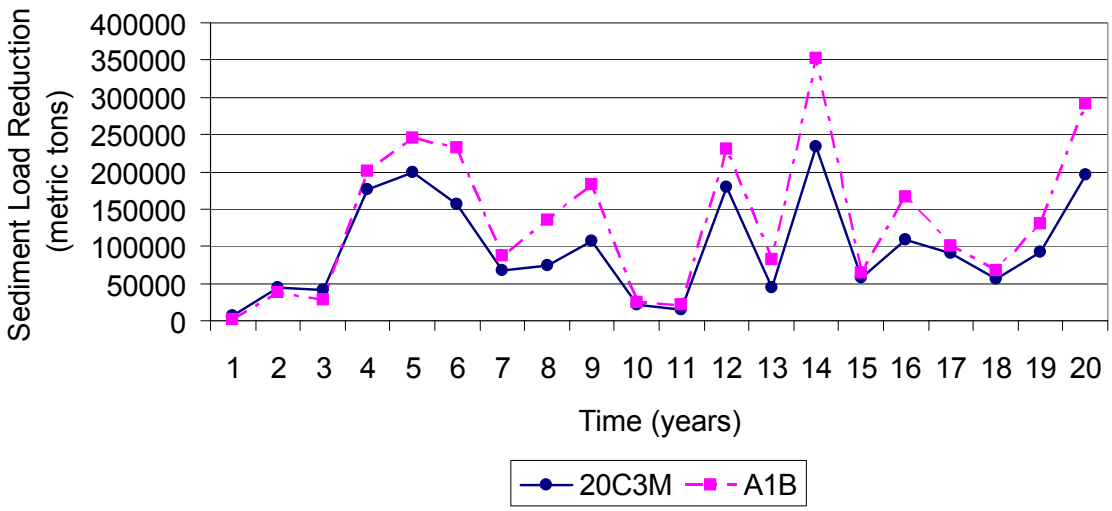

Figure 4-13. Conservation tillage sediment reduction at the field scale

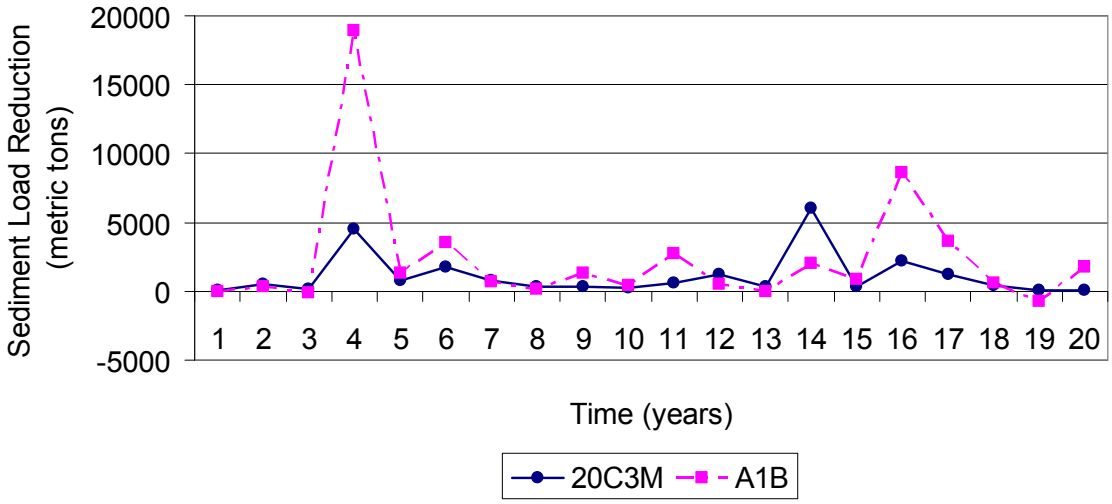

Figure 4-14. Conservation tillage sediment reduction at the watershed scale

Porous gully plugs do not show any significant change in performance under any climate change scenario for any pollutant. The lack of change in performance is likely due to the nature of these BMPs and their implementation in SWAT. Porous gully plugs are less intensive than other BMPs, and therefore do not have a great impact on reduction and are not effective under any future climate scenario.

Terraces and contour farming consistently show the greatest increases in efficiency and load reduction at both the field and watershed scale in future climate scenarios. This is due to the manner in which they are physically represented in SWAT, including a large reduction in both runoff curve number and the USLE practice factor. In large slope areas, the USLE_P factor becomes a significant factor for increasing pollutant reduction.

Native grass resulted in a significant decrease in sediment load reduction at the field between the current and future climate scenarios, while there was a significant increase in sediment load reduction at the outlet when applied. Decreases in sediment load reduction at the field is likely due to increased runoff in future climate scenarios, which allows for less sediment to be trapped by the grass in extreme precipitation events. Although sediment load reduction at the outlet was increased in the future climate scenario, it was still an overall decrease from the conventional tillage (base) scenario.

Grazing management shows significant decreases in percent reduction for sediment and nitrogen in all three future climate scenarios. Significant decreases in percent reduction were observed at the watershed scale in future climate scenarios. With an increase in precipitation, decreasing biomass removal from range land may not have enough of a large scale impact to enhance performance in future climate scenarios.

No-tillage in future climate scenarios generally showed an increase in sediment and total nitrogen load reduction. An increase was also observed in sediment and total nitrogen reduction efficiency at the field scale in future climate scenarios. At the watershed scale there was no significant difference in performance of the no-tillage BMP.

Conservation tillage in future climate scenarios increased load reduction at the field scale for sediment, total nitrogen, and total phosphorus. In some future scenarios increases in sediment and total nitrogen percent reduction at the field scale was observed. At the watershed outlet there was no significant difference in reduction for any future climate scenario.

Filter strips observed a significant increase in load reduction and efficiency for all pollutants at the field scale in future climate scenarios. Filter strip performance did not change on the watershed scale much, only sediment load reduction efficiency increased in future climate scenarios.

4.5 CONCLUSION

This study examined the effects of climate change on best management practice efficiency in the Tuttle Creek Lake watershed in Kansas and Nebraska. Using SWAT, the effects of three SRES emissions scenario outputs (A1B, A2, and B1) of the CCSM-3 model on the performance eight agricultural BMPs was determined.

The Tuttle Creek Lake watershed is projected to experience an increase in precipitation of up to 66% and an increase in mean daily temperature of up to 3.6 °C by the middle 21st century according to CCSM-3 model runs for the A1B, A2, and B1 SRES emissions scenarios provided by NCAR. As precipitation and temperature increase in this watershed, the effectiveness of BMPs for mitigation of NPS pollution is uncertain. The SWAT model was coupled with CCSM-3 statistically downscaled temperature and precipitation data to assess the impact of climate change on BMP implementation strategies.

The impacts of climate change on water quantity were observed in the conventional tillage scenario. All three water quantity (runoff, baseflow, and water yield) increased in each future climate scenario, which is likely due to the substantial increases in precipitation. The A1B scenario showed the greatest increase and B1 showed the smallest increase from the 20C3M scenario.

Water quality impacts of climate change in the current climate were also studied in the conventional tillage scenario. Sediment, nitrogen, and phosphorus load at the watershed outlet increased in all three future climate scenarios. Similar to the observed changes in water quantity, pollutant load increases were the largest in the A1B scenario and the smallest in the B1 scenario.

In the current climate, the most effective BMPs at the field scale to reduce sediment, nitrogen and phosphorus are terraces, contour farming, and native grass. Porous gully plugs, filter strips, and conservation tillage had the least effect on pollution reduction, while in some cases no-tillage had actually increased pollution generation at the field scale. Grazing management was moderately effective at the field scale. Native grass, terraces, contour farming, and no-tillage had highly variable reduction efficiencies, reducing confidence in these BMPs.

Under future climate, variability in native grass and no-tillage reduction efficiency at the field scale increased. Terraces, contour farming, and native grass were the most effective in pollution reduction at the field scale. Once again, porous gully plugs and filter strips were ineffective in field scale, with reduction efficiencies close to zero. At the watershed scale, terraces, contour farming, and native grass increased in pollutant

load reduction from current to future climate. All other BMPs did not significantly change performance consistently at the watershed scale.

Finally, significant change in BMP performance between the current climate and future climate scenarios was determined using t-tests. There were more significant changes in BMP performance at the field scale than at the watershed scale. Contour farming and terraces showed significant increases in reduction at both the field and watershed scale. Porous gully plugs showed no significant change in performance under any scenario, which is likely due to how they were represented within SWAT. Grazing management and no-tillage showed significant decreases in performance at the field scale in future scenarios. At the watershed scale, native grass increased sediment reduction.

The results of this study demonstrate that changing climate affects BMP performance in terms of percent reduction and load reduction of sediment, nitrogen, and phosphorus. Significant changes in performance were more commonly observed at the field scale, while most BMPs did not affect pollution reduction at the watershed outlet.

5 BEST MANAGEMENT PRACTICE SENSITIVITY ANALYSIS UNDER CLIMATE CHANGE SCENARIOS

Sean A. Woznicki, A. Pouyan Nejadhashemi

5.1 ABSTRACT

As global climate changes, its effect on water resources and nonpoint source (NPS) pollution is uncertain. To mitigate the effects of climate change on water resources, agricultural best management practices (BMPs), such as reduced tillage operations or structural BMPs such as porous gully plugs, may be used to reduce NPS pollution. The reduction capabilities of BMPs in future climates are unknown partially because the extent and impact of climate change and its affects on water resources are uncertain. Understanding the sensitivity of BMPs implementation as climate changes will be important for decision makers to consider what type of BMP is more reliable when developing implementation plans. The objective of this study was to determine how sensitivity of BMPs varies due to changes in precipitation, temperature, and CO_2 using the Soil and Water Assessment Tool (SWAT). Downscaled climate change data was obtained from the National Center for Atmospheric Research (NCAR) Geographic Information System Initiative Community Climate System Model (CCSM-3) model for the Tuttle Creek Lake watershed in Kansas and Nebraska. Three Special Report on Emissions Scenarios (SRES) storylines (A1B, A2, and B1), developed by the Intergovernmental Panel on Climate Change (IPCC), were compared to historical model output from CCSM-3. Sensitivity of eight agricultural BMPs (conservation tillage, contour farming, filter strips, grazing management, native grass, no-tillage, porous gully

plugs, and terraces) was determined for each climate change scenario by estimating the effects on sediment, total nitrogen, and total phosphorus on an annual and monthly basis. For all BMPs, NPS pollution was greatest under the A1B scenario, likely because this scenario had the largest annual average precipitation increase compared to current climate. Using a relative sensitivity index, native grass, grazing management, and filter strips were determined to be the most sensitive for all climate change scenarios, while porous gully plugs, no-tillage, and conservation tillage were the least sensitive on an annual basis. The monthly sensitivity analysis revealed that BMP sensitivity varies largely on a seasonal basis for all climate change scenarios. Meanwhile, grazing management, filter strips, and porous gully plugs were the only BMPs with sensitivities that did not significantly change in climate change scenarios. The results of this research suggest that majority of agricultural BMPs tested in this study are sensitive to climate change, and caution should be exercised in the decision making processes.

5.2 INTRODUCTION

The Intergovernmental Panel on Climate Change (IPCC, 2007) has determined that the global climate system is changing. Increases in atmospheric greenhouse gas (GHG) concentration, primarily due to fossil fuel use, have resulted in a global average net warming effect of the earth (IPCC, 2007). Global surface temperature has increased by 0.76°C in the past 100 years, and in the latter half of the 20th century the earth has warmed by 0.13°C per decade (IPCC, 2007). As GHG emissions continue to increase, global average surface temperature is predicted to increase anywhere from 1.8°C to 4.0°C by 2100, along with changes in rainfall volume and intensity (IPCC, 2007). This change

will greatly depend on future GHG emissions and technological development (Ficklin et al., 2009).

The potential effects of changing climate are far reaching: human health, ecosystem health and biodiversity, food production and global food supply, economic growth, tourism, and water resources all can be affected. As temperatures rise, heat waves are expected to increase mortality related to exposure during extreme events (Patz et al., 2005). Changing climate may induce changes in incidence of disease transmission as well as geographic distribution of disease vectors (Haines et al., 2006). Ecosystem dynamics have been affected by recent changes in climate. Many organisms in various geographic regions have been affected and common changes are related to timing of spring activities: earlier breeding of birds, spawning of amphibians, and flowering of plants (Walther et al., 2002). Food production is affected by climate change through alterations of crop yields and land suitability (Schmidhuber and Tubiello, 2007). Warming may benefit crop and pasture yields in temperate regions and decrease yields in tropical and arid regions (Tubiello et al., 2007). Economically, climate change is likely to reduce the rate of economic growth, although per capita income is likely to continue to increase (Fankhauser and Tol, 2005). Tourism is very sensitive to climatic variations, and popular destinations may become too hot, while other destinations with predominantly cool climates may warm and become more desirable globally (Berritella et al., 2004). Finally, climate change coupled with population growth and consumption needs will severely alter the hydrological cycle in most regions of the world (Jackson et al., 2001).

Fresh water is the most important resource in the world for humans: it is used for drinking, food production, industrial applications, transportation, and recreation.

Ecosystems also require fresh water to function properly: this essential resource provides life and habitat to numerous organisms. However, changes in the hydrologic cycle due to alterations in regional and seasonal patterns in temperature and precipitation are not well understood (Ficklin et al., 2009).

Therefore, the potential affects of climate change on watershed processes are of great concern to watershed managers (Marshall and Randhir, 2008).

Water Quantity. Many studies have explored the interaction between climate change and watershed hydrology. Precipitation, temperature, and atmospheric CO_2 changes have been predicted to affect streamflow and surface runoff in varying ways. Increases in atmospheric CO_2 have been shown to increase water yield and surface runoff (Chaplot 2007; Eckhardt and Ulbrich, 2003; Jha et al., 2006). This is likely due to decreases in plant stomatal conductance, which decreases transpiration and leaves more water available for runoff (Ficklin et al., 2009). Alteration in magnitudes and variability of precipitation are expected to have the greatest effect on watershed hydrology. Marshall and Randhir (2008) concluded for the Connecticut River watershed that surface runoff may increase in winter months due to increases in liquid precipitation, while spring surface runoff will likely decrease in spring due to less snowmelt. Chaplot (2007) determined that watershed hydrology in Iowa and Texas watersheds was more sensitive to changes in precipitation than temperature or CO_2. Streamflow in the Upper Mississippi River basin was predicted widely vary based on GCM predicted precipitation patterns, from a 6% decrease to a 51% increase (Jha et al., 2006). Franczyk and Chang (2009) predicted that winter surface runoff increases in an Oregon watershed due to

increased precipitation falling as rain. Stone et al. (2003) concluded that a higher resolution Regional Climate Models (RCM) predicted significantly greater increases in water yield than a GCM due higher magnitude of precipitation increases in projections of the Missouri River Basin. Temperature changes are also expected to alter the hydrological cycle, mostly through changes in evapotranspiration. Using high and low warming global climate model (GCM) scenarios, July surface runoff was predicted to decrease by 71% and 67%, respectively, due to increases in evapotranspiration attributed to temperature increases in the Connecticut River watershed. Eckhardt and Ulbrich (2003) determined that temperature increases caused increases in evapotranspiration in a mountainous German watershed, but the effects were minimal on groundwater recharge (3% decreases) and streamflow (4% decrease). Ficklin et al. (2010) determined that with precipitation held constant, as temperature increases, annual water yield decreases due to evapotranspiration increases.

Water Quality. Determining the impacts of climate change on water quality has been the focus of various studies. As climate change affects watershed hydrology, NPS pollution is also likely to be affected. Chaplot (2007) determined that sediment loads were most significantly affected by changes in precipitation, because runoff is a driving force of sedimentation. Increases in nitrate loads were attributed to increases in atmospheric CO_2, which was attributed to increased vegetation assimilation and soil fixation (Chaplot, 2007). The impacts of climate change on agricultural runoff yields in a California watershed were studied by Ficklin et al. (2010). Temperature, precipitation, and atmospheric CO_2 increases were predicted to increase nitrate yield by up to 40% and decrease chlorpyrifos pesticide yields by 32%. Ficklin et al. (2010) concluded that nitrate

and total phosphorus yield decreased the most in increased temperature scenarios without precipitation changes, while total phosphorus was highly correlated to sediment yield, and subsequently, precipitation and surface runoff. Marshall and Randhir (2008) observed that climate change caused significant alterations to the timing and runoff of sediment loading (20-40% increases in October and 50% decreases in March) in the Connecticut River watershed. Average annual organic nitrogen and organic phosphorus yield were predicted to decrease by up to 19% and 46%, respectively (Marshall and Randhir, 2008).

As described above, results from climate change impacts studies conclude that alterations in precipitation, temperature, and atmospheric CO_2, whether it be in magnitude, timing, or both, have a significant impact on water quantity and quality of watershed systems. In order to counter the effects of climate change, mitigation strategies have been developed. Mitigation strategies reduce the impacts of climate change through managing land use to increase resiliency of the watershed (Marshall and Randhir, 2008). For example, agricultural best management practices (BMPs) are a series of mitigation techniques designed to reduce surface runoff and pollution (sediment, nutrients, and pesticides) that reach water bodies through targeting sensitive areas of a watershed and is widely used in modeling studies by Arabi et al. (2007), Behera and Panda (2006), Bracmort et al. (2006), Jha et al. (2007), Parajuli et al. (2008), Santhi et al. (2006), Tuppad and Srinivasan (2008), and Tuppad et al. (2010). In many cases, BMP implementation by farmers is encouraged through incentive programs such as cost-sharing, tax breaks, and monetary compensation (Marshall and Randhir, 2008).

Assessing the sensitivity of BMP performance in scenarios of possible climate change will provide insight into the future pollution reduction capabilities of mitigation strategies. Sensitivity analysis provides a comprehensive understanding of the relationship between the model and the physical processes being modeled, and may be defined as the ratio of change in model output to change in a model parameter (McCuen, 1973). Performing a sensitivity analysis allows for a better understanding and estimating model parameters, which leads to reduced model uncertainty (Lenhart et al., 2002). There are two general methods of sensitivity analysis: local and global. Local sensitivity determines the impact of changes in a parameter value on model output, while global sensitivity analyzes the complete parameter space simultaneously (van Griensven et al., 2006). Lenhart et al. (2002) performed local sensitivity analysis through variation of hydrological parameters by developing ranges based on initial values and entire parameter ranges centered on the parameter mean, and concluded that both methods produced similar results. Through development of a combination local-global sensitivity analysis to limit model runs, van Griensven et al. (2006) determined the most sensitive hydrologic and water quality parameters through ranking. Sensitivity analysis is an important tool in BMP modeling to establish appropriate parameter ranges for proper representation in a watershed model (Tuppad et al., 2010). Luo and Zhang (2009) performed a management oriented sensitivity analysis using parameters related to BMP implementation through relative random sampling of parameter values in a one-at-a-time method. The need was identified to determine sensitivity of other pollution reduction parameters in terms of BMPs such as contour farming, terraces, cover crops, and strip-cropping (Luo and Zhang, 2009). A similar BMP sensitivity analysis was performed by

Tuppad et al. (2010) on physically realistic ranges of parameters related to conservation practice implementation.

The objective of this study was to perform a sensitivity analysis of BMPs across future climate change scenarios for the Tuttle Creek Lake watershed (TCLW) of Kansas and Nebraska using SWAT2009 model. Determining how sensitivity of BMPs may change with climate will allow for watershed managers and planners to determine, which BMPs may be relied on for future implementation while understanding the possible consequences of employing others.

5.3 MATERIALS AND METHODS

5.3.1 Study Area

The TCLW is part of the 6-digit hydrologic unit (HUC-6) Big Blue watershed and is comprised of two HUC-8 subwatersheds: the Lower Big Blue (HUC 10270205) and the Lower Little Blue (HUC 10270207). The five other HUC-8 subwatersheds of the Big Blue are the Upper Big Blue (HUC 10270201), Middle Big Blue (HUC 10270202), West Fork Big Blue (HUC 10270203), Turkey (HUC 10270204), and the Upper Little Blue (HUC 10270206). Two major rivers (the Little Blue River and Big Blue River) enter the TCLW from the north. In order to incorporate these inputs into the model, the entire Big Blue watershed (HUC 102702) was split into three sections for modeling, called the upper left, upper right, and TCLW in this study (Figure 5-1).

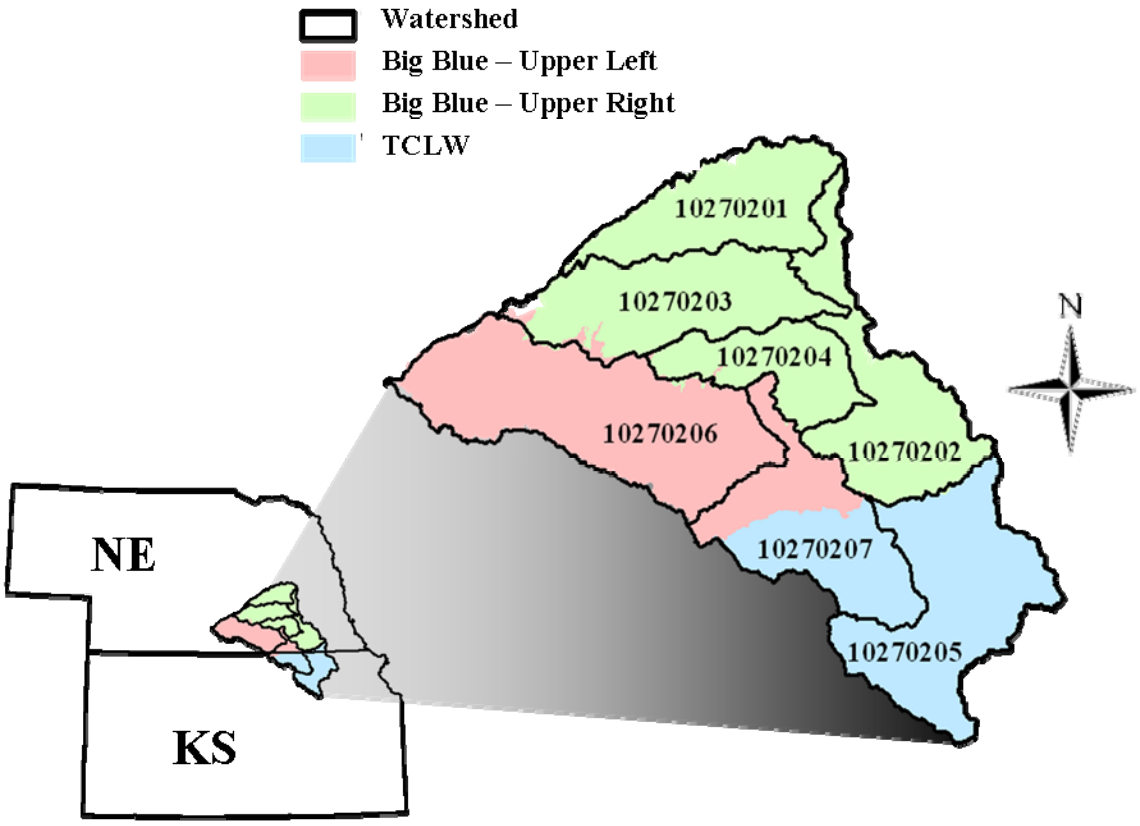

Figure 5-1. Study Area

The upper left watershed land use consists primarily of agricultural and range lands. Agricultural row crops make up 66% of the watershed, 25% of the watershed is designated as range land, and 5% is urban. Minimum and maximum elevations are 381 m and 668 m above mean sea level, respectively. The average watershed elevation is 530 m.

The upper right watershed has similar land use characteristics to the upper left. Agricultural row crops cover 79% of the land area, while range land takes up 12% of the watershed and urban is 5%. Minimum elevation is 363 m and maximum elevation is 601 m above mean sea level and the average watershed elevation is 480 m.

The TCLW is the focus of this study and is predominantly agricultural, with 40% of the watershed area devoted to agricultural row crops and 42% consisting of range land.

Total area of the TCLW is 6,158 km^2. Elevation in the TCLW ranges from 305 m to 513 m.

5.3.2 SWAT Model

SWAT is a watershed hydrology and water quality model developed by the United States Department of Agricultural Research – Agricultural Research Service (USDA-ARS) (Arnold et al., 1998). The model is physically based, spatially distributed, and designed to predict the impact of management practices on water, sediment, and agricultural chemical yields in complex watersheds with varying soils, land use, and land management practices over long time periods on a daily time-step (Gassman et al., 2007). In SWAT, a watershed is divided into subwatersheds based on elevation and river network. The subwatersheds are further divided into hydrologic response units (HRUs), which are areas consisting of homogeneous land use, soil type, slope, and management practices. Surface runoff, sediment, nutrients, and pesticides are generated at the HRU level, aggregated to the subbasin levels, and routed through the river network to the watershed outlet.

The user has two options for runoff volume calculations: the SCS curve number procedure and the Green and Ampt infiltration method (Neitsch et al., 2005).). The SCS curve number procedure is an empirical equation that calculates accumulated runoff with rainfall depth, initial abstraction (surface storage, infiltration, interception), and retention (spatial parameter based on soil, land use, management, and slope).

There are two options for calculating runoff volume in SWAT: the SCS curve number procedure and the Green and Ampt infiltration method (Neitsch et al. 2005). The SCS curve number procedure is an empirical equation that calculates accumulated runoff

with rainfall depth, initial abstraction (surface storage, infiltration, interception), and retention (spatial parameter based on soil, land use, management, and slope). Curve number drops as soil approaches wilting point and increases as the soil approaches saturation. The Green and Ampt infiltration method predicts infiltration assuming excess water at the surface at all time. Infiltration is calculated as a function of porosity, matric potential, and hydraulic conductivity. Water that does not infiltrate becomes surface runoff. The Green and Ampt infiltration method requires sub-daily precipitation data; however, this data is not available within the study area. Therefore, the SCS curve number procedure was used in this study.

In SWAT, soil erosion caused by rainfall and surface runoff is computed using the Modified Universal Soil Loss Equation (MUSLE) (Neitsch et al. 2005). MUSLE predicts sediment yield as a function of surface runoff volume, peak runoff rate, area, soil erodibility, land cover, land support practices, topography, and percent coarse fragments in top soil layer.

Channel sediment routing in SWAT is based on the maximum amount of sediment that can be transported from a reach segment, which is a function of peak channel velocity (Neitsch et al. 2005). Sediment routing is dominated by two processes: deposition and degradation. Degradation occurs when sediment concentration is less than maximum amount of sediment that can be transported from a reach segment, while deposition occurs when sediment concentration is greater than the maximum amount. In-stream nutrient processes are defined by the nitrogen and phosphorus cycle (Neitsch et al., 2005). The nitrogen cycle is a transformation of organic nitrogen to ammonia, nitrite, and finally to nitrate in aerobic water, which is a function of algal biomass that is

nitrogen and algal respiration rate. The in-stream phosphorus cycle is similar to the nitrogen cycle, where organic phosphorus is converted to soluble phosphorus available for uptake by algae or removed from the stream by settling (Neitsch et al., 2005).

Sediment deposition and degradation are the dominant processes in sediment routing, depending on whether sediment concentration is less than (degradation) or greater than (deposition) the maximum amount of sediment that can be transported from a reach segment. Nutrient routing in SWAT is modeled using the nitrogen cycle and the phosphorus cycle (Neitsch et al. 2005). Organic nitrogen and organic phosphorus may be removed from the stream by settling.

5.3.3 Observed Climate Data

Observed daily climate data from 1980-2002 was obtained from the National Climatic Data Center (NCDC) cooperative weather network. Average annual precipitation from 1978-2008 in the watershed was 839 mm. In TCLW, eight precipitation and six temperature stations were used. The upper left watershed contained 11 precipitation stations and seven temperature stations, while 14 precipitation and 11 temperature stations were used in the upper right watershed. Precipitation and temperature station locations are presented in Figure 5-2.

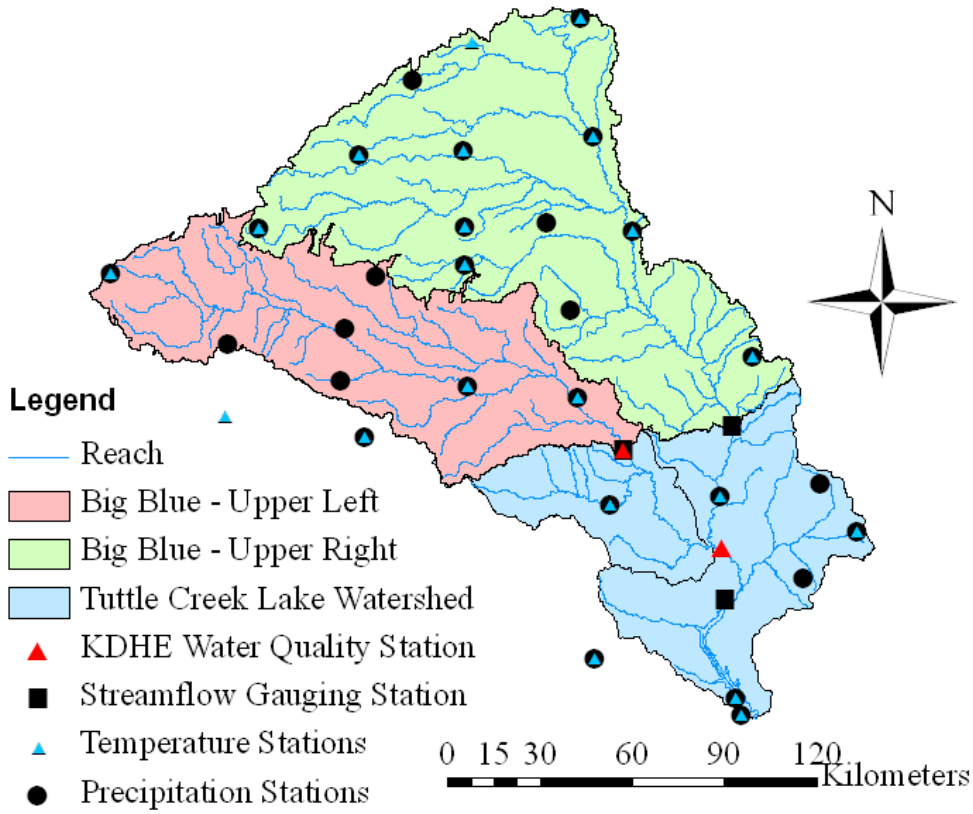

Figure 5-2. Precipitation stations, temperature stations, and model calibration locations (Right)

5.3.4 Climate Change Data

Data for the climate change scenarios was provided by the Community Climate System Model (CCSM-3) project (http://www.ccsm.ucar.edu), supported by the Directorate for Geosciences of the National Science Foundation and the Office of Biological and Environmental Research of the U.S. Department of Energy. The National Center for Atmospheric Research (NCAR) GIS Initiative provided CCSM-3 data in a geographic information system (GIS) format through GIS Climate Change Scenarios portal (http://www.gisclimatechange.org). The original monthly temperature and precipitation projection outputs from the National Center for Atmospheric Research (NCAR) GIS Initiative CCSM-3 are too coarse for use on the watershed scale. However,

the NCAR GIS Initiative also provided downscaled monthly temperature and precipitation at a scale of 4.5 km, which was used in this study (Hoar and Nychka, 2008).

Three Special Report on Emissions Scenarios (SRES) emissions scenarios were used in this research, as defined by Nakicenovic et al. (2000): A2, A1B, and B1. SRES scenarios are plausible alternative futures rather than specific predictions of future climate. The A2 scenario features prominent fossil fuel usage by developing countries and slow development of alternative fuel technologies by developed nations. By 2100, A2 has the highest atmospheric CO_2 concentration of the three scenarios used in this study. The A1B scenario is characterized by rapid economic growth and low population growth, while alternative energy and fossil fuel technologies have relatively equal market shares. The B1 scenario illustrates a world relying on resource conservation and environmental sustainability. Alternative energy dominates the market and fossil fuel use declines globally, leading to a slower increase in atmospheric CO_2 concentrations. A fourth non-SRES scenario was also used, entitled 20C3M. This scenario is a historical experiment characterized by greenhouse gases increasing as observed through the 20th century. 20C3M was used to compare results with the A1B, A2, and B1 climate change scenarios.

5.3.5 Model Setup

The SWAT model requires various spatial datasets for model setup, including elevation, land use, and soils data. Land use data was obtained from the Multi-Resolution Land Characteristics Consortium (MRLC) in the form of the National Land Cover Database 2001 (NLCD 2001) map. NLCD 2001 has a resolution of 30 m and contains 21

different land use classes (Homer et al., 2007). The NLCD 2001 does not subdivide agricultural lands to specific crops such as corn, soybean, or wheat. However, based on information obtained from the agricultural statistics (USDA-NASS, 2007) and stakeholder knowledge from common crop rotations in the watershed, the generic agricultural land within TCLW was split into six different land uses: corn-soybean (25%), continuous soybean (5%), continuous corn (15%), soybean-wheat (25%), continuous soybean (10%), and grain sorghum-soybean-wheat (20%).

Soil data was obtained from the U.S. Department of Agriculture (USDA) State Soil Geographic (STATSGO) database. STATSGO data is a 1:250,000 scale map that is linked to tabular data containing estimated physical and chemical soil properties (Muttiah and Wurbs, 2002). Elevation data (90 m resolution) was obtained from the Better Assessment Science Integrating point and Nonpoint Sources (BASINS) software version 4.0 (BASINS, 2007).

The SWAT model was setup separately for three sections of the Big Blue watershed (the upper left, upper right, and the TCLW). Twenty-three years (1980-2002) of daily observed climate data along with digital elevation model, land use maps, and soil maps were used to set up each model. A threshold value of 40 hectares was selected to define the HRU area. Five slope classes were used in HRU definition: 0-2%, 2-4%, 4-6%, 6-8%, and 8-99%.

5.3.6 Model Calibration and Validation

The TCLW, upper right, and upper left SWAT models were previously calibrated and validated for streamflow, sediment, total Kjeldahl nitrogen (TKN), and total phosphorus (TP) loads using historical observed climate data (Woznicki et al., 2010).

Daily calibration (1998-2000) and validation (2001-2002) was performed for the upper left at USGS #06884025 and TCLW at the US Army Corps Gauging Station. For the upper right, the daily calibration (1986-1989) and validation (1990-1993) location was USGS gage station number 06882000. A one year model warm up period was used prior to calibration. Calibration/validation locations are presented in Figure 2. Time steps vary for different constituents and watersheds due to limited data availability, particularly regarding sediment and nutrient observations.

Evaluation of model prediction capability was completed using the Nash-Sutcliffe Efficiency (NSE) (Nash and Sutcliffe, 1970) and coefficient of determination (R^2). NSE values can range from negative infinity to 1, where 1 indicates a perfect fit between observed data and model output data. Daily NSE values (combined calibration and validation) for the TCLW were 0.625 for streamflow, 0.563 for sediment, 0.256 for TKN, and 0.756 for TP. TCLW calibration and validation compared to observed data is presented in Figure 5-3.

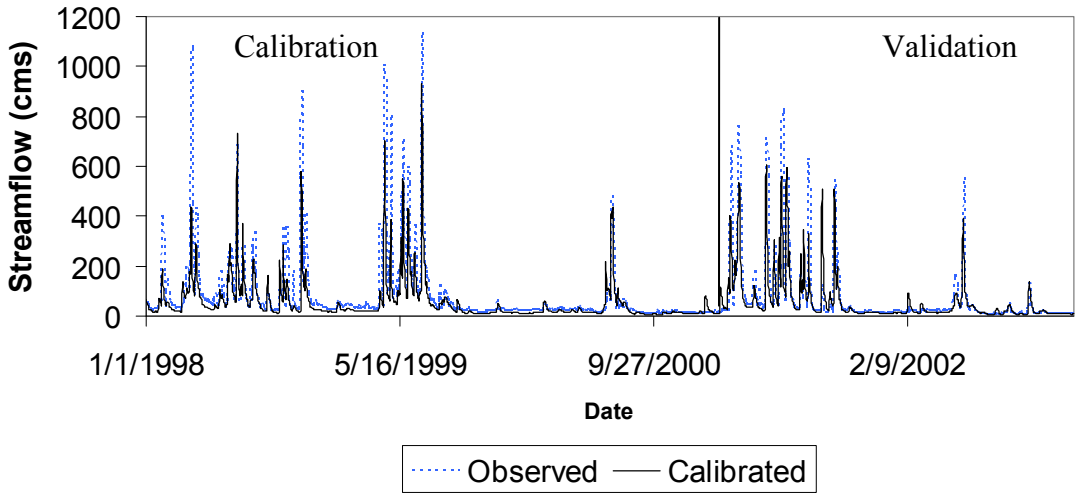

Figure 5-3. TCLW Calibration and Validation

According to performance ratings for NSE defined by Moriasi et al. (2007), streamflow and sediment can be considered satisfactory, TP can be considered very good, and TKN is unsatisfactory. Problems with TKN calibration and validation were likely due to lack of data for daily calibration (ten observations over the 20 year study period). In daily calibration, this quantity of observed data is inadequate for satisfactory calibration results. In addition, septic system usage and manure applications on agricultural land were not modeled. Although TKN calibration results were unsatisfactory, relative comparisons between model scenarios can still be made. Complete details regarding calibration and validation methods and results can be found in Woznicki et al. (2010).

5.3.7 Climate Change Scenarios

Downscaled monthly average total precipitation and monthly mean temperature data from the NCAR GIS Initiative were used to develop climate change scenarios. Monthly precipitation and temperature from the historical model (20C3M) spatial layer was extracted from each 4.5 km by 4.5 km cell containing a weather station with observed data. The 20C3M baseline time period selected was 1980-1999 for comparison of climate model data with observed temperature and precipitation data from the same time period. Future climate scenarios (A1B, A2, and B1) time periods were selected to be middle of the 21st century (2041-2060) centered on 2050. Observed average monthly precipitation and temperature data was then calculated for the period of study (1980-1999). The delta change method was used to generate daily precipitation and temperature

data from 20C3M for input into SWAT. Using differences in mean monthly temperature and precipitation between climate scenarios, the delta change method adjusts historical observed daily temperature and precipitation data on a monthly basis (Snover et al., 2003). Assumptions of the delta change method include: GCMs are more accurate in simulating relative changes between climate scenarios than the absolute values of a future scenario, there are no changes in climate variability, there are constant spatial patterns of climate, the number of wet days will remain constant, and minimum and maximum values of climate variables are scaled (Fowler et al., 2007).

Precipitation deltas (ratio) are calculated based on a percentage change between monthly 20C3M average and the monthly observed average and applied to daily observed data. Precipitation is not additive because precipitation is zero bounded (negative precipitation is not possible). The precipitation delta change method is described in equation 6.

$$P_{daily,20C3M} = P_{daily,obs}\left(\frac{P_{monthly,20C3M}}{P_{monthly,obs}}\right) \quad (6)$$

Where $P_{daily,\ 20C3M}$ is adjusted daily precipitation, $P_{daily,\ obs}$ is observed daily precipitation, $P_{monthly,\ 20C3M}$ is monthly average for 20C3M (1980-1999) precipitation, and $P_{monthly,\ obs}$ is monthly average (1980-1999) precipitation for the observed data from 1980-1999.

Temperature deltas (additive) are calculated based on the difference between monthly 20C3M average and the monthly observed average and applied to daily observed data. The temperature delta method is presented in equation 7.

$$T_{daily,20C3M} = T_{daily,obs} + \left(T_{monthly,20C3M} - T_{monthly,obs}\right) \quad (7)$$

Where $T_{daily,\ 20C3M}$ is adjusted mean daily temperature, $T_{daily,\ obs}$ is observed mean daily temperature, $T_{monthly,\ 20C3M}$ is monthly average temperature for 20C3M (1980-1999), and $T_{monthly,\ obs}$ is monthly average temperature for observed data (1980-1999). Monthly mean temperature deltas were applied to both minimum and maximum observed daily temperature.

Six temperature and eight precipitation stations were used to estimate delta change values between observed historical data and 20C3M for TCLW. The minimum and maximum deltas over all weather stations are presented in Figure 5-4. The 20C3M scenario over predicts by up to 116% in January and under predicts by about -72% in August. November and December precipitation is simulated most accurately by 20C3M, while January, August, and September are not reproduced well. Mean monthly temperature is under predicted by up to -0.6 °C in November and over predicted by up to 6.2 °C in August. Observed mean monthly temperature is simulated best by 20C3M in June and November and worst in July, August, and September.

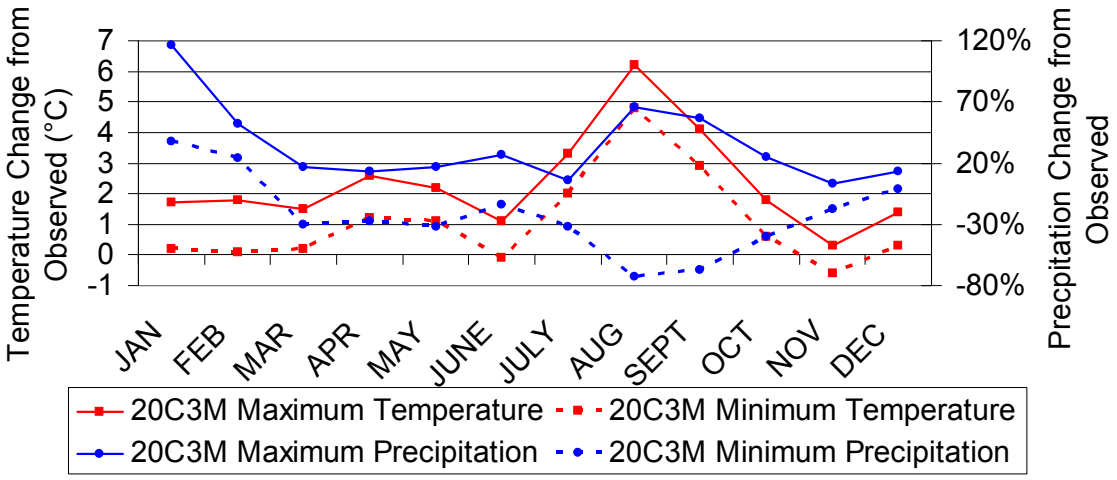

Figure 5-4. Minimum and maximum temperature deltas between observed historical and 20C3M

The delta change method was repeated using deltas calculated between observed data and each SRES emissions scenario (A1B, A2, B1). Delta ranges for each precipitation station between 20C3M and the future climate scenarios are presented in Figure 5-5. The A2 scenario had the greatest increase in precipitation (66.2% in August), while the A1B and A2 scenarios had the greatest temperature increases at 3.6 °C (September). Overall, B1 showed the smallest magnitude of changes from 20C3M.

Based on IPCC predictions for each emission scenario, atmospheric carbon dioxide (CO_2) concentration was considered to be constant. The atmospheric carbon dioxide concentration of 330 parts per million (ppm) CO_2 was used for the historical model and the 20C3M scenario. For year 2050, under the A2 and A1B scenario 525 ppm CO_2 was used and for the B1 scenario 475 ppm CO_2 was used (Houghton et al., 2001).

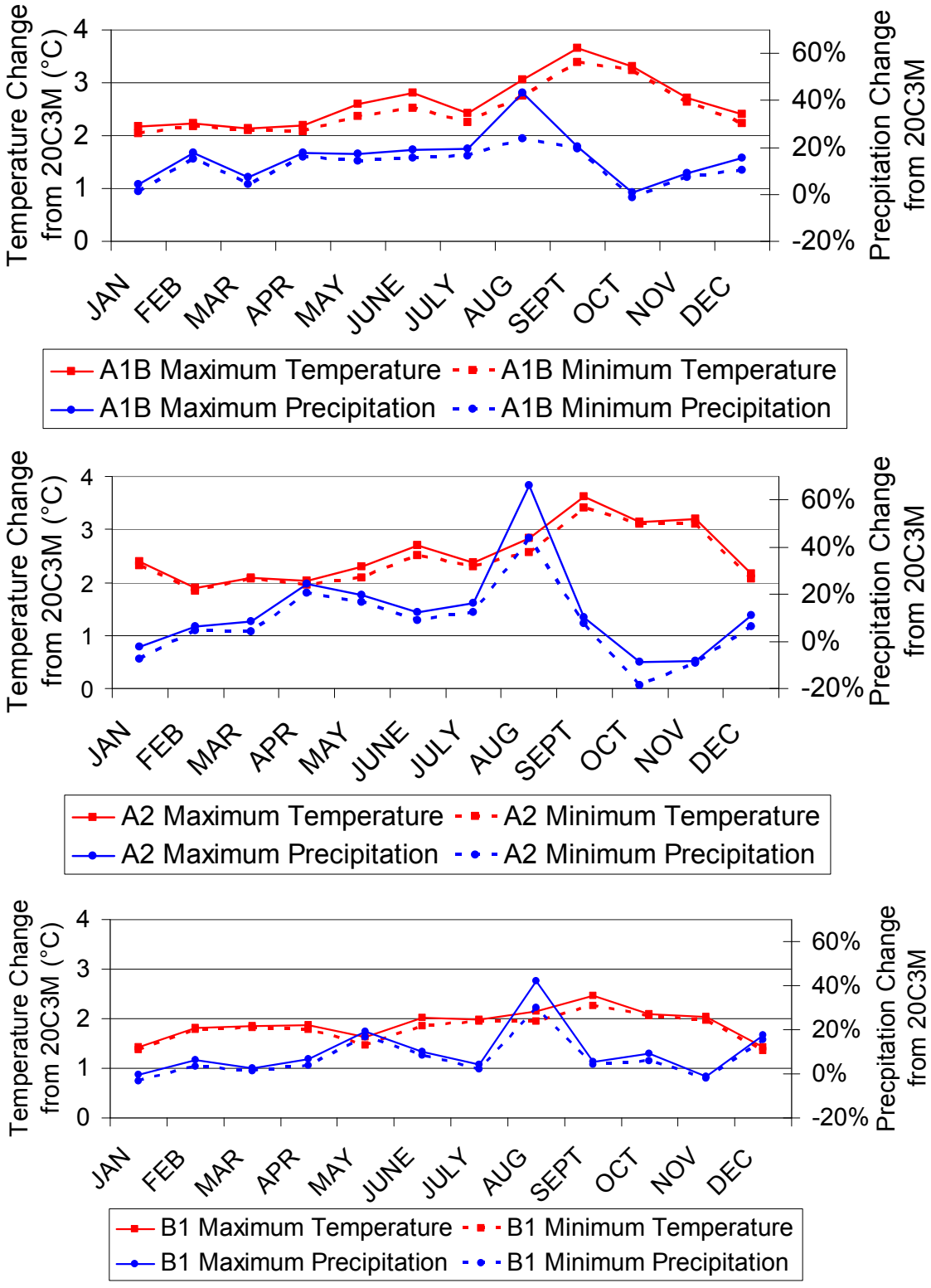

Figure 5-5. Minimum and maximum temperature deltas between 20C3M and A1B, A2, and B1

5.3.8 Representation of Best Management Practices in SWAT

Eight agricultural BMPs and a baseline scenario were implemented within SWAT for each climate scenario, for a total of 32 unique climate/BMP scenarios. No-tillage farming, conservation tillage farming, contour farming, terraces, filter strips, porous gully plugs, grazing management, and replacement of row crops with native grass were selected for representation within SWAT. The base scenario applied conventional tillage operations to each agricultural row crop.

5.3.8.1 Base Scenario (Conventional Tillage)

Conventional tillage operations on agricultural land were considered to represent the base scenario. One conventional tillage operations schedule was developed for each agricultural land use. An example of the soybean-winter wheat conventional tillage schedule is presented in Table 5-1. BMP applications that are not tillage operation based had conventional tillage applied in addition to the BMP. For example, the grazing management, porous gully plugs, filter strips, terraces, and contour farming scenarios also use conventional tillage on agricultural land.

Table 5-1. Example of a soybean-winter wheat conventional tillage operations schedule

Year	Crop	Operation	Application Rate	Date
1	SOYB	Tillage		March 27
1	SOYB	Tillage		April 15
1	SOYB	Tillage		May 14
1	SOYB	Planting		May 16
1	SOYB	Phosphorus fertilizer application	33 kg/ha	May 16
1	SOYB	Pesticide application	0.9 kg/ha	June 14
1	SOYB	Harvest and kill		October 1
1	WWHT	Tillage		October 10
1	WWHT	Nitrogen fertilizer application	65 kg/ha	October 15
1	WWHT	Phosphorus fertilizer application	31 kg/ha	October 15
1	WWHT	Planting		October 16
2	WWHT	Harvest and kill		July 1
2	WWHT	Tillage		August 1
2	WWHT	Tillage		September 1

5.3.8.2 No-Tillage Farming

No-tillage farming limits soil-disturbing activities of field operations to those necessary for planting crops and applying nutrients. No-tillage farming aims to reduce erosion caused by soil disturbing activities.

No-tillage operations were developed for the six crop rotations (corn-soybean, continuous corn, grain sorghum-soybean-winter wheat, continuous soybean, soybean-wheat, and continuous winter wheat) designated to agricultural land. One operations schedule was applied to a land use type based on the crops included in the schedule. An example of one of six no-tillage operations schedules (soybean-winter wheat) based on land use is presented in Table 5-2. The tillage operation that occurs on the day of planting is a no-till planter with a 5% mixing efficiency (EFTMIX). Mixing efficiency defines the fraction of materials (residue, nutrients, and pesticides) on the soil surface that are mixed through the soil depth specified by the tillage operation (Tuppad et al., 2010).

Table 5-2. Example of a soybean-winter wheat no-tillage operations schedule

Year	Crop	Operation	Application Rate	Date
1	SOYB	Pesticide application	0.9 kg/ha	April 30
1	SOYB	Tillage		May 5
1	SOYB	Planting		May 5
1	SOYB	Phosphorus fertilizer application	33 kg/ha	May 5
1	SOYB	Pesticide application	0.9 kg/ha	June 1
1	SOYB	Harvest and kill		October 1
1	WWHT	Nitrogen fertilizer application	65 kg/ha	October 15
1	WWHT	Phosphorus fertilizer application	31 kg/ha	October 15
1	WWHT	Planting		October 16
2	WWHT	Harvest and kill		July 1
2	WWHT	Pesticide application	0.9 kg/ha	August 1
2	WWHT	Pesticide application	0.9 kg/ha	October 15

5.3.8.3 Conservation Tillage Farming

Conservation tillage operations reduce soil disturbing activities to increase surface residue, but usually include some tillage practices (Tuppad and Srinivisan, 2008). Implementation of this BMP will reduce sheet and rill erosion while increasing soil moisture. Mixing efficiency for tillage operations in conservation tillage is specified to be 30% (Tuppad et al., 2010). An example of one of six conservation tillage operations schedules (soybean-winter wheat) is presented in Table 5-3.

Table 5-3. Example of a corn-soybean conservation tillage operations schedule

Year	Crop	Operation	Application Rate	Date
1	SOYB	Tillage		April 15
1	SOYB	Tillage		May 14
1	SOYB	Planting		May 16
1	SOYB	Phosphorus fertilizer application	33 kg/ha	May 16
1	SOYB	Pesticide application	0.9 kg/ha	June 14
1	SOYB	Harvest and kill		October 1
1	WWHT	Nitrogen fertilizer application	65 kg/ha	October 15
1	WWHT	Phosphorus fertilizer application	31 kg/ha	October 15
1	WWHT	Planting		October 16
2	WWHT	Harvest and Kill		July 1
2	SOYB	Tillage		August 1

5.3.8.4 Contour Farming

Contour farming changes runoff direction from downslope to around hill slopes through utilization of ridges formed by tillage and planting (USDA-NRCS, 2005). Sediment and contaminant transport is expected to be reduced by decreasing surface runoff energy, impounding water in depressions, and retaining more water on the field (Arabi et al., 2007).

To implement this practice in SWAT, the curve number (CN2) was reduced by three for agricultural land and the USLE practice factor (USLE_P) was reduced from its initial value of 1.0 to 0.5 or 0.6 based on slope. This method has previously been used in Arabi et al. (2007), Tuppad and Srinivasan (2008), and Tuppad et al. (2010).

5.3.8.5 Terraces

A terrace is an earth embankment, or a combination ridge and channel, constructed across a field slope (USDA-NRCS, 2005). Gully formation is limited and hill slope length is decreased to reduce erosion (Tuppad and Srinivasan, 2008). Surface runoff volume is also decreased by impoundment of water in small depressions (Arabi et

al., 2007). Sediment settling is increased by decreasing surface runoff energy (Arabi et al., 2007).

Terraces are incorporated in SWAT through adjustment of CN and USLE_P on agricultural row cropland in a similar manner to contour farming. CN value was reduced by five for agricultural land, while USLE_P was set to 0.12 or 0.10 based on the land slope (Arabi et al., 2007; Tuppad et al., 2010).

5.3.8.6 Filter Strips

Filter strips are areas of herbaceous vegetation placed between cropland, grazing land, or disturbed land and environmentally sensitive areas (USDA-NRCS, 2005). The purpose of filter strips is to reduce sediment, particulate organic nutrients, sediment absorbed contaminants, and dissolved contaminant loadings in runoff (Nejadhashemi and Mankin, 2007). Filter strips may also serve as a riparian buffer along streams.

SWAT has a built-in filter strip component (FILTERW) to add an edge-of-field filter strip of desired width to an HRU. Filter strip trapping efficiency for sediment, nutrients, and pesticides in surface runoff is calculated using an empirical equation based on the width of the filter strip (Neitsch et al., 2005). Filter strips were applied to all agricultural land in this study.

5.3.8.7 Porous Gully Plugs

Porous gully plugs are rocks or logs used to reduce surface runoff energy in ephemeral gullies and induce sediment settling (Tuppad and Srinivasan, 2008). This BMP is represented in SWAT through adjustment of the Manning's roughness coefficient (CH_N1), also known as Manning's "n" value, for tributary channels on subbasins

considered erodible. The CH_N1 value for BMP implementation was 0.05 on land with a subbasin slope greater than 0.05, while the initial CH_N1 value is 0.014 in SWAT (Tuppad and Srinivasan, 2008; Tuppad et al., 2010).

5.3.8.8 Grazing Management

Grazing management is used to prevent overgrazing of range grasses through reducing excessive biomass removal by animals. Sediment and nutrient yields are increased when land is overgrazed due to exposure of bare soil and increased soil compaction because of decreased infiltration and increased soil erosion and surface runoff (Tuppad and Srinivasan, 2008).

Grazing management is incorporated into SWAT through reduction of the harvest index (HVSTI) of range grass (Tuppad and Srinivasan, 2008). The harvest index is defined as the percentage of biomass removed in a harvest operation (in this case animal grazing). Remaining biomass is converted to residue on the soil surface, which protects soil from rain (reducing erosion) and decreases soil compaction (increasing infiltration). Initially, HVSTI is set to 90% for range grass, while in the initial BMP implementation scenario, HVSTI was set to 70%. A HVSTI greater than 100% results in the harvesting of below-ground biomass.

5.3.8.9 Native Grass

Native grass replacement consists of replacing land containing agricultural row crops with native tall grasses such as Indian switchgrass or big bluestem (Nejadhashemi and Mankin, 2007). Reduced sediment and nutrient transport to streams is expected because tillage and fertilizer needs are eliminated, while vegetative cover on the soil is

increased. To implement native grass (representing a mixture of native tall grass species) within SWAT, all agricultural row cropland was converted to range grass.

5.3.9 BMP Sensitivity Analysis

A BMP sensitivity analysis was performed under the four climate scenarios (20C3M, A1B, A2, and B1) to determine the range of possible impacts of BMP implementation on sediment and nutrient yields in the TCLW. The sensitivity analysis was performed on the calibrated model, which means that results presented in this study are "actual" sensitivities of the BMPs rather than theoretical sensitivity of the model by performing a global sensitivity analysis of all model parameters (Luo and Zhang, 2009). Parameters selected for the sensitivity analysis were obtained from previous studies regarding BMP implementation in SWAT (Behera and Panda 2006, Bracmort et al. 2006, Santhi et al. 2006, Arabi et al. 2007, Jha et al. 2007, Parajuli et al. 2008, Tuppad and Srinivasan 2008, and Tuppad et al. 2010). Ranges of sensitivity were determined by considering a reasonable range of the BMP implementation parameter obtained from published studies. Based on the type of studied parameters, variation may include entire defined parameter range, while in others it may be a percentage of the parameter range or a percentage of the initial BMP parameter value. Lenhart et al. (2003) performed a one-at-a-time sensitivity analysis by varying parameters by defining the variation range as a percentage of the parameter initial value or as a percentage of the entire parameter range and found that the results of each sensitivity analysis were not significantly different. For each BMP, one parameter that physically defines the process was altered randomly within the selected range of variation (Table 4) 50 times (Luo and Zhang, 2009). Therefore, eight BMPs were varied 50 times each for four climate scenarios, resulting in

1600 simulations. For each simulation, one input parameter was changed at a time while all other model parameters were kept constant. Relative sensitivity index was calculated for each BMP using equation 8:

$$S = \frac{y_i - y_o}{x_i - x_o} \frac{x_o}{y_o} \tag{8}$$

Where S is the relative sensitivity index, x_i is the ith BMP parameter value, x_o is the initial BMP parameter value, y_i is the model prediction of specific pollution resulting from the ith BMP parameter value, and y_o is the initial model prediction of specific pollution resulting from the initial BMP parameter value. BMP sensitivity was evaluated in terms of sediment, total nitrogen, and total phosphorus yields under each climate scenario. Greater magnitude of relative sensitivity index indicates higher sensitivity of the BMP. A positive relative sensitivity index indicates that increasing the parameter value increases the pollution yield relative to base scenario (initial parameter value used for a BMP), while a negative number indicates that increasing the parameter decreases the pollution yield relative to base scenario.

Table 5-4. BMP sensitivity analysis parameters

BMP	Parameter	Initial BMP Value	Range	Range Selection Method
No-tillage	EFTMIX	0.05	0.01 – 0.15	10% of entire range
Conservation tillage	EFTMIX	0.30	0.20 – 0.40	10% of entire range
Contour Farming	CN2	-3 from default	-1.5 – (-4.5)	50% of initial value
Terraces	CN2	-5 from default	-7.5 – (-2.5)	50% of initial value
Filter Strips	FILTERW	0	0 – 50	Entire range
Porous Gully Plugs	CH_N1	0.05	0.025 – 0.075	50% of initial value
Grazing Management	HVSTI	0.7	0 – 1.25	Entire range
Native Grass	CN2	Variable	-10% – 10%	10% of initial value

5.4 RESULTS AND DISCUSSION

5.4.1 BMP Relative Sensitivity

The results from long-term (twenty year) SWAT modeling showed that under the conventional tillage (base BMP) scenario, sediment, total nitrogen (TN), and total phosphorus (TP) yields increase in future climate scenarios (Table 5-5). The A1B scenario exhibits the greatest yields since it is experiencing the largest changes in climatological variables (precipitation, temperature, and carbon dioxide).

Annual sensitivity of BMPs allows us to make general inferences regarding how propagation of input variances (within the reasonable range) for BMPs will affect spatial planning and development decisions regarding water quality protection under future climate scenarios. Trends present in the BMP sensitivity analysis across climate change scenarios for sediment, TN, and TP are shown in Figures 5-6 through 5-9, 9-1 through 9-4, and 9-5 through 9-8, respectively. In addition, these figures tell us how BMP effectiveness may vary under future climate scenarios. For most BMPs, the annual

sensitivity indices for sediment, TN, and TP are relatively small across climate scenarios, although grazing management and native grass have sensitivities considerably greater than zero. The grazing management median sediment sensitivity index is 0.25 for 20C3M and 0.21 for the future climate scenarios, while native grass median sediment sensitivity is 1.70 for 20C3M and 3.00, 3.18, and 3.69 for A1B, A2, and B1, respectively. Conversely, no-tillage and porous gully plugs have the smallest median sensitivities for all pollutants. Therefore, it is expected that the native grass performance will be improved but more uncertain under future climate scenarios. We also observed that as we move from 20C3M to future climate scenarios, relative sensitivity index increases from A1B (lowest) to B1 (highest).

Table 5-5. Sediment, TN, and TP from the field for the base scenario

	20C3M	A1B	A2	B1
Sediment (metric tons)	1908000	2609000	2422000	2177000
TN (metric tons)	5762	7516	6982	6403
TP (metric tons)	1032	1384	1287	1180

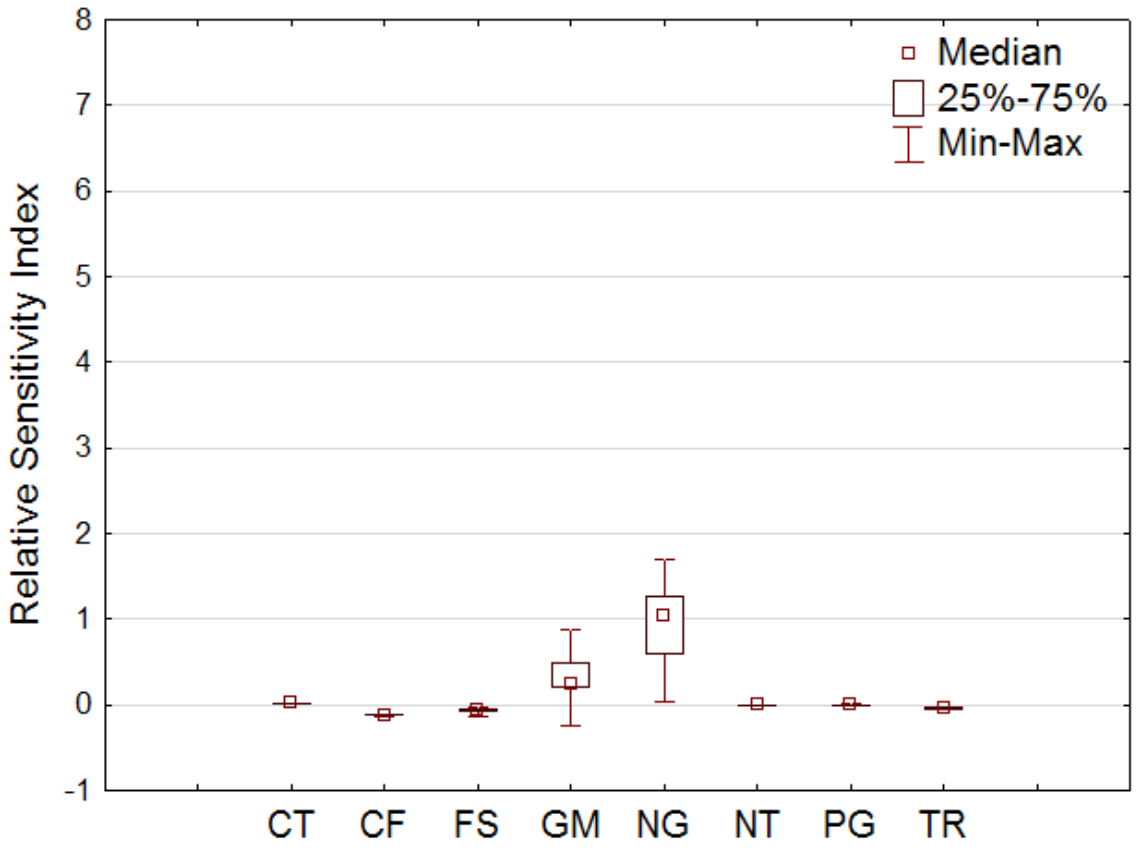

Figure 5-6. 20C3M sediment BMP sensitivity indices: conservation tillage (CT), contour farming (CF), filter strips (FS), grazing management (GM), native grass (NG), no-tillage (NT), porous gully plug (PG), and terraces (TR)

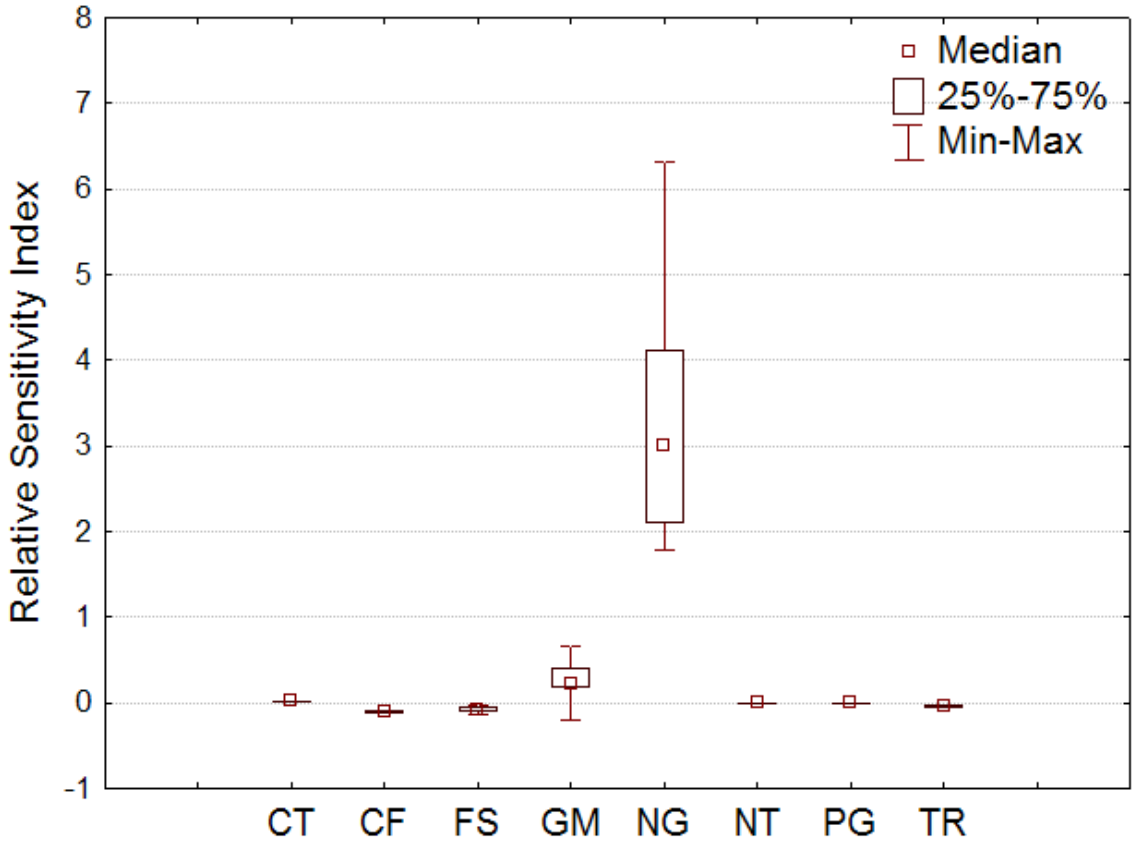

Figure 5-7. A1B sediment BMP sensitivity indices

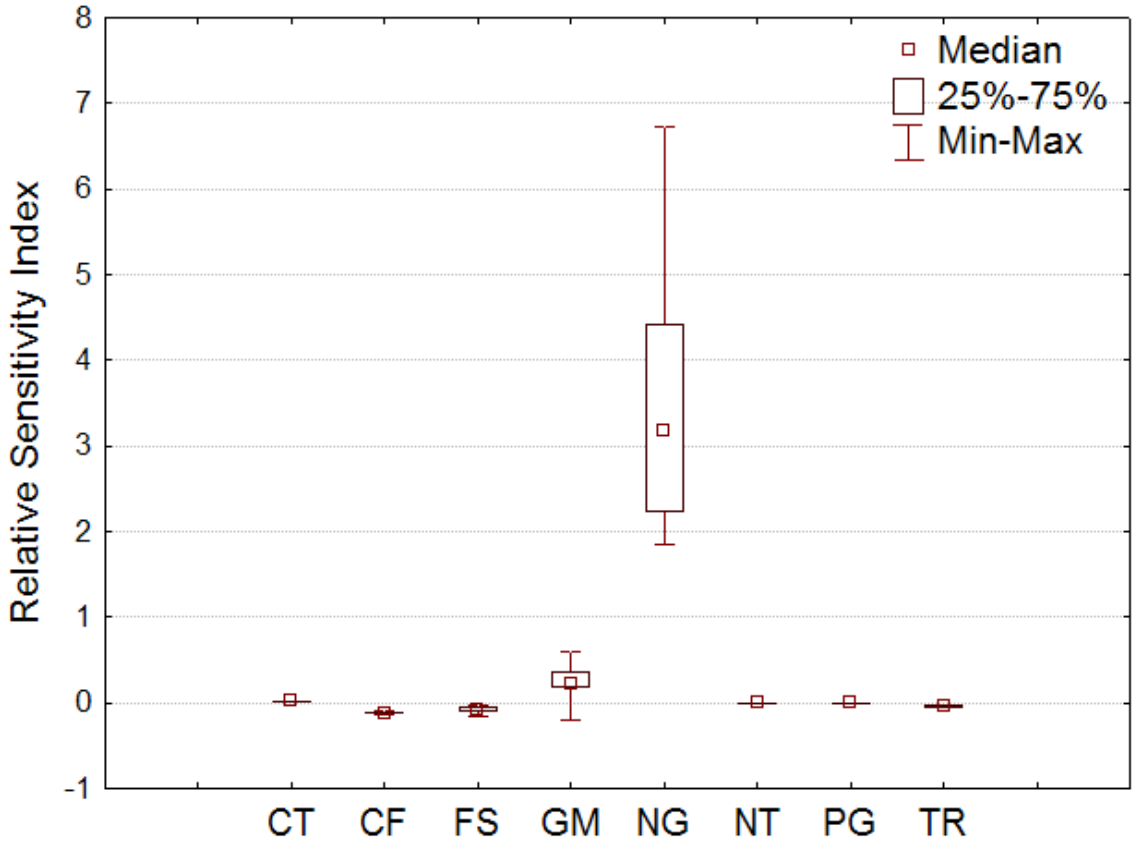

Figure 5-8. A2 sediment BMP sensitivity indices

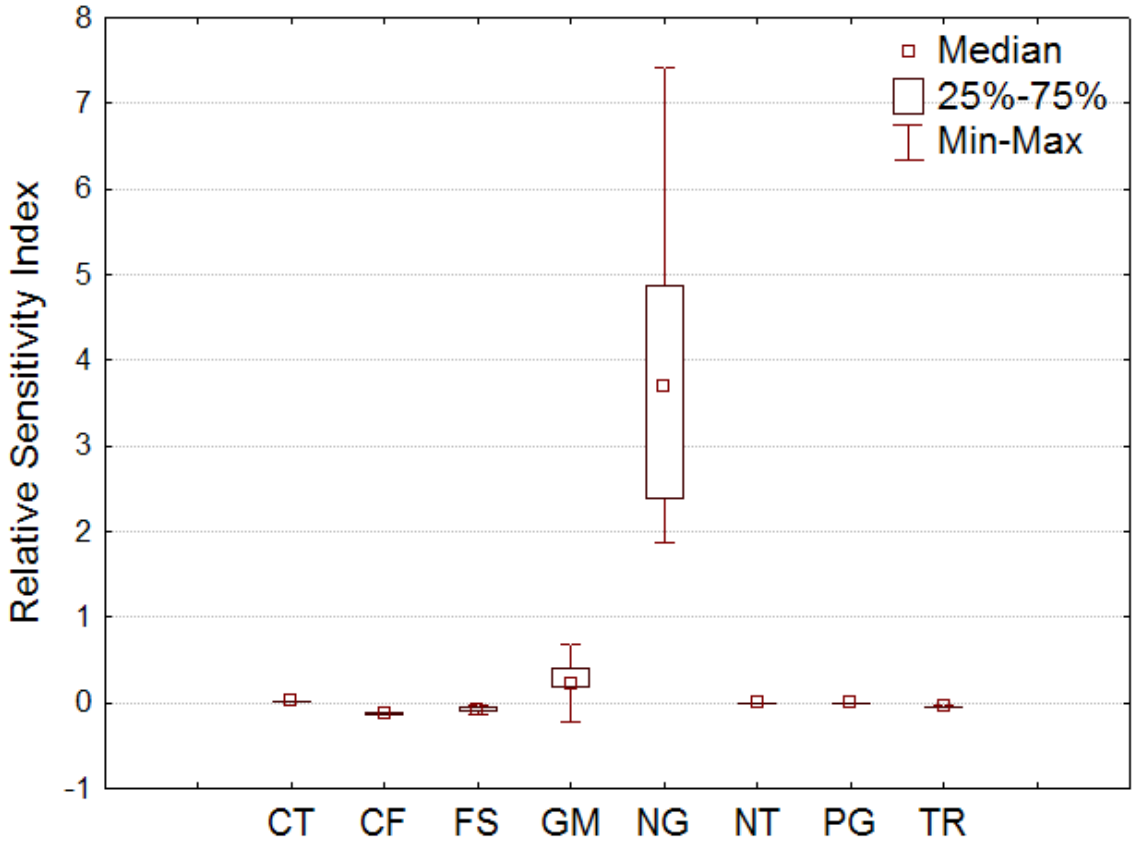

Figure 5-9. B1 sediment BMP sensitivity indices

5.5 Relative Sensitivity Impacts on Pollution Reduction

Sediment, TN, and TP yields from the field at the watershed scale as a function of parameter variation for each BMP application and climate scenario are presented in figures 5-10 through 5-17, and 9-9 through 9-24. These figures provide a visual representation of sensitivity trend and how it may change with changing climate. In the case of filter strips, variation in BMP performance is presented in the form changes in the filter strip width. Overall, some BMPs are revealed to be more sensitive than others. Within a certain climate scenario, as the physical parameters defining conservation tillage, porous gully plugs, no-tillage, and terraces change, graphically there is little change in sediment, TN, and TP produced from agricultural fields. However, for native

grass, filter strips, contour farming, and grazing management, the reverse is true: the relationship between input parameters and pollution generation is profound across the parameter range, which represent higher sensitivities. Sediment, TN, and TP reduction efficiency ranges are presented in Table 5-9. Greater efficiency ranges indicate that the BMP is less reliable across its implementation range. Meanwhile, higher efficiency values indicate that the BMP is more effective at sediment and nutrients reduction. In the following section, BMP variability is discussed in more detail across and within each climate scenario:

Table 5-6. Sediment, TN, and TP reduction efficiency ranges

	BMP	20C3M	A1B	A2	B1
Sediment Reduction	Conservation Tillage	5.0 – 6.0%	4.5 – 5.6%	4.9 – 6.0%	4.9 – 6.1%
	Contour Farming	32.1 – 39.5%	33.6 – 40.2%	34.0 – 41.0%	34.2 – 41.7%
	Filter Strips	31.3 – 57.5%	33.6 – 61.6%	33.7 – 61.9%	33.6 – 61.7%
	Grazing Management	-11.5 – 32.1%	-8.8 – 28.1%	-7.8 – 27.8%	-9.0 – 28.6%
	Native Grass	46.0 – 56.1%	4.3 – 51.4%	2.1 – 51.8%	0.7 – 52.5%
	No Tillage	10.0 – 10.2%	10.2 – 10.4%	10.6 – 10.8%	10.3 – 10.5%
	Porous Gully Plug	0.1 – 0.3%	0.1 – 0.3%	0.1 – 0.3%	0.1 – 0.3%
	Terraces	53.0 – 54.9%	56.6 – 58.2%	56.9 – 58.6%	56-8 – 58.7%
TN Reduction	Conservation Tillage	2.5 – 3.4%	2.6 – 4.1%	2.6 – 4.0%	2.6 – 3.8%
	Contour Farming	25.5 – 34.7%	25.4 – 33.1%	25.8 – 34.0%	26.3 – 35.2%
	Filter Strips	32.5 – 60.2%	33.9 – 62.8%	33.9 – 62.9%	33.9 – 62.8%
	Grazing Management	-5.9 – 24.1%	-4.3 – 19.6%	-3.8 – 19.3%	-4.6% - 20.8%
	Native Grass	44.7 – 56.4%	17.0 – 50.2%	15.2 – 50.6%	12.6 – 51.4%
	No Tillage	1.1 – 2.2%	4 – 5.8%	3.3 – 4.9%	2.1 – 3.5%
	Porous Gully Plug	0.0 – 0.2%	0.0 – 0.2%	0.0 – 0.2%	0.1 – 0.2%
	Terraces	49.0 – 52.8%	51.2 – 53.8%	51.3 – 54.2%	51.6 – 54.7%
TP Reduction	Conservation Tillage	1.0 – 1.3%	1.3 – 1.3%	1.2 – 1.3%	1.1 – 1.2%
	Contour Farming	31 – 41.5%	30.6 – 39.7%	31.0 – 40.7%	31.6 – 41.9%
	Filter Strips	38.2 – 70.1%	40.2 – 73.7%	40.2 – 73.7%	40.0 – 73.4%
	Grazing Management	-4.6 – 19.2%	-3.2 – 15.0%	-2.9 – 14.7%	-3.4 – 16.0%
	Native Grass	59.4 – 68.0%	39.9 – 64.6%	38.5 – 64.8%	36.3 – 65.1%
	No Tillage	-9.7 – (-6.7%)	-6.1 – (-3.8%)	-7.2 – (-4.7%)	-9.0 – (-6.3%)
	Porous Gully Plug	0.1 – 0.2%	0.1 – 0.2%	0.0 – 0.1%	0.0 – 0.2%
	Terraces	59.5 – 63.8%	61.5 – 65.2%	61.7 – 65.6%	61.8 – 65.9%

Filter strips: Median filter strip sensitivity increases in future climate scenarios for sediment, TN, and TP (Figures 5-6 through 5-9, 9-1 through 9-4, and 9-5 through 9-8). The scenario with the greatest precipitation (A1B) has the highest sensitivity and the

lowest sensitivity is in the scenario with the least precipitation (20C3M). As it shown in Figures 5-10, 9-11, and 9-19, for all climate scenarios, as width of the filter strips was increased, sediment, TN, and TP from agricultural fields was reduced. At about 30 m, filter strips reached 99% of their possible reduction capabilities. The trend followed the empirical equation, $Trapping\ Efficiency = 0.367(width\ of\ filter\ strip\ in\ meters)^{0.2967}$ (Neitsch et al., 2005), that is used to represent sediment, TN, and TP trapping efficiency in SWAT. Therefore, it can be concluded that filter strips were more sensitive at smaller widths, while sensitivity was greatly decreased if the width was increased to 30 m or greater. Across climate change scenarios, sensitivity slightly increases from 20C3M to A1B, A2, and B1. There is slight maximum reduction efficiency increases in future climate scenarios from conventional tillage (no-BMP scenario): 58% for 20C3M, 62% for A1B, 62% for A2, and 62% for B1 (sediment), but range of reduction (maximum minus minimum) increases: 26% for 20C3M, 28% for A1B, 28% for A2, and 28% for B1 (Table 5-9). Similar trends are present for TN and TP, although maximum TP reduction is greater than sediment and TN (Table 5-9).

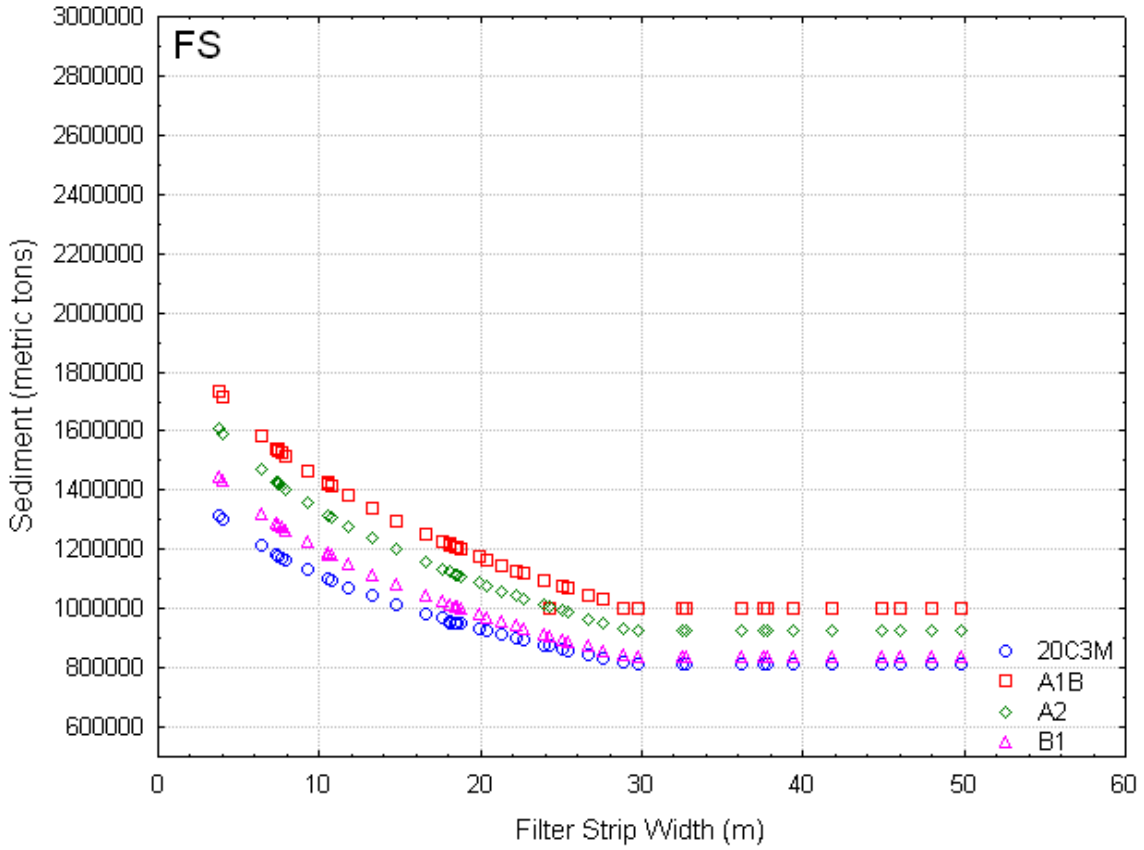

Figure 5-10. Filter strip sediment yield versus filter strip width

Grazing management: Grazing management on rangeland within TCLW was the second most sensitive BMP in all climate scenarios (Figures 5-6 through 5-9, 9-1 through 9-4, and 9-5 through 9-8) for sediment and TN, and third for TP. For example, the median sediment sensitivity was greatest for 20C3M (0.25) and smallest for A1B (0.21) and A2 (0.21). This trend among the climate scenarios suggests that as climate variables increases, grazing management becomes less sensitive to input variation. Maximum reduction efficiencies under all climate scenarios are around 30% for sediment, while they are close to 20% for TN and TP (Table 5-9). Meanwhile, smaller ranges of reduction efficiencies for sediment, TN, and TP in future climates were observed, as presented in Table 5-9. Grazing management reduction efficiency for sediment is 44% for 20C3M,

37% for A1B, 36% for A2, and 38% for B1. Therefore, grazing management may be more reliable for BMP implementation in future climate, but less effective in overall pollution reduction. Figures 5-11, 9-12, and 9-20 depict two specific trends regarding changes in grazing management performance. As the harvest index increases from 0% to 100%, pollutants yield increases due to residue losses, which protect the soil from erosion. When the parameter is increased to greater than 40% of its initial value (100% of harvest index), sediment, TN, and TP generation from agricultural fields dramatically decreases. At this point, all above-ground biomass has been harvested and below-ground biomass is now removed from the system. It is expected that sediment and nutrient yields would further increase due to increases in harvest index greater than 100%, however model results show this is not the case. Poor representation of this BMP within the model or a model artifact may cause this problem.

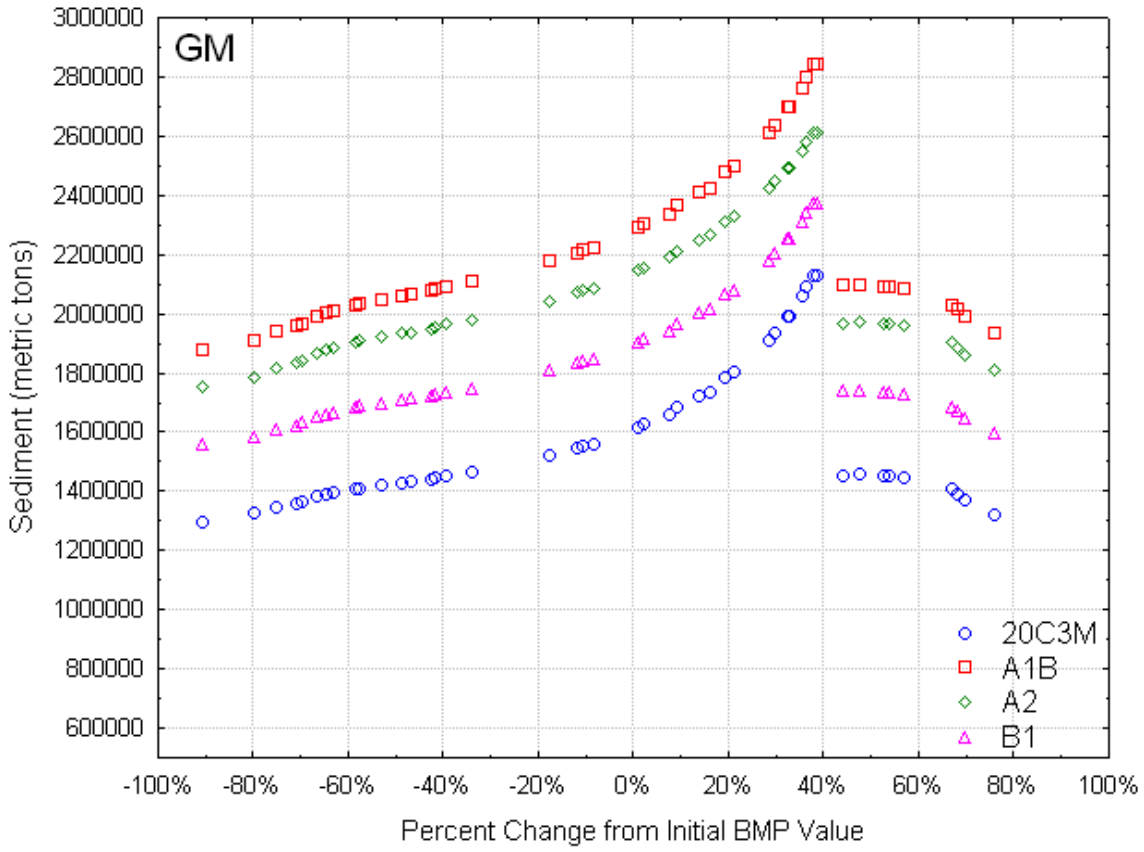

Figure 5-11. Grazing management sediment yield versus percent parameter change

Native Grass: Conversion of agricultural lands to native grass or conservation reserve program is highly effective at sediment, TN, and TP reduction in the TCLW (Table 5-9). Meanwhile, the sensitivity index increases for all three future climate scenarios from 20C3M (Figures 5-6 through 5-9, 9-1 through 9-4, and 9-5 through 9-8). Native grass is also highly sensitive to changes in its manner of implementation (especially large increases in curve number) and climate, as shown in Figures 5-12, 9-13, and 9-21. As curve number is increased by 4% or more, the slope of the input/output graph increases significantly, indicating increased sensitivity with greater curve numbers on native grass. Increases in sensitivity with changing climate suggest that increasing precipitation on native grass has a large impact on pollution generation due to increased

runoff. Similarly, increasing curve number of native grass has a large effect on NPS pollution generation. Maximum reduction efficiencies for native grass are high for all climate scenarios: sediment and TN are about 50% and TP is about 65%. Range of reduction efficiency changes as in sediment: 10% for 20C3M, 47% for A1B, 50% for A2, and 53% for B1. Similar trends were observed for TN and TP. Although reduction efficiency of native grass is highest of any BMP, the highly variable magnitudes of sediment, TN, and TP reduction ranges with changing climate indicates the application of native grass on agricultural lands will be more effective but less reliable under future climate scenarios.

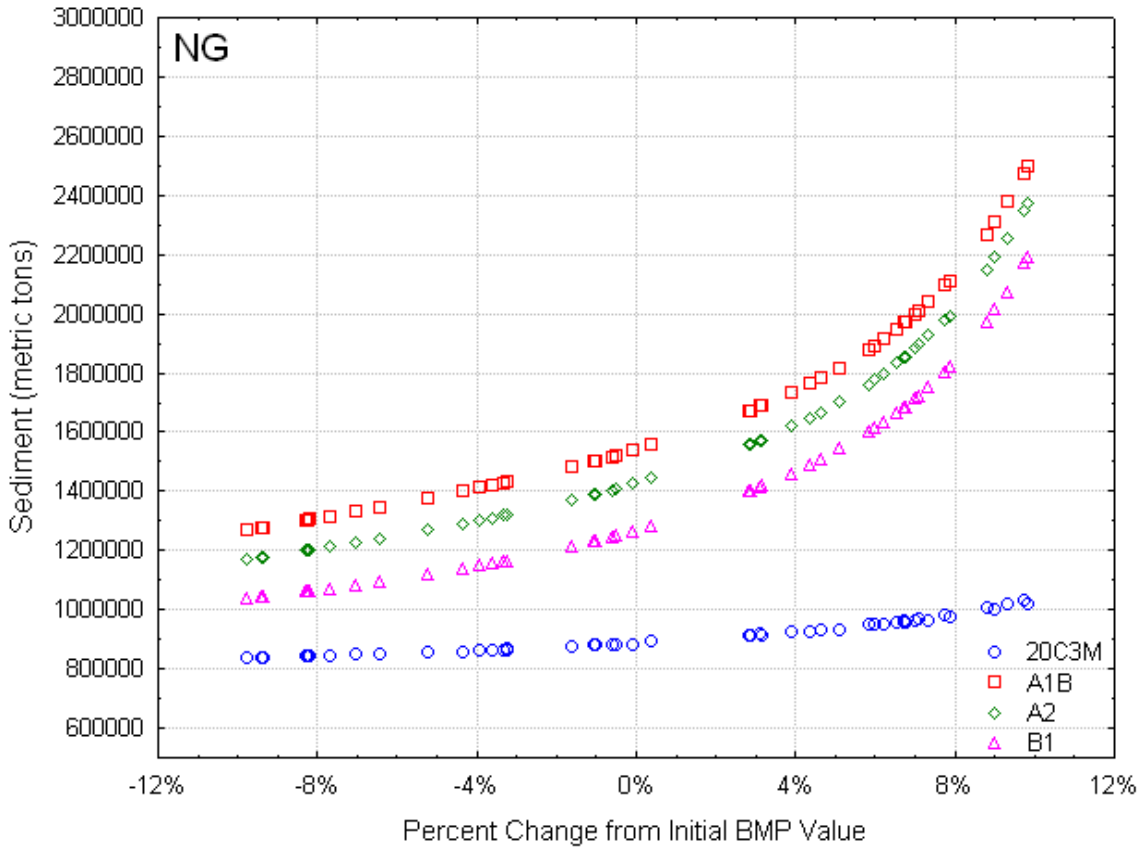

Figure 5-12. Native grass sediment yield versus percent parameter change

Conservation tillage: Conservation tillage does not exhibit much change in sensitivity between climate scenarios (Figures 5-6 through 5-9, 9-1 through 9-4, and 9-5 through 9-8). This is supported by the small range of pollution reduction within acceptable level of parameter changes that control conservation tillage. Sediment reduction from conventional tillage (no BMP scenario) ranges between 5-6% for each climate scenario, indicating that sensitivity and performance do not change much in future climate (Table 5-9). Reduction efficiency for conservation tillage ranges are about 3-4% for TN and 1% for TP (Table 5-9). Figures 5-13, 9-10,and 9-18 depict the lack of changes in sediment, TN, and TP yields from agricultural fields due to implementation of conservation tillage (altering mixing efficiency in tillage operations). Slightly higher

reduction efficiencies occur as the mixing efficiency decreases. This indicates that while the BMP does not have high reduction efficiency, if implementation deviates from recommended mixing efficiency, performance will change little in current and future climate scenarios.

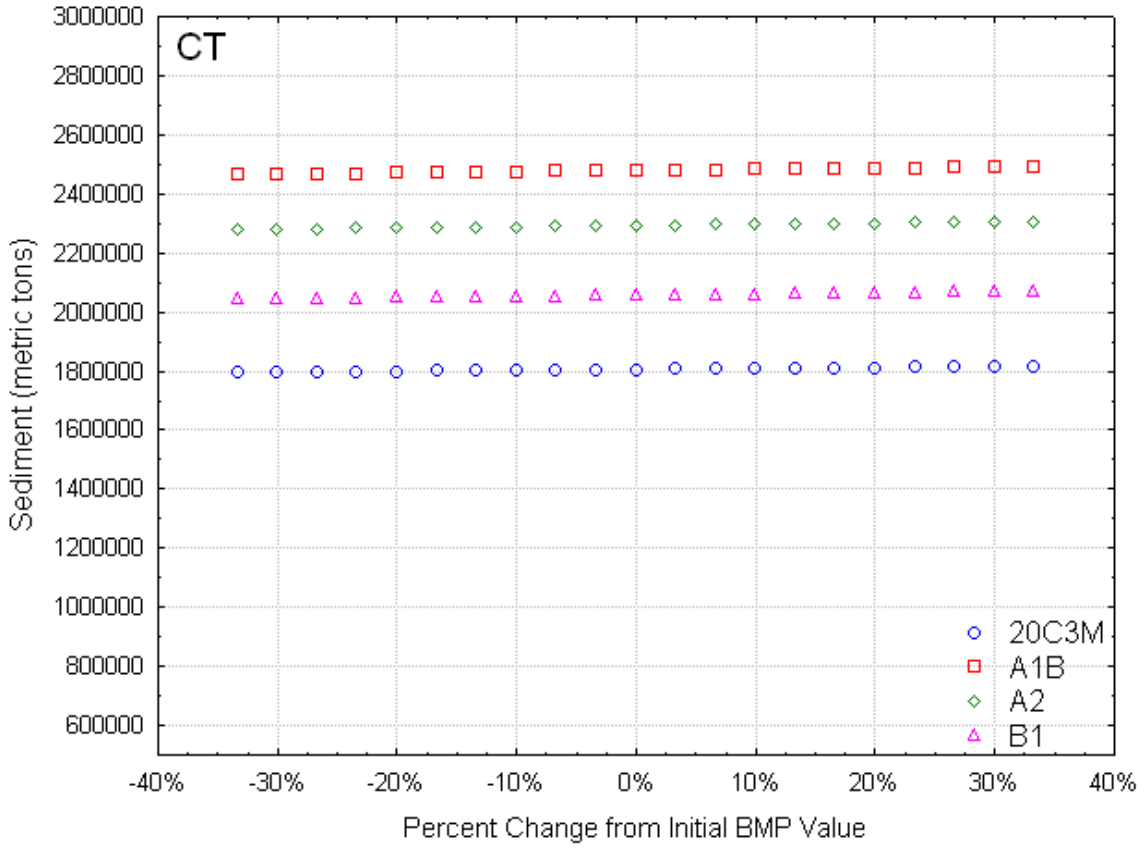

Figure 5-13. Conservation tillage sediment yield versus percent parameter change

No-Tillage: The no-tillage BMP is very similar to conservation tillage; there is little change in sensitivity between climate scenarios (Figures 5-6 through 5-9, 9-1 through 9-4, and 9-5 through 9-8). The difference between minimum and maximum reduction efficiency for each climate scenario is 0.2% for sediment and TN, indicating that the BMP is insensitive to changes in climate (Table 5-9). Figures 5-14, 9-14, and 9-22 demonstrate the lack of changes in sediment yield, TN, and TP from agricultural fields

due to implementation of no-till practice (altering mixing efficiency of tillage operations). Maximum sediment and phosphorus reduction efficiencies occurred at the lowest mixing efficiencies while maximum nitrogen reduction efficiency occurred at the highest mixing efficiency. Meanwhile, small changes for sediment, TN, and TP yields were estimated across climate scenarios: 10.2% in 20C3M, 10.4% in A1B, 10.8% in A2, and 10.5% in B1. Overall, compared to other BMPs, reduction efficiency of no-till practices are limited; however, the relative low sensitivity allows for dependable implementation in current and future climates.

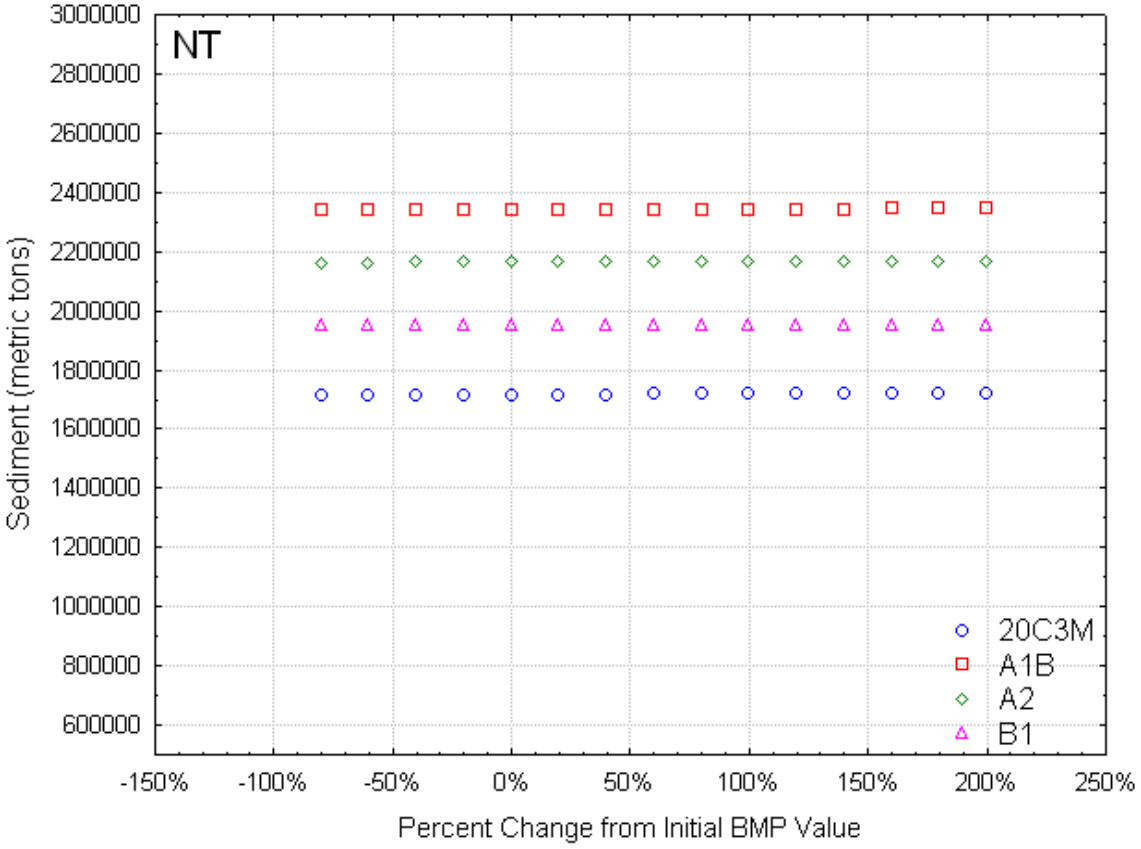

Figure 5-14. No-tillage sediment yield versus percent parameter change

Porous gully plugs: Relative sensitivity for porous gully plugs was the lowest among studied BMPs across all climate scenarios (-0.005 for sediment, -0.002 for TN,

and 0.001 for TP). Minimum and maximum reduction efficiency range with change in BMP implementation is relatively small across climate change scenarios: 0.3% for 20C3M, 0.2% for A1B, 0.2% for A2, and 0.3% for B1. This suggests that porous gully plugs effectiveness is not sensitive and limited to climate changes. Figures 5-15, 9-15, and 9-23 show that changes in the physical parameter that defines porous gully plugs (CH_N1) does not have a large effect on sediment, TN, and TP yields from agricultural fields. Luo and Zhang (2009) reported similar results for sediment load, where Manning's roughness for the tributary channel had an average sensitivity of 0.01, while TN and TP sensitivities were not reported in their study. Visually, the slopes in Figures 5-15, 9-15, and 9-23 are close to zero, confirming the low sensitivity. Maximum sediment, TN, and TP reduction (0.3%, 0.2%, and 0.2%, respectively) occurred with maximum increase in the BMP parameter. Although the BMP may be reliable in future climate scenarios, low reduction efficiency of porous gully plugs makes this BMP a less attractive alternative for pollution control in this watershed. However, this BMP can be very useful in areas that gully erosion is the primary source of pollution.

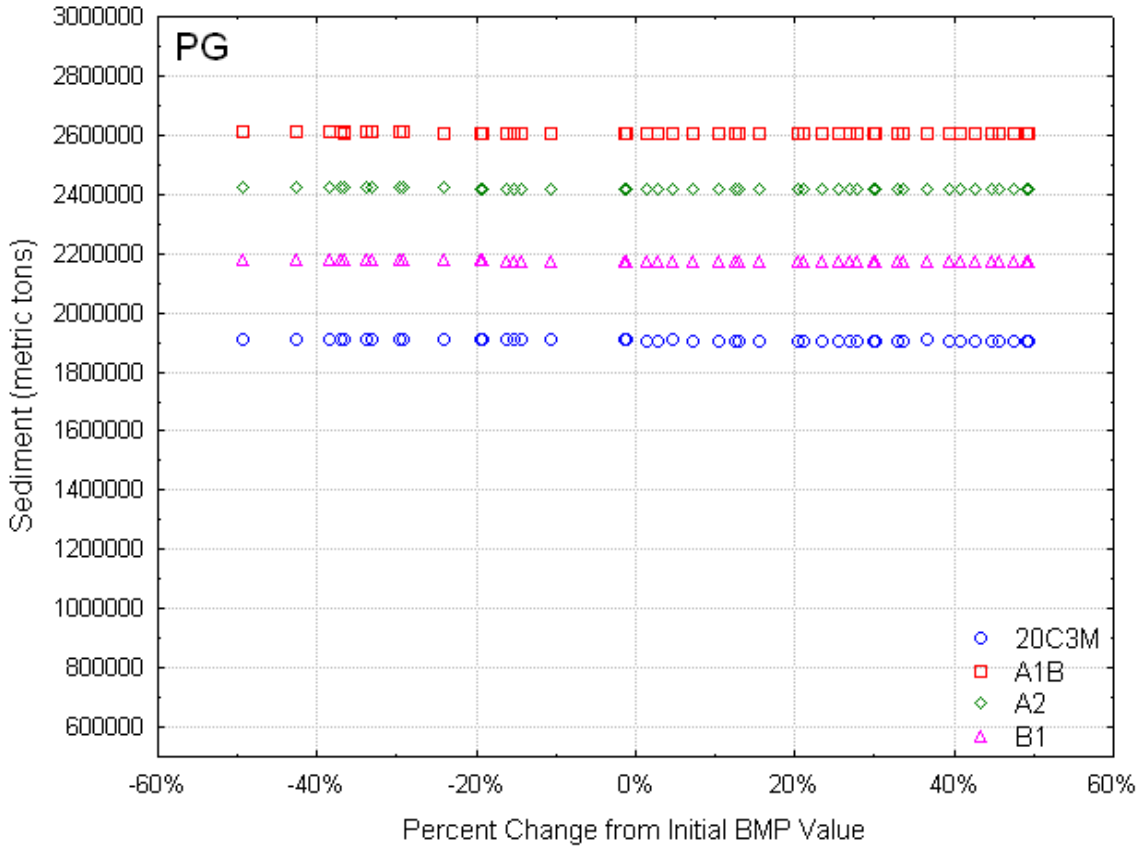

Figure 5-15. Porous gully plug sediment yield versus percent parameter change

Contour farming: Contour farming annual sediment, TN, and TP sensitivity is relatively constant across climate scenarios (Figures 5-6 through 5-9, 9-1 through 9-4, and 9-5 through 9-8). This BMP is the third most sensitive for sediment and TN, only native grass and grazing management are higher, while it is the second most sensitive for TP. Range between maximum and minimum reduction efficiency are mixed between different climate scenarios. For example, sediment reduction efficiency is 7.4% for 20C3M, 6.6% for A1B, 7% for A2, and 7.5% for A1B. This makes it difficult to reach a solid conclusion about overall impact of climate change on this BMP. Visually there is little slope in the sediment/TN/TP versus percent change in BMP implementation, as shown in Figures 5-16, 9-9, and 9-17. As curve number increases, the sediment, TN, and

TP from agricultural fields increases. This is expected due to increased runoff and therefore, increased sediment and nutrient transport. The effect of increasing curve number is not as severe as for the native grass scenario, which is due to the added implementation of the USLE practice factor (USLE_P) for both terraces and contour farming. Maximum reduction efficiency was relatively high under all climate scenarios: for sediment, it was 40% for 20C3M, 40% for A1B, 41% for A2, and 42% for B1. Similar trends were observed for TN and TP. These results demonstrate that contour farming is very effective at NPS pollution reduction from the field, and in future climates, deviation from recommended implementation as described in SWAT will have little effect on reduction outcomes.

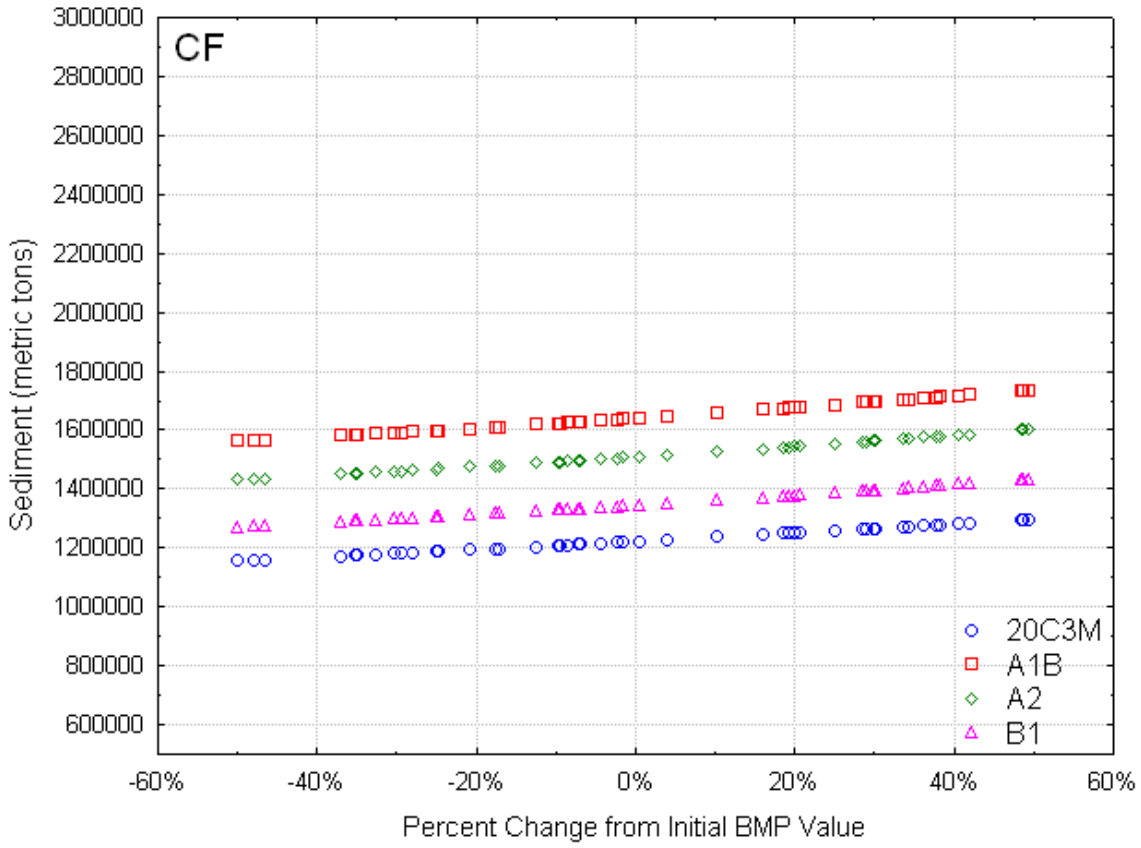

Figure 5-16. Contour farming sediment yield versus percent parameter change

Terraces: Terraces have comparable sensitivity trends across climate scenarios; although the sensitivity is relatively lower (Figures 5-6 through 5-9, 9-1 through 9-4, and 9-5 through 9-8). Ranges of minimum and maximum reduction with changes in parameter are small and similar across all for sediment, TN, and TP: 2%, 3%, and 4%, respectively for all climate scenarios. These small ranges indicate that terraces have a relatively high reliability in performance compared to other BMPs. Figures 5-17, 9-16, and 9-24 demonstrate the small changes in sediment, TN, and TP across parameter changes for terraces. With increasing curve number, reduction efficiency is lower, but the lower efficiency is mitigated by the implementation of the USLE practice factor, similar to contour farming. Maximum reduction efficiencies are high for terraces, as sediment is

55% (20C3M), 58% (A1B), 57% (A2), and 59% (B1);TN is 53% (20C3M), 54% (A1B), 54% (A2), and 55% (B1);TP is 64% (20C3M) 65% (A1B), 66% (A2), and 66% (B1). Therefore, terraces are an effective BMP for sediment, TN, and TP reduction in current and future climate and their reliability of implementation is high as well due to low relative sensitivity.

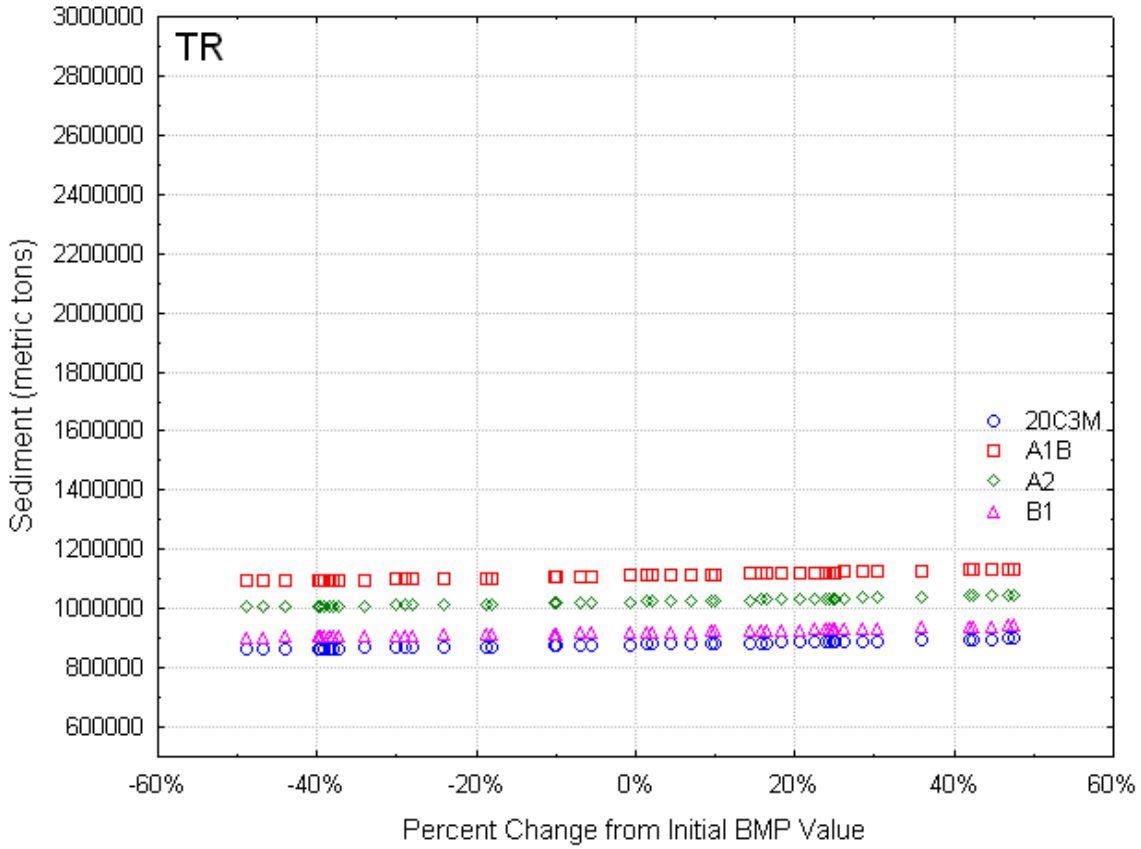

Figure 5-17. Terrace sediment yield versus percent parameter change

5.5.1 Monthly Sensitivity

Monthly BMP sensitivity demonstrates how seasonal changes in precipitation and temperature affect sediment, TN, and TP yields, and therefore, which months are likely to be more susceptible to future climates. Average monthly sensitivity for each BMP across four climate scenarios is presented in Figures 5-18 through 5-25 for sediment and Figures

9-25 through 9-32 (TN) and 9-33 through 9-40 (TP) in the appendix. Analyzing monthly trends also reveals tendencies that are not evident in the annual sensitivity data.

Conservation tillage (Figures 5-18, 9-25, 9-33) and no-tillage (Figures 5-19, 9-30, 9-38) have similar trends of higher sensitivities in wetter months and lower sensitivities in drier months. The wetter months (May and June) are also when planting and tillage occurs for most of the crop rotations. Therefore, altering the mixing efficiency of tillage-based BMPs has a greater impact on pollution generation from agricultural lands during wetter months. For conservation tillage and no-tillage, as mixing efficiency is increased, TP from the field decreases. As a result, applied phosphorus is more evenly distributed through the shallow soil layers in which the phosphorus is bound to soil particles, reducing transport ability. Meanwhile, across climate scenarios, there is modest change in sensitivity, indicating that there is little uncertainty about performance of these BMPs in plausible future climates. Furthermore, the low sensitivity indicates small changes in mixing efficiency of tillage operations may have little impact on BMP performance under future climate scenarios.

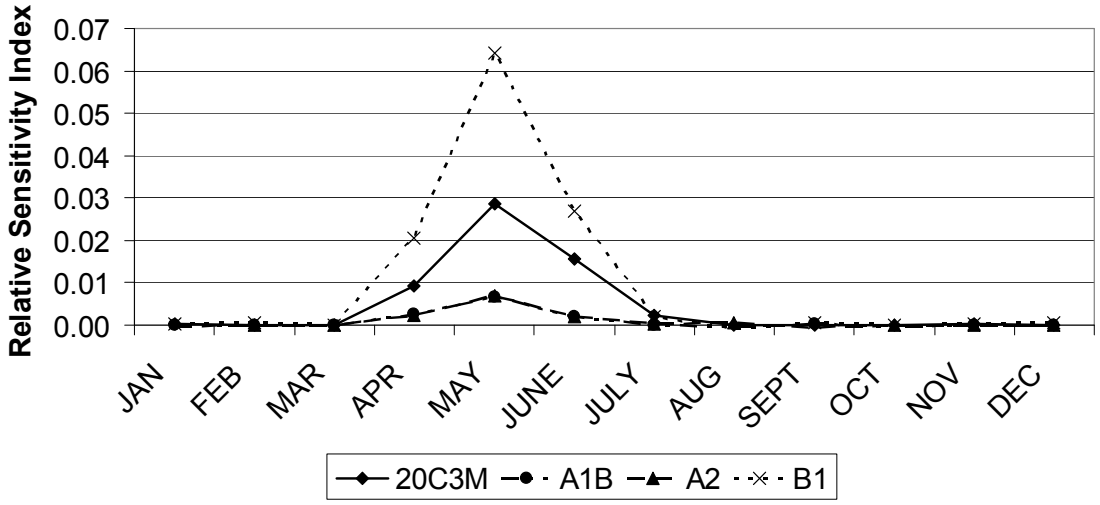

Figure 5-18. Conservation tillage average monthly sediment sensitivity

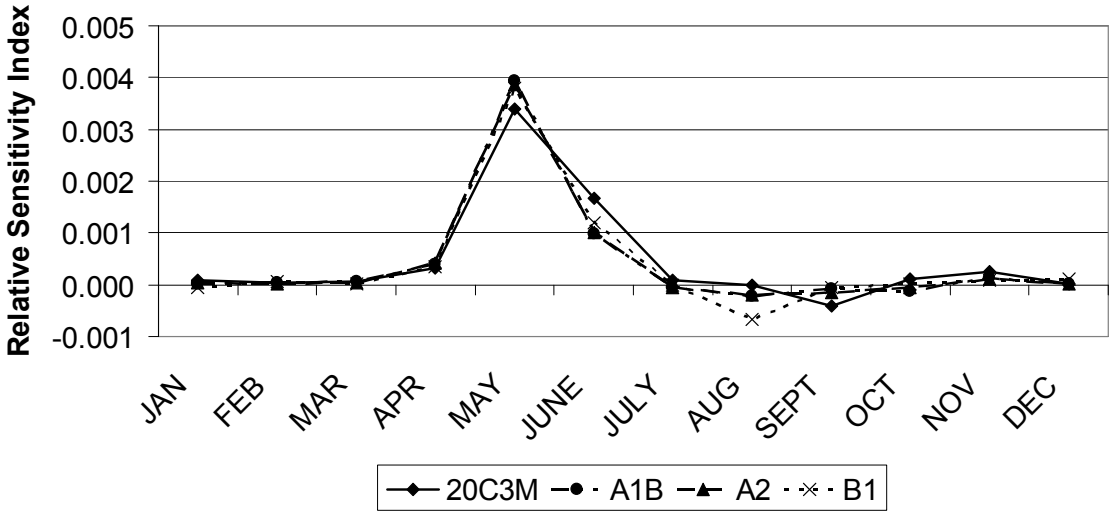

Figure 5-19. No-tillage average monthly sediment sensitivity

Contour farming (Figure 5-20, 9-26, 9-34) and terraces (Figures 5-21, 9-32, 9-40) have a similar monthly trend. Due to the similarity of their representation in SWAT (changes in curve number and USLE practice factor), the trends and sensitivities are similar. August has the highest magnitude sensitivity, which is similar to what was observed in native grass, likely because curve number is a factor in the implementation of native grass, contour farming, and terraces. The 20C3M scenario has the greatest

sensitivity each month for both contour farming and terraces, while the scenario with the most precipitation (A1B) has the lowest magnitude sensitivity.

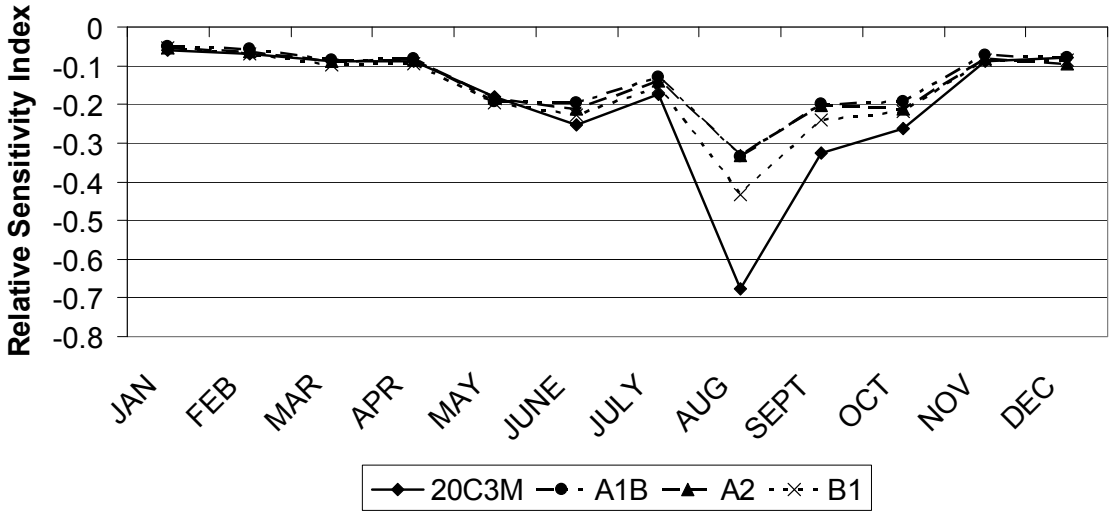

Figure 5-20. Contour farming average monthly sediment sensitivity

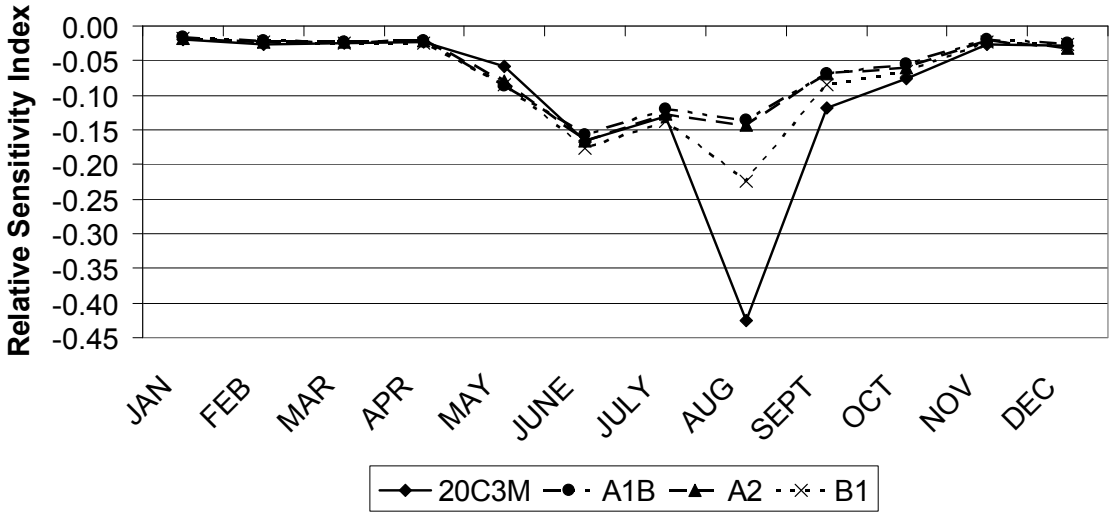

Figure 5-21. Terrace average monthly sediment sensitivity

Filter strip sensitivity is highly variable for all climate scenarios on a monthly basis (Figures 5-22, 9-27, 9-35). Sensitivity was determined to be greatest (about -0.16) in the months with the most precipitation (May-July), which suggests that filter strip width has a greater effect on NPS pollution in months with greater precipitation. In

months with less precipitation, filter strip width does not have a comparatively large average sensitivity (about -0.04) because of decreased NPS yield. This conclusion is supported by Lee et al. (2003), where it was determined that trapping effectiveness of filter strip and total rainfall are negatively correlated. Across climate scenarios, the monthly trends and sensitivity indices are very similar. Therefore, filter strip performance with respect to width impacts on pollution reduction is likely to undergo insignificant changes in future climate scenarios.

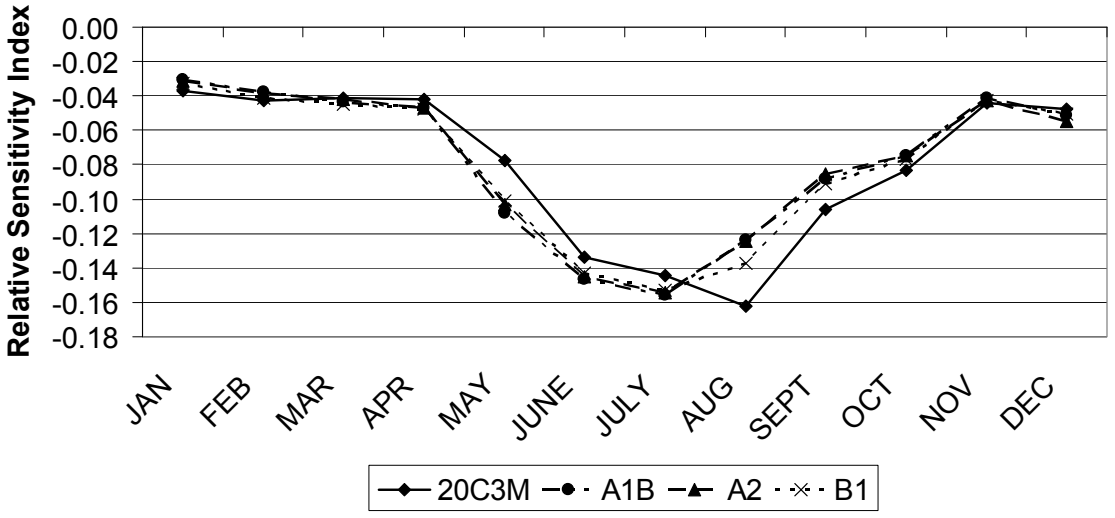

Figure 5-22. Filter strip average monthly sediment sensitivity

Grazing management sensitivity is largely consistent with the growing season and biomass fluctuations (Figures 5-23, 9-28, 9-36). As biomass accumulates in the spring until August, sensitivity decreases. As the range grass is harvested, and there is less biomass on the field, sensitivity increases to a peak in November and December. This suggests that sensitivity is highest when there is less biomass on the ground, indicating that changing the harvest index plays a larger role in pollution reduction after harvest. In the A1B, A2, and B1 scenarios the time to maturity of range grass is reached one month earlier (July) than in 20C3M (August), which results in an earlier harvest. Therefore,

20C3M lags behind A1B, A2, and B1 in magnitude of sensitivity and carries on into the beginning of the growing season. This lag is likely due to the increased temperatures in future climate scenarios, causing the beginning of the growing season and harvest date to shift forward one month.

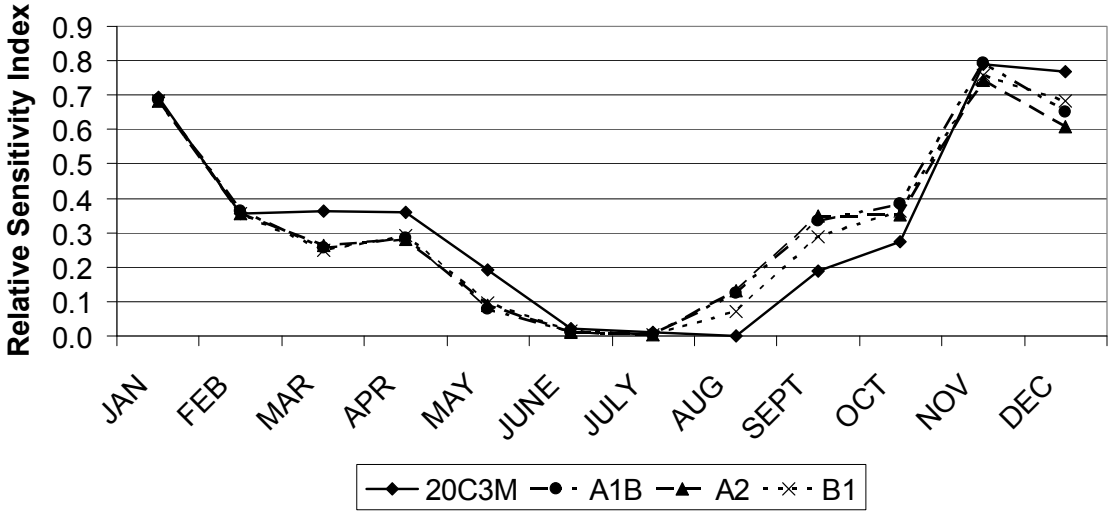

Figure 5-23. Grazing management average monthly sediment sensitivity

Native grass monthly sensitivity trends are similar for sediment, TN, and TP (Figures 5-24, 9-29, 9-37). Between climate scenarios, 20C3M monthly sensitivity is significantly lower than the future climate scenarios, which is consistent with the annual sensitivity in Figure 5-6 through 5-9 This suggests that native grass becomes more sensitive as temperature and precipitation increase. Monthly sensitivity trends are generally consistent with sensitivity of surface runoff and water yield for the future climate scenarios: beginning in March, sensitivity decreases with time into the growing season. As harvest takes place at the end of the growing season, sensitivity increases to a local maximum in October and then decreases again until February. The peak sensitivity in March also coincides with beginning of snowmelt and increased water yield, where combined with lack of biomass, results in high sensitivity of the native grass curve

number. Conversely, the local minimum sensitivity in winter months (November through February) is likely due to snow cover limiting runoff combined with lack of biomass on the field, meaning that changes in biomass cover do not affect sediment, TN, and TP yield during the winter months as much as March and October. The 20C3M scenario generally follows this trend, although the magnitudes of sensitivity are not as extreme, except for the peak in sediment and TP sensitivity in August. August in 20C3M has the lowest precipitation of any climate scenario, which results in a relatively small pollutant yield. For example, when curve number is reduced by 5% from the initial BMP value in 20C3M August, sediment yield is reduced from 277 tons to 237 tons (14% reduction), whereas for August in A1B sediment yield is reduced from 2967 tons to 2916 tons (2% reduction). Although load reduction is more for A1B (51 tons) than for 20C3M (40 tons), percent reduction is considerably greater for 20C3M. Therefore, in August 20C3M, changing curve number has a much greater impact on sensitivity because of the large percent reduction due to limited sediment and TP yield. This suggests that although reduction efficiency is higher in August for 20C3M than A1B, A2, or B1, native grass is less reliable in August because of the high reduction variation with respect changes in implementation.

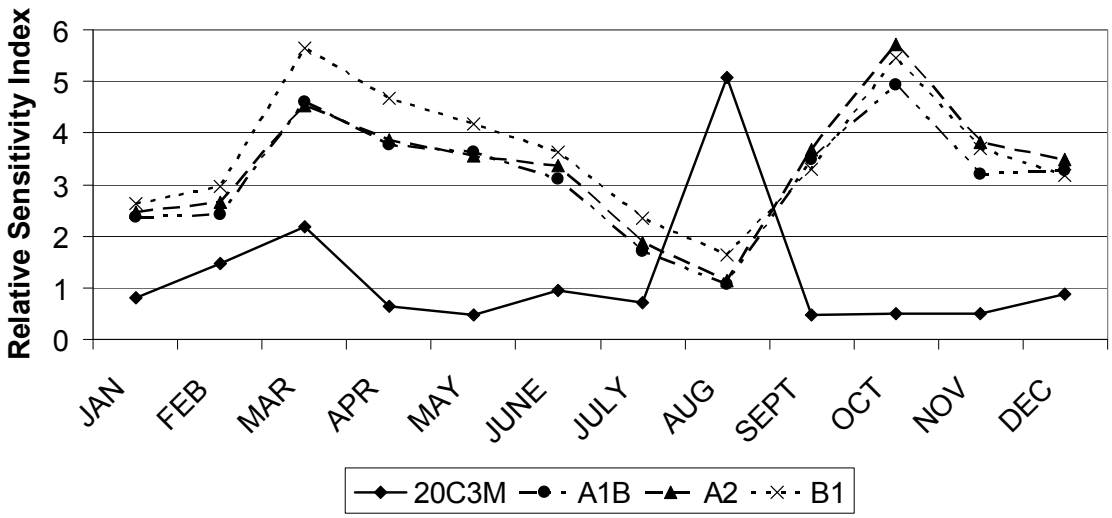

Figure 5-24. Native grass average monthly sediment sensitivity

Porous gully plug monthly sensitivity stays close to zero for most of the year, with peaks in March and November for sediment, TN, and TP under all climate scenarios (Figures 5-25, 9-31, 9-39). Between climate scenarios, A1B is the most sensitive, followed by A2 and B1, while 20C3M is the least sensitive. This indicates that porous gully plugs is relatively more sensitive to precipitation and temperature increases during these months.

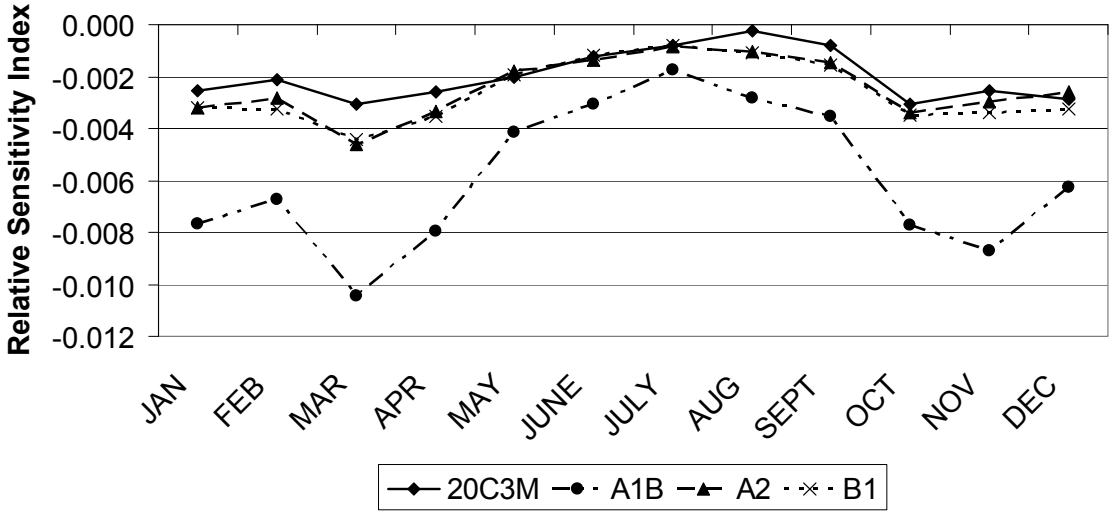

Figure 5-25. Porous gully plug average monthly sediment sensitivity

5.5.2 Significant Differences of BMP Sensitivity between Climate Scenarios

To determine significant differences of sediment, TN, and TP sensitivities for each BMP across climate scenarios, a one-way analysis of variance (ANOVA) was performed at a 0.05 level of significance. The p-values for each BMP pair-wise comparison of climate change scenario sensitivity is presented in Table 5-10 for sediment, Table 9-1 for TN, and Table 9-2 for TP, where significant differences between scenarios are highlighted. Filter strips, grazing management, and porous gully plugs do not show significant differences between climate scenarios for all three pollutants. Contour farming and terraces generally have statistically significant differences in sensitivity across all climate scenarios for sediment, TN, and TP, except under terraces for sediment and TP between 20C3M and A2. Under the native grass scenario, 20C3M is shows statistically significant differences from the future climate scenarios for all pollutants, which is expected, based on the annual and monthly sensitivity results. Finally, conservation tillage and no-tillage generally have statistically significant

differences between climate change scenarios, especially TN and TP. These results suggest that climate change plays a significant role in determining BMPs performance in regards to pollution control.

Table 5-7. ANOVA sediment p-values (highlighted cells indicate significance)

Conservation Tillage					Contour Farming				
	20C3M	A1B	A2	B1		20C3M	A1B	A2	B1
20C3M		0.89	<0.01	<0.01	20C3M		<0.01	<0.01	0.02
A1B	0.89		<0.01	<0.01	A1B	<0.01		<0.01	<0.01
A2	<0.01	<0.01		0.97	A2	<0.01	<0.01		<0.01
B1	<0.01	<0.01	0.97		B1	0.02	<0.01	<0.01	
Filter Strips					Grazing Management				
	20C3M	A1B	A2	B1		20C3M	A1B	A2	B1
20C3M		0.17	0.15	0.18	20C3M		0.30	0.19	0.36
A1B	0.17		0.96	0.98	A1B	0.30		0.79	0.91
A2	0.15	0.96		0.94	A2	0.19	0.79		0.71
B1	0.18	0.98	0.94		B1	0.36	0.91	0.71	
Native Grass					No-Tillage				
	20C3M	A1B	A2	B1		20C3M	A1B	A2	B1
20C3M		<0.01	<0.01	<0.01	20C3M		0.17	<0.01	<0.01
A1B	<0.01		0.434	0.03	A1B	0.17		<0.01	<0.01
A2	<0.01	0.44		0.18	A2	<0.01	<0.01		0.26
B1	<0.01	0.03	0.18		B1	<0.01	<0.01	0.26	
Porous Gully Plug					Terraces				
	20C3M	A1B	A2	B1		20C3M	A1B	A2	B1
20C3M		0.57	0.24	0.11	20C3M		<0.01	0.76	0.01
A1B	0.57		0.54	0.29	A1B	<0.01		<0.01	<0.01
A2	0.24	0.54		0.66	A2	0.76	<0.01		<0.01
B1	0.11	0.29	0.66		B1	0.01	<0.01	<0.01	

5.6 CONCLUSION

This study evaluated the sensitivity of eight agricultural BMPs with respect to sediment, TN, and TP pollution from the field under various climate change scenarios. Three SRES emissions scenarios (A.1B, A.2, and B.1) and a 20th century simulation (20C3M) from the CCSM-3 GCM were used in the comparison in the Tuttle Creek Lake

watershed (TCLW) located in Kansas and Nebraska. By changing model parameters related to the physical implementation of conservation tillage, contour farming, filter strips, grazing management, native grass, no-tillage, porous gully plugs, and terraces, annual and monthly sensitivities were calculated for each climate scenario.

Using the delta method, daily precipitation and temperature data were constructed for future climate scenarios (A1B, A2, and B1) and the 20C3M model from observed data to be used for the sensitivity analysis. With respect to the 20C3M scenario, A1B was determined to have the greatest increase in temperature, while A2 had the greatest precipitation increase by the middle 21st century.

Results of conventional tillage (considered the no BMP applied scenario) across climate change scenarios determined that A1B produced the greatest amount of sediment, TN, and TP yields from the field at the watershed scale, while 20C3M produced the least. In terms of sediment, TN, and TP reduction efficiency, filter strips, contour farming, terraces, and native grass were most effective, while porous gully plugs and conservation tillage were the least effective for all climate scenarios

The sensitivity analysis was performed by using a one-at-a-time parameter perturbation method to determine the sensitivity of each BMP with respect to sediment, TN, and TP within the TCLW under each climate scenario. Native grass replacement of agricultural row crops was determined to be the most sensitive BMP under all climate scenarios, while grazing management and filter strips were also highly sensitive on an annual and monthly basis. The least sensitive BMPs were determined to be porous gully plugs, no-tillage, and conservation tillage. Comparing BMP sensitivity across climate scenarios, it was determined that filter strips, grazing management, and porous gully

plugs do not experience significant sensitivity differences in future climate scenarios for sediment, TN, and TP. All other BMPs exhibited at least some significant differences between climate scenarios.

Comparing monthly and annual sensitivity, it was determined that analyzing sensitivity on a monthly basis reveals more regarding BMP performance and uncertainty. Most BMPs had highly variable sensitivity depending on the month, which was attributed to variation in seasonal precipitation, temperature and time of the growing season across all climate scenarios. Therefore, it is recommended caution should be exercised in the decision-making processes for developing future BMP implementation strategies.

This study provides valuable information to watershed managers and decision-makers regarding BMP implementation in current and possible future climates. Through use of sensitivity analysis, variations in BMP performance can be determined, which ultimately, affect spatial planning and development decisions regarding water quality protection under future climate scenarios. In addition, determining sensitivity of BMPs allow us to understand the reliability, risk, and uncertainty involved in both modeling and real world implementation of BMPs at the watershed scale to mitigate the negative impacts of climate changes on water resources.

6 CONCLUSION

This research examined the effects of climate change on water quantity, water quality, BMP effectiveness, and BMP reliability in the Tuttle Creek Lake watershed located in Kansas and Nebraska. A physically-based watershed model (SWAT) was used in conjunction with downscaled climate change data of three SRES emission scenario outputs (A1B, A2, and B1) from the National Center for Atmospheric Research CCSM-3 climate model. Eight agricultural BMPs were modeled within SWAT: conservation tillage, contour farming, filter strips, grazing management, native grass, no-tillage, porous gully plugs, and terraces. In the first study, sediment and nutrient load reduction and percent reduction efficiency of each BMP was determined at the field and watershed scales for all climate scenarios. In the second study, a sensitivity analysis was performed across all climate scenarios for each BMP. Initial BMP implementation parameters were adjusted based on reasonable ranges, and a relative sensitivity index was calculated to quantify sensitivity. Annual and monthly relative BMP sensitivity indices were determined for sediment, total nitrogen, and total phosphorus. The following general conclusions were made:

- Water quantity (surface runoff, baseflow, and water yield) increased in future climate scenarios within the study area.
- Water quality parameters (sediment, total nitrogen, and total phosphorus) increased in magnitude in future climate scenarios, which was mainly attributed to increases in surface runoff and water yield.
- Under both current and future climate scenarios, efficiency was determined to be greatest for more intensive BMPs, such as native grass, terraces, and contour

farming. Conversely, porous gully plugs and conservation tillage had lower efficiencies.

- Under future climate scenarios, most BMPs experienced decreased efficiencies for sediment or nutrients, particularly grazing management and native grass.
- Native grass, grazing management, and filter strips were determined to be the most sensitive among studied BMPs under all climate scenarios and therefore, the least reliable for implementation in future climates. Therefore, a slight change from predefined implementation conditions may increase uncertainty in performance. Porous gully plugs, no-tillage, and conservation tillage were the least sensitive among studied BMPs.
- In terms of significant changes in sensitivity between climate change scenarios, filter strips, grazing management, and porous gully plugs were the only BMPs that did not change for sediment and nutrient loads.

7 FUTURE RESEARCH

This study provides valuable insight into the manner in which future climate change may affect hydrology and NPS pollutant transport in agricultural watersheds. In addition, the impacts of climate change on BMP efficiency and sensitivity to method of implementation were determined. However, there is significant research to be done to enhance our understanding of the relationship between climate change, watershed dynamics, and BMP implementation strategy. Suggestions for future research include:

- *Quantifying the uncertainty of BMP implementation in current and future climates*: while a BMP sensitivity analysis allows for understanding of how reduction efficiency changes to different sources of variation in the input of the model, more research must be completed to include uncertainty of BMP efficiency and associated risk under future climate scenarios to aid watershed decision makers in developing implementation plans.
- *Exploring additional climate scenarios, models, and downscaling methods*: this study used three SRES emissions scenarios from one climate model. Introducing more plausible future SRES emissions scenarios under a wide array of climate models will allow for further understanding of the possibilities of change in water resources.
- *Determining optimal resolution of climate change data for water resources studies*: climate change data is often available for various spatial and temporal resolutions, usually in forms not acceptable for watershed impacts studies. Exploration of optimal spatial and temporal resolutions will allow for

standardized approaches to integration of climate change data and watershed models in future studies.

APPENDICES

8 APPENDIX A

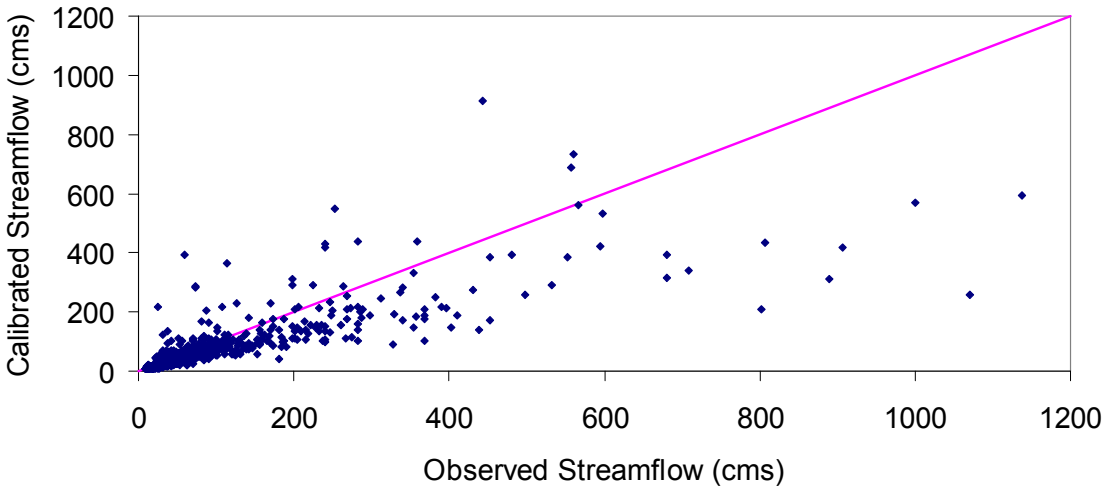

Figure 8-1. Observed versus calibrated streamflow

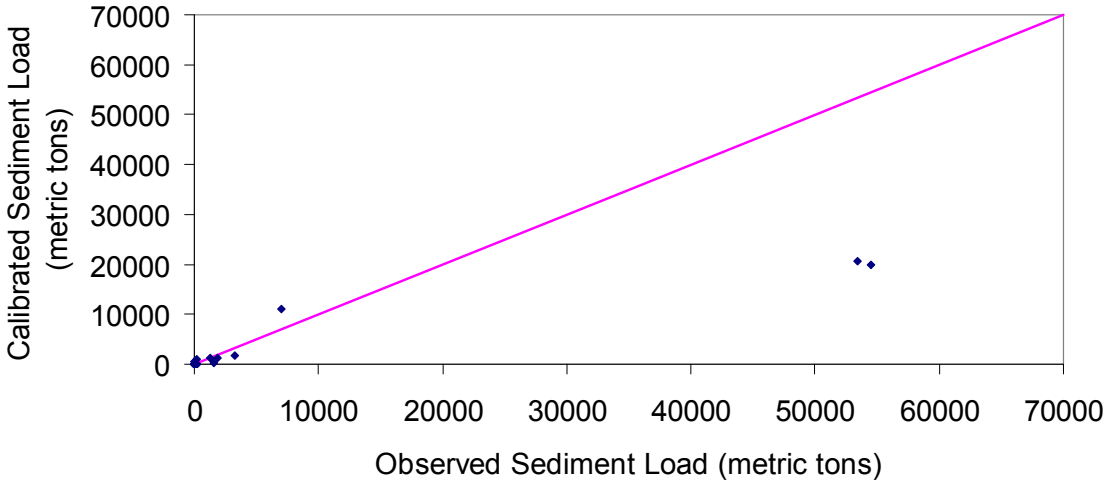

Figure 8-2. Observed versus calibrated sediment load

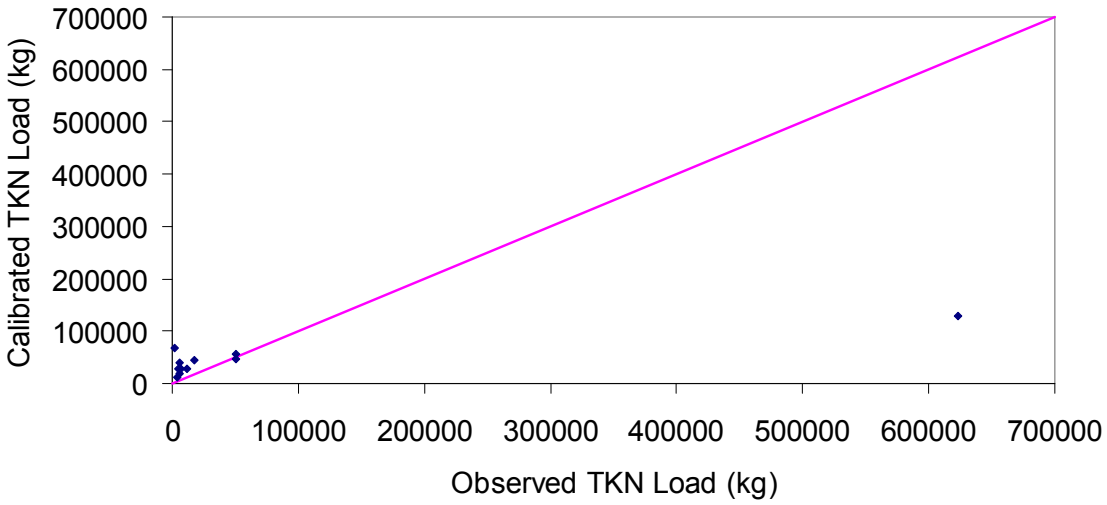

Figure 8-3. Observed versus calibrated TKN load

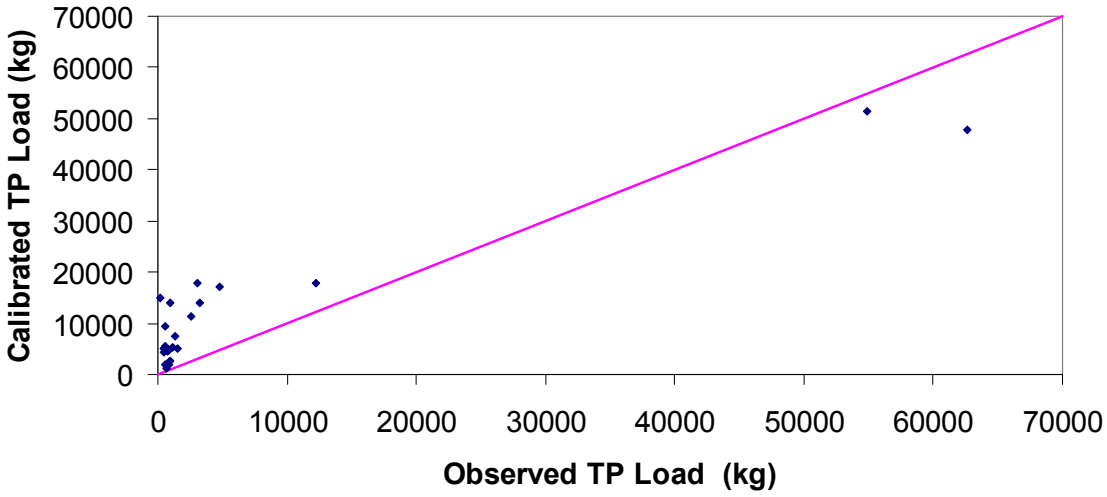

Figure 8-4. Observed versus calibrated TP load

Table 8-1. Significant difference (p-value) in BMP performance at the field scale between 20C3M and A2.

	Sediment		Total Nitrogen		Total Phosphorus	
BMP	% Red	Load Red	% Red	Load Red	% Red	Load Red
Contour Farming	↑ <0.01	↑ <0.01	0.36	↑ <0.01	0.33	↑ <0.01
Filter Strips	↑ <0.01	↑ <0.01	↑ 0.02	↑ <0.01	↑ <0.01	↑ <0.01
Grazing Management	↓ <0.01	↓ 0.01	↓ <0.01	↓ 0.01	↓ <0.01	↓ 0.01
Native Grass	<0.01	0.08	<0.01	↓ 0.05	<0.01	↓ 0.65
No-Tillage	0.10	↑ 0.01	↑ <0.01	↑ <0.01	0.07	0.13
Porous Gully Plugs	0.29	0.11	0.64	0.22	0.36	0.08
Conservation Tillage	↑ 0.05	↑ <0.01	↑ <0.01	↑ <0.01	0.09	↑ 0.01
Terraces	0.02	↑ <0.01	0.83	↑ 0.04	0.90	↑ <0.01

Table 8-2. Significant difference (p-value) in BMP performance at the watershed scale between 20C3M and A2.

	Sediment		Total Nitrogen		Total Phosphorus	
BMP	% Red	Load Red	% Red	Load Red	% Red	Load Red
Contour Farming	↑ <0.01	↑ <0.01	0.84	0.19	0.71	0.21
Filter Strips	↑ 0.05	↑ <0.01	0.16	0.70	↓ 0.01	0.17
Grazing Management	0.72	0.57	↓ 0.01	0.19	↓ 0.01	0.17
Native Grass	↑ <0.01	↑ <0.01	0.54	0.49	0.54	0.61
No-Tillage	↑ 0.05	↑ 0.03	0.81	0.91	0.82	0.82
Porous Gully Plugs	0.32	0.26	0.11	0.21	0.07	0.12
Conservation Tillage	↑ 0.04	0.05	0.30	0.52	0.98	0.37
Terraces	↑ <0.01	↑ <0.01	0.61	↑ 0.03	0.77	↑ 0.01

Table 8-3. Significant difference (p-value) in BMP performance at the field scale between 20C3M and B1.

	Sediment		Total Nitrogen		Total Phosphorus	
BMP	% Red	Load Red	% Red	Load Red	% Red	Load Red
Contour Farming	↑ <0.01	↑ <0.01	0.07	↑ <0.01	0.05	↑ <0.01
Filter Strips	↑ <0.01	↑ <0.01	↑ <0.01	↑ <0.01	↑ <0.01	↑ <0.01
Grazing Management	↓ <0.01	↓ 0.04	↓ 0.01	0.08	↓ <0.01	0.08
Native Grass	↓ <0.01	↓ 0.01	↓ <0.01	↓ 0.01	↓ <0.01	0.29
No-Tillage	0.14	↑ 0.02	↑ <0.01	↑ <0.01	0.18	0.21
Porous Gully Plugs	0.43	0.22	0.31	0.75	0.18	0.48
Conservation Tillage	↑ 0.04	↑ 0.01	↑ <0.01	↑ <0.01	0.06	↑ 0.02
Terraces	0.47	0.09	0.51	0.39	0.61	0.16

Table 8-4. Significant difference (p-value) in BMP performance at the watershed scale between 20C3M and B1.

	Sediment		Total Nitrogen		Total Phosphorus	
BMP	% Red	Load Red	% Red	Load Red	% Red	Load Red
Contour Farming	↑ 0.01	↑ <0.01	0.65	0.27	0.40	0.15
Filter Strips	0.53	↑ <0.01	↓ 0.02	0.11	0.08	0.20
Grazing Management	0.97	0.70	↓ <0.01	0.24	↓ <0.01	0.22
Native Grass	↑ <0.01	↑ <0.01	0.50	0.70	0.67	0.98
No-Tillage	0.21	0.09	0.68	0.91	0.75	0.84
Porous Gully Plugs	0.34	0.31	0.28	0.31	0.05	0.21
Conservation Tillage	0.14	0.31	0.62	0.33	0.54	0.63
Terraces	↑ <0.01	↑ <0.01	0.06	↑ 0.05	↑ <0.01	↑ 0.02

9 APPENDIX B

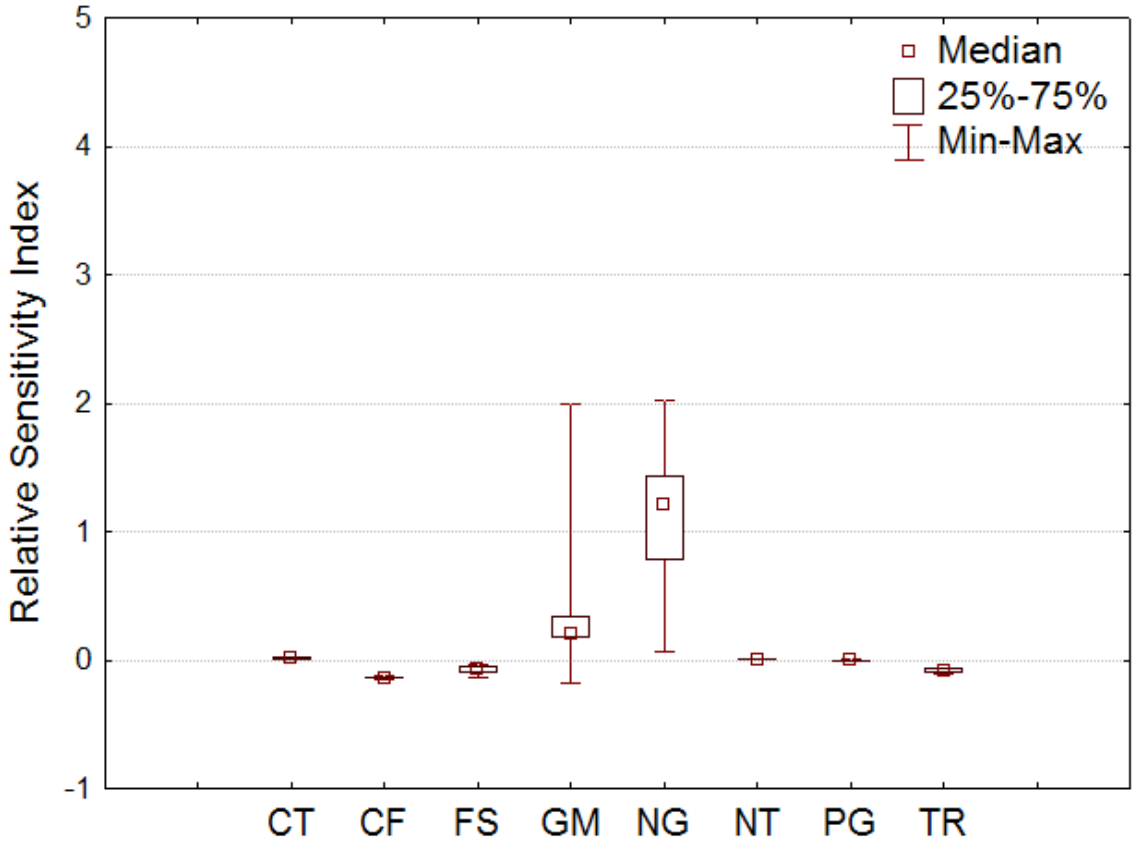

Figure 9-1. 20C3M total nitrogen BMP relative sensitivity indices

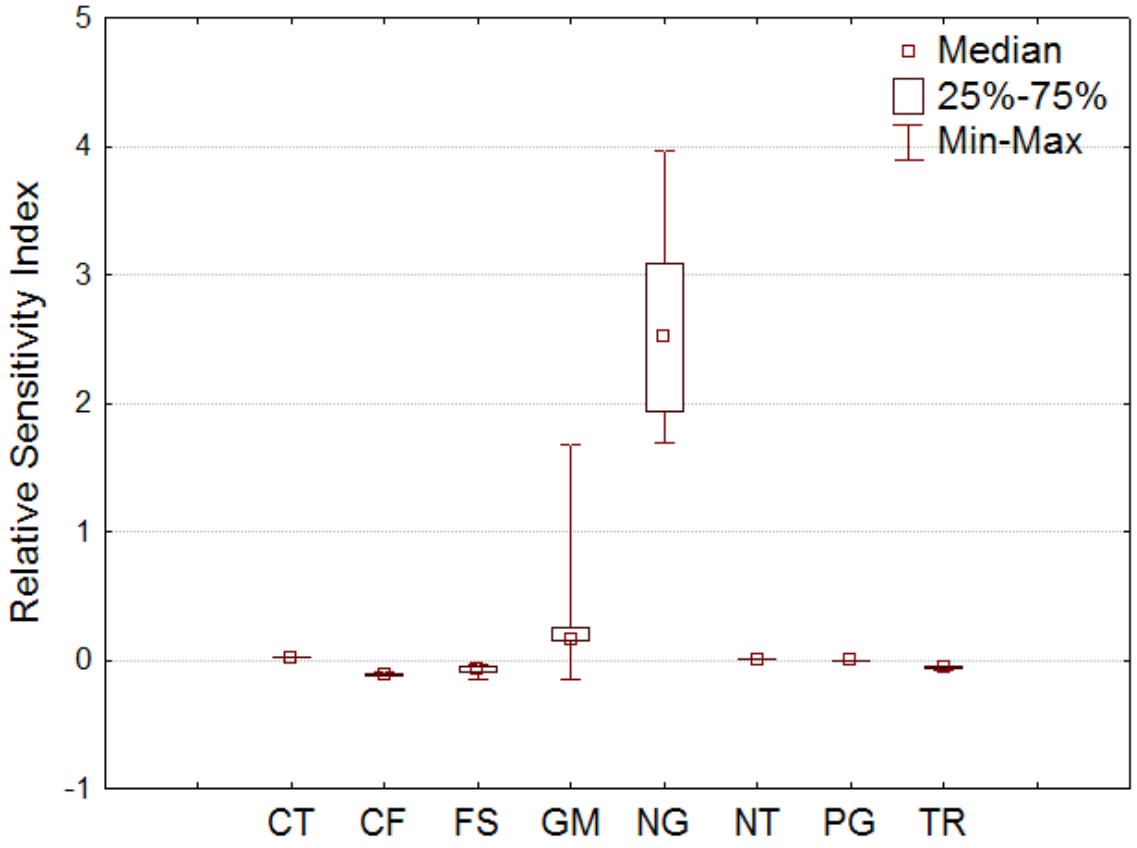

Figure 9-2. A1B total nitrogen BMP relative sensitivity indices

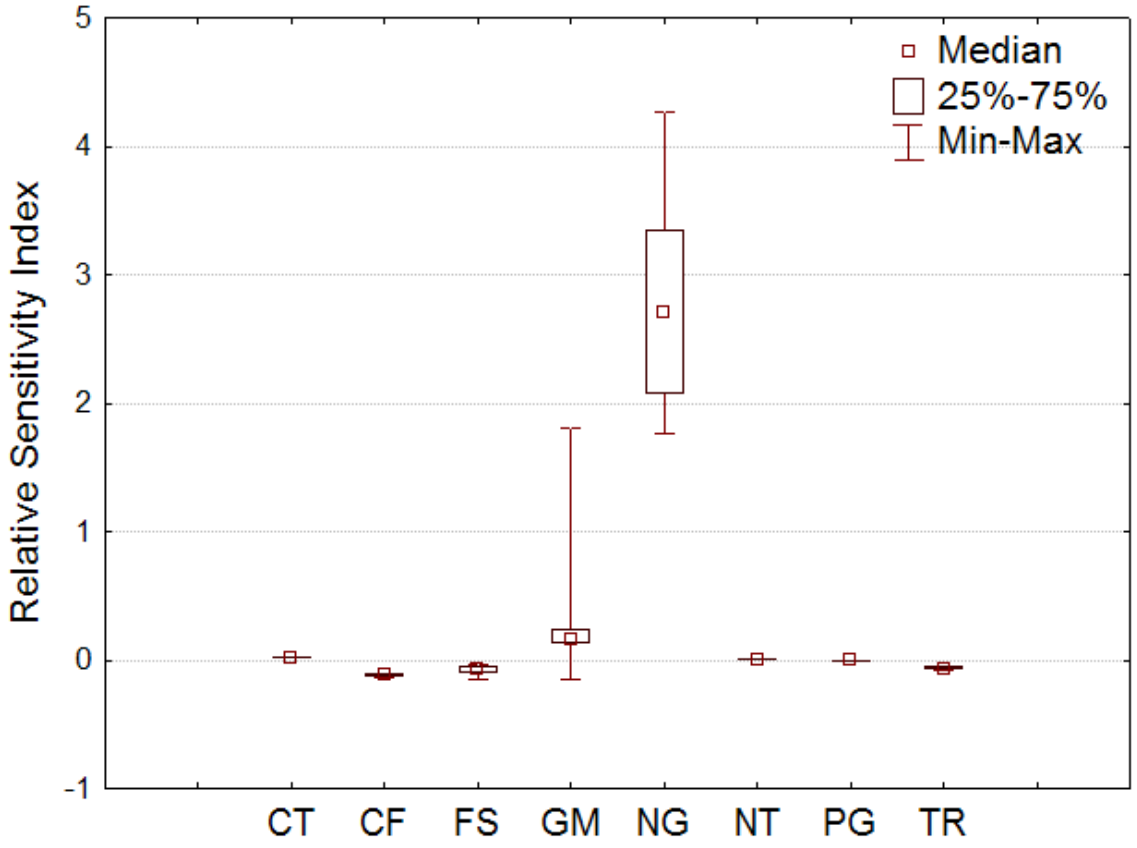

Figure 9-3. A2 total nitrogen BMP relative sensitivity indices

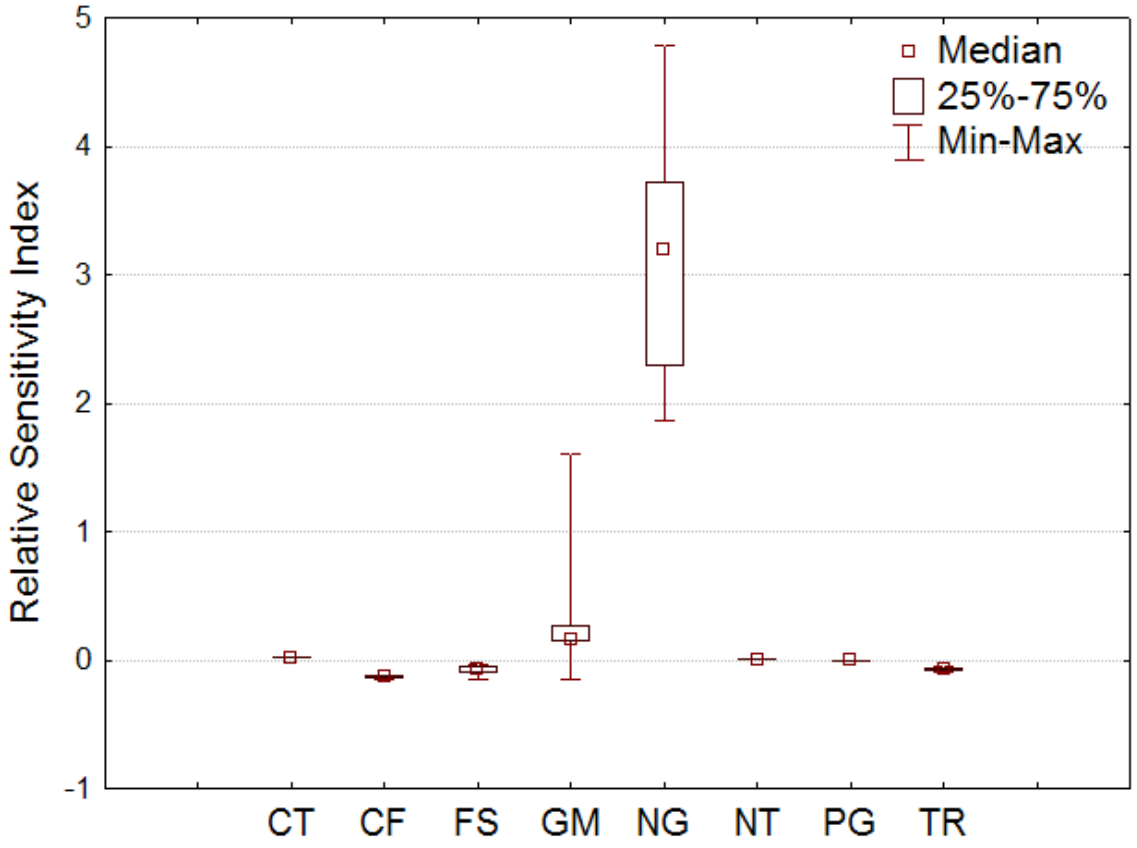

Figure 9-4. B1 total nitrogen BMP relative sensitivity indices

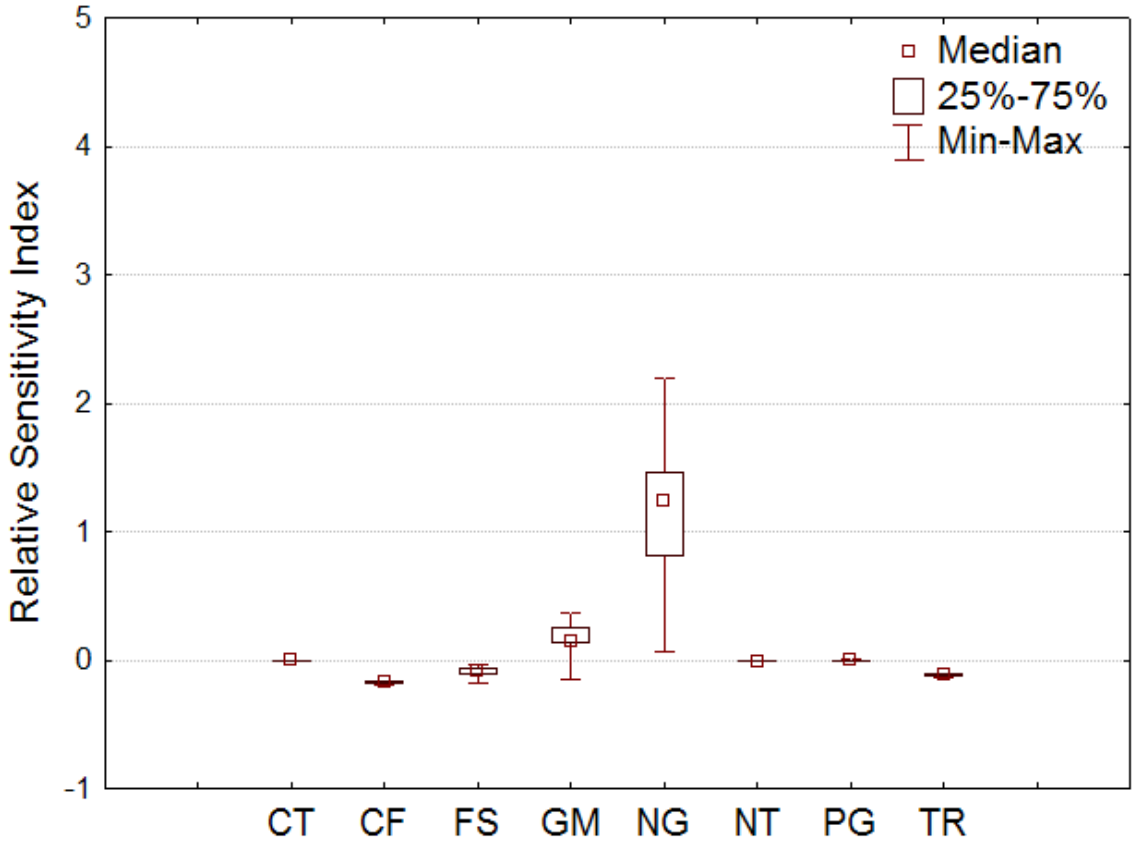

Figure 9-5. 20C3M total phosphorus BMP relative sensitivity indices

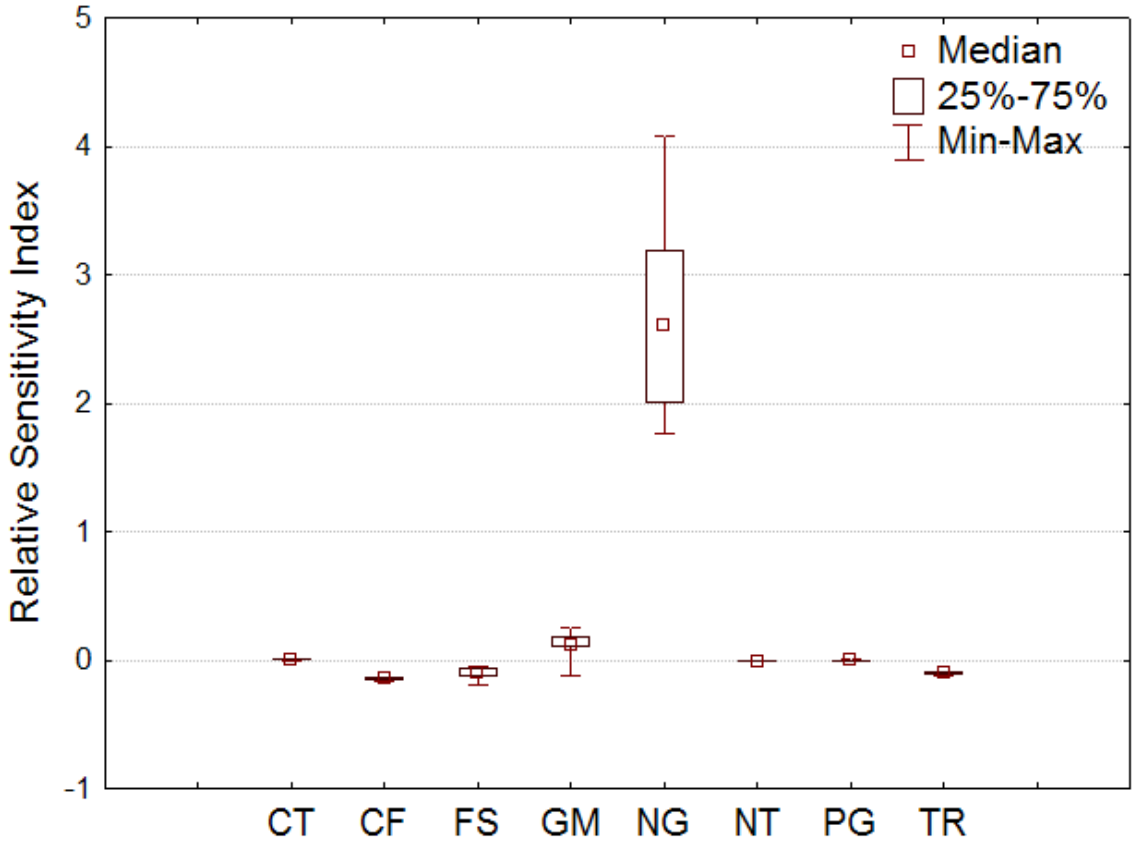

Figure 9-6. A1B total phosphorus BMP relative sensitivity indices

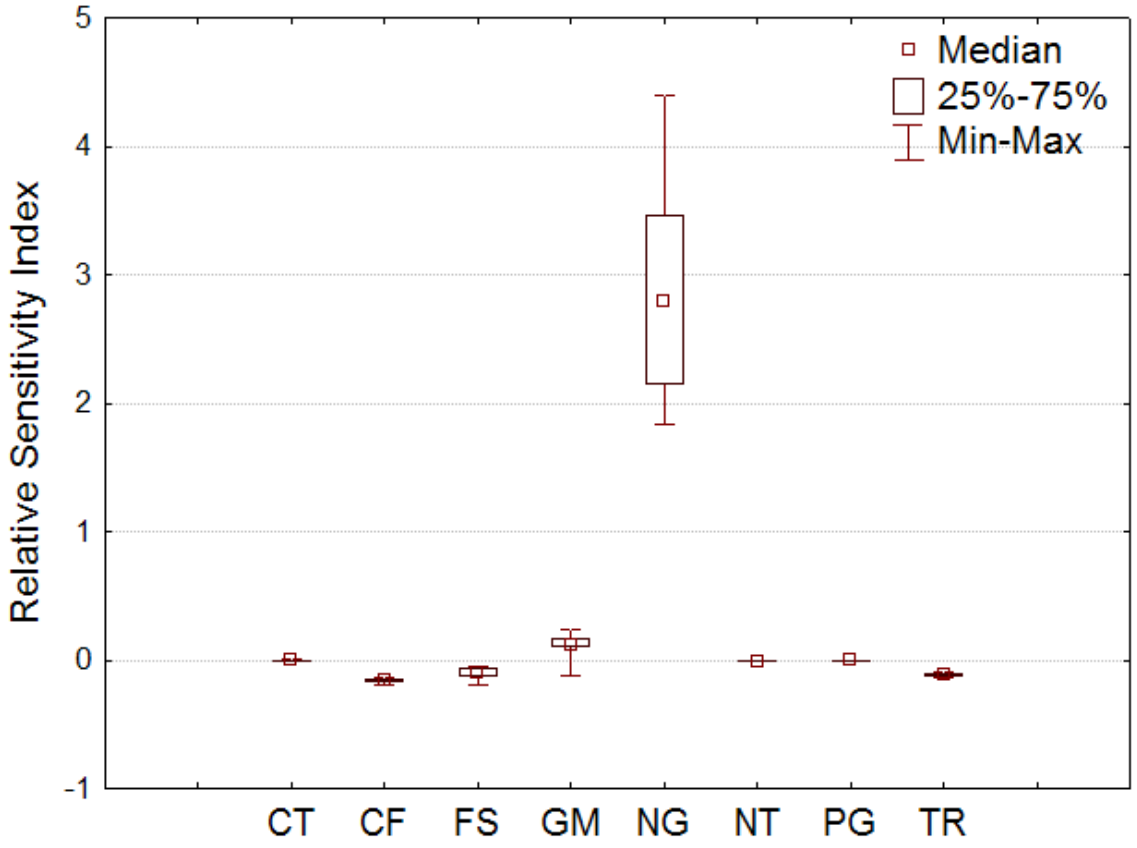

Figure 9-7. A2 total phosphorus BMP relative sensitivity indices

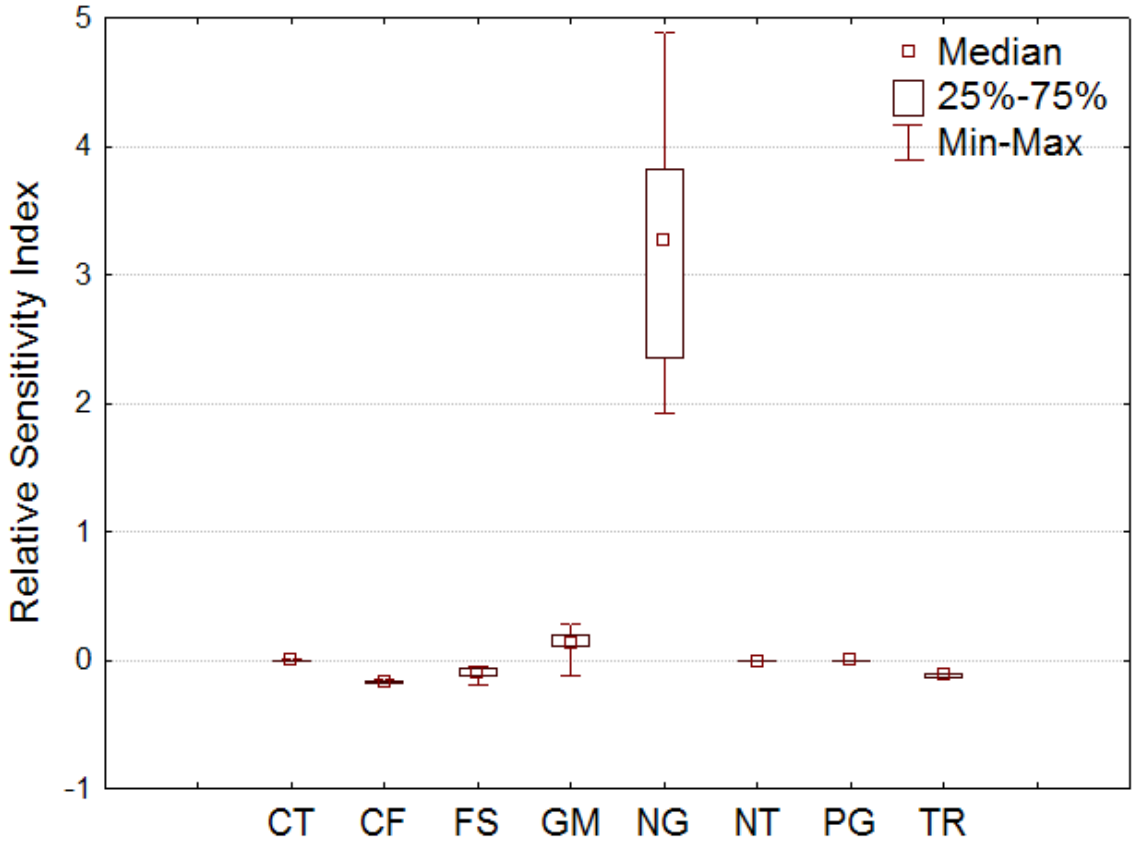

Figure 9-8. B1 total phosphorus BMP relative sensitivity indices

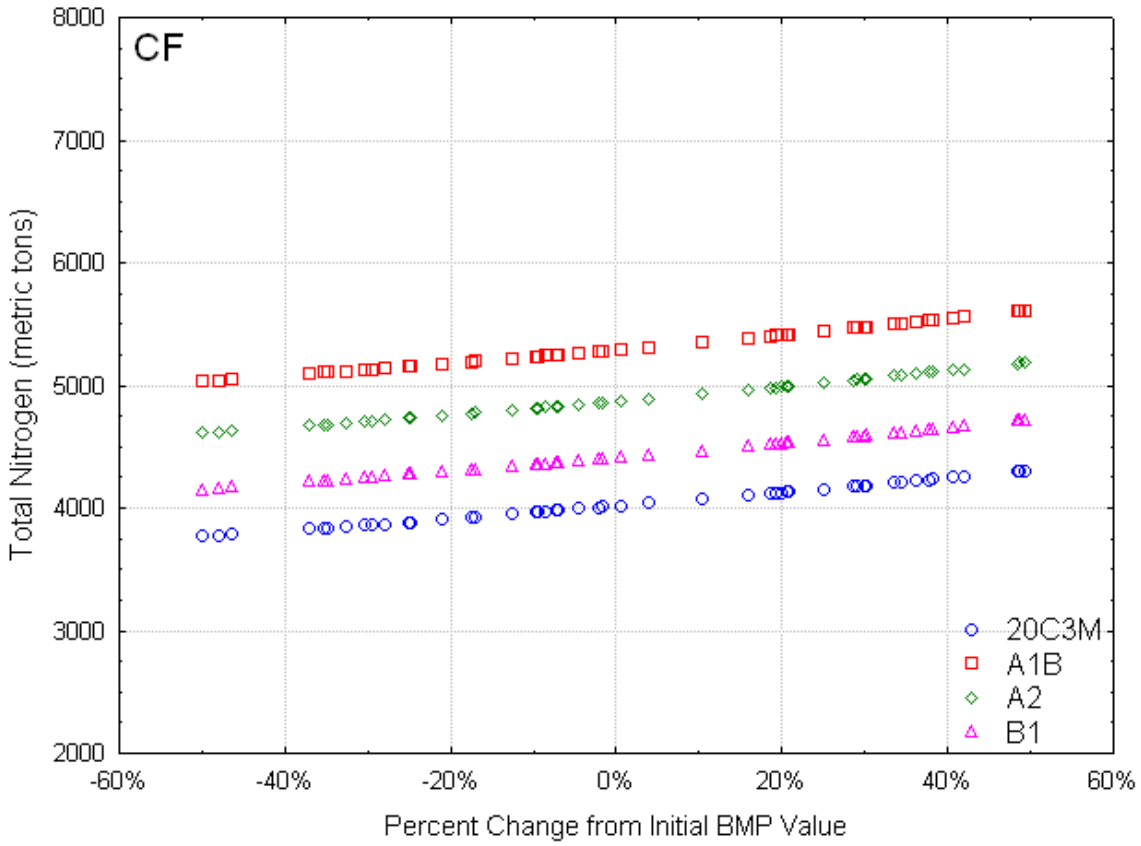

Figure 9-9. Contour farming TN yield versus percent parameter change

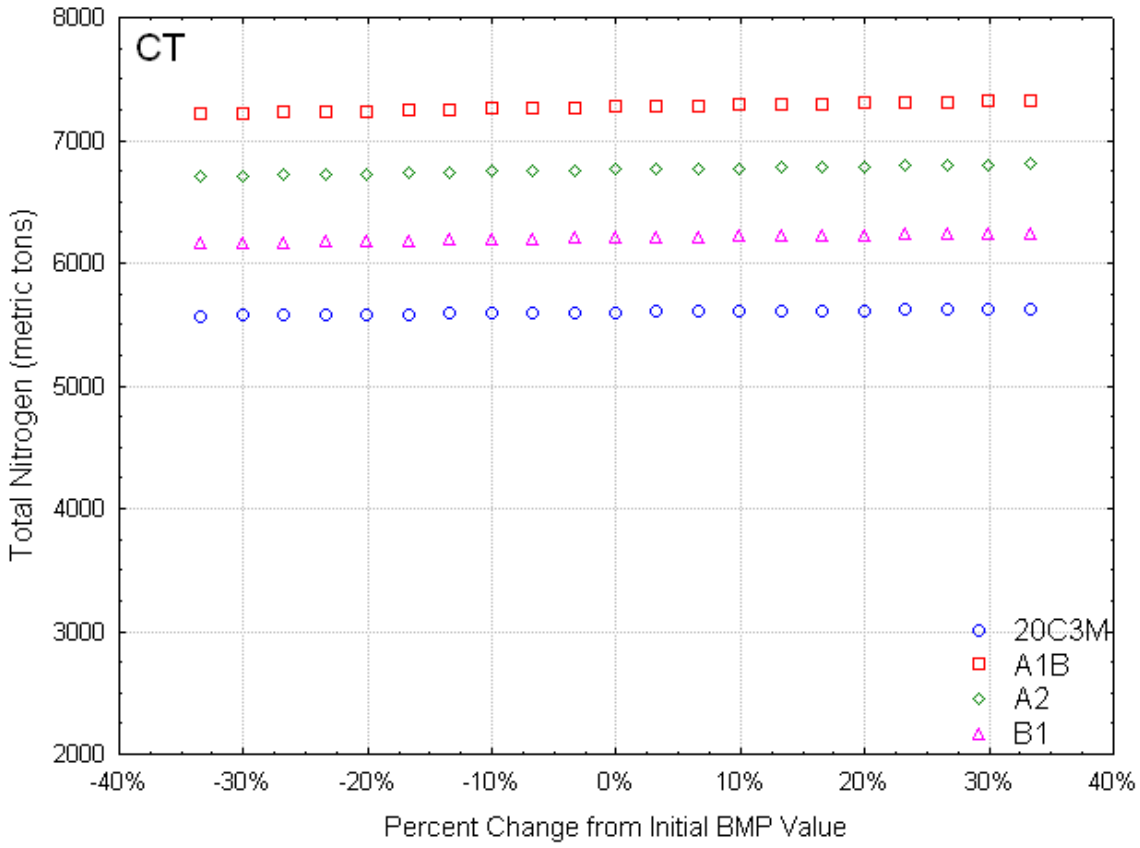

Figure 9-10. Conservation tillage TN yield versus percent parameter change

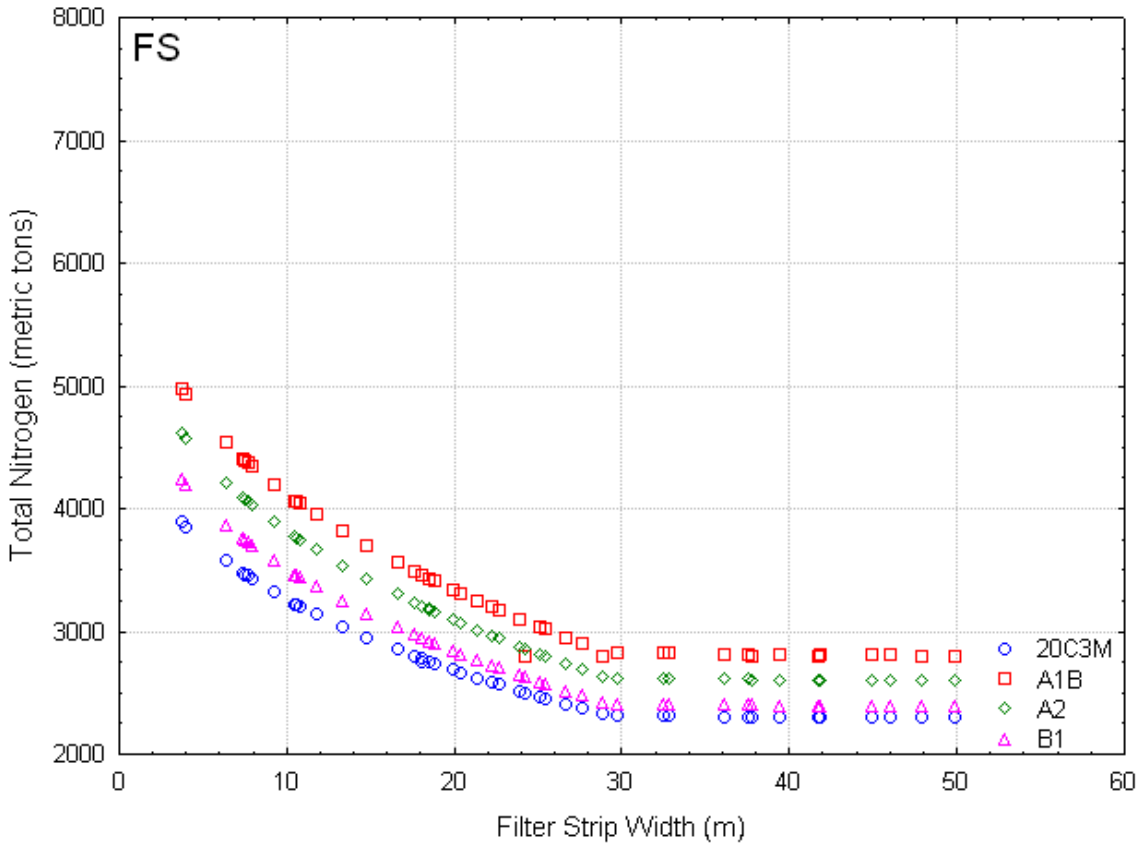

Figure 9-11. Filter strip TN yield versus filter strip width

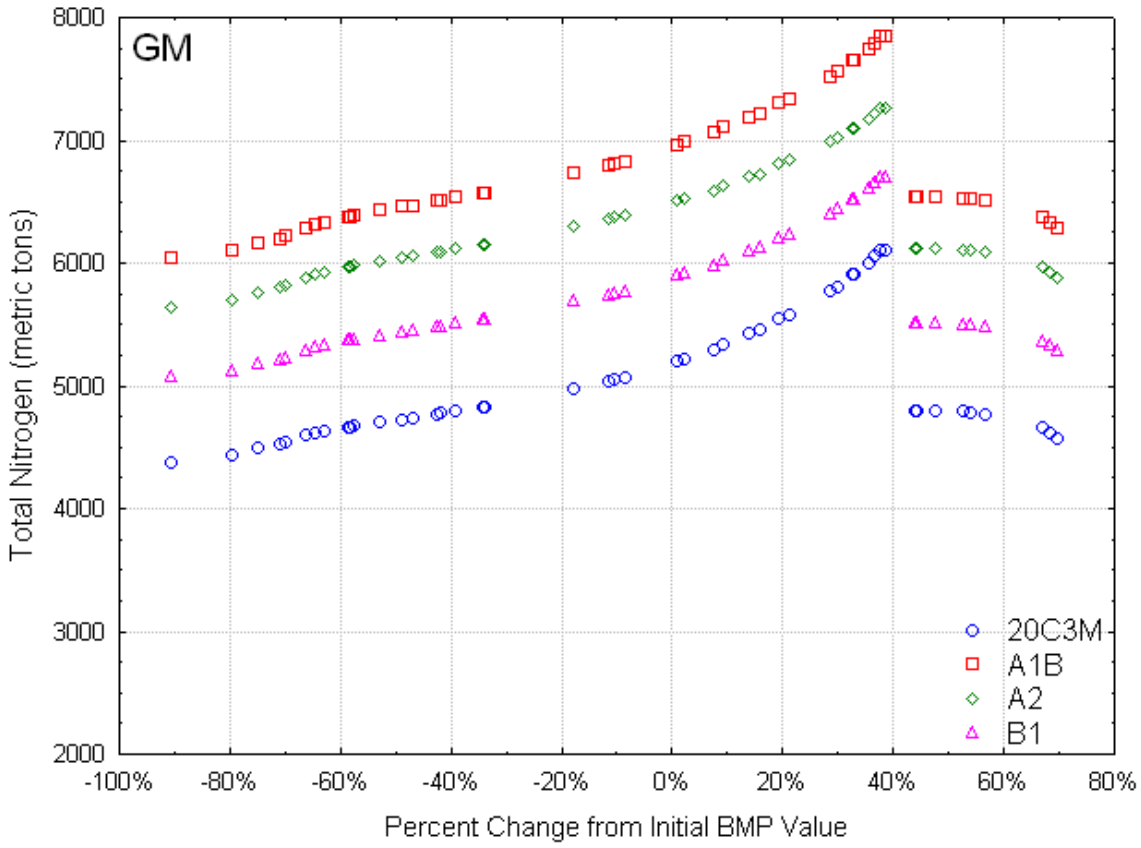

Figure 9-12. Grazing management TN yield versus percent parameter change

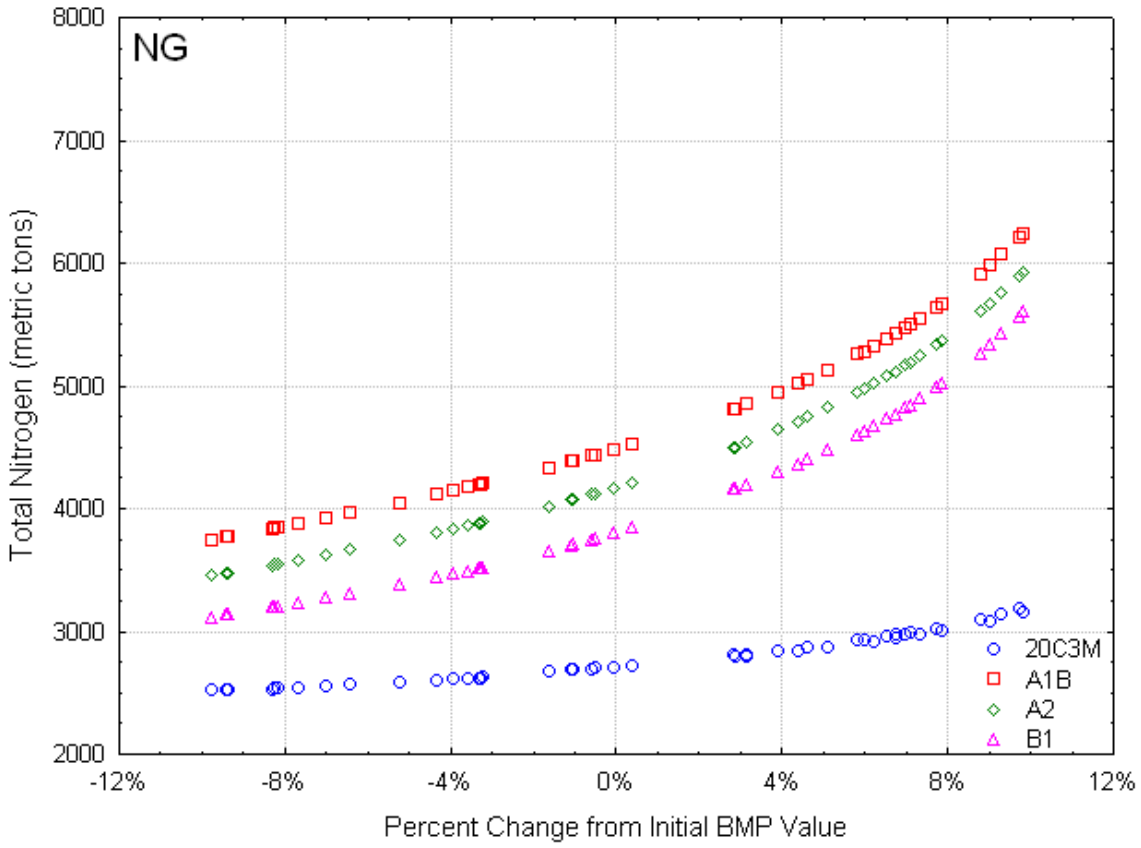

Figure 9-13. Native grass TN yield versus percent parameter change

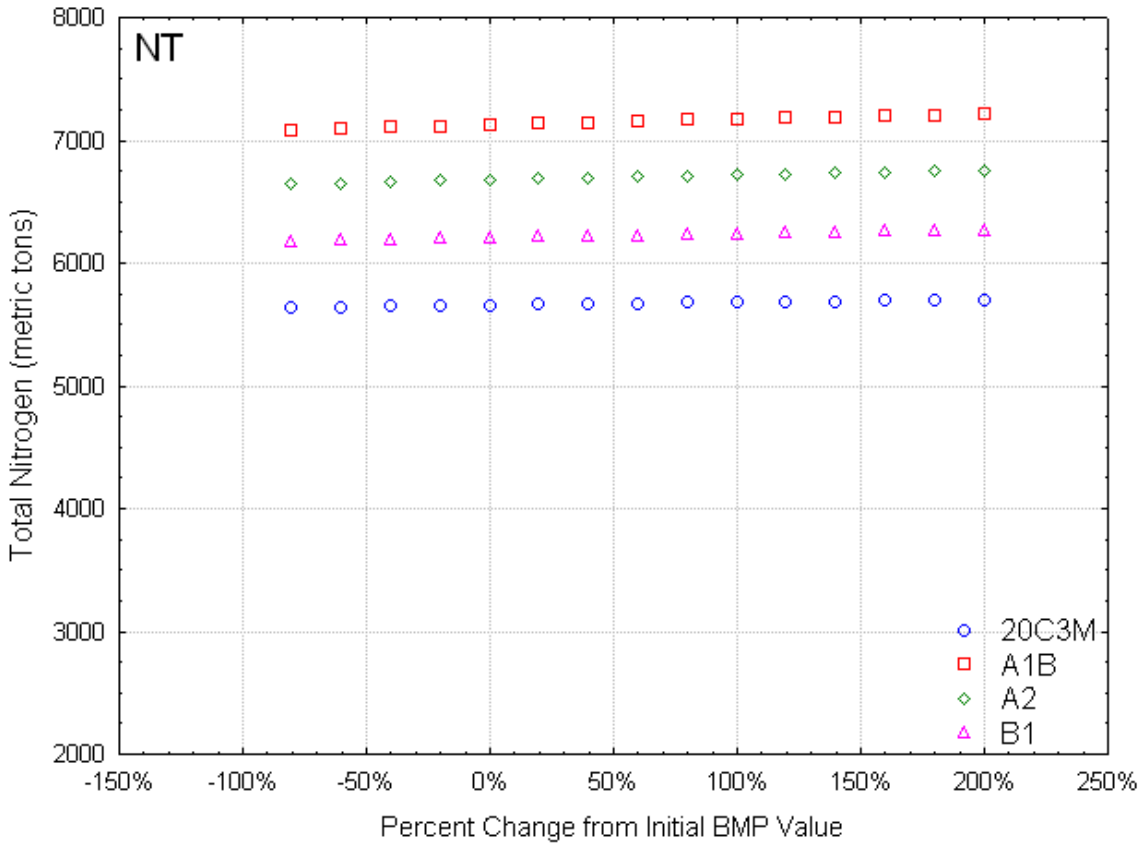

Figure 9-14. No-tillage TN yield versus percent parameter change

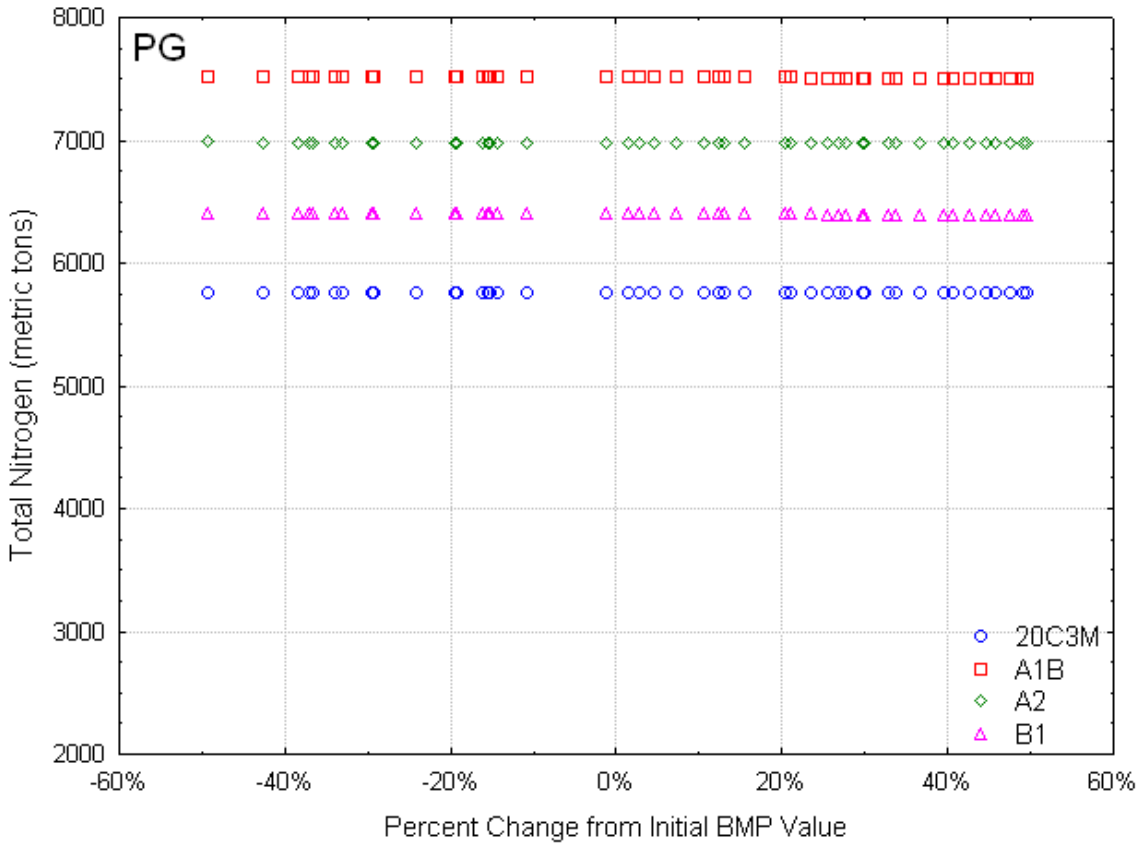

Figure 9-15. Porous gully plug TN yield versus percent parameter change

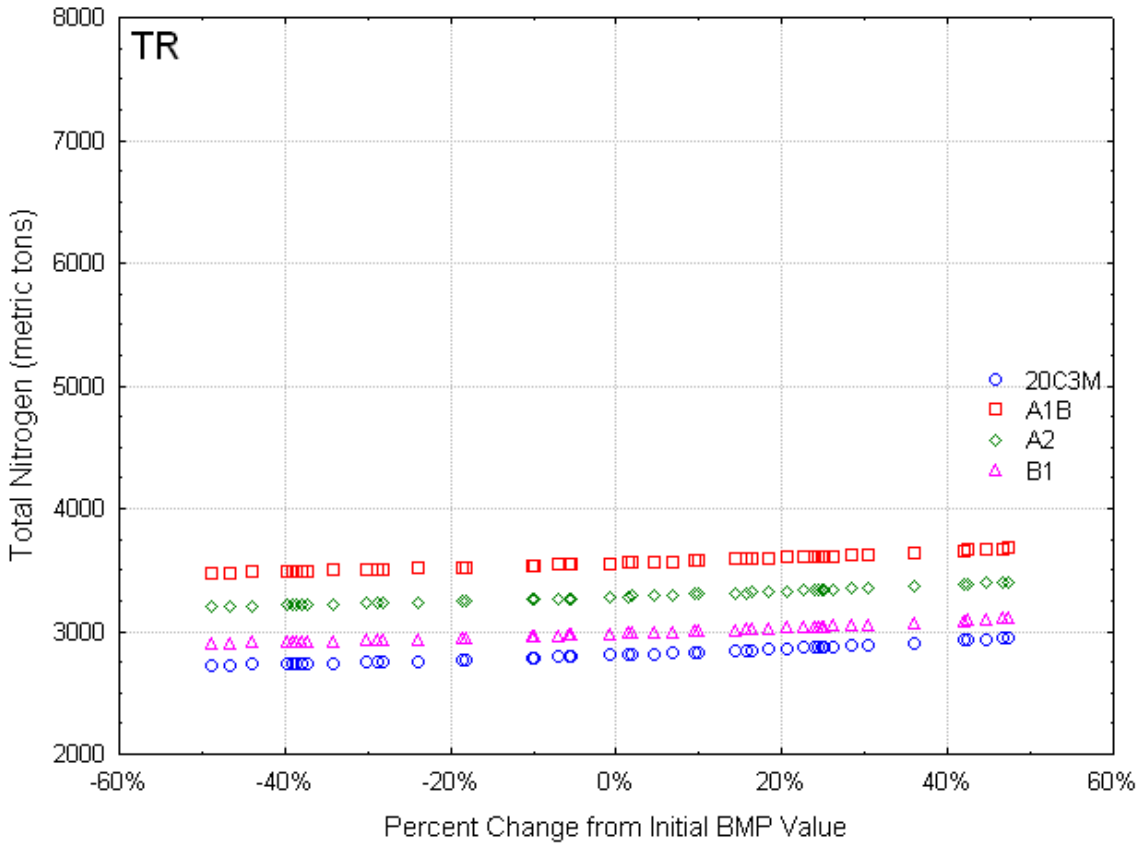

Figure 9-16. Terrace TN yield versus percent parameter change

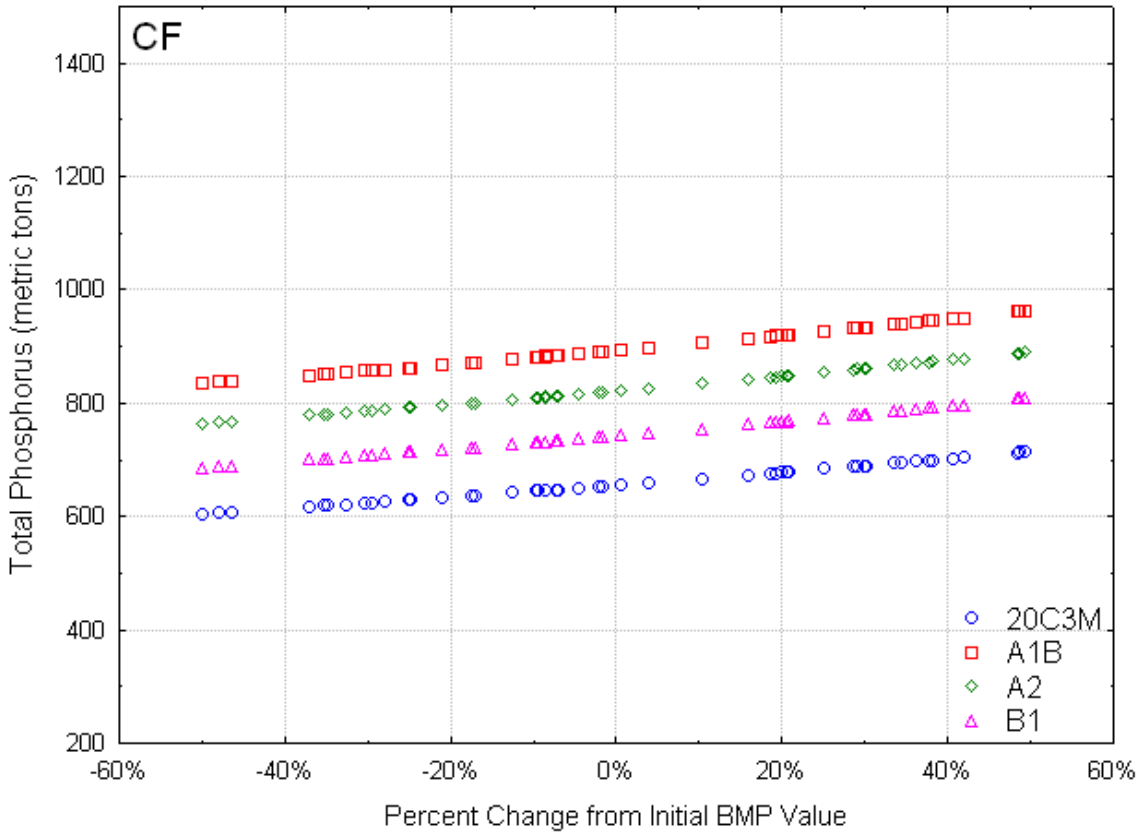

Figure 9-17. Contour farming TP yield versus percent parameter change

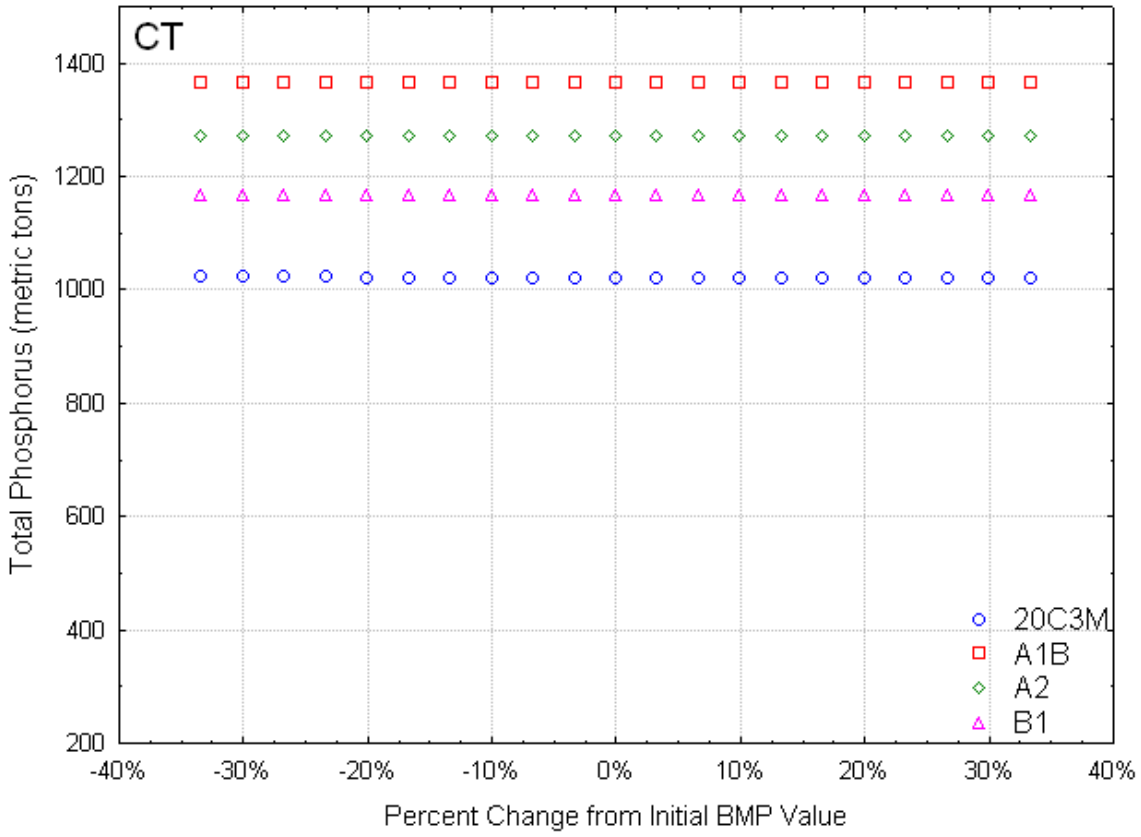

Figure 9-18. Conservation tillage TP yield versus percent parameter change

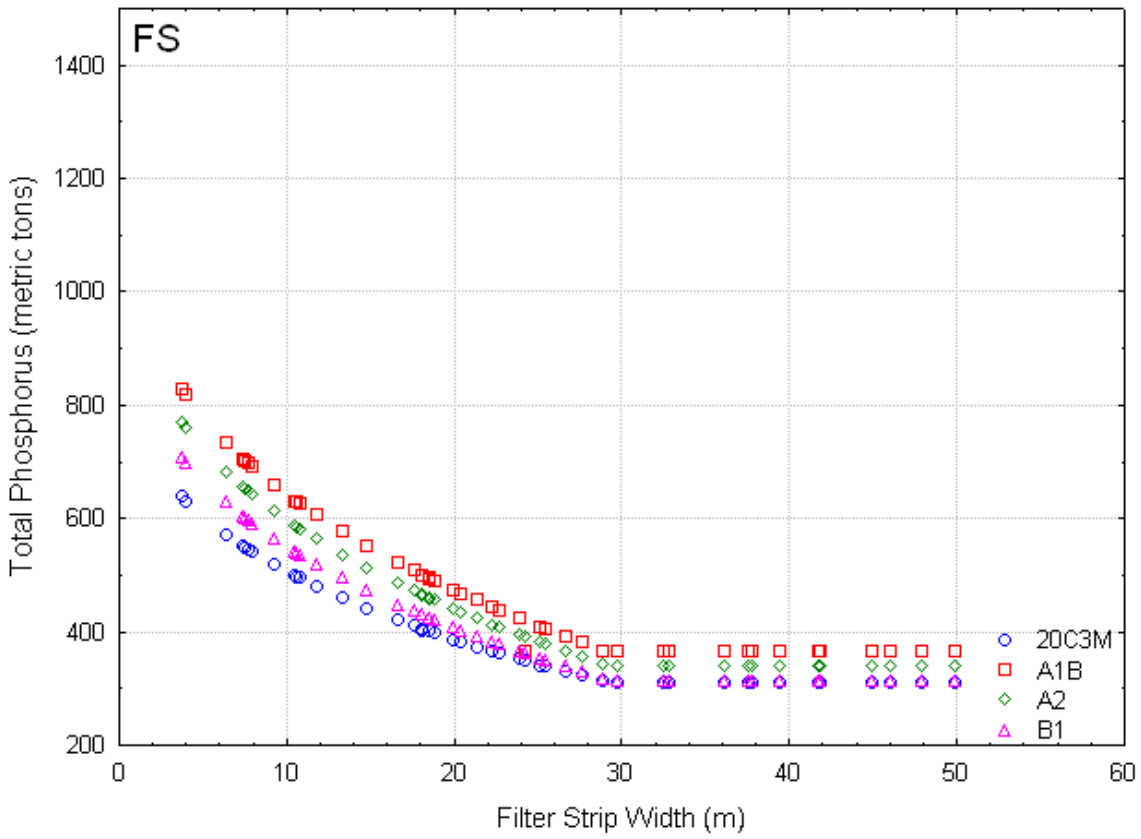

Figure 9-19. Filter strip TP yield versus filter strip width

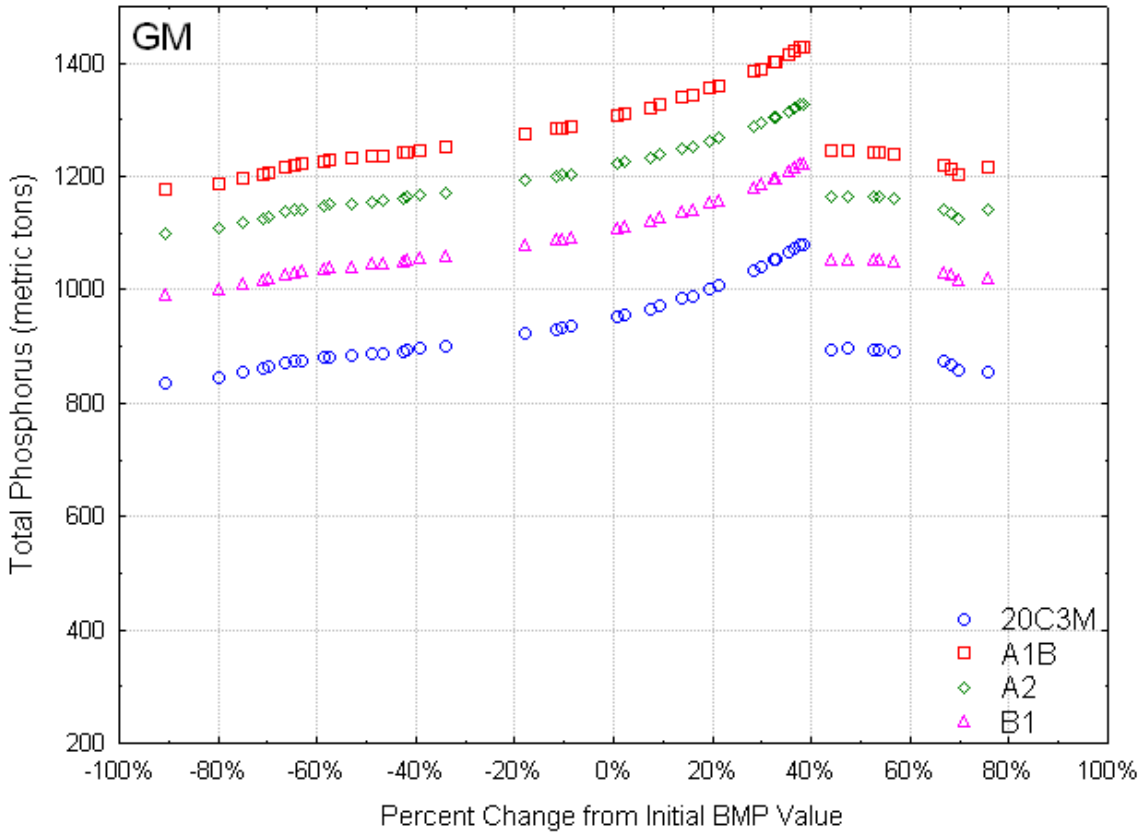

Figure 9-20. Grazing management TP yield versus percent parameter change

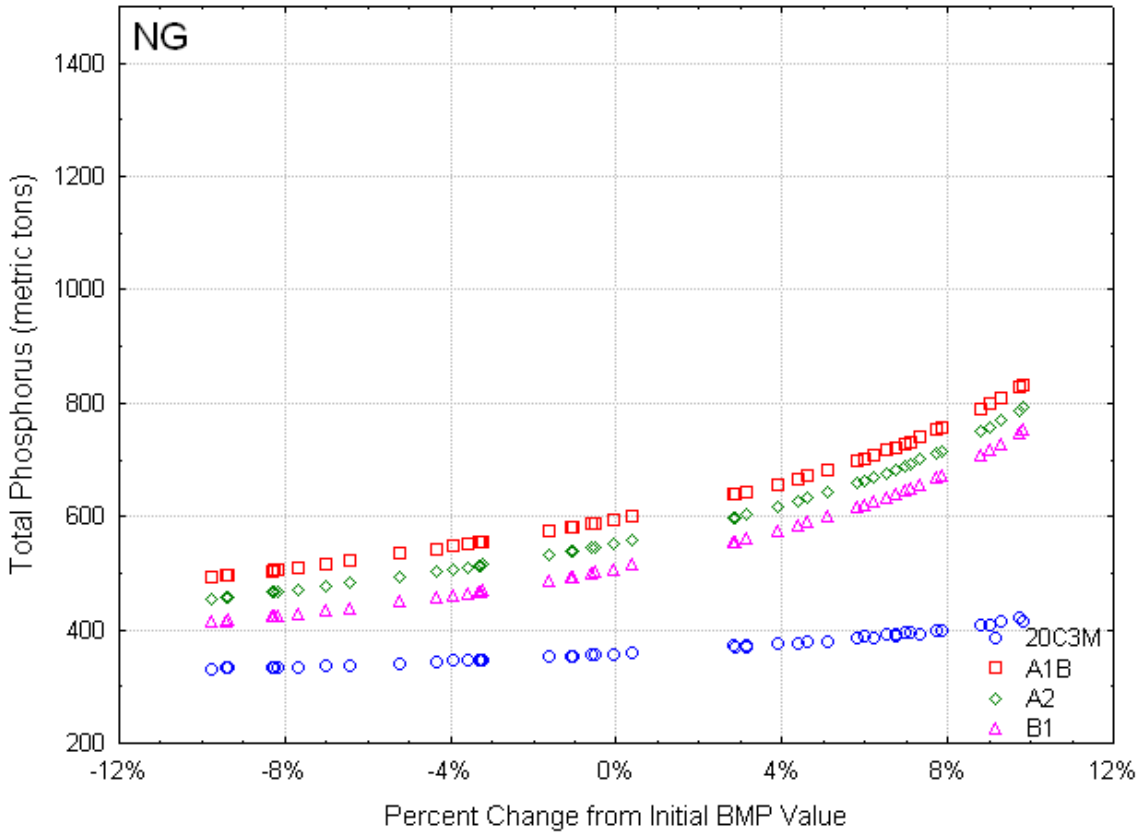

Figure 9-21. Native grass TP yield versus percent parameter change

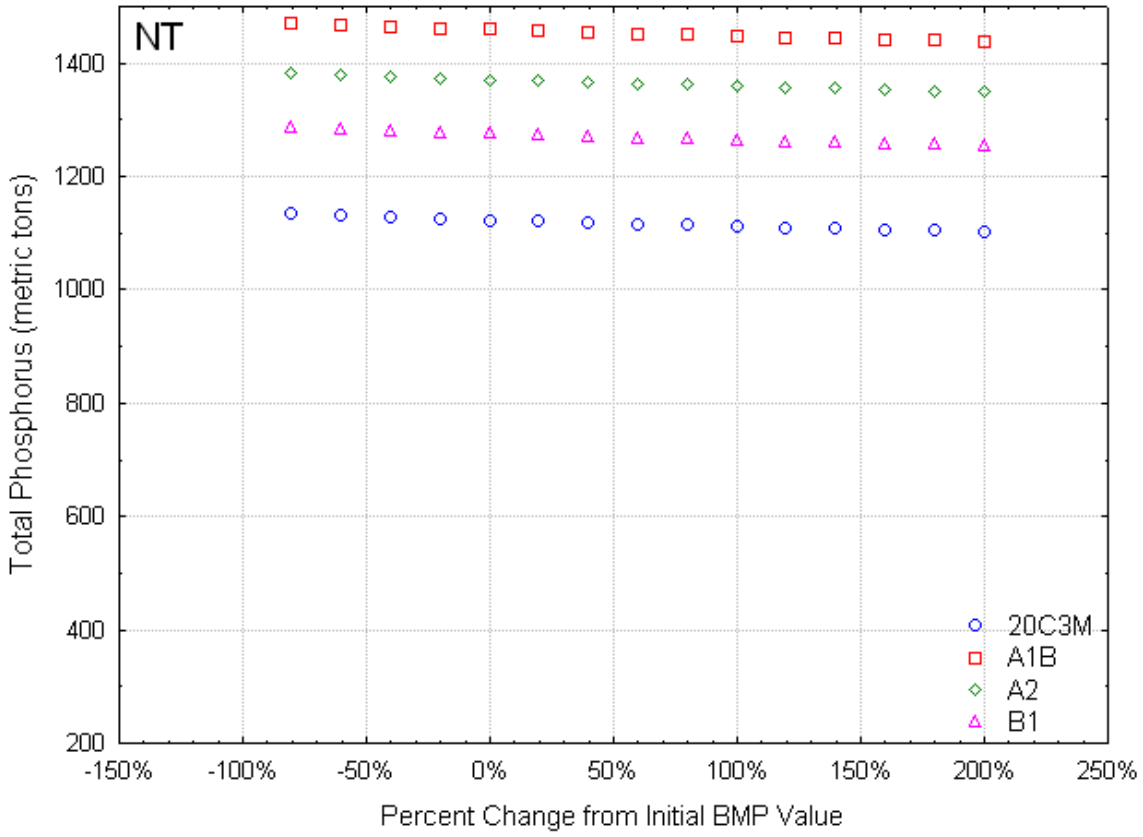

Figure 9-22. No-tillage TP yield versus percent parameter change

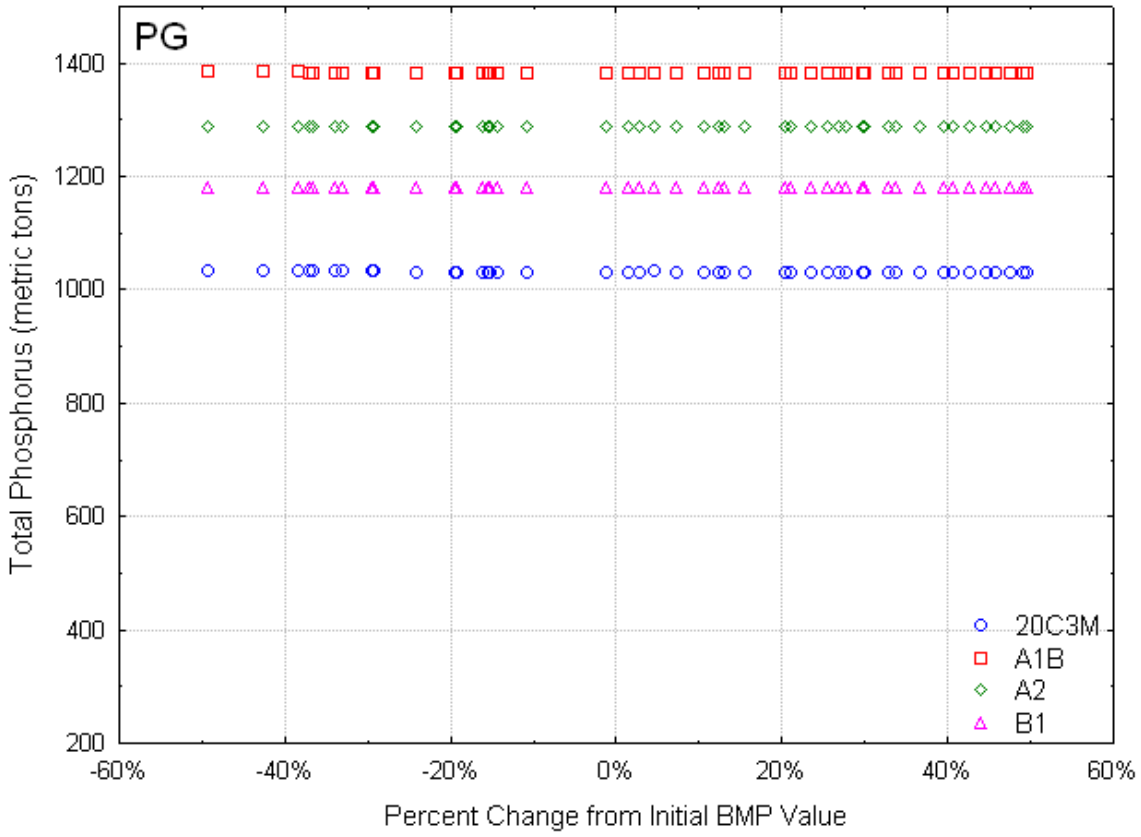

Figure 9-23. Porous gully plug TP yield versus percent parameter change

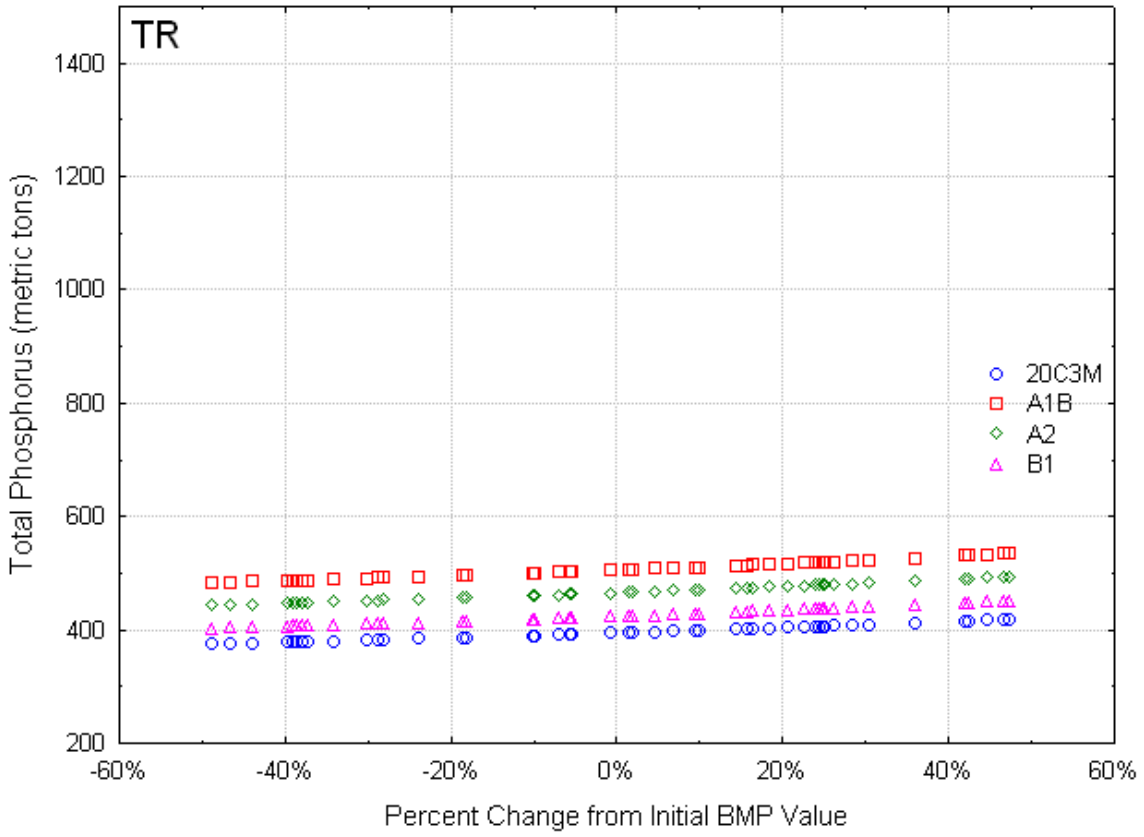

Figure 9-24. Terrace TP yield versus percent parameter change

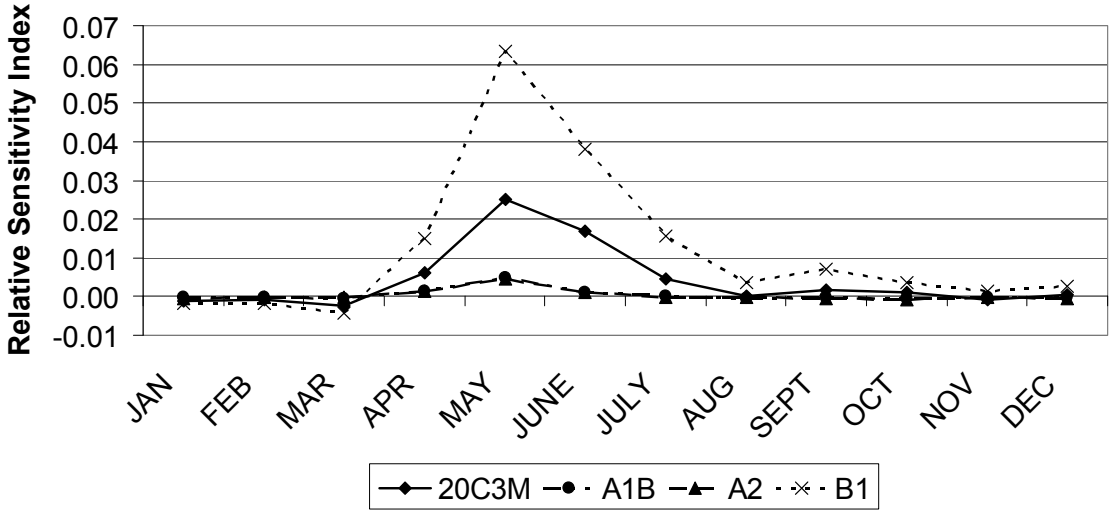

Figure 9-25. Conservation tillage average monthly TN sensitivity

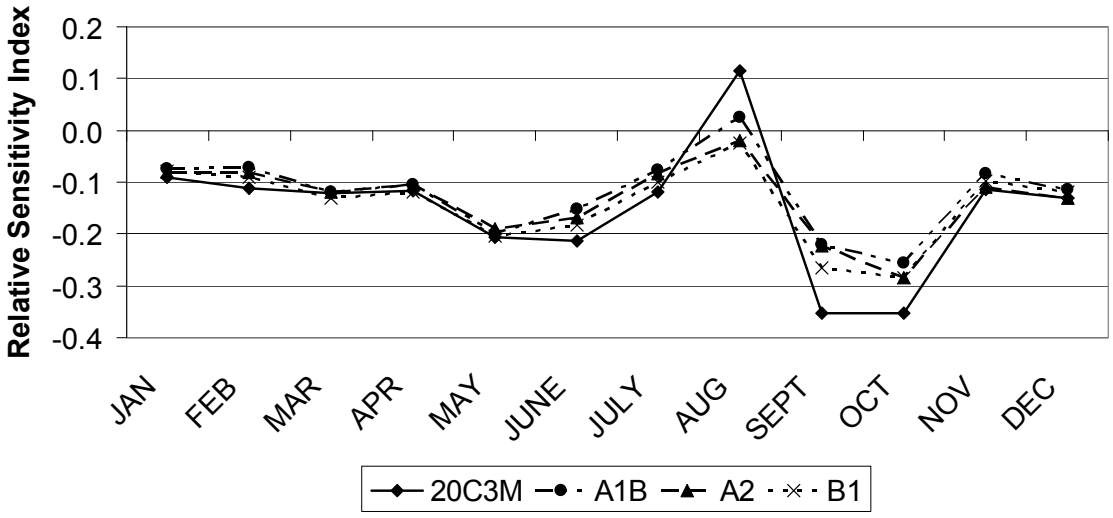

Figure 9-26. Contour farming average monthly TN sensitivity

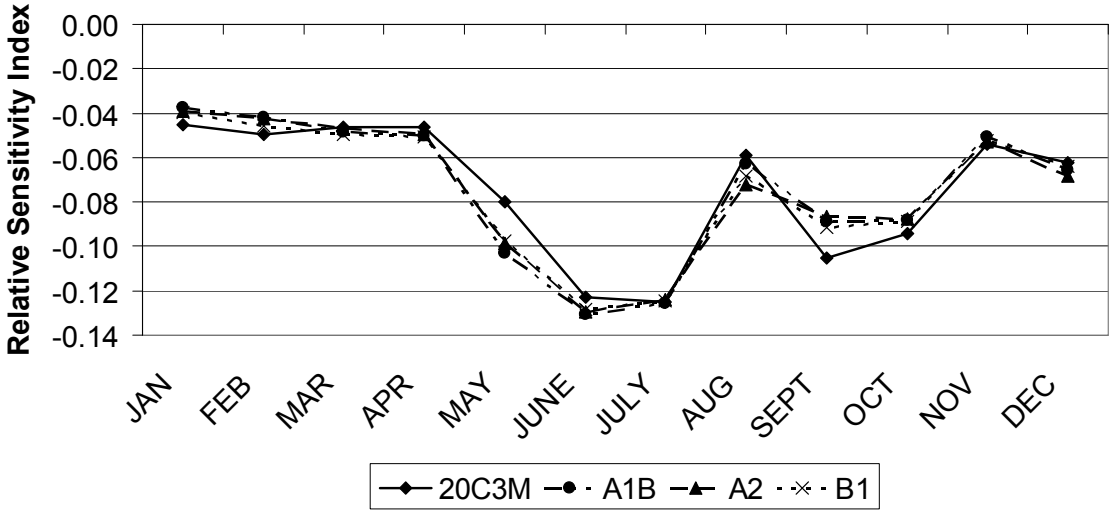

Figure 9-27. Filter strip average monthly TN sensitivity

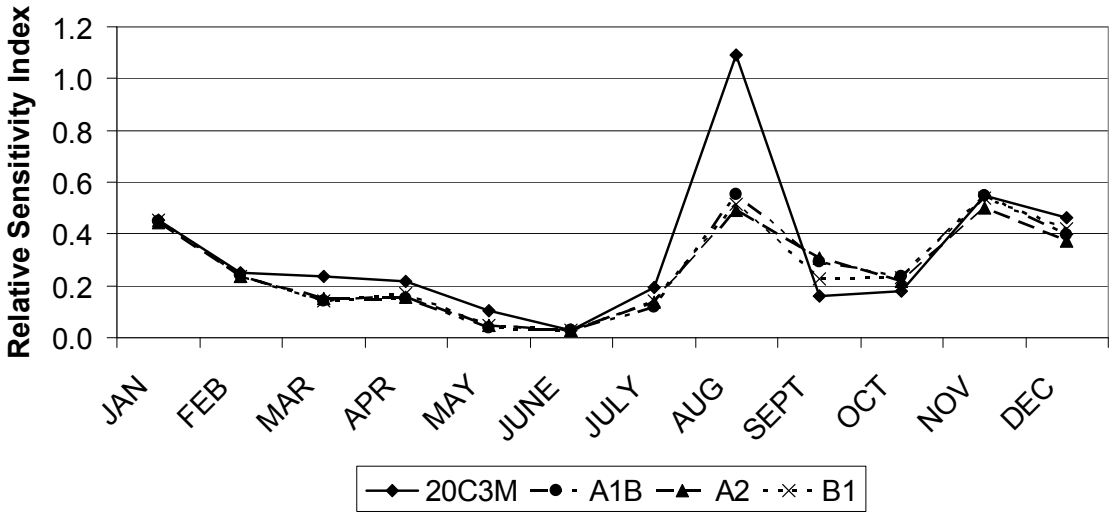

Figure 9-28. Grazing management average monthly TN sensitivity

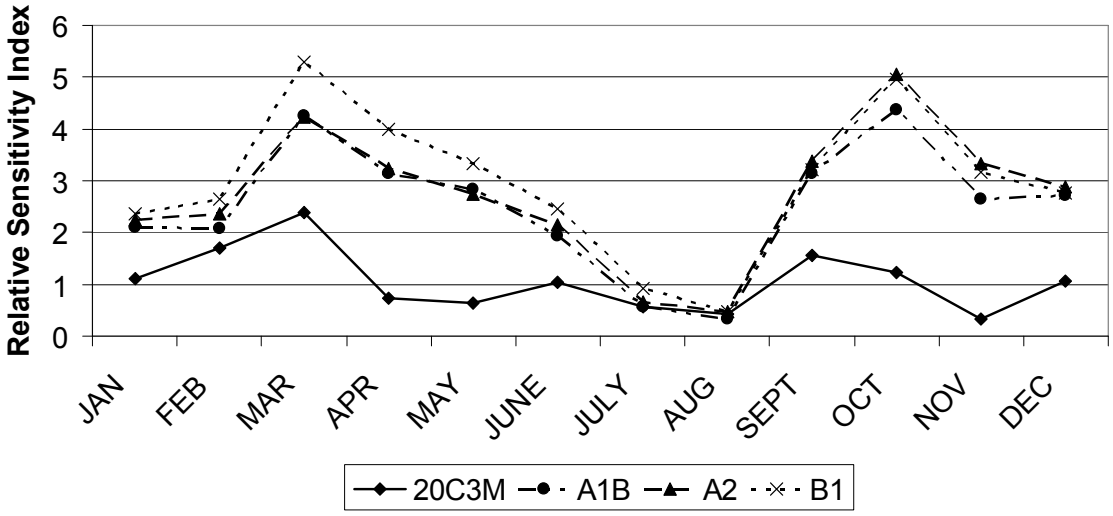

Figure 9-29. Native grass average monthly TN sensitivity

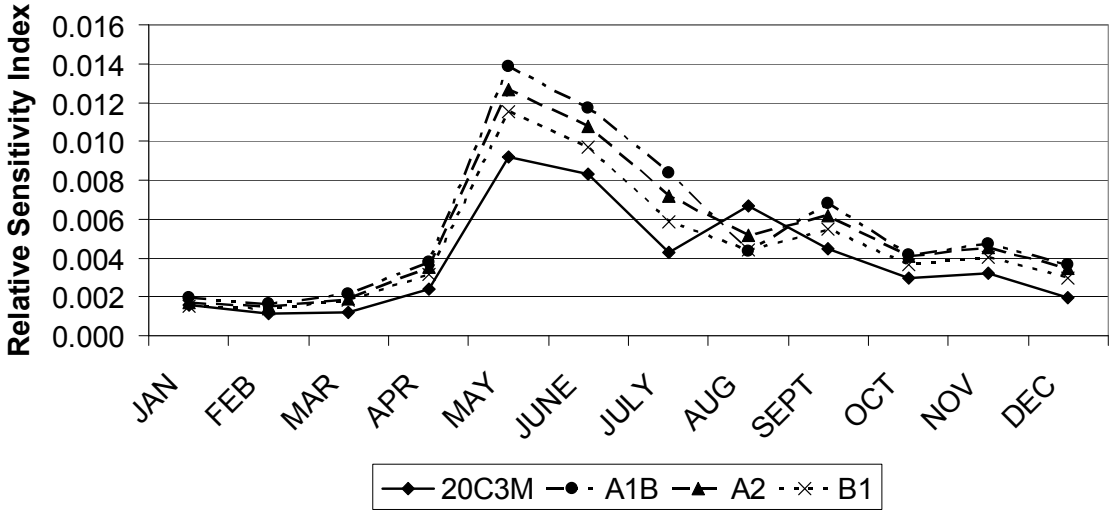

Figure 9-30. No-tillage average monthly TN sensitivity

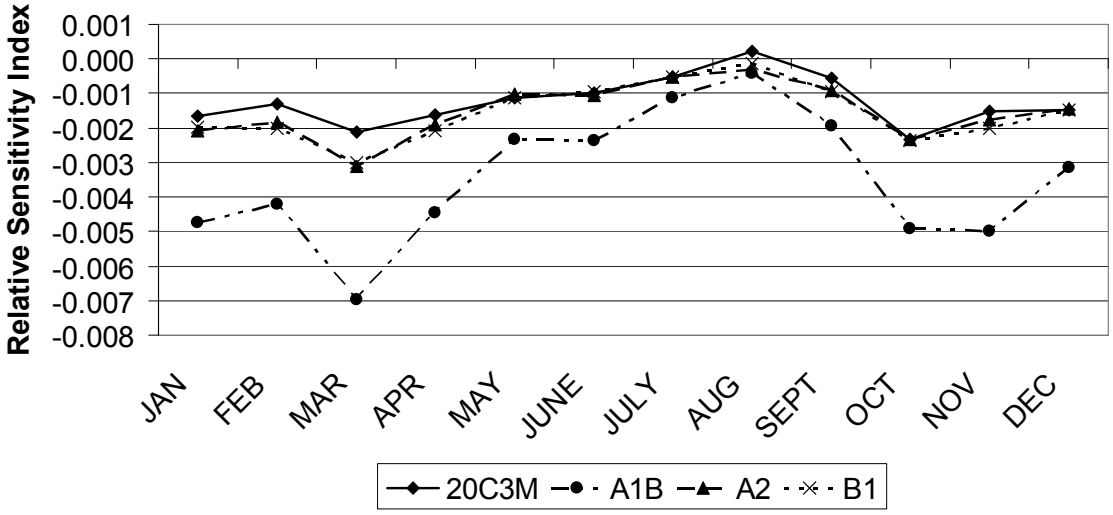

Figure 9-31. Porous gully plug average monthly TN sensitivity

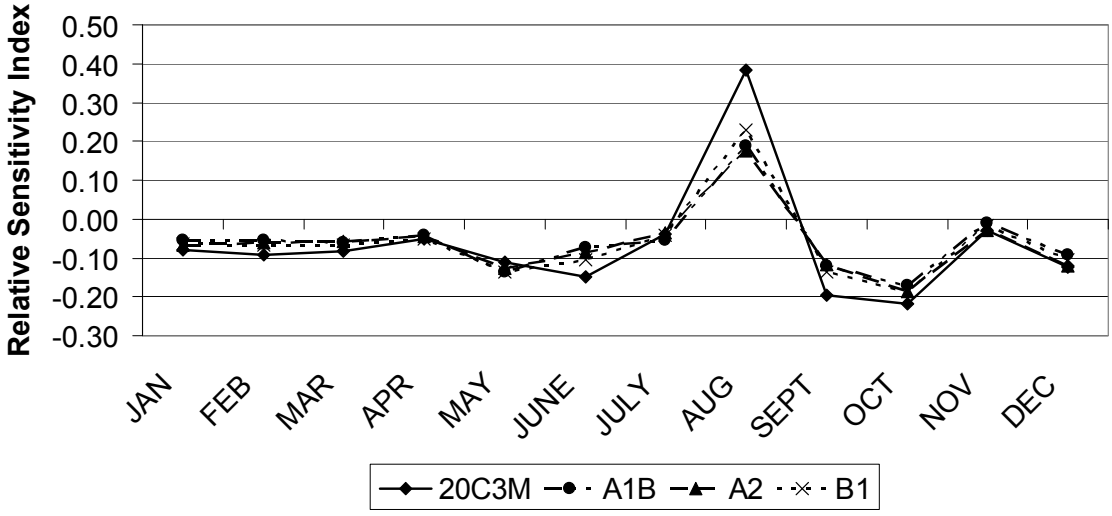

Figure 9-32. Terrace average monthly TN sensitivity

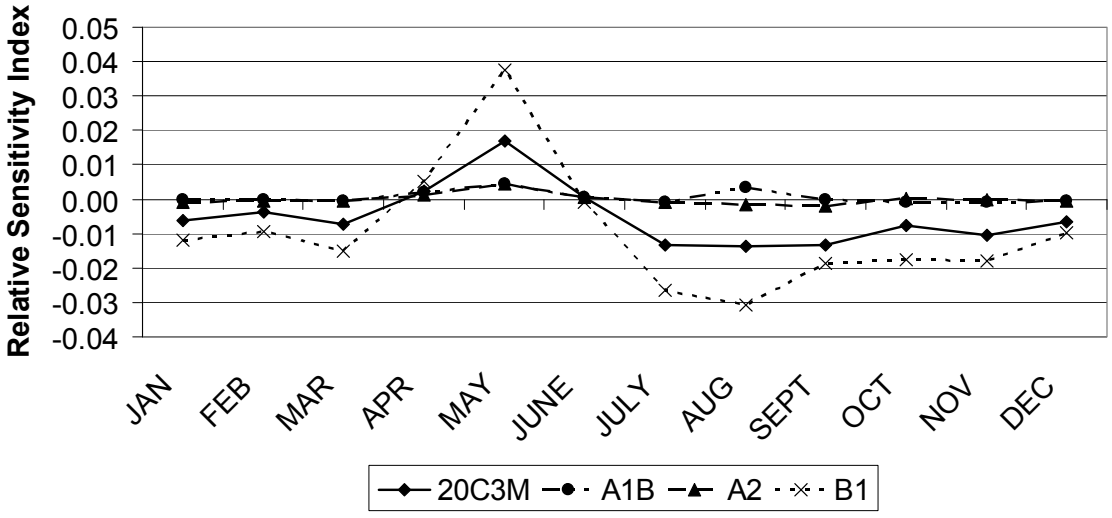

Figure 9-33. Conservation tillage average monthly TP sensitivity

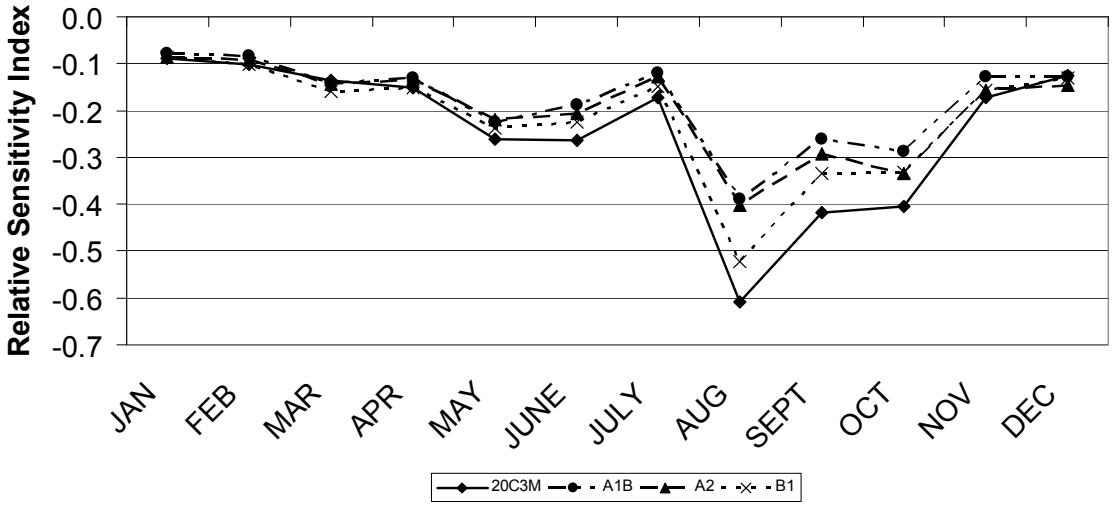

Figure 9-34. Contour farming average monthly TP sensitivity

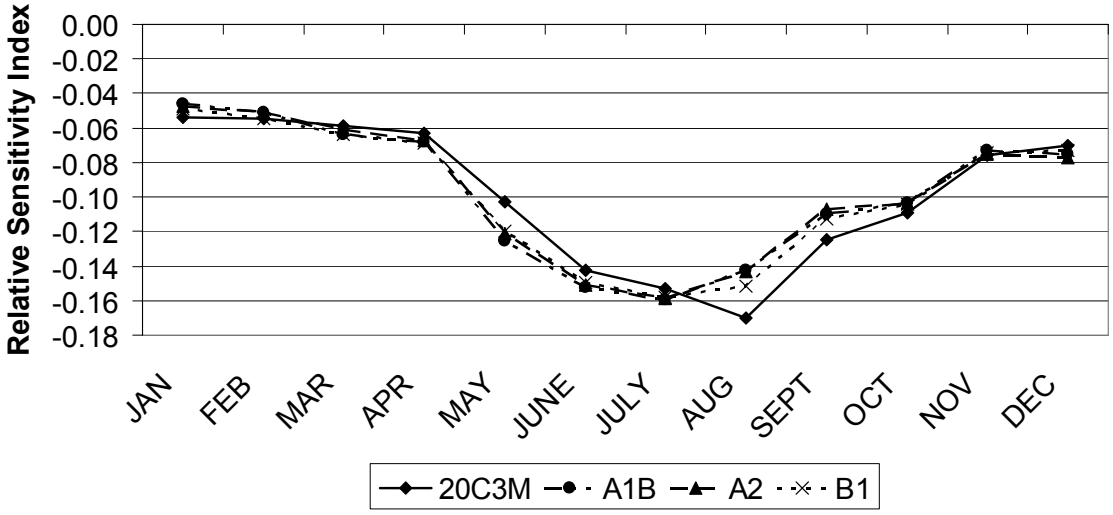

Figure 9-35. Filter strip average monthly TP sensitivity

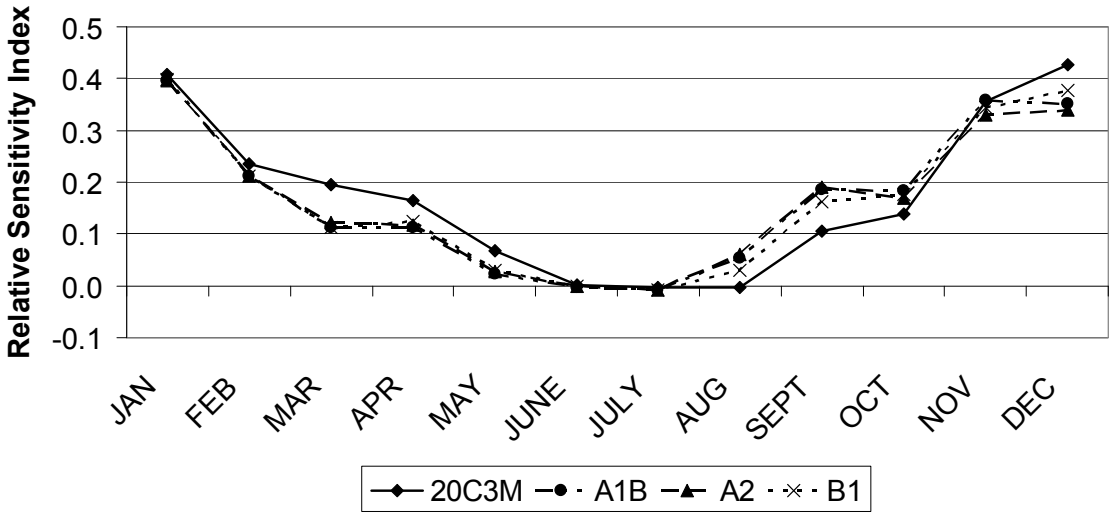

Figure 9-36. Grazing management average monthly TP sensitivity

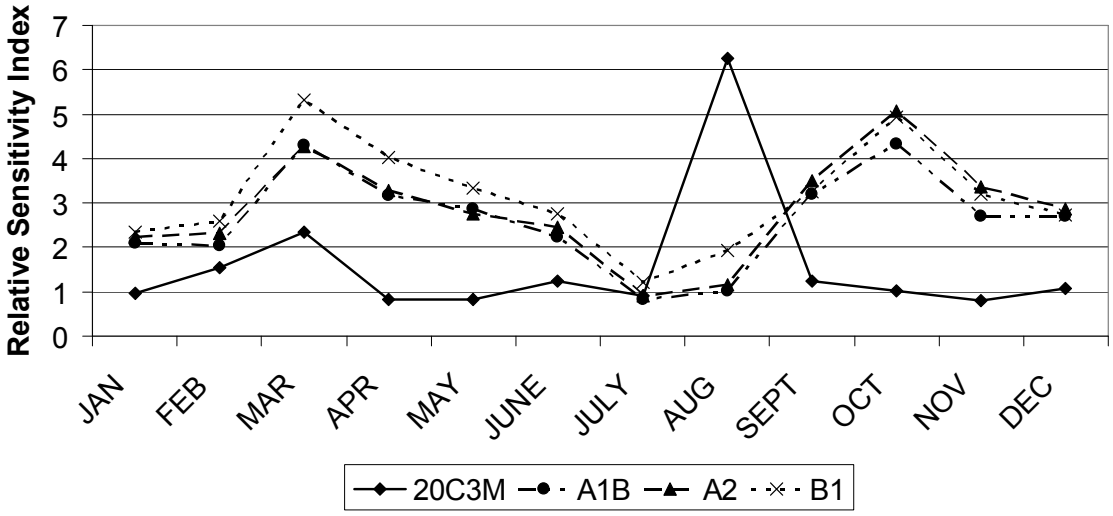

Figure 9-37. Native grass average monthly TP sensitivity

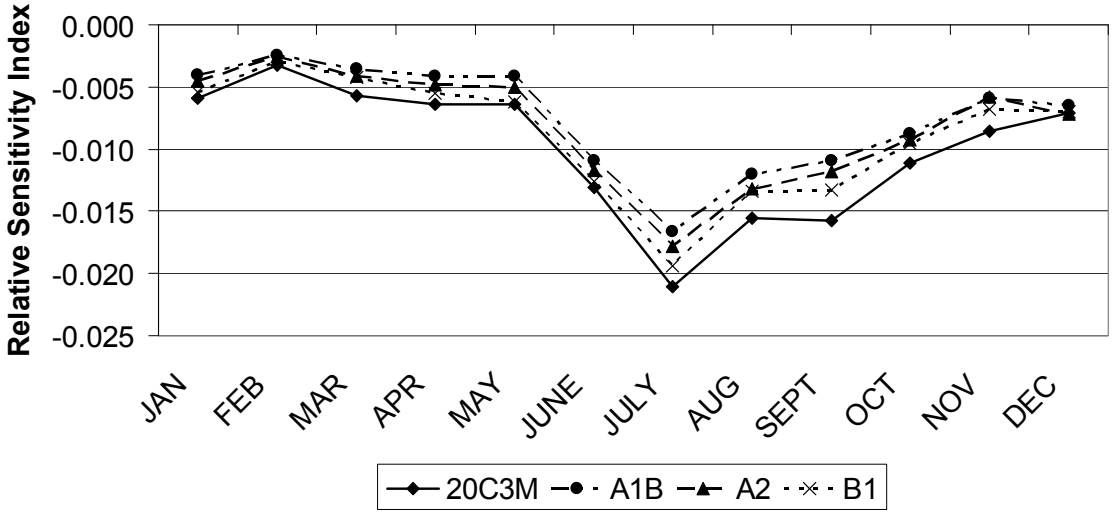

Figure 9-38. No-tillage average monthly TP sensitivity

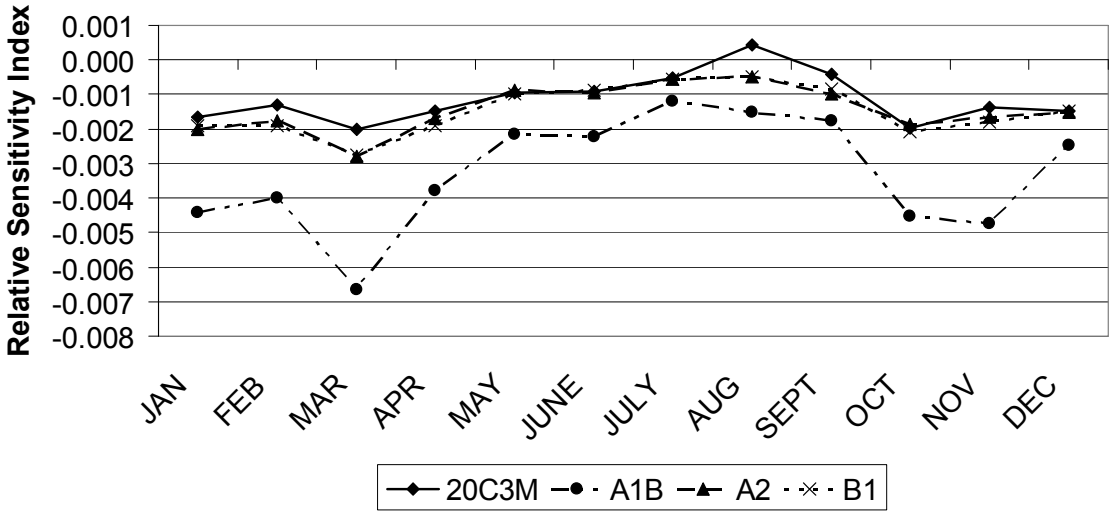

Figure 9-39. Porous gully plug average monthly TP sensitivity

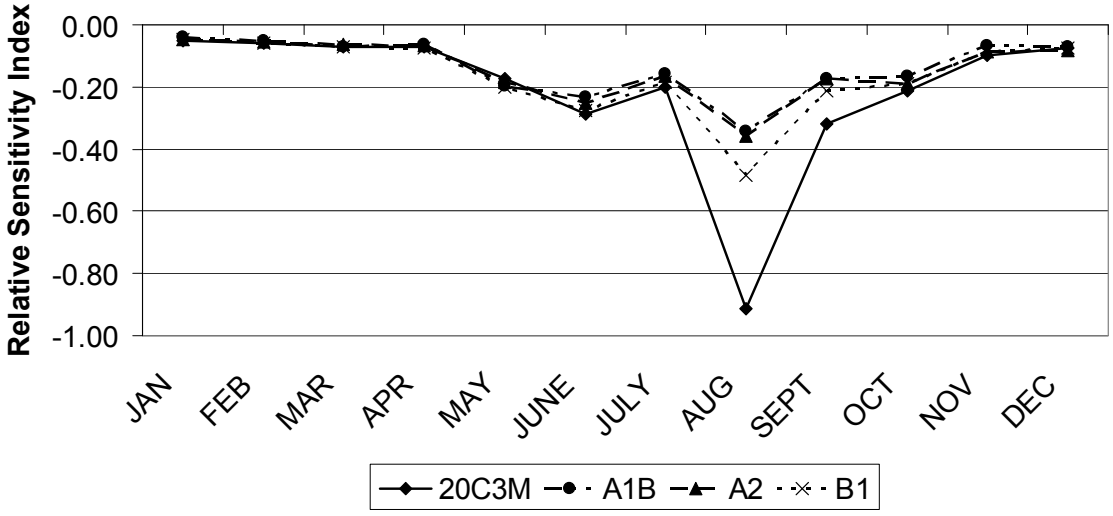

Figure 9-40. Terrace average monthly TP sensitivity

Table 9-1. ANOVA TN p-values (highlighted cells indicate significance)

Conservation Tillage					Contour Farming				
	20C3M	A1B	A2	B1		20C3M	A1B	A2	B1
20C3M		<0.01	<0.01	<0.01	20C3M		<0.01	<0.01	<0.01
A1B	<0.01		0.04	<0.01	A1B	<0.01		<0.01	<0.01
A2	<0.01	0.04		<0.01	A2	<0.01	<0.01		<0.01
B1	<0.01	<0.01	<0.01		B1	<0.01	<0.01	<0.01	
Filter Strips					Grazing Management				
	20C3M	A1B	A2	B1		20C3M	A1B	A2	B1
20C3M		0.39	0.39	0.42	20C3M		0.36	0.31	0.45
A1B	0.39		0.99	0.96	A1B	0.36		0.9225	0.88
A2	0.39	0.99		0.97	A2	0.31	0.92		0.80
B1	0.42	0.96	0.97		B1	0.45	0.88	0.80	
Native Grass					No-Tillage				
	20C3M	A1B	A2	B1		20C3M	A1B	A2	B1
20C3M		<0.01	<0.01	<0.01	20C3M		<0.01	<0.01	<0.01
A1B	<0.01		0.189	0.0004	A1B	<0.01		<0.01	<0.01
A2	<0.01	0.19		0.0223	A2	<0.01	<0.01		<0.01
B1	<0.01	0.0004	0.0223		B1	<0.01	<0.01	<0.01	
Porous Gully Plug					Terraces				
	20C3M	A1B	A2	B1		20C3M	A1B	A2	B1
20C3M		0.87	0.37	0.23	20C3M		<0.01	<0.01	<0.01
A1B	0.87		0.46	0.29	A1B	<0.01		0.02	<0.01
A2	0.37	0.46		0.75	A2	<0.01	0.02		0.01
B1	0.23	0.29	0.75		B1	<0.01	<0.01	0.01	

Table 9-2. ANOVA TP p-values (highlighted cells indicate significance)

Conservation Tillage					Contour Farming				
	20C3M	A1B	A2	B1		20C3M	A1B	A2	B1
20C3M		<0.01	<0.01	<0.01	20C3M		<0.01	<0.01	0.0180
A1B	<0.01		<0.01	<0.01	A1B	<0.01		<0.01	<0.01
A2	<0.01	<0.01		<0.01	A2	<0.01	<0.01		<0.01
B1	<0.01	<0.01	<0.01		B1	0.0180	<0.01	<0.01	
Filter Strips					Grazing Management				
	20C3M	A1B	A2	B1		20C3M	A1B	A2	B1
20C3M		0.26	0.27	0.32	20C3M		0.15	0.09	0.25
A1B	0.26		0.99	0.89	A1B	0.15		0.81	0.78
A2	0.27	0.99		0.91	A2	0.09	0.81		0.60
B1	0.32	0.89	0.91		B1	0.25	0.78	0.60	
Native Grass					No-Tillage				
	20C3M	A1B	A2	B1		20C3M	A1B	A2	B1
20C3M		<0.01	<0.01	<0.01	20C3M		<0.01	<0.01	<0.01
A1B	<0.01		0.18	0.0006	A1B	<0.01		<0.01	<0.01
A2	<0.01	0.18		0.0320	A2	<0.01	<0.01		0.01
B1	<0.01	0.0006	0.0320		B1	<0.01	<0.01	0.01	
Porous Gully Plug					Terraces				
	20C3M	A1B	A2	B1		20C3M	A1B	A2	B1
20C3M		0.79	0.42	0.27	20C3M		<0.01	0.11	0.0202
A1B	0.79		0.58	0.39	A1B	<0.01		<0.01	<0.01
A2	0.42	0.58		0.76	A2	0.11	<0.01		<0.01
B1	0.27	0.39	0.76		B1	0.0202	<0.01	<0.01	

REFERENCES

REFERENCES

Abbaspour, K.C., M., Faramarzi, S.S. Ghasemi, and H. Yang. 2009. Assessing the impact of climate change on water resources in Iran. Water Resources. Research, 45: W10434.

Abu-Zreig, M., R.P. Rudra, M.N.Lalonde, H.R. Whiteley, and N.K. Kaushik. 2004. Experimental investigation of runoff reduction and sediment removal by vegetated filter strips. Hydrological Processes, 18(11): 2029-2037.

Arabi, M., J.R. Frankenberger, B.A. Engel, and J.G. Arnold. 2007. Representation of agricultural conservation practices with SWAT. Hydrological Processes, 22(16): 3042-3055.

Arnell, N.W. 2004. Climate change and global water resources: SRES emissions and socio-economic scenarios. Global Environmental Change-Human and Policy Dimensions, 14(1): 31-52.

Arnold, J.G., R.Srinivasan, R.S. Muttiah, and J.R.Williams. 1998. Large area hydrologic modeling and assessment - Part 1: Model development. Journal of the American Water Resources Association, 34(1): 73-89.

Bahremand A., F. De Smedt, J. Corluy, Y.B. Liu, J. Poórová, L. Velcická, and E. Kuniková. 2007. WetSpa model application for assessing reforestation impacts on floods in Margecany-Hornad watershed, Slovakia. Water Resource Management, 21(8): 1373-1391.

BASINS, 2007. Better assessment science integrating point & nonpoint sources. Available at : http://www.epa.gov/waterscience/basins/. Accessed 22 September 2009.

Bates, B.C., Z.W. Kundzewicz, S. Wu and J.P. Palutikof, Eds. 2008. Climate Change and Water. Technical Paper of the Intergovernmental Panel on Climate Change, IPCC Secretariat, Geneva: 210 pp.

Behera, S., and R.K. Panda. 2006. Evaluation of management alternatives for an agricultural watershed in a sub-humid subtropical region using a physical process based model. Agriculture, Ecosystems, and Environment, 13: 62-72.

Berritella, M., A. Bigano, R. Roson, and R.S.J. Tol. 2004. A general equilibrium analysis of climate change impacts on tourism. Research Unit Sustainability and Global Change Working Paper FNU-49, Hamburg University and Centre for Marine and Atmospheric Science, Hamburg, Germany.

Bhaduri, B., J. Harbor, B.A. Engel, and M. Grove. 2000. Assessing watershed-scale, long-term hydrologic impacts of land use change using a GIS-NPS model. Environmental Management, 26(6): 643–658.

Bhaduri, B., M. Minner, S. Tatalovich and J. Harbor. 2001. Long-term hydrologic impact of urbanization: A tale of two models. Journal of Water Resources Planning and Management, 127: 13–19.

Bicknell, B.R., J.C. Imhoff, J.L. Kittle, Jr., A.S. Donigian, Jr., and R.C. Johanson. 1997. Hydrological simulation program—Fortran: User's manual for version 11. US Environmental rotection Agency, National Exposure Research Laboratory, Athens, Georgia. EPA/600/R-97/080, 755 pp.

Borah, D.K., and M. Bera. 2003. Watershed-scale hydrologic and nonpoint-source pollution models: Review of mathematical bases. Transactions of the ASAE, 46(6): 1553-1566.

Borah, D.K., and M. Bera. 2004. Watershed-scale hydrologic and nonpoint-source pollution models: Review of applications. Transactions of the ASAE, 47(3): 789-803.

Bosch, D., F. Theurer, R. Bingner, G. Felton and I. Chaubey. 1998. Evaluation of the AnnAGNPS Water Quality Model. ASAE Paper No. 98-2195, St. Joseph, Michigan. 12 p.

Bracmort, K.S., M. Arabi, J.R. Frankenberger, B.A. Engel, and J.G. Arnold. 2006. Modeling long-term water quality impact of structural BMPs. Transactions of the ASABE, 49(2): 367-374.

Castro, C.L., R.A. Pielke Sr., and G. Leoncini. 2005. Dynamical downscaling: Assessment of value retained and added using the Regional Atmospheric Modeling System (RAMS). Journal of Geophyiscal Research, 110: D05108.

Chaplot, V. 2007. Water and soil resources response to rising levels of atmospheric CO2 concentration and to changes in precipitation and air temperature. Journal of Hydrology, 337: 159-171.

Christensen, J.H., B. Hewitson, A. Busuioc, A. Chen, X. Gao, I. Held, R. Jones, R.K. Kolli, W.-T. Kwon, R. Laprise, V. Magaña Rueda, L. Mearns, C.G. Menéndez, J. Räisänen, A. Rinke, A. Sarr, and P. Whetton. 2007: Regional climate projections. In: Climate Change 2007: The Physical Basis. Contribution of Working Group I to the Fourth Assessment Report of the Intergovernmental Panel on Climate Change [Solomon, S., D. Qin, M. Manning, Z. Chen, M. Marquis, K.B. Averyt, M. Tignor, and H.L. Miller (eds.)]. Cambridge University Press, Cambridge, UK, and New York, pp. 847-940.

Covich, A.P., S.C. Fritz, P.J. Lamb, R.D. Marzolf, W.J. Matthews, K.A. Poiani, E.E. Prepas, M.B. Richman, and T.C. Winter. 1997. Potential effects of climate change on aquatic ecosystems of the Great Plains of North America. Hydrological Processes, 11: 993–1021.

Das, S., R.P. Rudra, B. Gharabaghi, P.K. Goel, A. Singh, and I. Ahmed. 2007. Comparing the performance of SWAT and AnnAGNPS model in a watershed in

Ontario. Proceedings of the ASABE fourth conference on watershed management to meet water quality standards and TMDLs. Publication no: 701P0207. San Antonio, Texas. March 10–14, 2007.

Debano, L.F., and L.J. Schmidt. 1990. Potential for enhancing riparian habitats in the southwestern United States with watershed practices. Forest Ecology and Management, 33/34: 385–403.

Dibike, Y.B., and P. Coulibaly. 2005. Hydrologic impact of climate change in the Saguenay watershed: comparison of downscaling methods and hydrologic models. Journal of Hydrology, 307: 145-163.

Duan, Q.Y., V.K. Gupta, and S. Sorooshian. 1993. Shuffled complex evolution approach for effective and efficient global minimization. Journal of Optimaztion Theory and Applications, 76(3): 501-521.

Easterling, W., and M. Apps. 2005. Assessing the consequences of climate change for food and forest resources: A view from the IPCC. Climatic Change, 70(1-2): 165-189.

Ebi, K.L., D.M. Mills, J.B. Smith, and A. Grambsch. 2006. Climate change and human health impacts in the United States: An update on the results of the US National Assessment. Environmental Health Perspectives, 114(9): 1318-1324.

Eckhardt, K., and U. Ulbrich. 2003. Potential impacts of climate change on groundwater recharge and streamflow in a central European low mountain range. Journal of Hydrology, 285(1-4): 244-252.

Fankhauser, S., and R.S.J. Tol. 2005. On climate change and economic growth. Resource and Energy Economics, 27(1): 1-17.

Ficklin, D.L., Y.Z. Luo, E. Luedeling, and M.H. Zhang. 2009. Climate change sensitivity assessment of a highly agricultural watershed using SWAT. Journal of Hydrology, 374(1-2): 16-29.

Ficklin, D.L., Y.Z Luo, E. Luedeling, S.E. Gatzke, and M.H. Zhang. 2010. Sensitivity of agricultural runoff loads to rising levels of CO2 and climate change in the San Joaquin Valley watershed of California. Environmental Pollution, 158: 223-234.

Fowler, H. J., S. Blenkinsop, and C. Tebaldi. 2007. Linking climate change modelling to impacts studies: recent advances in downscaling techniques for hydrological modelling. International Journal of Climatology 27: 1547-1578.

Franczyk, J. and H. Chang. 2009. The effects of climate change and urbanization on the runoff of the Rock Creek basin in the Portland metropolitan area, Oregon, USA. Hydrological Processes, 23(6): 805-815.

Gassman, P.W., M.R. Reyes, C.H. Green, and J.G.Arnold. 2007. The soil and water assessment tool: Historical development, applications, and future research directions. Transactions of the Asabe, 50(4): 1211-1250.

Giorgi, F., and L.O. Mearns. 1999. Introduction to special section: regional climate modeling revisited. Journal of Geophyiscal Research, 104: 6335-6352.

Gitau, M.W., T.L. Veith, W.J. Gburek, and A.R. Jarrett. 2006. Watershed level best management practice selection and placement in the town brook watershed, New York. Journal of the American Water Resources Association, 42(6): 1565-1581.

Githui, F., W. Gitau, F. Mutua, and W. Bauwens. 2009. Climate change impact on SWAT simulated streamflow in western Kenya. International Journal of Climatology, 29: 1823–1834.

Göncü, S., and E. Albek. 2009. Modeling climate change effects on streams and reservoirs with HSPF. Water Resources Management 24(4): 707-726.

Gosain, A.K., S. Rao, and D. Basuray. 2006. Climate change impact assessment on hydrology of Indian river basins. Current Scence, 90(3): 346-353.

Graham, L.P., J. Andreasson, and B. Carlsson. 2007. Assessing climate change impacts on hydrology from an ensemble of regional climate models, model scales, and linking models – a case study on the Lule River basin. Climatic Change, 81: 293-307.

Gregory, P.J., J.S.I. Ingram, and M. Brklacich. 2005. Climate change and food security. Philosophical Transactions of the Royal Society B-Biological Sciences, 360(1463): 2139-2148.

Gül, G.O., and D. Rosbjerg. 2010. Modelling of hydrologic processes and potential response to climate change through the use of a multisite SWAT. Water and Environment Journal, 24(1): 21-31

Gutowski, W.J., G.C. Hegerl, G.J. Holland, T.R. Knutson, L.O. Mearns, R.J. Stouffer, P.J. Webster, M.F. Wehner, and F.W. Zwiers, 2008. Causes of observed changes in extremes and projections of future changes. In: Weather and Climate Extremes in a Changing Climate: Regions of Focus: North America, Hawaii, Caribbean, and U.S. Pacific Islands [Karl, T.R., G.A. Meehl, C.D. Miller, S.J. Hassol, A.M. Waple, and W.L. Murray (eds.)]. Synthesis and Assessment Product 3.3. U.S. Climate Change Science Program, Washington, DC, pp. 81-116.

Haines A., R.S. Kovats, D. Campbell-Lendrum, C. Corvalan. 2006. Climate change and human health: impacts, vulnerability, and mitigation. The Lancet, 367: 2101-2109.

Hay, L.E., R.L. Wilby, and G.H. Leavesly. 2000. A comparison of delta change downscaled GCM scenarios for three mountainous basins in the United States. Journal of the American Water Resources Association, 36(2): 387-397.

Hoar, T., and D. Nychka. 2008. Statistical Downscaling of the Community Climate System Model (CCSM) monthly temperature and precipitation projections. White paper by IMAGe/NCAR.

Homer, C. et al. 2007. Completion of the 2001 National Land Cover Database for the conterminous United States. Photogrammetric Engineering and Remote Sensing, 73(4): 337-341.

Howden, S.M., J-F. Soussana, F.N. Tubiello, N. Chhetri, M. Dunlop, and H. Meinke. 2007. Adapting agriculture to climate change. Proceedings of the National Academy of Sciences, USA, 104: 19691–19696.

Houghton, J. T., Y. Ding, D. J. Griggs, M. Noguer, P. J. van der Linden, X. Dai, K. Maskell and C. A. Johnson, (eds). 2001. IPCC, 2001: Climate Change 2001: The Scientific Basis. Contribution of Working Group I to the Third Assessment Report of the Intergovernmental Panel on Climate Change. Cambridge University Press, Cambridge, United Kingdom and New York, NY, USA: 881 pp.

Hulme, P.E. 2005. Adapting to climate change: is there scope for ecological management in the face of a global threat? Journal of Applied Ecology, 42(5): 784-794.

Hurd, B.H., M. Callaway, J. Smith, and P. Kirshen. 2004. Climatic change and US water resources: From modeled watershed impacts to national estimates. Journal of the American Water Resources Association, 40(1): 129-148.

IPCC. 2007. Summary for Policymakers. In: Climate Change 2007: The Physical Science Basis. Contribution of Working Group I to the Fourth Assessment Report of the Intergovernmental Panel on Climate Change [Solomon, S., Qin, D., Manning, M., Chen, Z., Marquis, M., Averyt, K.B., Tignor, M., Miller, H.L. (eds.)]. Cambridge University Press, Cambridge, United Kingdom and New York, NY, USA.

Jackson, R.B., S.R. Carpenter, C. N. Dahm, D. M. McKnight, R.J. Naiman, S.L. Postel and S.W. Running. 2001. Water in a changing world. Ecological Applications, 11(4): 1027-1045.

Jha, M., J.G. Arnold, P.W. Gassman, F. Giorgi, and R. Gu. 2006. Climate change sensitivity assessment on upper Mississippi river basin steamflows using SWAT. Journal of the American Water Resources Association, 42(4): 997-1015.

Jha, M.K., P.W. Gassman, and J.G. Arnold. 2007. Water quality modeling for the Raccoon River watershed using SWAT. Transactions of the ASABE, 50(2): 479-493.

Joos, F., I.C. Prentice, S. Sitch, R. Meyer, G. Hooss, G.K. Plattner, S. Gerber, and K. Hasselmann. 2001. Global warming feedbacks on terrestrial carbon uptake under the Intergovernmental Panel on Climate Change (IPCC) emission scenarios. Global Biogeochemical. Cycles, 15(4): 891-908.

Karl, T.R., W.C. Wang, M.E. Schlesinger, R.W Knight, and D. Portman. 1990. A method of relating general circulation model simulated climate to the observed local climate. Part I: Seasonal statistics. Journal of Climate 3, 1053–1079.

Karl, T.R., and K.E. Trenberth. 2003. Modern global climate change. Science, 302: 1719-1723

Karl, T.R., J.M. Melillo, and T.C. Peterson. 2009. Global climate change impacts in the United States. Global climate change impacts in the United States: 188 pp.

Kovats, R.S., D. Campbell-Lendrum, and F. Matthies. 2005. Climate change and human health: Estimating avoidable deaths and disease. Risk Analysis, 25(6): 1409-1418.

Kundzewicz, Z.W., L.J. Mata, N.W. Arnell, P. Döll, P. Kabat, B. Jiménez, K.A. Miller, T. Oki, Z. Sen, and I.A. Shiklomanov. 2007: Freshwater resources and their management. Climate Change 2007: Impacts, Adaptation and Vulnerability. Contribution of Working Group II to the Fourth Assessment Report of the Intergovernmental Panel on Climate Change, M.L. Parry, O.F. Canziani, J.P. Palutikof, P.J. van der Linden and C.E. Hanson, Eds., Cambridge University Press, Cambridge, UK, 173-210.

Lenderink, G., A. Buishand, and W. van Deursen. 2007. Estimates of future discharges of the river Rhine using two scenario methodologies: direct versus delta approach. Hydrology and Earth System Sciences, 11(3): 1145-1159.

Lenhart, T., K. Eckhardt, N. Fohrer, and H.G. Frede. 2002. Comparison of two different approaches of sensitivity analysis. Physics and Chemistry of the Earth, 27: 645-654.

Liu, A.J., S.T.Y. Tong, and J.A. Goodrich. 2000. Land use as a mitigation strategy for the water-quality impacts of global warming: A scenario analysis on two watersheds in the Ohio River Basin. Environmental Engineering and Policy, 2: 65-76.

Liu Y.B., and F. De Smedt. 2004. WetSpa extension, documentation and user manual. Department of Hydrology and Hydraulic Engineering, Vrije Universiteit Brussel, Belgium.

Luo, Y., and M. Zhang. 2009. Management oriented sensitivity analysis for pesticide transport in watershed-scale water quality modeling using SWAT. Environmental Pollution, 157: 3370-3378.

Marshall, E., and T.Randhir. 2008. Effect of climate change on watershed system: a regional analysis. Climatic Change, 89(3-4): 263-280.

Maurer, E.P. 2007. Uncertainty in hydrologic impacts of climate change in the Sierra Nevada Mountains, California under two emissions scenarios. Climatic Change, 82: 309-325

McCuen, R.H. 1973. The role of sensitivity in hydrologic modeling. Journal of Hydrology, 18(1): 37-53.

Meehl, G.A., T.F. Stocker, W.D. Collins, P. Friedlingstein, A.T. Gaye, J.M. Gregory, A. Kitoh, R. Knutti, J.M. Murphy, A. Noda, S.C.B. Raper, I.G. Watterson, A.J. Weaver and Z.C. Zhao. 2007: Global Climate Projections. In: Climate Change 2007: The Physical Science Basis. Contribution of Working Group I to the Fourth Assessment Report of the Intergovernmental Panel on Climate Change [Solomon, S., D. Qin, M. Manning, Z. Chen, M. Marquis, K.B. Averyt, M. Tignor and H.L. Miller (eds.)]. Cambridge University Press, Cambridge, United Kingdom and New York, NY, USA.

Meyer, J.L., M.J. Sale, P.J. Mulholland, and N.L. Poff. 1999. Impacts of climate change on aquatic ecosystem functioning and health. Journal of the American Water Resources Association, 35(6): 1373-1386.

Moriasi, D.N. et al. 2007. Model evaluation guidelines for systematic quantification of accuracy in watershed simulations. Transactions of the Asabe, 50(3): 885-900.

Muleta, M.K., and J.W. Nicklow. 2005. Sensitivity and uncertainty analysis coupled with automatic calibration for a distributed watershed model. Journal of Hydrology, 306(1-4): 127-145.

Murdoch, P.S., J.S. Baron, and T.L.Miller. 2000. Potential effects of climate chance on surface-water quality in North America. Journal of the American Water Resources Association, 36(2): 347-366.

Muttiah, R.S., and R.A. Wurbs. 2002. Scale-dependent soil and climate variability effects on watershed water balance of the SWAT model. Journal of Hydrology, 256(3-4): 264-285.

Nakicenovic et al. 2000. Special Report on Emissions Scenarios. A Special Report of Working Group III of the Intergovernmental Panel on Climate Change. Cambridge University Press: Cambridge. 599 pp.

Nash, J. E., and J. V. Sutcliffe. 1970. River flow forecasting through conceptual models part I — A discussion of principles. Journal of Hydrology, 10 (3): 282–290.

National Academies. 2008. Understanding and responding to climate change: highlights of National Acadamies Reports, 2008 Edition.

Nejadhashemi, A.P., and K.R. Mankin. 2007. Comparison of four water quality models (STEPL, PLOAD, L-THIA, and AVSWAT-X) in simulating sediment and nutrient dynamics in a watershed. Minneapolis, MN: ASABE Annual International Meeting. Paper no: 072211. June 17–20.

Nejadhashemi, A.P., and K.R. Mankin. 2007. Recommended Practices for Modeling BMPs Using SWAT Model. Kansas Water Office.

Neitsch, S.L., J.G. Arnold, J.R. Kiniry, and J.R. Williams. 2005. Soil and water assessment tool theoretical documentation, Grassland, Soil and Water Research Laboratory, Agricultural Research Service, Tempe, TX 76502.

NRCS-NHCP. 2010. USDA Natural Resources Conservation Service - National Conservation Practice Standards. Available at: http://www.nrcs.usda.gov/technical/standards/nhcp.html. Accessed: January 2010.

Nurmohamed, R., S. Naipal, and F. De Smedt. 2007. Modeling hydrological response of the Upper Suriname river basin to climate change. Journal of Spatial Hydrology, 7(1).

Nyenje, P.M. and O. Batelaan. 2009. Estimating the effects of climate change on groundwater recharge and baseflow in the upper Ssezibwa catchment, Uganda, Hydrological Sciences Journal, 54(4): 713-726.

Parajuli, P.B., K.R. Mankin, and P.L. Barnes. 2008. Applicability of targeting vegetative filter strips to abate fecal bacteria and sediment yield using SWAT. Agricultural Water Management, 95(10): 1189-1200.

Parker, G.T., R.L. Droste, and K.J. Kennedy. 2008 Modelling the effect of agricultural best management practices on water quality under various climatic scenarios. Journal of Environmental Engineering and Science, 7(1): 9-19.

Parmesan, C. 2006. Ecological and evolutionary responses to recent climate change. Annual Review of Ecololgy, Evolution, and Systematics, 37: 637-669.

Patz, J.A., and R.S. Kovats. 2002. Hotspots in climate change and human health. British Medical Journal, 325: 1094–1098.

Patz, J.A., D. Campbell-Lendrum, T. Holloway, and J.A. Foley. 2005. Impact of regional climate change on human health. Nature, 438: 310–317.

PLOAD. 2001. PLOAD version 3.0: An ArcView GIS Tool to Calculate Nonpoint Sources of Pollution in Watershed and Stormwater Projects, User's Manual. USEPA.

PRUDENCE. 2005 Prediction of regional scenarios and uncertainties for defining European climate change risks and effects, Project EVK2-CT2001-00132 in the EU 5th Framework Program for Energy, Environment, and Sustainable Development.

Rosenberg, N.J., R.A. Brown, R.C. Izaurralde, and A.M. Thomson. 2003. Integrated assessment of Hadley Centre (HadCM2) climate change projections on agricultural productivity and irrigation water supply in the conterminous United States - I. Climate change scenarios and impacts on irrigation water supply simulated with the HUMUS model. Agricultural and Forest Meteorology, 117(1-2): 73-96.

Rosenberg, E.A., P.W. Keys, D.B. Booth, D. Hartley, J. Burkey, A.C. Steinemann, and D.P. Lettenmaier. 2010. Precipitation extremes and the impacts of climate change on stormwater infrastructure in Washington State. Climatic Change, 102: 319-349

Santhi, C., R. Srinivasan, J.G. Arnold, and J.R. Williams. 2006. A modeling approach to evaluate the impacts of water quality management plans implemented in a watershedi n Texas. Environmental Modeling and Software, 21: 1141-1157.

Schmidhuber, J., and F.N. Tubiello. 2007. Global food security under climate change. Proceedings of the National Academy of Sciences, 104: 19703–19708.

Scott, D., G. McBoyle, and M. Schwartzentruber. 2004. Climate change and the distribution of climatic resources for tourism in North America. Climate Research, 27: 105-117.

Senhorst, H.A.J., and J.J.G. Zwolsman. 2005. Climate change and effects on water quality: a first impression. I W a Publishing, pp. 53-59.

Slingo, J.M., A.J. Challinor, B.J. Hoskins, and T.R. Wheeler. 2005. Introduction: food crops in a changing climate. Philosophical Transactions of the Royal Society B-Biological Sciences, 360(1463): 1983-1989.

Snover, A. K., A. F. Hamlet, and D. P. Lettenmaier. 2003: Climate-change scenarios for water planning studies: Pilot applicationsin the Pacific Northwest. Bulletin of the American Meteorological Society, 84: 1513–1518.

Solomon, S., G.-K. Plattner, R. Knutti, and P. Friedlingstein. 2009. Irreversible climate change due to carbon dioxide emissions. Proceedings of the National Academy of Sciences, 106(6): 1704-1709.

Stone, M.C., R.C. Hotchkiss, and L.O. Mearns. 2003. Water yield responses to high and low spatial resolution climate change scenarios in the Missouri River basin. Geophysical Research Letters, 30(4): 35.1-35.4.

Tans, P. 2010. NOAA/ESRL (www.esrl.noaa.gov/gmd/ccgg/trends/). Accessed November 16, 2010.

Thomas, C.D., et al. 2004. Extinction risk from climate change. Nature, 427: 145-148.

Tubiello, F.N., J.F. Soussana, and S.M. Howden. 2007. Crop and pasture response to climate change. Proceedings of the National Academy of Sciences of the United States of America, 104: 19686–19690.

Tuppad, P. and R. Srinivasan. 2008. Bosque River environmental infrastructure improvement plan: Phase II BMP modeling report. Texas AgriLife Research, Texas A&M University.

Tuppad, P., N. Kannan, R. Srinivasan, C.G. Rossi, and J.G. Arnold. 2010. Simulation of agricultural management alternatives for watershed protection. Water Resources Management, 24(12): 3115-3144.

Ullrich, A., and M.Volk. 2009. Application of the Soil and Water Assessment Tool (SWAT) to predict the impact of alternative management practices on water quality and quantity. Agricultural Water Management, 96: 1207-1217.

USDA-NASS, 2007. 2007 Census of Agriculture. USDA-National Agricultural Statistics Service 2007

USDA-NRCS, 2005. National Conservation Practice Standards-NHCP. Available online at http://www.nrcs.usda.gov/Technical/Standards/nhcp.html

van Griensven, A., T. Meixner, S. Grunwald, T. Bishop, M. Diluzio, and R. Srinivasan. 2006. A global sensitivity analysis tool for the parameters of multi-variable catchment models. Journal of Hydrology, 324(1-4): 10-23.

Walther, G.R., E. Post, P. Convery, A. Menzel, C. Parmesan, et al. 2002. Ecological responses to recent climate change. Nature, 416: 389-395.

Woznicki, S.A., A.P. Nejadhashemi, C. Smith. 2010. Assessing best management practice implementation strategies under climate change scenarios. Transactions of the ASABE, under review.

Wilby, R.L., C.W. Dawson, and E.M. Barrow. 2002. SDSM – a decision support tool for the assessment of regional climate change impacts. Environmental Modeling and Software, 17: 147-159.

Wilby, R.L., H.G. Orr, M. Hedger, D. Forrow, and M. Blackmore. 2006. Risks posed by climate change to the delivery of Water Framework Directive objectives in the UK. Environment International, 32(8): 1043-1055.

Yuan, Y., R.L. Bingner, and R.A. Rebich. 2001. Evaluation of AnnAGNPS on Mississippi Delta MSEA watersheds. Transactions of the ASAE, 44(5): 1183-1190.